PROPERDIN IN IMMUNITY

In vitro and *in vivo* investigations

Thesis submitted for the degree of

Doctor of Philosophy

by

Aline Dupont M.Sc. (DEA – Lille)

Department of Infection, Immunity and Inflammation

November 2008

Statement of Originality

This accompanying thesis submitted for the degree of PhD entitled “Properdin in immunity – *In vitro* and *in vivo* investigations” is based on work conducted by the author in the Department of Infection, Immunity and Inflammation of the University of Leicester during the period between October 2004 and September 2007.

All the work recorded in this thesis is original unless otherwise acknowledged in the text or by references.

None of the work has been submitted for another degree in this or any other University.

Signed: _____ Date: _____

Acknowledgments

I would first like to thank my supervisor, Dr. Cordula Stover, for giving me the opportunity to realise this work and for her help and continuous support during the 4 years of this PhD. Mille mercis pour vos précieux conseils et votre patience, Chef.

I would also like to thank all the other people who have contributed to this work: Dr. Aras Kadioglu for his great contribution for all the animal work, Dr. Rana El-Rachkidy Lonnen for her always useful advices whenever I had a problem (science-related or not, and even when I didn't have any problem…), Dr. Claire Smith, Dr. Adam Wright, Dr. Karl Staples, Dr. Nicholas Lynch and Dr. Chris Jones for initiating me to ELISA, flow cytometry, real-time PCR and rotational thromboelastography, respectively. Many thanks go as well to Stefan Hyman and Natalie Allcock for the electron microscopic analyses. I am thankful too to all the staff from the animal house and the Transgenic Unit, especially Jane Brown. Thanks too to my postgraduate tutor Prof. Richard Camp, not forgetting Prof. Peter Bradding and Prof. Alison Goodall for their useful discussions.

I would like to thank of course as well my labmates from lab 211 (Chrissy, Claudia, Irina, Kathryn, Nur'ain, Petra and Sen) and members of staff from the III and other departments, especially Sonia (and Sergio), Sarah, James, George, Christine, Rob, Mahmut, Luisa, Barbara, Areej, Hind, Sara and Girish.

I am grateful too to Prof. Stéphane Bouquelet and Dr. Olivier Vidal from the Université de Lille for welcoming me to their lab 6 years ago and introducing me to the "lab world". I would never have been able to go that far without you.

Also, most importantly, I would like to thank my family and my friends, here in Leicester and back in France, for their endless support and for always being present in both the good and the bad moments. Merci pour tout.

Abstract

The complement system is one of the defence systems used by the host to protect itself against pathogens. It is divided into three complement pathways: the antibody-dependent classical pathway, the lectin pathway and the alternative pathway. This latter antibody-independent pathway is auto-activated and leads to the generation and the deposition of C3b molecules on the pathogen's surface. Properdin, the only positive regulator of this pathway, plays a major role by stabilising the alternative C3 convertase that leads to the creation of the amplification loop. Only little was known about the biology of properdin at the beginning of this project, despite the fact that properdin was discovered more than 50 years ago and despite the important role played by this molecule in immunity, as illustrated by the higher susceptibility to severe meningococcal disease encountered by properdin-deficient people. My thesis dealt with three experimental outlines to determine the role of properdin in immunity

Properdin was examined from its global expression by various organs to its specific expression by different cell types. I have first shown using molecular biology and bioinformatics tools that properdin was expressed at a relatively high level in different lymphoid organs. I have then examined in more detail the expression of properdin by one of these organs, namely the spleen, using immunofluorescence. Properdin was thus shown to be present only in the white pulp compartment of this organ, where it was organised in clusters of properdin-positive cells possessing long cytoplasmic extensions.

Next, I studied the expression of properdin by auxiliary cells. I have first given evidence that properdin was deposited on the surface of platelets and that this level of deposition was related to the activation state of the platelets. I have then shown for the first time that properdin was expressed by two mast cell lines. Microscopic analyses then demonstrated that properdin was present on the mast cell membrane and was present mainly as clusters on membrane extensions similar to vesicles in the process of being released. Further analyses on vesicles released by mast cells confirmed that properdin was enriched in a fraction of vesicles similar in size and in shape to microvesicles.

Finally, the role played by properdin during bacterial infection was investigated using a pneumococcal pneumonia model. This study showed that properdin-deficient mice presented a worse level of infection than their wild-type littermates 2 days post-infection. This was associated with an unexpected higher survival rate for properdin-deficient animals one week following the challenge. Therefore, in this model, while properdin was seen to be beneficial during the first 48 hours post-infection, by controlling the infection, the absence of properdin led to increased survival following infection. This study thus showed for the first time that properdin could play a bivalent role during infection, the higher inflammatory response engendered by properdin turning from being beneficial to being detrimental to the host over time.

Table of Contents

List of Figures

List of Tables

Abbreviations

ACD	Acid citrate dextrose
ADP	Adenosin tri-phosphate
AP	Alkaline phosphatase
AU	Arbitrary unit
BHI	Brain heart infusion
bp	Base pairs
BSA	Bovine serum albumin
C	Complement component
CD	Cluster of differentiation
CFP	Complement factor properdin
CFU	Colony forming unit
CLP	Caecum ligation and puncture
CR	Complement receptor
CRP	Collagen related protein
DAPI	4',6-diamidino-2-phenylindole
DMSO	Dimethyl sulfoxide
DNA	Deoxyribonucleic acid
dNTP	Deoxy-nucleotide tri-phosphate
E.	*Escherichia*
ECL	Enhanced chemiluminescence
EDTA	Ethylenediaminetetraacetic acid
ELISA	Enzyme-linked immunosorbent assay
EMBL	European molecular biology laboratory
EST	Expressed sequence tag
FACS	Fluorescence-activated cell sorting
FCS	Foetal calf serum
FITC	Fluorescein isothiocyanate
GAPDH	Glyceraldehyde-3-phosphate dehydrogenase
GM-CSF	Granulocyte-macrophage colony-stimulating factor
HMC	Human mast cell
HRP	Horse radish peroxidase
IFN	Interferon
Ig	Immunoglobulin
IL	Interleukin
IMS	Industrial methylated spirit
IPTG	Isopropyl-β-D-thiogalactopyranoside
KDa	Kilodaltons
LAD	Laboratory of allergic disease
LB	Luria Broth
LBP	LPS binding protein
LPS	Lipopolysaccharide
MAC	Membrane attack complex
MASP	MBL-associated serine protease
MBL	Mannose-binding lectin
MCP	Membrane co-factor protein
MFI	Mean fluorescence intensity
MOI	Multiplicity of infection
N.	*Neisseria*

NCTC	National collection of type cultures
OCT	Optimal cutting temperature
OD	Optical density
PBMC	Peripheral blood mononuclear cell
PBS	Phosphate buffered saline
PCR	Polymerase chain reaction
PE	Phycoerythrin
PMA	Phorbol 12-myristate 13-acetate
PMN	Polymorphonuclear
PN	Properdin
pNPP	para-nitrophenylphosphate
Psp	Pneumococcal surface protein
RNA	Ribonucleic acid
ROTEG	Rotational thromboelastography
S.	*Streptococcus*
SCF	Stem cell factor
SD	Standard deviation
SDS	Sodium dodecyl sulphate
SDS-PAGE	SDS-Polyacrylamide gel electrophoresis
SEM	Standard error of the mean
TAE	Tris acetate EDTA
TBS	Tris buffered saline
TEG	Thromboelastography
TEM	Transmission electron microscopy
TEMED	N,N,N,N’-tetramethylethylenediamine
TGF	Transforming growth factor
Tm	Melting temperature
TMB	3,3’,5,5’-tetramethylbenzidine
TNF	Tumor necrosis factor
TPM	Transcript per million
TRAP	Thrombin Receptor Activation Protein
TRITC	Tetramethyl rhodamine isothiocyanate
TSR	Thrombospondin structural homology repeat
U	Unit
UV	Ultraviolet
X-Gal	5-bromo-4-chloro-3-indolyl-β-D-galactoside

1 General introduction

Immunology is by definition the study of immunity, the English word "*immunity*" coming from the Latin term "*immunitas*" meaning "*exempt*". The immune system comprises thus all the tissues, cells and molecules used by the body to protect itself from a foreign pathogenic agent and so keep itself exempt of this agent.

1.1 The immune system

Initially, there is a phase of recognition of the target, followed by an effector phase in which the target is neutralised and/or eliminated. The immune system is divided into two categories: the innate immunity and the adaptive immunity.

The innate immunity is the first line of defence against pathogenic agents. It is non-specific and includes elements that do not adapt. The innate immunity thus consists of physical barriers – such as the skin or the mucous membranes – physiological barriers – such as the pH or soluble factors, including complement components – and phagocytic cells – such as monocytes, macrophages and neutrophils.

The adaptive immunity by contrast is specific and acquired during the life of an individual. It requires more time than the innate immunity to develop as it involves the formation of specific antibodies and of T-cell receptor repertoire directed against the specific antigens carried by the pathogen. Cells of the adaptive immunity include B lymphocytes, T lymphocytes and antigen-presenting cells.

1.2 The complement system

The complement system functions within both the innate and the adaptive immunity, as it can be activated either by the formation of an immune complex, or by contact with the surface of a pathogen.

The first people to describe this system and to mention the word "complement" were Jules Bordet and Paul Ehrlich at the very end of the 19th century (Lachmann, 2006). Nowadays, the complement system is divided into three pathways: the classical pathway, the alternative pathway and the lectin pathway, and is composed of more than 30 circulating and membrane-bound proteins. These three

pathways all converge, after different proteolytic cascades, to the formation of a complex called the C3 convertase. Even though the molecules constituting the diverse C3 convertases are different, a same terminal pathway is then shared by the 3 systems as illustrated by the figure 1-1. These three complement cascades result in the same final activities: cytolysis, production of opsonins and anaphylatoxins, and initiation of an inflammatory reaction.

1.2.1 Classical complement pathway

It was the first complement pathway discovered. The initiation of this pathway is triggered by the C1 complex, itself formed by C1q and a tetramer comprising two copies of the C1r and of the C1s molecules. The formation of an immune complex induces conformational changes of the Fc region portion of IgM, IgG1, IgG2 and IgG3 molecules. This modification allows C1q to bind to adjacent Fc regions and this binding triggers C1r auto-activation. Activated C1r then cleaves the C1s molecule and activated C1s binds to and cleaves C4 into two fragments: C4a and C4b; C4a acting as an anaphylatoxin whereas C4b, while staying attached to the pathogen's surface, binds to the C2 component. This newly-formed C4b2 complex is then cleaved by the activated C1s. This cleavage leads to the formation of two new molecules: C2a and C2b, causing the creation of the C4b2a complex, the so-called classical C3 convertase (figure 1-1A) (Duncan et al., 2008).

The classical pathway has been shown to be as well induced by non-immune proteins such as serum amyloid P protein, C-reactive protein, polyanions or viral membranes (Gasque, 2004).

1.2.2 Lectin complement pathway

The lectin pathway was the last complement pathway to be discovered (Ikeda et al., 1987). It is antibody-independent and is activated when MBL (Mannose-Binding Lectin) or ficolins bind to carbohydrate groups present at the surface of certain pathogens. When activated, MBL or ficolins can interact with one of the three Mannose-binding lectin Associated Serine Proteases (MASP-1, MASP-2 and MASP-3) or with the non-protease MAp19 (MBL-Associated protein 19) (Gaboriaud et al., 2007). The complex formed by the association of activated ficolin or MBL to MASP-2 activates and cleaves C4 and C2 as the activated C1 does for the classical pathway and this results in the formation of the C4b2a complex, which is the lectin C3

convertase, and the release of C4a and C2b fragments (figure 1-1B) (Duncan et al., 2008).

The MBL-MASP-1 complex may as well play a role by directly inducing the cleavage of C3, although this still remains unclear (Dommett et al., 2006).

1.2.3 Alternative complement pathway

The alternative complement pathway was first described by Louis Pillemer in 1954 as the "properdin system" (Pillemer et al., 1954). It plays an important role in host defence against pathogens as it leads to the elimination of the pathogen without the help of any specific antibodies. To indicate their belonging to this pathway, all the alternative pathway's proteins were called "factors", with the exception of C3 as this component is common to the three pathways.

This pathway is originally known to be initiated by auto-activation of C3. This non-specific mechanism is called "tick-over". Spontaneously 1% of the serum C3 is hydrolysed, thus altering the conformation of the molecule. The so-called C3(H_2O) molecule generated has then the ability to bind to the serine protease factor B. When bound to C3(H_2O), factor B is cleaved, in presence of factor D, into Ba and Bb, the Bb fragment remaining associated to the C3(H_2O) to generate a C3(H_2O)Bb complex that has a C3 convertase-like activity. C3(H_2O)Bb is also able to cleave C3 molecules into C3a and C3b. Once C3b is generated, it then covalently binds to factor B and, in presence of factor D, leads to the creation of a C3bBb complex (and to the release of a Ba molecule), which is the C3 convertase of the alternative pathway (figure 1-2) (Thurman and Holers, 2006). Properdin, by binding to this C3bBb complex, stabilises the C3 convertase and enhances by 10-fold the half-life of this convertase (Fearon and Austen, 1975). By stabilising the C3 convertase, properdin amplifies the C3 turn-over and therefore the generation of more C3b molecules and the deposition of more C3b onto the pathogen's surface.

Recent publications however suggested that the alternative C3 convertase could be formed following another succession of events, involving the binding of properdin directly to C3b or even directly to the surface of the pathogen (Hourcade, 2006; Spitzer et al., 2007). This new function of properdin is described in more detail in chapter 1.3.4.

The fact that the alternative pathway is initiated by a hydrolysed form of C3 means that this pathway can be activated as well by both the classical and the lectin pathway: the C3b molecules obtained after activation of these two complement pathways bind to the surface of a pathogen and, in presence of both factor B and factor D, generate alternative C3 convertases. The alternative pathway acts therefore as an amplifier of the two other complement pathway (Brouwer et al., 2006).

1.2.4 C3 convertase and C5 convertase

As mentioned earlier, both the C4b2a complex and the C3bBb complex act as a C3 convertase, which means that they both cleave the C3 component into two fragments: the C3a anaphylatoxin and the C3b opsonin.

The binding of C3b molecules to a C3 convertase then leads to the creation of a C5 convertase. This convertase is therefore the C4b2a3b complex for both the classical and the lectin pathway, and the C3bBb3b complex for the alternative pathway. Both types of C5 convertase share the same activity: they bind to the C5 component, hydrolyse it and release the C5a anaphylatoxin and the C5b fragment. This latter molecule next binds to the pathogen's surface and this constitutes the first step of the common lytic terminal complement pathway (figures 1-1D and 1-2).

1.2.5 Terminal pathway

This terminal pathway starts with the binding of the C5b fragment to the pathogenic surface and ends with the creation of the Membrane Attack Complex (MAC). After binding to the surface of the target cells, C5b is stabilised by C6 and this creates the C5b6 complex. It is then successively joined by C7 and C8. This newly-formed C5b678 complex initiates the creation of a small pore into the membrane of the target cell. Multiple C9 molecules then bind to this complex and polymerise. This allows the MAC to get fully inserted into the membrane and creates a pore inside the cell surface, preventing the cell to keep its osmotic stability, and therefore leads to the cell lysis (figure 1-1D) (Wurzner, 2003).

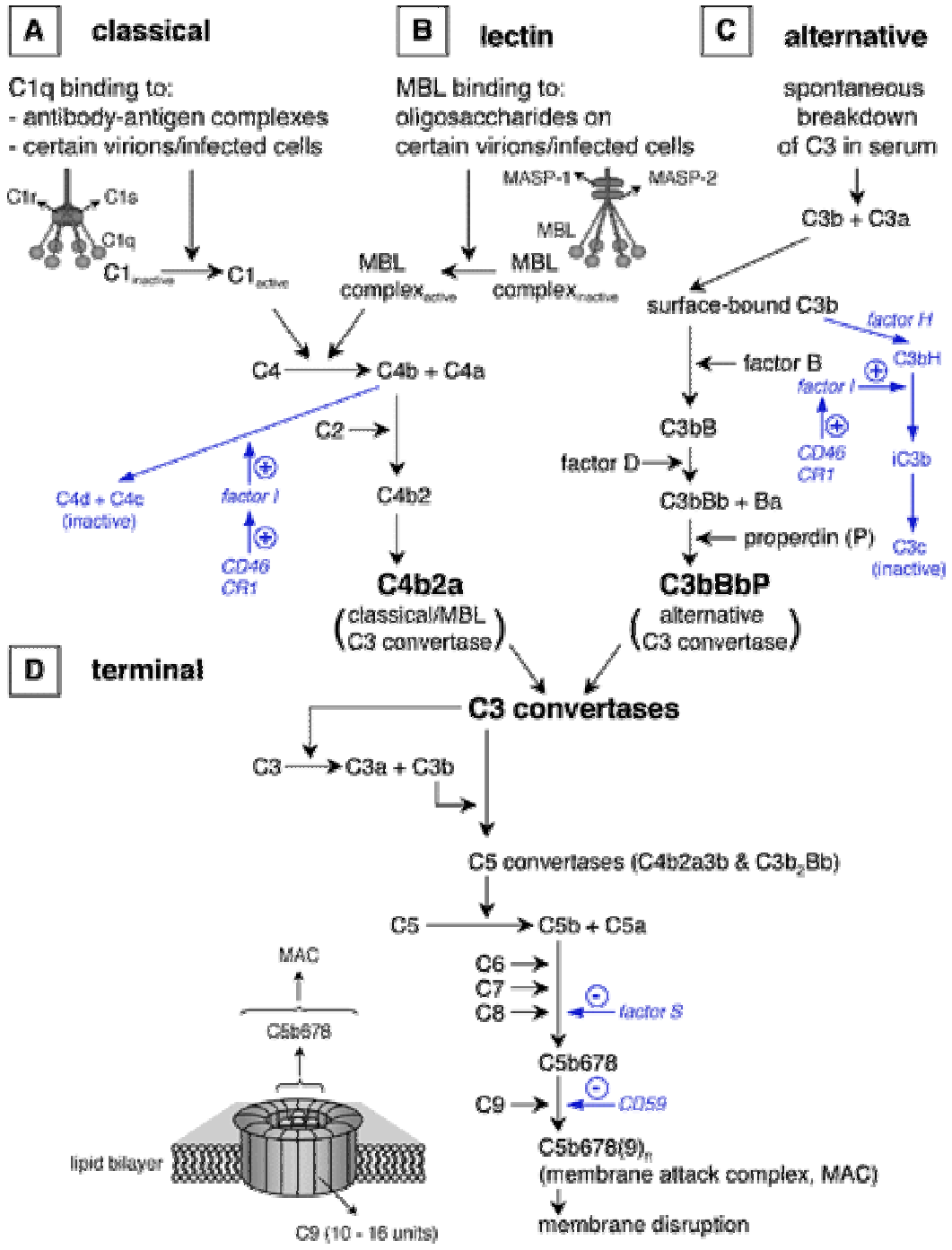

Figure 1-1: The complement pathways. A: the classical pathway; B: the lectin pathway; C: the alternative pathway and D: the common terminal pathway. Positions of regulatory molecules (factor H, factor I, factor S, CD46, CD59 and CR1) are indicated in blue (from Favoreel et al., 2003).

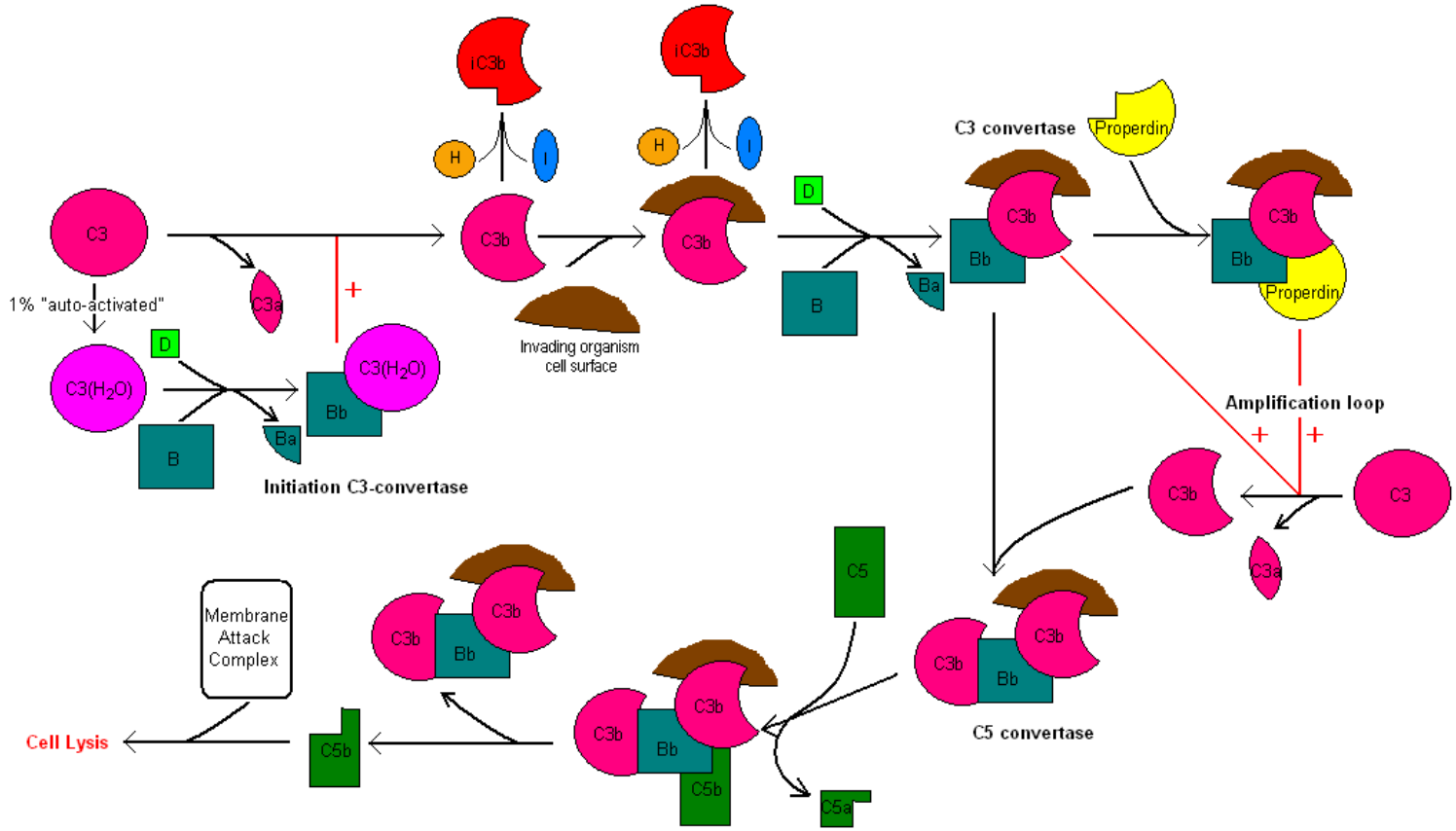

Figure 1-2: The standard model of the alternative complement pathway. This pathway is auto-activated and leads to the formation of anaphylatoxins (C3a, C5a), opsonins (C3b, iC3b) and of the membrane attack complex. This pathway is functional in absence of properdin, but in its presence, the C3 convertase is stabilised, which results in the creation of an amplification loop.

1.2.6 Regulation of the complement system

Several finely regulatory mechanisms control the complement pathway to allow it to keep its specificity to pathogenic cells.

The lability of some major complement components is one effective regulatory mechanism used to avoid impromptu activation of the complement system. For example, the half-life of the C3 convertase and the stability of the C5b fragment are considerably reduced if they are not quickly stabilised by properdin and C6, respectively (Fearon and Austen, 1975; Wurzner, 2003). In the same way, the very short half-life of C3b prevents it from diffusing far from its generating site and thus from binding to healthy non-pathologic cells.

Another strategy used by the complement system to protect its host pertains to soluble or membrane-bound factors (figure 1-1). The membrane-associated regulatory proteins are often found on the surface of host cells, but are absent on foreign surfaces, while the soluble factors are present at high concentration in the blood. These proteins act at different points of the complement cascade. It is the case of C1-Inh (C1 Inhibitor), a major inhibitor of the classical pathway as it can either dissociate C1q from the rest of the C1 molecule or prevent the autoactivation of the C1s and C1r sub-units (Duncan et al., 2008). C4bBP (C4b Binding Protein), CR1 (Complement Receptor 1) and MCP (Membrane Co-factor Protein or CD46) all bind to C4b. For the alternative pathway, the regulatory role is played by factor H, CR1 and MCP, which all bind to C3b. Factor I then cleaves inhibitor-bound C3b and C4b molecules respectively into iC3b and C3f, and into C4c and C4d, inactivating irreversibly C3b and C4b (Favoreel et al., 2003).

The complement system can as well be regulated after the formation of the C3 convertase. In fact, all the proteins mentioned in the previous paragraph, except for MCP, are able to dissociate the C3 convertase after its formation. This role is played too by DAF (Decay Accelerating Factor) (Harris et al., 2007).

The generation of the MAC is finely regulated as well by CD59 and by the S-protein (CD55), which, by binding to the C5b67 complex, prevents its insertion into the membrane (Favoreel et al., 2003).

1.2.7 Complement activities

Activation of the complement system results in a variety of biological actions, such as cell lysis, opsonophagocytosis and inflammatory responses. In addition to these acute responses, the complement system has been shown to play an important role during chronic conditions such as both ischemic and autoimmune diseases.

1.2.7.1 C3 component

C3 is the central component of the complement system. While native C3 in serum is an inert molecule, C3 is cleaved into 2 fragments: C3a and C3b, during complement activation. Due to the important role played by C3b in immunity, C3b is highly regulated and therefore can be inactivated by factor I into two cleavage products: C3f and iC3b. Further cleavage of iC3b leads to the formation of C3c and C3dg, this latter being itself cleaved into C3d and C3g (figure 1-3) (Law and Dodds, 1997). Many of these C3 activation/degradation products play a crucial role: C3a is an anaphylatoxin (see chapter 1.2.7.4), C3b and iC3b are opsonins (see chapter 1.2.7.3), while C3dg and C3d are ligands for CR2, a non-phagocytic receptor present on B lymphocytes. The association of C3dg and C3d to CR2 influences B cell activation and development and plays a role in antibody production, antibody class switching and memory functions (Lyubchenko et al., 2005).

1.2.7.2 Lytic action

As seen in the chapter 1.2.5, the generation of the membrane attack complex at the end of the communal terminal pathway results in the formation of pores on the surface of target cells and therefore leads to the death of these cells. This constitutes a major defence mechanism against certain bacterial and viral infections as its initiation can happen in absence of specific antibodies, via both the alternative and the lectin pathway. However, due to the thick cell wall that prevents the insertion of the complex into their membrane, Gram-positive bacteria are often resistant to MAC-mediated lysis. Few Gram-negative bacteria can as well evade this mechanism via their long polysaccharide side chains associated to their LPS: this prevents, here again, the insertion of the MAC into the membrane of the bacteria (Kindt et al., 2007).

1.2.7.3 Opsonisation

Complement activation leads to the formation of opsonin molecules. These molecules can bind both the antigen present at the surface of a pathogen and the opsonin receptor present at the surface of several phagocytic cell types. They thus act

as a bridge between pathogens and phagocytic cells and allow the elimination of a pathogen without requiring the presence of antibody. Because opsonisation happens on both Gram-positive and Gram-negative bacteria, opsonophagocytosis is one of the major mechanisms used in innate immunity against pathogens (Jarva et al., 2003; Rautemaa and Meri, 1999).

The three complement-derived opsonins are named C3b, iC3b and C4b. C3b and C4b result respectively from the cleavage of C3 and C4 during complement activation, while iC3b is a further cleavage product of C3b (see chapter 1.2.7.1 and figure 1-3). Three complement-derived opsonin receptors have been described as well: the complement receptors CR1, CR3 and CR4. CR1 possesses a binding site for both C3b and C4b, while iC3b is a ligand for both CR3 and CR4. These three complement receptors are present on the surface of many phagocytic cell types including macrophages, monocytes and neutrophils (Hostetter, 2000; Ren et al., 2004).

As the bacterial capsule can act as a barrier between the opsonin fixed on the bacterial surface and its receptor, some capsular bacteria are able to evade opsonophagocytosis (Kindt et al., 2007).

1.2.7.4 Production of anaphylatoxins

Others products of complement activation are the C3a and C5a anaphylatoxins, which are strong inducers of inflammation. They are ligands for specific G-protein-coupled receptor, namely C3aR and C5aR, present on inflammatory cells. Both C3a and C5a are strong chemoattractants for neutrophils and lymphocytes and their release during complement activation contributes to the clearance of pathogens by quickly attracting phagocytic cells (such as macrophages and monocytes) at the site of infection. They induce smooth muscles contraction, as well as mast cells and basophils recruitment and degranulation, resulting in the liberation of histamine and other mediators that increase vascular permeability (Kindt et al., 2007).

In addition to that, C3a possesses an anti-microbial activity as it can generate breaks in the plasma membrane of some bacteria, as described for anti-microbial peptides (Nordahl et al., 2004).

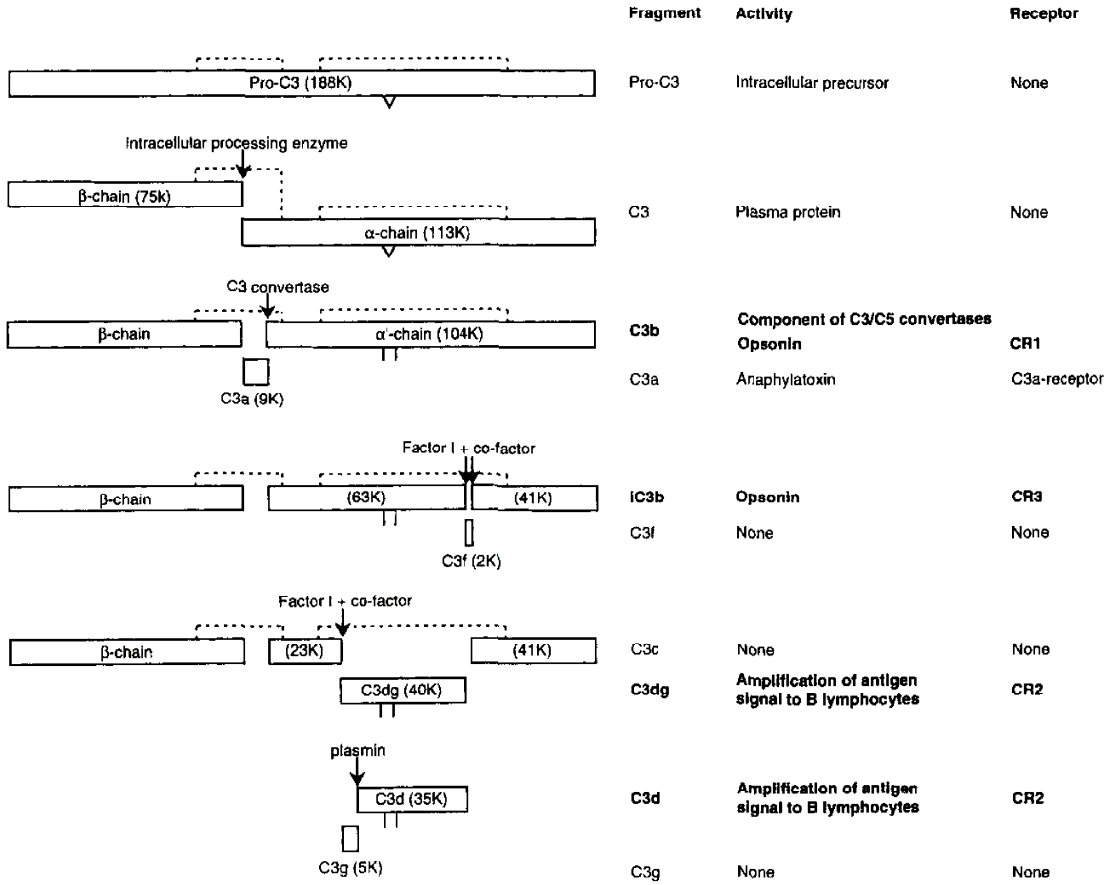

Figure 1-3: C3 activation and degradation products (from Law and Dodds, 1997).

1.3 Properdin

Properdin functions within the alternative pathway of complement activation. It is the only positive regulator of this pathway.

1.3.1 History of properdin

It is difficult to mention properdin without relaying its controversial discovery. In 1954, when failing to isolate the "C'3" component of the complement (which was at this time considered as a single molecule, but corresponds to the C3, C5, C6, C7, C8 and C9 components nowadays) by treating human serum with zymosan, a component of the yeast wall, Louis Pillemer discovered a new serum protein; Hans Hirschmann named this molecule "properdin" (Pillemer et al., 1954).

Believing properdin was of major importance, Pillemer, with the help of numerous collaborators, decided to characterise more precisely this molecule. Properdin was found to have bactericidal, virus-neutralising and haemolytic activities. Pillemer then introduced the concept of a "properdin system" consisting of different serum components – including properdin – which together were allegedly playing a protective role against pathogens without requiring the presence of immune complexes (Pillemer et al., 1954). The paper relating this discovery, published in 1954 in Science, generated a huge interest by the public and quickly properdin was seen as a "modern day, biologic philosopher's stone" (Lepow, 1980). However, quickly after the publication of this paper, some scientists, reluctant to the concept of the properdin system, came forward with another interpretation of Pillemer's results. In 1957, during this period of scientific scepticism surrounding the properdin system, Louis Pillemer died from an overdose of barbiturate; barbiturate was actually the buffer used in Pillemer's complement assay (Maves and Weiler, 1993). His death, seen as suicide even though it has never been proved, intensified even more the polemic around the properdin system. A year after Pillemer's death, Robert Nelson Jr. published in the Journal of Experimental Medicine the first paper rejecting the properdin system. In this paper, Nelson explained Pillemer's "observed phenomena by a mechanism involving natural antibodies and complement components instead of a single and discrete new substance, properdin" (Nelson, 1958). For a decade, this will be the view adopted by the scientific community as it was in accordance with the existing dogma

introduced by Ehrlich that defined complement activation as being immune complex-dependent (Figueroa and Densen, 1991).

However in 1968, Pillemer's former colleagues, using properdin highly purified by column chromatography, showed that properdin appeared as a single molecule using density gradient ultracentrifugation and electrophoresis. This highly purified properdin had the same properties as previously observed using partially purified properdin. Using immunoelectrophoresis, they confirmed as well that properdin was distinct from immunoglobulins (Pensky et al., 1968). More data published in the early 1970s suggested the existence of an alternative complement pathway as complement activation was observed independently of the presence of C1, C2 or C4 and as new complement factors were purified (Maves and Weiler, 1993). All this finally leaded to the acceptance by the scientific community of Pillemer's properdin and "properdin system", which was renamed the alternative complement pathway.

It is worth mentioning that factor B, one of the factors of the alternative complement pathway, has long been named properdin factor B to emphasise the fact it belonged to this newly found complement pathway. This leaded to confusions in terminology in some articles when mentioning properdin instead of factor B, some of them still being observed in recent publications (Taylor et al., 2004).

1.3.2 Gene

The human properdin gene, known as *CFP* (Complement Factor Properdin), represents around 6kb of the genome. It is located in the Xp11.3-Xp11.23 region of the short arm of the X chromosome (Coleman et al., 1991; Goundis et al., 1989). It was first partially sequenced by Reid and Gagnon in 1981 and its full sequence was obtained by Nolan and coworkers in 1991 from the PMA-stimulated U-937 cell line cDNA (Nolan et al., 1991; Reid and Gagnon, 1981). The human properdin gene is composed of 10 exons: the first exon is not translated, the second one includes the translation start site, the TSR-0 to TSR-5 regions are each represented by a unique exon (from exon 3 to exon 8), while the last TSR – TSR-6 – is encoded by both exon 9 and exon 10 (Nolan et al., 1992). The open reading frame (ORF) of human properdin is 1410bp long (from 243 to 1652 of the mRNA sequence with the Genbank accession number NM_002621) (from http://www.ncbi.nlm.nih.gov/projects/gorf/).

Mouse and guinea-pig properdin have been sequenced as well and showed respectively 72% and 75% homology with the human properdin at a nucleic acid level (Goundis and Reid, 1988; Maves et al., 1995). The ORF of mouse properdin is 1395bp long (from 71 to 1461 of the mRNA sequence with the Genbank accession number NM_008823) (from http://www.ncbi.nlm.nih.gov/projects/gorf/).

1.3.3 Protein

Properdin is a mixture of cyclic polymers formed by head-to-tail association of flexible, rod-like, asymmetric monomers (Smith et al., 1984). This glycoprotein circulates in serum in a dimer, trimer or tetramer form (ratio 26:54:20) (figure 1-4), the highest oligomerised form having the highest activity (Pangburn, 1989). No monomer of properdin has been detected in serum suggesting oligomerisation is an early intracellular event (Farries and Atkinson, 1989).

An unglycosylated monomer of properdin has an apparent mass of 53KDa on an SDS gel under reducing conditions (Smith et al., 1984). It is made of 469 amino acids and consists of 7 repetitive, but non-identical, motifs of approximately 60 amino acids each that are called “thrombospondin type I repeats” or “thrombospondin structural homology repeats” (TSRs) (Sun et al., 2004). These modules possess a well-conserved CWR (Cysteine Tryptophan Arginine)-layered motif and are independently folded (Smith et al., 1991). Similar motifs are found in the structure of other modular proteins such as the C6, C7, C8 and C9 components of the complement pathway, the circumsporozoite of *Plasmodium falciparum* and thrombospondin I and II (Goundis and Reid, 1988).

Properdin’s TSRs are called from TSR-0 (N-terminal) to TSR-6 (C-terminal) (figure 1-4). TSR-0 is a truncated TSR and TSR-6 has 25 amino acids more than the other TSRs. The role of each TSR was studied using mutant forms of recombinant properdin lacking certain TSRs and using individual recombinant TSRs. The putative roles of each TSR are summarised on figure 1-5 (Higgins et al., 1995; Perdikoulis et al., 2001; Sun et al., 2004). It has been shown that, on their own, none of the TSRs were able to bind sulphatides, neither C3b, even though native properdin was able to bind both sulphatides and C3b, showing that the association of all the TSRs was important for the protein function (Perdikoulis et al., 2001). TSR-0 and TSR-6, being the extremities of the monomer, are thought to play an important role in the

oligomerisation of the protein (Higgins et al., 1995). X-ray scattering analyses of properdin suggested that TSR-0, TSR-1, TSR-2 and TSR-3 act as spacers to ensure that TSR-4 and TSR-5 are accessible to other molecules (Sun et al., 2004). Both TSR-4 and TSR-5 have been shown to be involved in the stabilisation of the C3bBbP complex (Higgins et al., 1995; Perdikoulis et al., 2001).

Properdin protein sustains different post-translational modifications. The N-glycosylation is carried by the extra 25 amino acids of the TSR-6 motif. This glycosylation does not play any role during secretion, polymerisation or binding of properdin to C3bBb (Farries and Atkinson, 1989). Properdin possesses as well 4 O-fucosylations and is highly C-mannosylated (on 15 sites) (Gonzalez de Peredo et al., 2002; Hartmann and Hofsteenge, 2000).

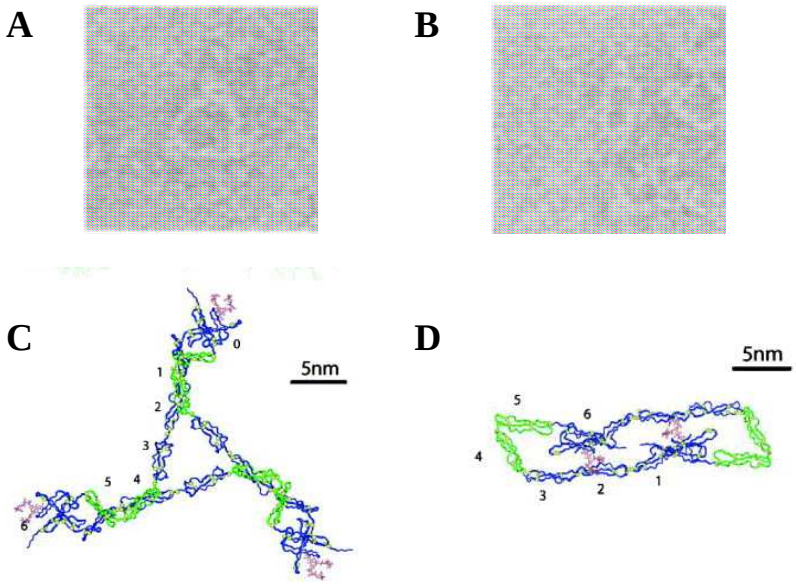

Figure 1-4: Representations of a dimer (B and D) and of a trimer (A and C) of properdin. A-B: Electron microscopy pictures (from Smith et al., 1984); C-D: Final best-fit representations (from Sun et al., 2004). The positions of the different TSRs are represented on the graphs by their numbers.

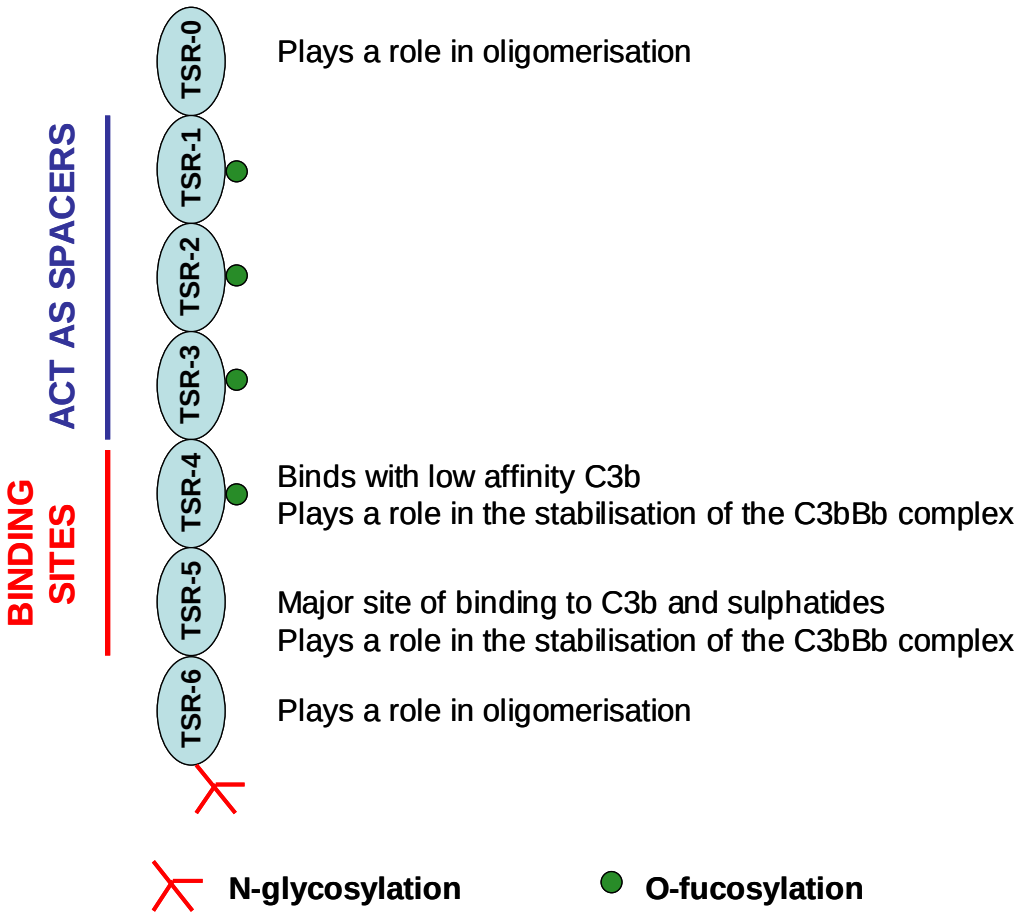

Figure 1-5: Schematic representation of a monomer of properdin and roles of its different TSRs. The functions of each TSRs are explained opposite their schematic representation.

1.3.4 Functions

Properdin is the only positive regulator of the complement alternative pathway. It plays its major role by preventing the dissociation of Bb from C3b and the inactivation of the C3 convertase by factor I and co-factors (Maves and Weiler, 1993). Therefore, by stabilising the labile C3 convertase (C3bBb) of the alternative pathway, properdin increases the half-life of this complex from 1-4 to 18-40 minutes (Fearon and Austen, 1975).

In order to amplify the complement reaction, properdin can bind to either C3b alone, or C3bBb complex, but has a greater affinity for the latter. Properdin's affinity for membrane bound C3b or C3bBb is as well known to be higher than its affinity for their soluble forms (Farries and Atkinson, 1989; Hourcade, 2006). However, a relatively recent publication by Hourcade demonstrated that properdin is able to bind to membrane bound C3b to form a C3b-properdin complex and that this complex can accelerate the association of factor B to C3b and promote the assembly of a pre-formed C3 convertase to another monomer of the properdin molecule. These results suggested that, in addition to its stabilising role, properdin could amplify the C3 convertase formation (Hourcade, 2006). The latest work of Hourcade's group showed that properdin could indeed directly bind to certain microbial targets and, recently, Kimura and collaborators showed properdin could bind to certain type of LPS and properdin affinity of LPS correlates with the restoration of alternative pathway activation in properdin-deficient mouse serum (Kimura et al., 2007; Spitzer et al., 2007). Spitzer and collaborators suggested that properdin can activate the alternative pathway in two manners: either non-specifically as described by the standard known model, or specifically by binding directly to the bacterial target or to apoptotic cells where it initiates the formation of the C3 convertase (figure 1-6) (Spitzer et al., 2007; Xu et al., 2008).

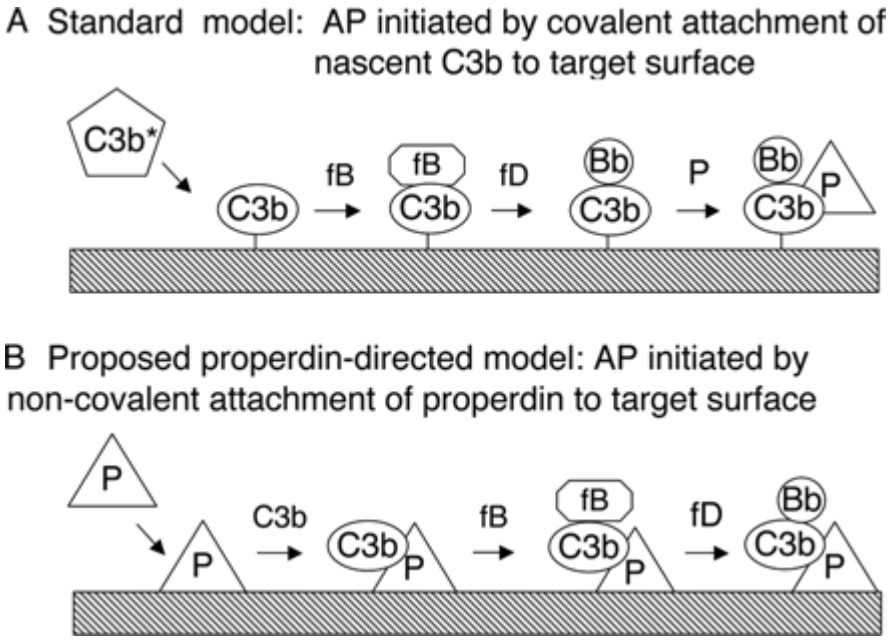

Figure 1-6: Role of properdin in the initiation of the alternative pathway of complement. A: the standard model where properdin binds to the pre-formed C3bBb complex; B: the new properdin-directed model where properdin binds first to the target surface before being joined by C3b and Bb (from Spitzer et al., 2007).

1.3.5 Properdin deficiency

Although it is the most frequent deficiency for a component of the alternative pathway, properdin deficiency remains a rather uncommon event linked to an increased susceptibility (250 times higher) to a severe (mortality rate of 34-63%) fulminant meningococcal disease, usually due to a rather uncommon serogroup (mainly Y and W-135) of *Neisseria meningitidis* (Fijen et al., 1999a; Fijen et al., 1999b; Spitzer et al., 2007). This meningococcal episode usually happens during adolescence (Fijen et al., 1999a). It is the only X-linked complement inheritance and it causes an impairment of the alternative pathway.

The association of properdin-deficiency with *N. meningitidis* infection may be explained by the fact that the alternative pathway plays a major role in anti-capsular antibody-dependent killing of *N. meningitidis in vitro* and that the presence of properdin seems to be crucial to obtain effective bactericidal activity against the serogroup W-135 of *N. meningitidis* (Sjoholm et al., 1991; Sjoholm et al., 2006; Soderstrom et al., 1991). In presence of a high concentration of anti-capsular antibodies, the lack of properdin in properdin-deficient individuals is masked by the antibody-dependent role played by the classical pathway, explaining why properdin-deficient patients do not develop recurrent infections (Fijen et al., 1999a). Thus, to protect properdin-deficient individuals towards *N. meningitidis* infection, a vaccination every 3 years with a tetravalent ACYW meningococcal capsular polysaccharide vaccine is advised (Fijen et al., 1998; Morgan and Orren, 1998). Detection of properdin-deficient families seems yet to be an issue as properdin deficiency is not tested routinely. However, a study carried out by Fijen and collaborators in the Netherlands showed that 33% of the persons who developed a meningococcal disease due to an uncommon serogroup of *N. meningitidis* were complement-deficient and 30% of these complement-deficient people were in fact properdin-deficient (Fijen et al., 1999a). Screening of all patients showing evidence of meningococcal disease due to uncommon serogroups of *N. meningitidis* and of their families should permit to detect and protect more properdin-deficient individuals by vaccination.

Properdin deficiency being a recessive X-linked trait, it affects mainly male individuals. An uneven Lyonisation occurs in female carriers of the inheritance, the mean level of properdin being half of the normal properdin level, with important

discrepancies between individuals according to the degree of inactivation of the mutated X chromosome (van den Bogaard et al., 2000). This pattern makes the detection of female carriers difficult.

The first properdin-deficient family to have been identified was a Swedish family in 1982 with 3 males affected (Sjoholm et al., 1982). Since then properdin-deficiency has been observed in more than 100 individuals belonging to more than 30 families (table 1-1) (Linton and Morgan, 1999). The fact that properdin deficiency has been reported in just a few countries suggested that it was a recent mutation. Although different point mutations affecting different exons of the properdin gene have been characterised, only three phenotypic forms of properdin deficiency – namely type I, type II and type III deficiency – have been identified so far (Truedsson et al., 1997).

The type I deficiency is the most common and the first one to have been identified (Sjoholm et al., 1982). It is characterised by a complete absence of the properdin antigen in serum despite a normal mRNA level. In this case, an early stop codon is created due to a point mutation in the properdin sequence, leading to the synthesis of a truncated properdin molecule, which will rapidly be degraded intracellularly (Sjoholm et al., 1982).

The type II deficiency is characterised by a low properdin antigen serum concentration (1 to 10% of the normal level) despite a normal mRNA level. The intracellular properdin concentration and the secretion of properdin by properdin-deficient monocytes are normal, suggesting the properdin protein is degraded extracellularly. A point mutation in the properdin sequence in fact results in a wrong oligomerisation of the properdin protein (nearly only dimers are visualised in this case), leading to an increased extracellular catabolism of the abnormal molecule (Nordin Fredrikson et al., 1998).

The type III deficiency is characterised by a normal serum concentration of properdin, but in a dysfunctional form. This deficiency has only been detected in one large Dutch family (Sjoholm et al., 1988a). In this case, the point mutation in the properdin sequence does not affect synthesis, secretion or oligomerisation of the protein, but by changing the conformation of the protein, it prevents its binding to C3b (Nordin Fredrikson et al., 1996).

All the published cases of properdin-deficiency are summarised in table 1-1. Over 26 years, 113 people have been diagnosed properdin-deficient. Properdin-deficiency has been inventoried in 12 different countries, mainly in European countries. The most common type of properdin-deficiency observed was the type I deficiency. Properdin-deficiency was detected either in patient suffering from bacterial infections or in the family of these patients. In patient suffering from bacterial infection, the average age for the onset of the infection was 17.9 year-old and the infection was in more than 90% of the cases due to *Neisseria meningitidis* (1 case of *S. pneumoniae* infection, 1 case of *H. influenza* type B infection and 1 case of chronic discoid lupus erythematosus), with 33% of serotype Y, 33% of serotype W-135, 13% of serotype B and 7% of serotype C. The patient developing an infection due to *S. pneumoniae* was deficient in both properdin and complement component 2.

Age of index patient	Year of report	Country (+origin)	Disease associated with the deficiency for the index patient	Type of deficiency	Number of cases of properdin deficiency in the family	Reference
15	1982	Sweden	*N. meningitidis* C	Type I	2	Sjoholm et al., 1982 ; Braconier et al., 1983
ND	1985	Switzerland	None	Type I	ND	Schifferli et al., 1985
30	1987	USA	*N. meningitidis* Y	Type I	2	Densen et al., 1987
9	1987	Canada	*S. pneumoniae*	Type I + C2 deficiency	0	Gelfand et al., 1987
11	1987	Denmark	*N. meningitidis* B	Type II	2	Nielsen and Koch, 1987
	1988	Sweden	None	Type II	2 in total	Sjoholm et al., 1988b
61	1988	The Netherlands	*N. meningitidis* C	Type III	9	Sjoholm et al., 1988a; Sjoholm, 1990
47	1989	UK (Scotland)	Chronic discoid lupus erythematosus	Type I	3	Holme et al., 1989
ND	1989	Denmark	ND	ND	5 from 4 families	Nielsen et al., 1989
18	1989	Sweden	*N. meningitidis* Y	Type I	2	Soderstrom et al., 1989
10	1990	Denmark	*N. meningitidis*	Type I	ND	Nielsen et al., 1990
14	1990	Israel (Tunisian origin)	*N. meningitidis* B	Type I or II	2	Schlesinger et al., 1990; Kolble et al., 1993; Schlesinger et al., 1993
16	1990	Israel (Tunisian origin)	*N. meningitidis* B	Type I	0	Schlesinger et al., 1990; Schlesinger et al., 1993
9	1993	UK (Scotland)	*N. meningitidis*	Type II	1	Kolble et al., 1993
1.5	1993	Israel (Tunisian origin)	*H. influenza* type B	Type I	4	Schlesinger et al., 1993

Age of index patient	Year of report	Country (+origin)	Disease associated to the deficiency for the index patient	Type of deficiency	Number of cases of properdin deficiency in the family	Reference
7	1995	The Netherlands	*N. meningitidis* Y	Type I + protein C deficiency	1	Derkx et al., 1995; Fijen et al., 1995
32	1995	UK	*N. meningitidis* B and then W-135	Type I	0	Cunliffe et al., 1995
12	1995	France	*N. meningitidis* Y	Type II	3	Fremeaux-Bacchi et al., 1995
ND	1997	South America	ND	Type I	?	Truedsson et al., 1997
ND	1998	Brazil	ND	ND	2 cases	Zelazko et al., 1998
14	1998	Israel (Tunisian origin)	*N. meningitidis* Y	Type I	5	Rottem et al., 1998
19	1998	Israel (Libyan origin)	*N. meningitidis* Y	Type I	0	Rottem et al., 1998
13	1999	Switzerland	*N. meningitidis* B	Type I	8	Spath et al., 1999
13 patients	1989 1996 1999	The Netherlands	9 *N. meningitidis* W-135 and 4 Y	11 Type I 2 Type II	11	Fijen et al., 1989; Fijen et al., 1996; Fijen et al., 1999a
5.5	2006	Turkey	***N.*** *meningitidis*	Type I	2	Genel et al., 2006
ND	2006	United States (Hispanic family)	ND	Type I	6	Mathew and Overturf, 2006
14	2006	Denmark	Uncommon *N. meningitidis*	Type I + MBL deficiency	5	Bathum et al., 2006

Table 1-1: Published cases of properdin deficiency. ND: information not disclosed in the original publication.

1.3.6 Source of properdin

Properdin is found at a concentration of 22 to 25µg/ml in human sera. Its concentration in sera of children under the age of 1 is lower (below 20µg/ml) (de Paula et al., 2003).

Properdin mRNA has been detected in spleen, liver, adipose tissue, sinonasal tissue and mammary gland (Avery et al., 1993; Choy and Spiegelman, 1996; Maves and Weiler, 1992; Nakamura et al., 2006; Vandermeer et al., 2004). Unlike most of the components of the complement system, the liver is not the major source of biosynthesis for properdin. As properdin expression is important in the spleen, it was suggested as being the main source of properdin synthesis. However, this hypothesis was rejected as splenectomy does not affect the serum concentration of properdin in human (Truedsson et al., 1990). The actual physiological source of properdin still remains unclear.

At a cellular level, properdin synthesis and/or secretion was observed in many cell types. All information to date, including results from this work, is collated in table 1-2. Thus properdin has been shown to be expressed by macrophages, monocytes, T cells, astrocytes, hepatoma cells, stromal vascular fibroblasts, neutrophils, shear stressed endothelial cells, bronchial epithelial cells and dendritic cells.

Cell type	Description	Technique used	Reference
Astrocytes	Detection of properdin mRNA in human astrocytes.	RT-PCR, Southern blot	Avery et al., 1993
Bronchial epithelial cells	Expression of properdin by BEAS-2B cells.	Real-time RT-PCR	Vandermeer et al., 2004
Dendritic cells	Expression of properdin by mature and immature human dendritic cells.	RT-PCR	Reis et al., 2006
Endothelial cells	Synthesis and secretion of properdin by shear-stressed HUVEC and HCMEC cells.	RT-PCR, Northern blot, Immunoprecipitation, Western blot	Bongrazio et al., 2003
Granulocytes	Detection of properdin mRNA in human peripheral blood granulocytes (without detection of *de novo* synthesis). Secretion of the properdin stored in the secondary granules of neutrophils stimulated with TNFα, C5a, IL-8 and fMLP.	In situ hybridisation, Northern blot, Western blot, ELISA, flow cytometry	Wirthmueller et al., 1997
Hepatocytes	Synthesis and secretion of an active form of properdin by the hepatoma cell line Hep-G2 (not regulated by IL-6).	RT-PCR, Southern blot, dot blot	Maves and Weiler, 1994
Lymphocytes	Expression of properdin in peripheral blood T-cells. Synthesis and secretion of properdin by H9, HuT78, Jurkat and T-ALL cells.	Northern blot, RT-PCR, ELISA, in situ hybridisation	Schwaeble et al., 1993
Macrophages	Synthesis and secretion of properdin by guinea-pig peritoneal macrophages. Expression of properdin by LPS-stimulated and immature macrophages.	Immunoelectrophoresis, RT-PCR	Bentley et al., 1978 ; Reis et al., 2006
Mast cells	Synthesis and secretion of properdin by HMC-1 cells. Properdin excretion via membrane vesicles.	RT-PCR, real-time RT-PCR, Western blot, immunofluorescence, ELISA, flow cytometry	This work

Cell type	Description	Technique used	Reference
Monocytes	Synthesis and secretion of an active form of properdin by human peripheral blood monocytes.	Functional assay, immunohistochemistry.	Whaley, 1980
	Synthesis and secretion of properdin by U-937 cells. Induction of the secretion by stimulation of the cells with PMA or IFNγ.	Slot blot, ELISA, immunoprecipitation.	Minta, 1988
	Synthesis of properdin by HL-60 cells after differentiation with DMSO.	Immunoprecipitation, Western blot.	Farries and Atkinson, 1989
	Detection of properdin mRNA in human peripheral blood monocytes.	RT-PCR, Southern blot.	Maves and Weiler, 1992
	Expression and secretion of properdin by peripheral blood monocytes, HL-60, U-937 and Mono Mac 6 cells. Secretion by Mono Mac 6 cells is regulated by certain cytokines.	Northern blot, ELISA.	Schwaeble et al., 1994
Platelets	Detection of properdin on unstimulated and ADP-, TRAP- and CRP-activated platelets.	Flow cytometry	This work
Stromal vascular fibroblasts	Detection of properdin mRNA in mouse stromal vascular fibroblasts isolated from fat tissue.	Northern blot, Western blot.	Choy and Spiegelman, 1996

Table 1-2: Cells expressing properdin.

1.3.7 Aims of the study

The aim of this study was to investigate the roles of properdin in immunity. In order to do so, the level of expression of properdin was assessed in different mouse organs before focusing of its expression pattern by one lymphoid organ, the spleen (chapter 2). Next, the expression of properdin by two auxiliary cells, namely platelets and mast cells, was examined (chapters 2.2.2.3 and 3, respectively). The synthesis and secretion of properdin by mast cells was then further characterised (chapter 3). Finally, the role played by properdin during bacterial infection was investigated using a mouse model of pneumococcal pneumonia and the properdin-deficient mouse line (chapter 4).

2 Properdin expression in mouse organs

2.1 Introduction

As mentioned earlier, only few studies have investigated properdin expression in murine or human tissues. The first study relating properdin expression in tissue was published by Maves and Weiler in 1992. Using RT-PCR, they found that properdin was expressed in human spleen (Maves and Weiler, 1992). Using a similar approach, Avery and collaborators reported in 1993 that properdin was expressed in human liver too (Avery et al., 1993). Three years later, properdin was shown to be expressed as well in adipose tissue (of mouse origin). This was found at both a RNA and protein level. This study was the first to compare the level of properdin expression between tissues: properdin was found to be expressed at a low similar level in liver and fat tissue and at a higher level in spleen. Moreover, Choy and Spiegelman demonstrated that the source of properdin in adipose tissue was not adipocytes, but stromal vascular cells (Choy and Spiegelman, 1996). More recently, properdin expression has been reported in the sinonasal tissue (at a lower level than in the liver) and in the mammary gland (Vandermeer et al., 2004; Nakamura et al., 2006).

The fact that properdin was found to be expressed by these various tissues suggests that properdin exerts a tissue-specific function. In fact, while properdin could play its complement regulatory function in many of these tissues (like the spleen, sinonasal tissue or mammary gland), the role of properdin in other tissue such as the adipose tissue may be different from its humoral function. In order to understand better the role played by properdin in tissue, it is important to establish a repertoire of tissues expressing properdin and to compare the level of properdin expression between each of these tissues.

The aim of the first chapter of this thesis was therefore to assess the level of properdin expression by mouse organs.

2.2 Material and methods

2.2.1 Tissue sample

Properdin-deficient (see chapter 4.1.2) or wild type mice (C57Bl/6 on Charles Rivers "gold line" background) were culled by cervical dislocation by an experienced animal technician (schedule 1 of the Animal welfare Act). Brain, heart, kidney, liver, lymph node, ear lobe, spleen and thymus were dissected and placed immediately into the appropriate medium until further use.

2.2.2 RNA extraction

Total RNA was extracted from mouse tissue using TRIzol reagent (Invitrogen, Paisley, UK) following the manufacturer's instructions. Tissue samples were placed into a tube containing an appropriate amount of TRIzol (1ml of Trizol per 50mg of sample) and homogenised using a glass Teflon homogeniser (Wheaton; Fisher Scientific, Loughborough, UK), and then centrifuged at 12,000g for 10 minutes. The clear supernatant was then left to stand at room temperature for 5 minutes. One fifth of the sample volume of chloroform (Fisher Scientific, Loughborough, UK) was added and high speed centrifugation of the sample then allowed a good separation of the pink organic phase (bottom) from the aqueous phase (top) containing the RNA. The aqueous phase was transferred and resuspended with isopropanol (Fisher Scientific) to precipitate the RNA and washed with 75% ethanol (Fisher Scientific). After drying, the pellet was resuspended in DEPC-treated water. To ensure no genomic DNA contamination, all RNA samples were then DNase I-treated: RNA was appropriately diluted using DEPC-treated water and the 10x buffer (100mM Tris-HCl (pH 7.5), 25mM $MgCl_2$, 5mM $CaCl_2$) to obtain a final RNA concentration of 150µg/ml in each sample. DNase I (10 units/ml; ABgene, Epsom, UK) was added to the RNA and samples were incubated at 37°C for 30 minutes. Another RNA extraction was then performed to remove any trace of protein present in the sample. For this RNA purification, only 500µl of TRIzol and half of the other reagents previously used for the RNA extraction were used.

2.2.3 Estimation of the RNA concentration

Xµl of each RNA sample were diluted into (1000-X)µlof DEPC-treated water and transferred into a quartz cuvette. The optical density (OD) of each sample was

then measured at 260nm using the 50 BIO UV-visible spectrophotometer (Varian). The RNA concentration was determined using the following formula:

$$\text{RNA concentration } (\mu g/\mu l) = \frac{\text{OD (260nm) x 40}}{X}$$

with X being the volume of the RNA sample used (in µl).

2.2.4 Reverse Transcriptase Polymerase Chain Reaction (RT-PCR)

2.2.4.1 cDNA synthesis

First strand cDNA was synthesised from total RNA using the SuperScript first strand synthesis system for RT-PCR (Invitrogen) following manufacturer's instructions. 5µg of total RNA were denatured for 5 minutes at 65°C. A mastermix containing dNTPs, oligo(dT) primers, 10X buffer, $MgCl_2$, DTT and recombinant RNase Inhibitor RNaseOUT was added to the denatured RNA and brought to 42°C to permit annealing, prior to add the SuperScript II Reverse Transcriptase and then left to incubate at 42°C for 50 more minutes. At the end of the cDNA synthesis, the mixture was incubated at 70°C for 15 minutes to inactivate the enzyme. The RNA template was finally removed by incubating the newly synthesised cDNA with RNase H at 37°C for 20 minutes. cDNA was then kept in the freezer at -20°C until further use.

2.2.4.2 Polymerase Chain Reaction (PCR)

2.2.4.2.1 Primers used in this study

The software used to design the primers used in this study was GeneTool Lite version 1.0. (Biotools). This software calculates the estimated melting temperature (Tm) of each primer and gives information about the risk of having primer dimers and hairpin formation. Thus, for each primer I designed, my attention was focused on the fact that Tms were similar for the two primers of a pair and that no primer dimers or secondary structure formation was predicted.

All the primers used in this thesis were synthesised, purified and lyophilised by MWG Biotech (Ebersberg, Germany), unless otherwise specified in the text. Primers were then reconstituted in dH_2O at a final concentration of 1fM and stored in the freezer at -20°C. Small aliquots of working stock were then regularly obtained by diluting the primer stock solution 1:5 in PCR-grade dH_2O.

2.2.4.2.2 PCR specific for the open reading frame of the mouse properdin gene

The reaction was performed by mixing the following reagents in a 0.5ml PCR reaction tube: 0.2mM of each dNTPs (PCR Nucleotide Mix; Promega, Southampton, UK), 2mM of $MgCl_2$ (ABgene), the 10x reaction buffer IV (ABgene) appropriately diluted in DEPC-treated H_2O, 4µM of each primer (forward and reverse MouPN primers (see table 2-1)), 40µl/ml of template cDNA (obtained in chapter 2.1.4.1) and 40U/ml of Thermoprime plus DNA polymerase (ABgene). The final volume of each PCR reaction was of 25µl.

The tube was then pulsed-centrifuged and placed into a thermocycler (Gene Amp PCR System 9700, PE Applied Biosystems). The following program was finally applied to the machine:

Step	**Temperature (°C)**	**Time (sec)**	**Number of cycles**	**Function**
1	95	180	1	Initial denaturation
2	95 63 72	60 60 150	40	Denaturation Annealing Extension
3	72 4	300 ∞	1	Final extension

The PCR products were analysed by agarose gel electrophoresis (see chapter 2.1.4.3).

Primers		Sequence	Product size	Reference
HumPN	Forward Reverse	ATG ATC ACA GAG GGA GCG CAG GC GGT TTG GAA GGT CAG GGG GCT CA	1451 bp	This study chapter 3
HumPNsh1	Forward Reverse	AGC ACC GCA CAC TCA CTT CA AGC CCA CCA CTA CGT TTC TG	451 bp	This study chapter 3
HumPNsh2	Forward Reverse	AAG TTG CTG CAC GCT CCT ATG CCG GAG GAT TCT TCA TAC TGG	220 bp	This study chapter 3
HumPNsh3	Forward Reverse	AGC ACC GCA CAC TCA CTT CA CCG GAG GAT TCT TCA TAC TGG	360 bp	This study chapter 3
HumPNsh4	Forward Reverse	AAG TTG CTG CAC GCT CCT ATG AGC CCA CCA CTA CGT TTC TG	314 bp	This study chapters 2 & 3
HumGAPDH	Forward Reverse	CAC CAG GGC TGC TTT TAA CTC TGG TA CCT TGA CGG TGC CAT GGA TTT GC	148 bp	Guo et al., 2002 chapter 3
MouGAPDH	Forward Reverse	ATC ACT GCC ACC CAG AAG AC CAC ATT GGG GGT AGG AAC AC	180 bp	Zhang and Insel, 2004 chapter 2
MouPN	Forward Reverse	ATG CCT GCT GAA ATG CAA GCC CC GGG GGT CAG AAT GGA AGC AAG GG	1422 bp	This study chapter 2
SP6		CAT TTA GGT GAC ACT A		PNACL chapter 2 & 3
T7		AAT ACG ACT CAC TAT AGG G		PNACL chapter 2 & 3

Table 2-1: Primers used in this study (Hum: human; Mou: mouse; PN: properdin; sh: short fragment; SP6: SP6 RNA polymerase promoter site; T7: T7 RNA polymerase promoter site).

2.2.4.3 Agarose gel electrophoresis

A 0.8% agarose gel was made by dissolving 0.4g of agarose into 50ml of 1x TAE (Tris-Acetate-EDTA) buffer (40mM Tris, 20mM glacial acetic acid, 1mM EDTA, pH 8.0) and heating it up for 1.5 minutes at moderate power in a microwave oven. The solution was then left to cool for 5 to 10 minutes before to add 1.3µM of ethidium bromide (Sigma-Aldrich, Gillingham, UK). The mixture was immediately poured into a casting apparatus and a comb was inserted to form the wells. The gel was left to set for 20 more minutes at room temperature. When the gel was set, it was transferred to the running tank and immersed with 1x TAE.

At this moment, DNA samples were mixed with a 6x bromophenol blue loading dye (30% (v/v) glycerol, 70% (v/v) TAE, 0.3% (w/v) bromophenol blue). Samples and the 1kb DNA Ladder (Promega) were next loaded into the agarose gel wells and electrophoresis was performed at a constant voltage of 90V. The electrophoresis was stopped when the line representing the dye had migrated through 3/4 of the gel. DNA on the gel was then visualised using a UV transluminator (UVP) and pictured using a DC120 digital camera (Kodak).

2.2.5 Cloning

2.2.5.1 Gel extraction

DNA extraction from agarose gel was done using Sephaglas BandPrep kit (Amersham Biosciences, Chalfont St Giles, UK) following manufacturer's instructions. Briefly, the band of interest was cut from the agarose gel using a clean scalpel and put into a pre-weighted reaction tube. An appropriate volume of solubiliser was added to this tube and it was heated up at 60°C for few minutes to allow a complete solubilisation of the agarose gel. Sephaglas BP beads were then added to the solubilised mixture and left to stand for few more minutes to allow the DNA to bind to the beads. The beads were then washed 3 times with a wash solution, allowed to dry and finally the purified DNA was eluted from the beads and stored at -20°C until further use.

2.2.5.2 Estimation of the DNA concentration

The concentration of each DNA sample extracted from the gel was estimated by mixing 4µl of each sample with 2µl of loading dye. These and 5µl of the molecular weight marker SmartLadder (Eurogentec, Aylesbury, UK) were run into an

agarose gel. As well as giving the size of the band, this ladder gave the concentration of the DNA contained in each step of the ladder, making it easy, by comparison, to estimate the DNA concentration of each sample.

2.2.5.3 Preparation of the competent cells

Top10F' competent cells (Invitrogen) were streaked out onto a plate of LB agar complemented with 1:100 tetracyclin (stock solution 30µg/ml, diluted in 70% ethanol). The plate was incubated overnight at 37°C. One single colony was picked from the plate and grown overnight in 5ml of TYM broth (2% bacto-tryptone, 0.5% bacto-yeast extract, 0.1M NaCl) complemented with tetracyclin in a shaking incubator at 30°C. 2.5ml of this culture were then used to inoculate 250ml of fresh TYM broth and was incubated approximately 3 hours at 37°C under agitation (until an OD of 0.5-0.6 at 550nm was obtained). Cells were then spun down at 900g for 30 minutes at 4°C and the pellet was resuspended into 85ml of tbf I solution (30mM KOAc, 50mM $MnCl_2$, 100mM KCl, 10mM $CaCl_2$, 15% glycerol (v/v)) and left to stand on ice for 30 minutes. Next, cells were spun down at 900g for 8 minutes at 4°C and the pellet was resuspended gently in 10ml of tbf II solution (10mM Na-MOPS, 75mM $CaCl_2$, 10mM KCl, 15% glycerol (v/v)). Competent cells were finally aliquoted by 50, 100 or 200µl and stored in the freezer at -80°C until further use.

2.2.5.4 Ligation

Ligation was performed using the PGEM-T easy vector system I (Promega). The amount of insert to add to the ligation reaction was calculated using the following formula:

$$\frac{\text{insert size (bp)}}{\text{vector size (bp)}} = \frac{\text{insert (ng)}}{\text{vector (ng)}},$$

which, in a molar ratio, means that: $\text{insert (ng)} = \frac{(\text{insert size (bp)} \times 25)}{3018}$.

The actual amount of insert used in a ligation reaction was 3 to 4 times the molar ratio. For the mouse properdin ORF, the insert had a size of 1422bp, therefore 40ng of this insert was used for the reaction. Thus, the ligation reaction mixture (final volume of 10µl) contained 25ng of the PGEM-T easy vector, 3U of the T4 DNA ligase, 40ng of the mouse properdin ORF insert and the 2x rapid ligation buffer appropriately diluted in dH_2O. To complete the ligation, the mixture was allowed to stand at room temperature for 1 hour.

2.2.5.5 Transformation

In preparation of this experiment, an empty universal tube was pre-cooled on ice and a universal tube containing LB broth was pre-warmed at 37°C.

An aliquot of Top10F' competent cells (50µl) was thawed on ice and transferred into the pre-cooled universal tube, where 10µl of the ligation product were added and the cells were incubated for 15 minutes on ice, followed by a 5 minutes incubation period at 37°C. 950µl of the pre-warmed LB broth were added to the cell preparation and incubated for 45 minutes at 37°C under agitation. 100µl and 200µl of this bacterial culture were then plated onto LB agar plates complemented with ampicillin (100µg/ml) and the selection markers X-Gal (Promega) and IPTG (Promega) (at a concentration of 80µg/ml and 0.5mM respectively). Plasmid-free top10F' cells being ampicillin sensitive, ampicillin prevented the growth of any contaminant on the plate. Concerning X-Gal and IPTG, they were used to discriminate the bacteria carrying an empty plasmid (blue colonies) from the bacteria carrying a plasmid containing an insert (white colonies).

2.2.5.6 Plasmid extraction

White colonies were picked up from the plate after transformation and grown overnight at 37°C in LB supplemented with ampicillin (100µg/ml). 1.5ml of each culture were transferred to a reaction tube and spun down at 12,000g for 1 minute. The bacterial pellet was first completely resuspended into 100µl of the ice-cold P1 buffer (50mM TrisHCl, 10mM EDTA, 50mM Glucose, 100µg/ml RNaseA, pH 8.0) before that 200µl of the P2 solution (0.2M NaOH, 1% SDS) were added and the mixture was left for 5 minutes on ice to permit bacterial lysis. 150µl of the ice-cold P3 buffer (60ml of 5M potassium acetate, 28ml of acetic acid, 12ml of H_20, pH 4.8) were then added to the mixture and it was left to stand on ice for 5 minutes to precipitate bacterial proteins, genomic DNA, carbohydrates and SDS. All this unwanted material was pelleted by centrifugation at 12,000g for 5 minutes and the supernatant was transferred to a new tube, where it was mixed with 2 volumes of 100% ethanol. The plasmid was finally pelleted by spinning it down for 15 minutes at 12,000g, washed with 70% ethanol, air-dried and resuspended in 50µl of TE buffer (10mM Tris-HCl pH 7.5, 1mM EDTA pH 8.0).

2.2.5.7 Restriction digest

Digests were performed following manufacturer's instructions. All restriction enzymes used in this thesis required the same conditions. Digest mastermix (final volume of 20µl) therefore contained 2µl of the plasmid (extracted as previously described in chapter 2.1.5.6), the appropriate 10x buffer (Promega) correctly diluted in dH_2O, 10 to 12U of the appropriate restriction enzyme (Promega) and 0.1mg/ml of acetylated BSA (Promega). The reaction was let to stand at optimal temperature for 1 hour before to be loaded onto an agarose gel (see chapter 2.1.4.3).

2.2.5.8 Sequencing

After extraction of the plasmid, the DNA concentration was measured as explained in chapter 2.1.5.2 and few microlitres of this plasmid preparation were appropriately diluted to obtain a final concentration of 50ng plasmid/µl TE buffer. Eight microlitres of this preparation were sent to PNACL (Protein and Nucleic Acid Chemistry Laboratory, University of Leicester) for sequencing. The PGEM-T easy vector having its insert region flanked by the T7 promoter region on one side and the SP6 promoter region on the other side, primers specific for T7 and for SP6 were therefore used to sequence our insert. The analysis was done using the 3730 automated sequencer (Applied Biosystem). T7 and SP6 primers were designed and synthesised by PNACL (table 2-1).

2.2.6 Northern blot

2.2.6.1 Agarose gel electrophoresis

Northern blot agarose gel was prepared in two steps: first, agarose (2% (v/w)) was dissolved in DEPC-treated water by heating up the solution at a moderate power in a microwave oven and poured into an RNase-free casting apparatus to obtain a 2mm-thick gel. This gel had just a supporting role by allowing a better handling of the Northern blot gel. While this supporting gel was setting, the Northern blot gel was prepared by dissolving agarose (1% (w/v)) in DEPC-treated water by heating up the solution at a moderate power in a microwave oven. The solution was left to cool down for 5 to 10 minutes before adding 1/3 volume of 5x MOPS (50mM sodium acetate, 0.22M MOPS (3-(N-Morpholino)-propanesulfonic acid), 5mM acetic acid, pH7.0), 1/3 volume of 37% formaldehyde solution (Sigma-Aldrich) and 1.3µM of ethidium bromide (Sigma-Aldrich). This solution was then immediately poured on top of the first gel in the fume hood. A comb was inserted in to form the wells and it

was left to set for 40 minutes at room temperature. When set, the gel was finally transferred into a running tank and immersed with 1x MOPS containing 0.25µM of ethidium bromide.

Fifteen micrograms of total RNA or 3µl of the 0.24-9.49kb RNA molecular weight ladder (Invitrogen) were then mixed into 20µl of RNA sample buffer (1x MOPS, 6.5% formaldehyde, 40% formamide) before being denatured for 15 minutes at 56°C. After chilling on ice for few minutes, samples were mixed with 2µl of RNA loading dye (10mM EDTA, 0.1% (w/v) bromophenol blue, 0.1% (w/v) xylene cyanol, 98% formamide) and loaded into the wells of the gel.

Electrophoresis was finally performed at a constant voltage of 35V overnight. RNA on the gel was then visualised using a UV transilluminator (Dual intensity, UVP)) to check the quality of the RNA and pictured using a Polaroid camera.

2.2.6.2 Northern blotting

Northern blotting was performed by standard capillary transfer as follows. An RNase-free glass tray was filled with 20x SSC (3M NaCl, 0.3M Tri-Sodium Citrate, pH 7.0). A glass plate covered with several sheets of 1mm Whatman paper was placed on top of the tray and each extremity of the Whatman paper was dipped into the 20x SSC solution (3M Sodium chloride, 0.3M sodium citrate, pH 7.0) to allow a constant hydration of the paper. The Northern blot gel (without its supporting gel) was placed on top of the Whatman papers and was covered itself by a nylon membrane (Hybond-N, Amersham Biosciences). The surface of the membrane was then wetted with 20x SSC and covered by 5 sheets of Whatman paper, 4cm of paper towels and some weights were placed on top to allow the RNA to transfer by capillarity from the gel to the membrane.

The next day, the nylon membrane was inserted between two sheets of Whatman paper and placed into an oven at 80°C for 2 hours to allow the RNA to fix to the membrane.

2.2.6.3 Molecular weight ladder staining

The part of the membrane containing the molecular weight ladder was cut off and stained in the RNA ladder stain solution (0.02% (w/v) methylene blue, 0.3M sodium acetate, pH 5.3) for 5 minutes, before being rinsed three times in dH_2O. This strip was then dried at room temperature and was used to estimate the size of the

products obtained after exposure of the hybridised nylon membrane with an X-ray film.

2.2.6.4 Labelling of the probes

This work was done after registering as an isotype user and following an appropriate training to work with radioactivity. The mouse DNA coding for the mouse properdin ORF previously synthesised (see chapter 2.2.1.1) was radioactively labelled using the random primed DNA labelling kit (Roche, Lewes, UK) following manufacturer's instructions. Briefly, 100ng of this cDNA was denatured at 95°C for 10 minutes and then mixed with hexanucleotide primers, dTTP, dATP, dGTP, ^{32}P dCTP and Klenow enzyme and incubated for 1 hour at 37°C to induce the synthesis of the complementary strand. A Biogel P4 Polyacrylamide gel column (Bio-Rad, Hemel Hempstead, UK) was then equilibrated with equilibrating buffer (0.1x SSC, 0.1% SDS) and the probe was purified by gel-filtration through this column to eliminate unincorporated ^{32}P dCTP.

2.2.6.5 Hybridisation

The nylon membrane was pre-hybridised for 1 hour at 56°C in 10ml of QuikHyb hybridization solution (Stratagene, Cambridge, UK). The radioactive probe was then heated up at 95°C for 10 minutes before being diluted into 10ml of hybridisation solution. The nylon membrane was incubated in this solution overnight at 56°C. The next day, the membrane was washed twice for 5 minutes in solution 1 (2x SSC) at room temperature and twice for 10 minutes in solution 2 (2x SSC, 0.1% (w/v) SDS) at 68°C. After the second wash, the radioactive background level of the membrane was checked using a Geiger counter. The membrane was then washed twice for 20 minutes in solution 3 (0.5x SSC, 0.1% SDS) at 68°C, allowed to dry at room temperature for 10 minutes before being wrapped in Safran film and finally exposed in a cassette to an X-ray film at -80°C for 3 to 5 days. The film was finally developed manually by soaking the X-ray film into successively a developing solution (Agfa-Gevaert, Brentford, UK) until the appearance of dark bands and a rapid fixer solution (Agfa-Gevaert), and by rinsing it abundantly under tap water.

All the radioactive work was performed in a designated area and protective shields were used. The work place was monitored frequently with a Geiger counter and all the material used during these experiments was discarded as instructed.

2.2.7 Immunohistochemistry

2.2.7.1 Embedding

After explantation, properdin-deficient and wild type mouse spleens were snap-frozen in liquid nitrogen and stored at -80°C until further use. They were then embedded in Tissue-Tek OCT compound (Sakura; Bayer Diagnostics, Newbury, UK) and cut into 7µm-thick sections using a cryostat (OTF 5000, Bright). Sections were picked up on a microscope slide (Histobond, Raymond A Lamb, Eastbourne, UK) and slides were stored in a slide box at -80°C until further use.

2.2.7.2 Immunostaining

Seven micrometres-thick cryostat sections were air-dried for 30 minutes at room temperature before being fixed in methanol for 10 minutes. Sections were then rinsed under running water and in TBS (0.15M NaCl, 2mM KCl, 20mM Tris Base, pH 7.5) for 10 minutes, treated with 0.3% H_2O_2-TBS for 10 minutes and rinsed again under running water and in TBS for 10 minutes each. After being blocked for 2 hours in 5% BSA-TBS and in Seroblock (Serotec, Kidlington, UK) diluted 1:100 in 1% BSA-TBS for 15 minutes in a humidification chamber, the slides were incubated at room temperature with the appropriate antibody diluted in 1% BSA-TBS (see table 2-2). After three washings in TBS, sections were mounted using the Vectashield hard set mounting medium with DAPI (Vector Laboratories, Peterborough, UK) and covered with a coverslip. Slides were then observed under an inverted TE300 fluorescence microscope (Nikon). FITC signals were visualised using the Chroma S484/15x excitation filter, TRITC signals using the Chroma S555/25x excitation filter and DAPI signals using the Chroma S395/10x excitation filter. Pictures were finally taken with a digital camera and analysed using the Openlab 4.03 software (Improvision).

2.2.7.3 Pre-absorption of the properdin antibody

To prove the specificity of the polyclonal antibody to mouse properdin, 10µg of the FITC-conjugated goat anti-human properdin antibody (Nordic Immunology; Tebu-Bio, Peterborough, UK) was pre-incubated with either 50µl of TBS, or 50µl of TBS containing 25µg of ultra-pure properdin antigen (Cortex Biochem; Europa Bioproducts, Ely, UK) for 2 hours at 37°C. The tubes were then centrifuged at 12,000g for 15 minutes at 4°C and 40µl of each supernatant were removed. The

pellets were resuspended in 40µl of 1% BSA-TBS. Each mixture was then applied on mouse sections as described in the previous chapter.

Target	Antibody used	Dilution	Time
Properdin	FITC-conjugated goat anti-human properdin antibody (Nordic Immunology)	1:75	2 hours
Tingible body macrophages	Rat anti-mouse CD68 antibody (Serotec)	1:75	2 hours
Follicular dendritic cells	Rat anti-mouse FDC-M1 antibody (BD Pharmingen, Oxford, UK)	1:40	2 hours
B cells	Rat anti-mouse CD45R/B220 antibody (BD Pharmingen)	1:50	2 hours
Secondary antibodies	FITC-labelled anti-rat IgG (Abcam; Cambridge, UK) TRITC-labelled donkey anti-rat IgG (Jackson Immunoresearch; Stratech Scientific, Soham, UK)	1:400 1:200	1 hour 1 hour
Double labelling	1- Cell-marker specific antibody 2- TRITC-labelled anti-IgG 3- FITC-conjugated goat anti-human properdin antibody	See above 1:200 1:75	2 hours 1 hour 1 hour

Table 2-2: Antibodies and conditions used for immunofluorescence studies.

2.2.8 Whole blood platelets flow cytometry

This work was done in Glenfield General Hospital in the laboratory of Prof. Alison Goodall (University of Leicester) under the supervision of Dr. Chris Jones.

The FITC-labelled mouse anti-human properdin antibody used in this study was obtained using the Zenon Fluorescein mouse IgG1 labeling kit (Invitrogen) following manufacturer's instructions. Briefly, for each sample, 5µl of Zenon Fluorescein mouse IgG1 labeling reagent was incubated for 5 minutes with 1µg of mouse anti-human properdin antibody HYB06 (Antibody Shop, Gentofte, Denmark) at room temperature in the dark. Five microlitres of the Zenon blocking reagent was then added to the mixture and left to stand in the dark at room temperature for an additional 5 minutes.

Flow cytometric analysis of whole blood platelets was performed as previously described (Goodall and Appleby, 2004). Briefly, 1µg of FITC-labelled

mouse anti-human properdin antibody or of its isotype control (Mouse IgG1κ MOPC 21 FITC-conjugated (Sigma-Aldrich)) was put into a tube containing 50µl of HEPES Buffered Saline (HBS) (150mM NaCl, 5mM KCl, 1mM $MgSO_4$, $7H_2O$, 10mM HEPES free salt) supplemented with 2mM $CaCl_2$, 0.5U hirudin (Sigma-Aldrich) and the appropriate concentration of agonist (ADP (Adenosin Tri Phosphate; Sigma-Aldrich): 0.01mM; TRAP (Thrombin Receptor Activation Protein; Sigma-Aldrich): 0.1mM; CRP (Collagen Related Protein; Sigma-Aldrich): 1µg/ml). 5µl of human blood freshly collected from a superficial arm vein of a healthy volunteer using Vacutainers with sodium citrate (Becton Dickinson, Oxford, UK) were then added to the preparation using a Barky pipette, gently mixed and left to stand at room temperature in the dark for 20 minutes. Samples were then diluted and fixed in 500µl of 0.2% formyl saline (37% formaldehyde solution, 0.85% (w/v) NaCl) for an additional 10 minutes. A further 1:10 dilution of each sample in 0.2% formyl saline was finally performed and the data were directly acquired by the Coulter Epics XL-MCL flow cytometer (Beckman Coulter, High Wycombe, UK) and analysed using the System II, version 3.0 software (Beckman Coulter).

2.3 Results

In this chapter, the expression of properdin was assessed at a transcriptional and at a translational level in different mouse organs.

2.3.1 At a transcriptional level

2.3.1.1 Cloning of mouse properdin ORF from mouse spleen cDNA

RNA was extracted from mouse spleen as explained in chapter 2.1.2 and this RNA was used as a template to synthesise single stranded cDNA (see chapter 2.1.4.1). PCR was then performed using this freshly synthesised cDNA and a pair of primers specific for the mouse properdin gene as described in chapter 2.1.4.2.2. These primers called "MouPN" were designed to obtain a PCR product that included the all open reading frame of the mouse properdin gene (table 2-1). Mouse properdin ORF has a length of 1395bp and the PCR product obtained using these primers was expected to be 1422bp long.

As shown on figure 2-1, a PCR product with the expected size of 1422bp was visualised on the agarose gel. In order to confirm the identity of this product, a consequent amount of DNA from the band of interest was needed. Six other PCRs using exactly the same conditions as previously were therefore performed and the PCR reactions were run into an agarose gel. The PCR products obtained at 1422bp were all excised from the gel, pooled together, and the DNA was extracted from the gel using the Sephaglas BandPrep kit (see chapter 2.1.5.1). The DNA concentration of the 1422bp fragment extracted was measured (see chapter 2.1.5.2) and this fragment was cloned into a PGEM-T easy vector (Promega) as described in chapter 2.1.5.4. The plasmid obtained was used to transform Top 10F' competent cells (see chapter 2.1.5.5) and the transformed bacteria were plated onto LB agar plates supplemented with ampicillin, X-Gal and IPTG. Six white single colonies were then selected (the white colour of the colonies meaning these cells had a fragment inserted in the insert region of the vector), picked up individually and grown overnight before to be submitted to a plasmid extraction (see chapter 2.1.5.6). The plasmids obtained were screened by restriction digest using *EcoR*I (see chapter 2.1.5.7), as bioinformatics analyses using Gene Tool Lite 1.0 software showed that the PGEM-T easy vector possessed two restriction sites for *EcoR*I, while the properdin insert had none. The PGEM-T easy vector was cut twice for all the samples tested following

*EcoR*I digest, as seen with the 3000bp band observed on the gel for the six samples corresponding to the size of the linearised vector (figure 2-2). In lane 2, an extra band with the expected size of the properdin fragment was visualised too, suggesting the fragment was successfully inserted into the plasmid for this sample. This plasmid was sent for sequencing to PNACL (see chapter 2.1.5.8) to confirm the identity of its insert. This work was done using primers specific for both the T7 and the SP6 promoter regions that flanked the insert region of the PGEM-T easy vector. The sequence obtained using the T7 promoter primer and the complementary sequence of the one obtained using the SP6 promoter primer were then aligned with the known sequence of the Mus musculus complement factor properdin mRNA (EMBL accession number: NM_008823) using the multi-align editor function of the Gene Tool Lite 1.0 software (figure 2-3). The sequence obtained using the T7 promoter primer showed 97% identity with the mouse properdin gene, whereas the one obtained using the SP6 promoter primer showed 96% identity with the mouse properdin gene. It is worth mentioning that the mismatches and gaps observed between the sequence of the insert and the sequence of the mouse properdin gene were mainly seen after the first 500bp sequenced; the best quality sequence with this technique being usually observed between 50bp and 500bp after the end of the sequencing primer (PNACL DNA sequencing service, personal communication). These results taken together therefore showed that the product previously obtained by RT-PCR using spleen cDNA was indeed properdin.

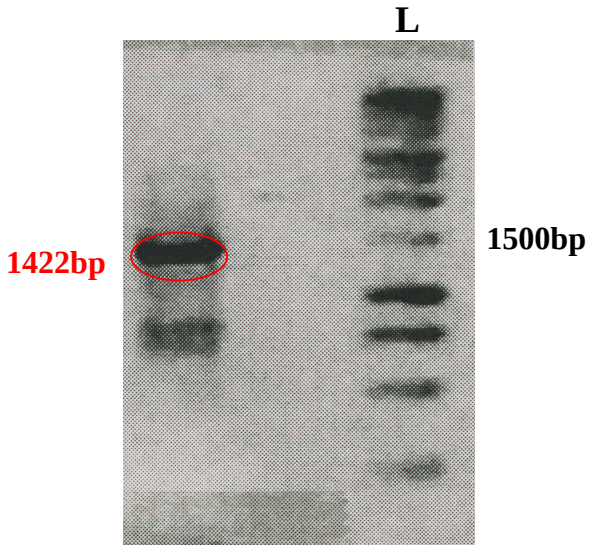

Figure 2-1: Representation of the PCR product obtained using mouse spleen cDNA and the MouPN primers pair after migration into a 0.8% agarose gel. L: benchtop 1kb DNA ladder (Promega).

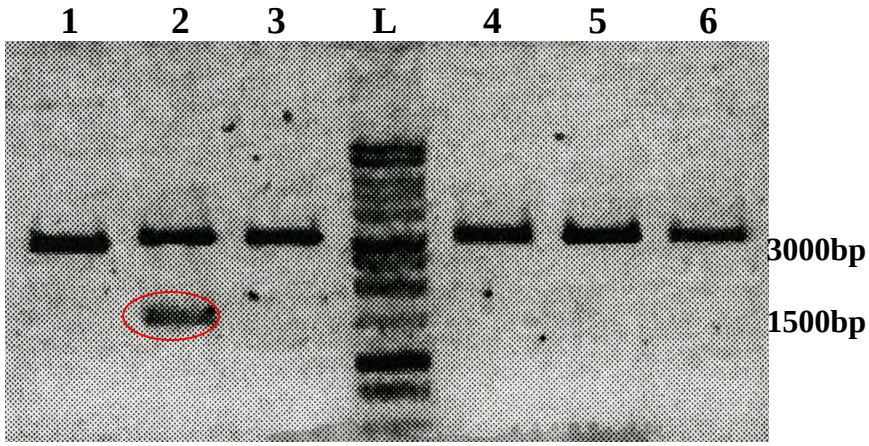

Figure 2-2: Representation of the products obtained after restriction digest by *EcoR*I of the plasmids extracted from Top10F' cells transformed with the PCR product obtained using mouse spleen cDNA and the MouPN primers pair. L: benchtop 1kb DNA ladder (Promega). 1, 2, 3, 4, 5 and 6: the six different plasmid preparations.

A

```
Consensus ATGCAAGCCC CTCAGTGGCT CCTGCTGCTA CTGGTTATCC TGCCAGCCAC AGGCTCAGAC
Properdin ATGCAAGCCC CTCAGTGGCT CCTGCTGCTA CTGGTTATCC TGCCAGCCAC AGGCTCAGAC 142
Insert T7 ATGCAAGCCC CTCAGTGGCT CCTGCTGCTA CTGGTTATCC TGCCAGCCAC AGGCTCAGAC 60

Consensus CCTGTGCTCT GCTTCACCCA GTATGAGGAG TCCTCTGGCA GGTGCAAAGG CCTACTTGGG
Properdin CCTGTGCTCT GCTTCACCCA GTATGAGGAG TCCTCTGGCA GGTGCAAAGG CCTACTTGGG 202
Insert T7 CCTGTGCTCT GCTTCACCCA GTATGAGGAG TCCTCTGGCA GGTGCAAAGG CCTACTTGGG 120

Consensus AGAGACATCA GGGTAGAAGA CTGCTGTCTC AACGCTGCCT ATGCCTTCCA GGAGCATGAT
Properdin AGAGACATCA GGGTAGAAGA CTGCTGTCTC AACGCTGCCT ATGCCTTCCA GGAGCATGAT 262
Insert T7 AGAGACATCA GGGTAGAAGA CTGCTGTCTC AACGCTGCCT ATGCCTTCCA GGAGCATGAT 180

Consensus GGTGGCCTCT GTCAGGCATG CAGGTCTCCA CAATGGTCAG CATGGTCCTT ATGGGGGCCC
Properdin GGTGGCCTCT GTCAGGCATG CAGGTCTCCA CAATGGTCAG CATGGTCCTT ATGGGGGCCC 322
Insert T7 GGTGGCCTCT GTCAGGCATG CAGGTCTCCA CAATGGTCAG CATGGTCCTT ATGGGGGCCC 240

Consensus TGCTCAGTTA CATGTTCTGA GGGGTCCCAG CTGCGACACA GGCGCTGTGT GGGCAGAGGT
Properdin TGCTCAGTTA CATGTTCTGA GGGGTCCCAG CTGCGACACA GGCGCTGTGT GGGCAGAGGT 382
Insert T7 TGCTCAGTTA CATGTTCTGA GGGGTCCCAG CTGCGACACA GGCGCTGTGT GGGCAGAGGT 300

Consensus GGTCAGTGCT CTGAGAATGT GGCTCCTGGA ACTCTTGAGT GGCAGCTACA GGCCTGTGAG
Properdin GGTCAGTGCT CTGAGAATGT GGCTCCTGGA ACTCTTGAGT GGCAGCTACA GGCCTGTGAG 442
Insert T7 GGTCAGTGCT CTGAGAATGT GGCTCCTGGA ACTCTTGAGT GGCAGCTACA GGCCTGTGAG 360

Consensus GACCAGCCAT GCTGTCCAGA GATGGGTGGC TGGTCTGAGT GGGGAC-CTG GGGGCCTTGC
Properdin GACCAGCCAT GCTGTCCAGA GATGGGTGGC TGGTCTGAGT GGGGACCCTG GGGGCCTTGC 502
Insert T7 GACCAGCCAT GCTGTCCAGA GATGGGTGGC TGGTCTGAGT GGGGACTCTG GGGGCCTTGC 420

Consensus TCTGTCACAT GCTCCAAAGG AACCCAGATC CGTCAACGAG TATGTGATAA TCCTGCTCCT
Properdin TCTGTCACAT GCTCCAAAGG AACCCAGATC CGTCAACGAG TATGTGATAA TCCTGCTCCT 562
Insert T7 TCTGTCACAT GCTCCAAAGG AACCCAGATC CGTCAACGAG TATGTGATAA TCCTGCTCCT 480

Consensus AAGTGTGGGG GCCACTGCCC AGGAGAGGCC CAGCAATCAC AGGCCTGTGA CACCCAGAAG
Properdin AAGTGTGGGG GCCACTGCCC AGGAGAGGCC CAGCAATCAC AGGCCTGTGA CACCCAGAAG 622
Insert T7 AAGTGTGGGG GCCACTGCCC AGGAGAGGCC CAGCAATCAC AGGCCTGTGA CACCCAGAAG 540

Consensus ACCTGCCCCA CACATGGGGC CTGGGCATCC TGGGGCCCCT GGAGCCCCTG CTCAGGATCC
Properdin ACCTGCCCCA CACATGGGGC CTGGGCATCC TGGGGCCCCT GGAGCCCCTG CTCAGGATCC 682
Insert T7 ACCTGCCCCA CACATGGGGC CTGGGCATCC TGGGGCCCCT GGAGCCCCTG CTCAGGATCC 600

Consensus TGCCTTGGTG GTGCTCAAGA ACCTAAGGAG AC-CGAAGCC GCTCATGTTC TGCACCAGCA
Properdin TGCCTTGGTG GTGCTCAAGA ACCTAAGGAG ACACGAAGCC GCTCATGTTC TGCACCAGCA 742
Insert T7 TGCCTTGGTG GTGCTCAAGA ACCTAAGGAG ACTCGAAGCC GCTCATGTTC TGCACCAGCA 660

Consensus -CTTCACACC AGCC-CCTGG GAAACCCTGC TCAGGACCAG CCTATGAGCA TAAGGCCTGC
Properdin CCTTCACACC AGCCCCCTGG GAAACCCTGC TCAGGACCAG CCTATGAGCA TAAGGCCTGC 802
Insert T7 TCTTCACACC AGCCTCCTGG GAAACCCTGC TCAGGACCAG CCTATGAGCA TAAGGCCTGC 720

Consensus AGTGGCCTAC CACCTTGCCC A-TGGCTGGT GGCTGGGGG- CCATGGAGCC CTTTGAGCC-
Properdin AGTGGCCTAC CACCTTGCCC AGTGGCTGGT GGCTGGGGG- CCATGGAGCC CTTTGAGCCC 861
Insert T7 AGTGGCCTAC CACCTTGCCC ACTGGCTGGT GGCTGGGGGT CCATGGAGCC CTTTGAGCCT 780

Consensus CTGCTCTGTG ACTTGTG-CC TG-GCC-GAC CCTAGAGC-A C-GGACATGT GATCACCCTG
Properdin CTGCTCTGTG ACTTGTGGCC TGGGCCAGAC CCTAGAGCAA C-GGACATGT GATCACCCTG 920
Insert T7 CTGCTCTGTG ACTTGTGCCC TGCGCCCGAC CCTAGAGCCA CCGGACATGT GATCACCCTG 840
Consensus CACCC-GTCA TGGGGG-CCC CTTT-G-GCT GGTGATGC-- -TCGGAACC- A-TGTGTAAC
Properdin CACCCCGTCA TGGGGG-CCC CTTTTGTGCT GGTGATGCCA CTCGGAACCA AATGTGTAAC 979
Insert T7 CACCC-GTCA TGGGGGGCCC CTTTGGGGCT GGTGATGCTC TTCGGAACCC A-TGTGTAAC 889

Consensus AA-GCCGTA- CTTGCC-TG- AAACG-G-A- TGG-A-GC-T -GG--AAATG -AG-G-CTGC
Properdin AAAGCCGTAC CTTGCCCTGT AAACGGGGAG TGGGAGGCCT GGGGAAAATG GAGTGACTGC 1039
Insert T7 AA-GCCGTAT CTTGCCTTGC AAACGTGAAT TGGTACGCTT CGGCCAAATG TAGCG-CTGC 957

Consensus --CC-GCT-- --ATG-TC-- TC---TGTG- AGGA
Properdin AGCCGGCTGA GAATG-TCCA TCAACTGTGA AGGA                          1072
Insert T7 CCCCCGCTTT ATATGCTCTT TCT--TGTGT AGGA                          989
```

B

```
Consensus  CCCCCAGTCT TACCTTCGTT CCCTAAAATC CCAAAGAAGA GAAGACCCAG AAACGTCTGT
Properdin  CCCCCAGTCT TACCTTCGTT CCCTAAAATC CCAAAGAAGA GAAGACCCAG AAACGTCTGT 1432
Insert SP6 CCCCCAGTCT TACCTTCGTT CCCTAAAATC CCAAAGAAGA GAAGACCCAG AAACGTCTGT 60

Consensus  CCGTGTACAT CTGTACTGGC AAAGAGAAGG TGGTGGTCGA AGACGGGGAC ATCGCGAAGT
Properdin  CCGTGTACAT CTGTACTGGC AAAGAGAAGG TGGTGGTCGA AGACGGGGAC ATCGCGAAGT 1372
Insert SP6 CCGTGTACAT CTGTACTGGC AAAGAGAAGG TGGTGGTCGA AGACGGGGAC ATCGCGAAGT 120

Consensus  GTGTCACCGG CACCTCAGGG GGTCTTCCAT TGTAAGAAGA GTGGGACTGG AAGTTGGTAA
Properdin  GTGTCACCGG CACCTCAGGG GGTCTTCCAT TGTAAGAAGA GTGGGACTGG AAGTTGGTAA 1312
Insert SP6 GTGTCACCGG CACCTCAGGG GGTCTTCCAT TGTAAGAAGA GTGGGACTGG AAGTTGGTAA 180

Consensus  CTTTGACATC CGCCCATGAA CCCCTCGTTT CCACACGTCT CCGCGACCGC CTGTGCCCAC
Properdin  CTTTGACATC CGCCCATGAA CCCCTCGTTT CCACACGTCT CCGCGACCGC CTGTGCCCAC 1252
Insert SP6 CTTTGACATC CGCCCATGAA CCCCTCGTTT CCACACGTCT CCGCGACCGC CTGTGCCCAC 240

Consensus  CGCAACCCTG ATGTACCACC ACACGTGTCT G-GGTCCATG AGGTGACACT GGTACTTGGA
Properdin  CGCAACCCTG ATGTACCACC ACACGTGTCT GAGGTCCATG AGGTGACACT GGTACTTGGA 1192
Insert SP6 CGCAACCCTG ATGTACCACC ACACGTGTCT GGGGTCCATG AGGTGACACT GGTACTTGGA 300

Consensus  AAGTACTATG TCAATACCTA CAATATCGTC ACAGCTTATA GGACCTCAAA AGGTCGTGTA
Properdin  AAGTACTATG TCAATACCTA CAATATCGTC ACAGCTTATA GGACCTCAAA AGGTCGTGTA 1132
Insert SP6 AAGTACTATG TCAATACCTA CAATATCGTC ACAGCTTATA GGACCTCAAA AGGTCGTGTA 360

Consensus  CCGAAGGGTA ATTTAAACGC CGGCGGTGTC GAGGAACTTG CACTGACGAC CGGACCCCAA
Properdin  CCGAAGGGTA ATTTAAACGC CGGCGGTGTC GAGGAACTTG CACTGACGAC CGGACCCCAA 1072
Insert SP6 CCGAAGGGTA ATTTAAACGC CGGCGGTGTC GAGGAACTTG CACTGACGAC CGGACCCCAA 400

Consensus  GGAAGTGTCA ACTACCTGTA AGA-TCGGCC GACG-CAG-G AGGTAAAAGG GGTCCGGAGG
Properdin  GGAAGTGTCA ACTACCTGTA AGAGTCGGCC GACGTCAGTG AGGTAAAAGG GGTCCGGAGG 1012
Insert SP6 GGAAGTGTCA ACTACCTGTA AGAATCGGCC GACGGCAGGG AGGTAAAAGG GGTCCGGAGG 480

Consensus  GTGAGGGGCA AATG--CCGT TCCATGCCGA A-----G-GT AAACCA-GGC TCACCGTAGT
Properdin  GTGAGGGGCA AATGTCCCGT TCCATGCCGA AACAATGTGT AAACCAAGGC TCACCGTAGT 952
Insert SP6 GTGAGGGGCA AATGGGCCGT TCCATGCCGA AGGGGGG-GT AAACCAGGGC TCACCGTAGT 540

Consensus  G-GT-GTG-T TT-CCCGGGG G-ACTG
Properdin  G-GTCGTGTT TTCCCCGGGG GTACTG                                  927
Insert SP6 GAGTGGTGGT TTGCCCGGGG GGACTG                                  566
```

Figure 2-3: Comparison of the sequence of the cloned insert (lane 3) sequenced using a primer annealing to the T7 promoter site (A) and of the complementary sequence of the cloned insert sequenced using a primer annealing to the SP6 promoter site (B) with the sequence of the mouse complement factor properdin mRNA (EMBL accession number: NM_008823) (lane 2). The consensus sequence (lane 1) was constructed from the alignment of the reference sequence (lane 2) with the sequence of the cloned insert (lane 3) using the multi-align editor function of the Gene Tool Lite 1.0 software. Identities between both sequences are represented in black, mismatches in red and gap in green. Lane 1: consensus sequence, lane 2: properdin sequence, lane 3: cloned insert sequence. A: Adenine, C: Cytosine, G: Guanine, T: Thymine.

2.3.1.2 Screening of mouse RNAs

Next, the expression of properdin by different murine organs (brain, gut, heart, kidney, liver, lung, spleen and thymus) was assessed by Northern blot analysis using three sets of mouse RNAs available in the laboratory that were labelled "normal", "LPS-treated" and "eye infected". The "LPS-treated" mouse was from a SJL background and had been infected intra-peritonally with 100ng of LPS per gram of body weight (gift of Dr Michael Bette, University of Marburg, Marburg, Germany) (Yirmiya et al., 2001). No further information was available concerning the time-point the animal was culled. The organs from the "normal" and "eye infected" mice were a kind gift from Dr Neill Gingles (University of Leicester). Unfortunately, no further information about the strain of these mice as well as on what caused the infection in the eye of the "eye infected" mouse was available. RNAs were prepared from these organs by guanidinium thiocyanate/caesium chloride gradient by Dr Cordula Stover and were stored in a freezer at -80ºC until further use. At the time of the experiment, these RNA samples seemed suitable to investigate a potential up-regulation of properdin expression. These RNAs were therefore first run into a denatured RNA agarose gel (figure 2-4) (see chapter 2.1.6.1) and transferred to a nylon membrane (see chapter 2.1.6.2). The expression of properdin by each of these organs was assessed by Northern blotting using a radioactive-labelled probe specific for mouse properdin (see chapter 2.1.6.5). This probe was synthesised using the DNA coding for the mouse properdin ORF obtained previously using spleen RNA and the MouPN primers (see chapters 2.1.6.4 and 2.2.1.1).

A representation of an X-Ray film obtained after exposure of the membrane with a sensitive film is shown in figure 2-5. Despite the multiple washes and the use of different times of exposure, a high background level was observed on the X-ray film. However, despite this high background, positive signals could still be identified on the film. Thus, for each mouse, a band of the expected size of approximately 1500bp was observed for the lane corresponding to the spleen sample (lanes 3, 8 and 18). The properdin signal was seen to be more intense for the "LPS-treated" mouse spleen RNA than for the "eye-infected" mouse spleen RNA. An extra band could be detected as well for the RNA extracted from the thymus of the eye-infected mouse (lane 14). No signal was detected for any of the other RNA samples extracted from the three mice.

Properdin signals being detected by Northern blot in only the two lymphoid organs of the three sets of organs tested, the expression of properdin by this particular type of organ was further assessed. Therefore, RNAs were extracted from the lymph nodes, the spleen and the thymus of a non-challenged C57Bl/6 mouse and these RNAs were used as templates to synthesise single stranded cDNAs. A PCR was then performed as previously described using the "MouPN" primers pair (see chapter 2.1.4.2.2) and the PCR reaction products were run into a 0.8% agarose gel. As shown on figure 2-6, a band with the expected size of the mouse properdin ORF was visualised when using both the spleen (lane 2) and the thymus (lane 3) cDNAs, but no product was observed for the lymph node cDNA (lane 1). The intensity of this band seemed much higher for the spleen than for the thymus, but as no internal control was run in parallel to ensure the same quantity of RNA was used in both cases, this was not a quantitative analysis.

The level of properdin expression was therefore next quantified using real-time PCR. Mouse spleen, thymus, lymph node and brain cDNAs were used as template and amplified using a pair of primers specific for human properdin called HumPNsh4 and a pair of primers specific for the mouse housekeeping gene GAPDH called MouGAPDH (table 2-1). Both pairs of primers were tested by RT-PCR to ensure they gave a single product of the expected size (see chapter 3.3.3.1.1) and to ensure HumPNsh4 reacted with mouse cDNA. Real-time PCR was performed as described in chapter 3.2.6 and the relative concentrations obtained for properdin were finally divided by the relative concentrations obtained for GAPDH (table 2-3). The variabilities in GAPDH expression observed between the different lymphoid tissues could be explained by a slightly different concentration of RNA at the beginning of the experiment or by a moreorless efficient cDNA synthesis. Moreover, data published on the GeoProfile website showed that the thymus expressed slightly more GAPDH than the spleen or the lymph node and that the level of GAPDH expression was higher in the brain than in any of the lymphoid organs.

The results, expressed as a percentage of properdin expression (table 2-3), confirmed the previous impression: they showed that the spleen expressed more properdin mRNA than the lymph node (6.5 times more), itself expressing more properdin mRNA than the thymus (1.7 times more). A very low signal was detected in the brain sample (almost 300 times lower than the transcript level detected for the

spleen). However, the brain and, at a lower extent, the thymus results may have been affected by the variablities previously reported between the different GAPDH expression levels.

Two other RNA samples called “brain infected” and “spleen infected” were run in parallel. These RNA were extracted from a C57Bl/6 “gold line” mouse 24 hours after intranasal infection with 5.10^5 *S. pneumoniae* D39 (see chapter 4.2.3.1). In both cases, more than twice more properdin was detected in the organs extracted from the infected mouse than in the organs taken from its healthy littermate (table 2-3).

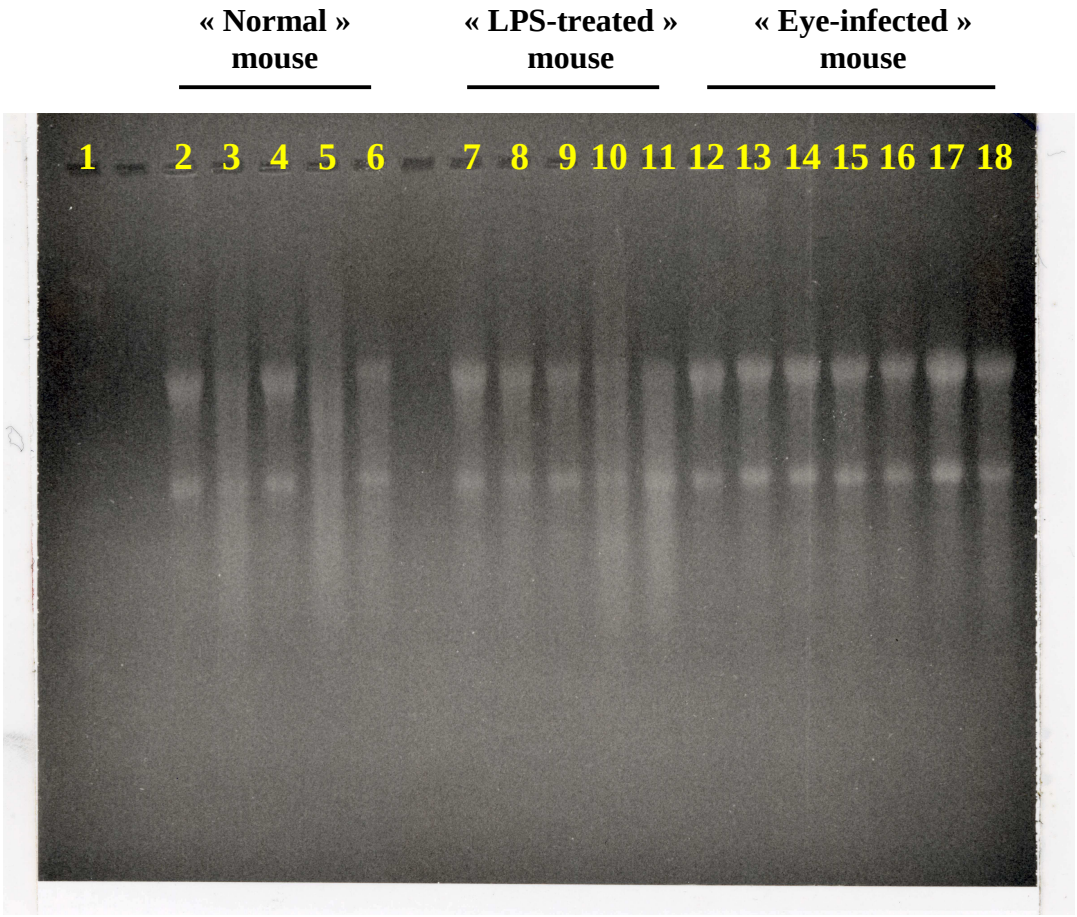

Figure 2-4: Picture of the Northern blot agarose gel taken under UV light.
Lane 1: RNA ladder. A: “normal” mouse - Lane 2: heart RNA, lane 3: spleen RNA, lane 4: kidney RNA, lane 5: liver RNA, lane 6: brain RNA; B: “LPS-treated” mouse - Lane 7: heart RNA, lane 8: spleen RNA, lane 9: kidney RNA, lane 10: liver RNA, lane 11: brain RNA; C: “eye-infected” mouse - Lane 12: brain RNA, lane 13: lung RNA, lane 14: thymus RNA, lane 15: heart RNA, lane 16: gut RNA, lane 17: kidney RNA and lane 18: spleen RNA.

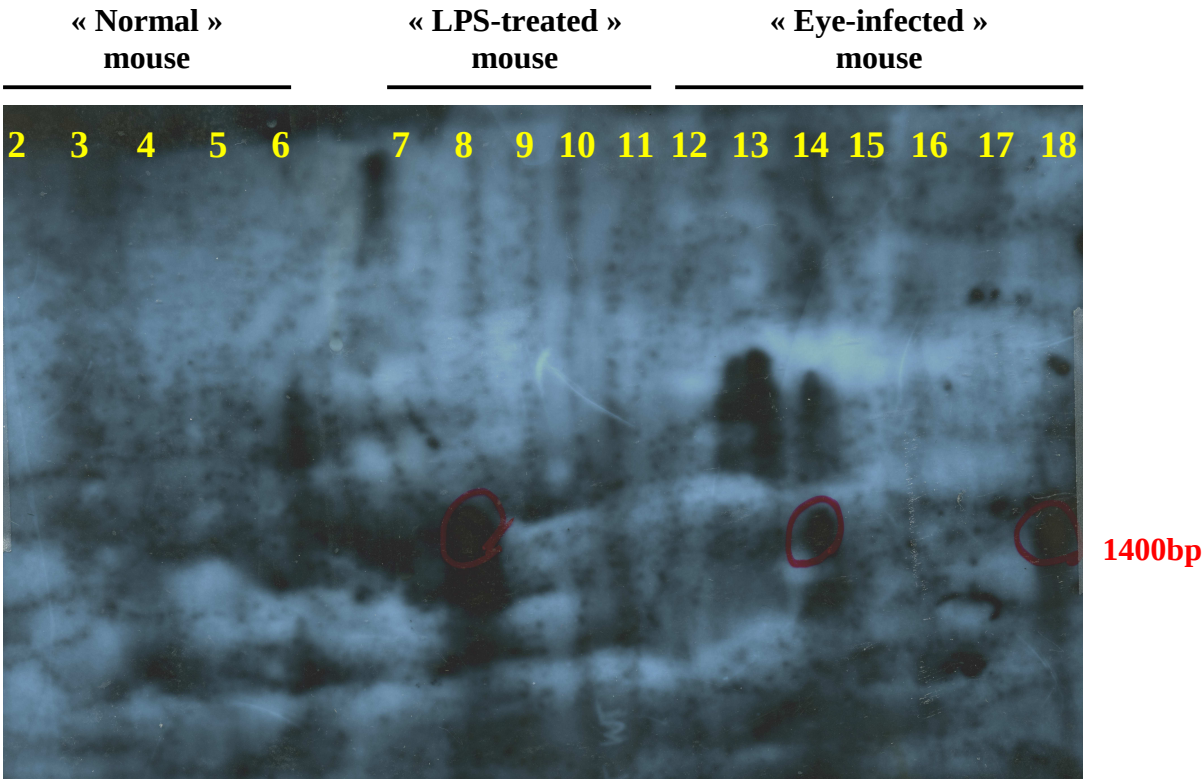

Figure 2-5: Northern blot analysis on different mouse tissues using a radiolabelled probe specific for mouse properdin. A: “normal” mouse - Lane 2: heart RNA, lane 3: spleen RNA, lane 4: kidney RNA, lane 5: liver RNA, lane 6: brain RNA; B: “LPS-treated” mouse - Lane 7: heart RNA, lane 8: spleen RNA, lane 9: kidney RNA, lane 10: liver RNA, lane 11: brain RNA; C: “eye-infected” mouse - Lane 12: brain RNA, lane 13: lung RNA, lane 14: thymus RNA, lane 15: heart RNA, lane 16: gut RNA, lane 17: kidney RNA and lane 18: spleen RNA. Representative results obtained from one of two experiments (using the same RNAs).

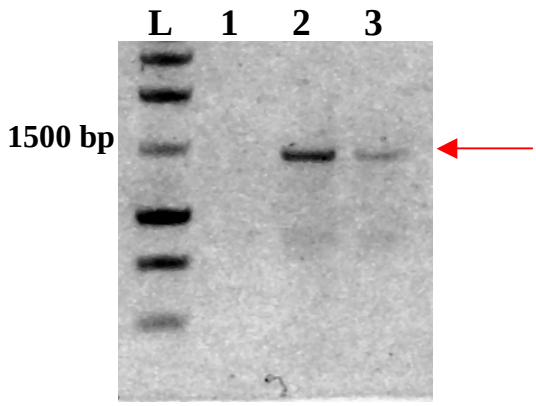

Figure 2-6: Representation of the RT-PCR products obtained using different mouse lymphoid organs and the MouPN primer pair after migration into a 0.8% agarose gel. L: benchtop 1kb DNA ladder (Promega). Lane 1: using lymph node cDNA, lane 2: using spleen cDNA, lane 3: using thymus cDNA. The RNAs for the thymus and the lymph node were a pool from organs obtained from two to three mice.

Organ		**Spleen control**	**Spleen Infected**	**Brain Control**	**Brain Infected**	**Lymph node**	**Thymus**
GAPDH	Crossing point	36.95	35.48	26.22	26.01	38.08	30.60
	Relative concentration	**1.6**	**3.5**	**528.1**	**592.5**	**0.9**	**49.5**
Properdin	Crossing point	25.43	22.95	25.21	23.56	29.38	23.76
	Relative concentration	**7.2**	**33.6**	**8.3**	**22.9**	**0.6**	**20.4**
Properdin expression (AU)		**100**	**210**	**0.34**	**0.85**	**16**	**9**

Table 2-3: Relative properdin expression of different mouse organs obtained after real-time PCR analysis. These results correspond to the quotient of the properdin concentration by the GAPDH concentration and are expressed in percentage. The "spleen control" sample was given the arbitrary value of 100. Results obtained from a single experiment.

2.3.2 At a translational level

In order to correlate the transcriptional level of properdin expression to its translational level of expression, the distribution of properdin on spleen sections issued from wild type and properdin-deficient mice was analysed using a FITC-labelled anti-properdin antibody.

2.3.2.1 Specificity of the antibody

The FITC-labelled goat anti-human properdin antibody used in this study has been shown to specifically bind to human properdin by immunohistochemistry on human tissue sections of atherosclerotic coronary lesions (Oksjoki et al., 2006). However, this antibody was used in my study to detect mouse properdin on mouse tissue sections. To test its specificity, this antibody was first pre-absorbed with properdin antigen prior to be applied on mouse spleen sections (see chapter 2.1.7.3). As seen on figure 2-7, the positive signal observed with the FITC-labelled antibody on spleen sections obtained from wild type animals was lost when this antibody was pre-absorbed with its antigen. However, this technique may not be sufficient to confirm the specificity of the signal for mouse properdin as the non-absorbed antibody could have bound to another protein with a similar epitope present on the tissue (Burry, 2000).

A negative control was therefore used to prove the specificity of the properdin antibody to mouse properdin. Sections of both properdin-deficient and wild type mouse spleens were stained with the anti-human properdin antibody and, whereas signals could be visualised on the wild type spleen sections, only background signal was detected on the properdin-deficient spleen sections (figure 2-8). The absence of signal on properdin-deficient mouse spleen tissue was most likely due to the absence of expression of the properdin protein and therefore showed that this goat anti-human properdin antibody stained specifically properdin on frozen mouse spleen section.

2.3.2.2 Properdin expression in spleen

As seen on figure 2-9A, immunofluorescent signals corresponding to properdin were only observed inside the white pulp compartment of the wild type mouse spleen. No signal was detected in the splenic red pulp area. Positive signals for properdin were mainly observed as one cluster of properdin positive signals in nearly every white pulp compartment of the mouse spleen (figure 2-9B); however, some white pulp compartments showed sometimes none or two clusters of positive cells. At

a higher magnification, properdin signals were seen to be localised in a specific location of the white pulp with a low cell density, as shown by the DAPI staining of this zone (representing cell nuclei, DAPI forming fluorescent complexes when bound to double-stranded DNA) (figures 2-9C and 2-9D).

In an attempt to identify the properdin positive cell population, spleen sections were stained with markers specific for particular sub-types of cells. First, spleen sections were stained with a rat anti-mouse CD68 antibody and positive signals were visualised using a FITC-labelled anti-rat IgG antibody (see chapter 2.1.7.2). As seen on figure 2-10A, CD68-positive signals were seen in both the red and the white pulp area of the spleen: strong signals were observed all over the red pulp compartment, whereas inside the white pulp, only few clusters of positive cells were visible in each compartment. This pattern in the white pulp was similar to the one observed using the anti-properdin antibody. To investigate whether CD68-positive cells in the white pulp area of the spleen were positive as well for properdin, spleen sections were then stained simultaneously with both the FITC-labelled goat anti-human properdin antibody and the rat anti-mouse CD68 antibody (the CD68 signal was then visualised using a TRITC-labelled anti-rat IgG antibody) (see chapter 2.1.7.2). As seen on figure 2-9B, despite the fact that properdin-positive cells were situated in the close vicinity of the CD68-positive cell population in the white pulp area of the spleen, both FITC-positive (properdin) and TRITC-positive (CD68) signals did not co-localise when merged on a same picture.

The exact nature of the cell type responsible for the properdin-positive signals observed in the white pulp area of the spleen was thus further investigated. Using the same technique as the one used for CD68, anti-FDC-M1 and anti-CD45R antibodies were tested to see if their signals superimposed with the properdin-positive signals. As seen on figure 2-11A, the FDC-M1-positive cells were observed in the white pulp compartment of the spleen, in the same area where properdin-positive cells were detected. However, despite this close proximity, it seemed that FDC-M1-positive cells were only adjacent to the properdin-positive cells. Concerning the CD45R-positive cells, they were observed all over the white pulp compartment, including the properdin-positive cell area, but, here again, signals did not superimpose, suggesting here again that properdin-positive cells were not CD45R positive (figure 2-11B).

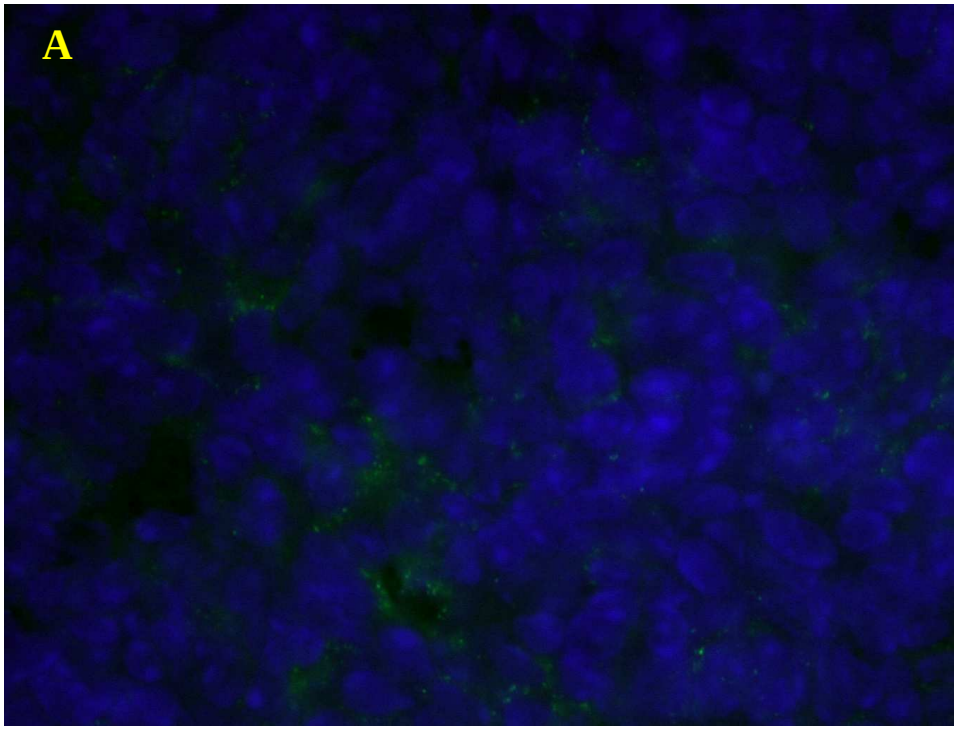

Original magnification x100

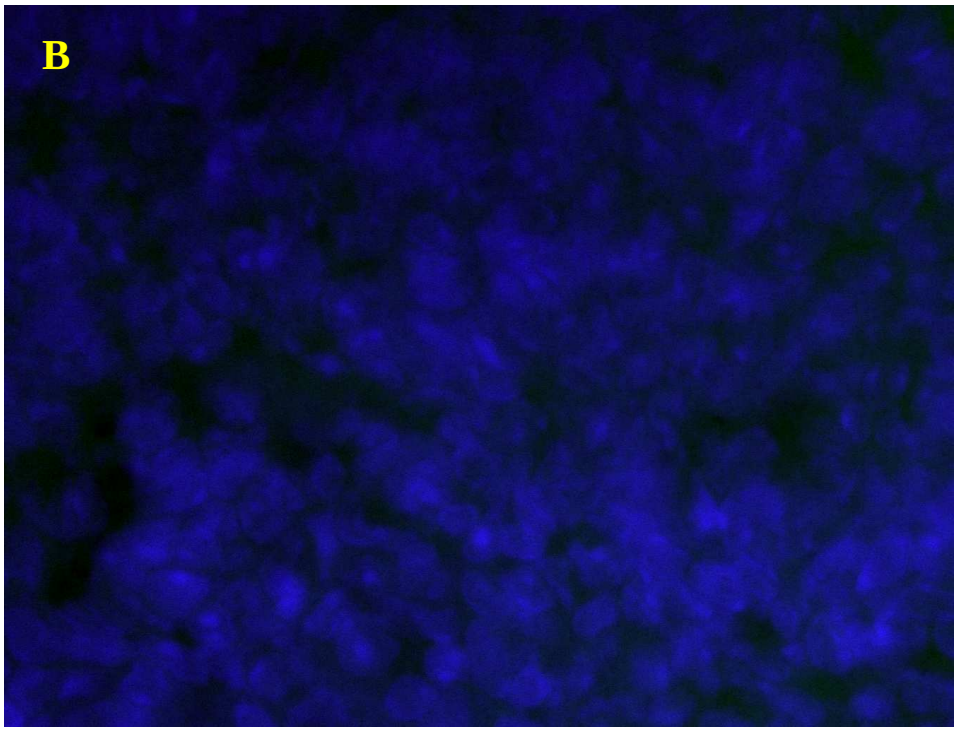

Original magnification x100

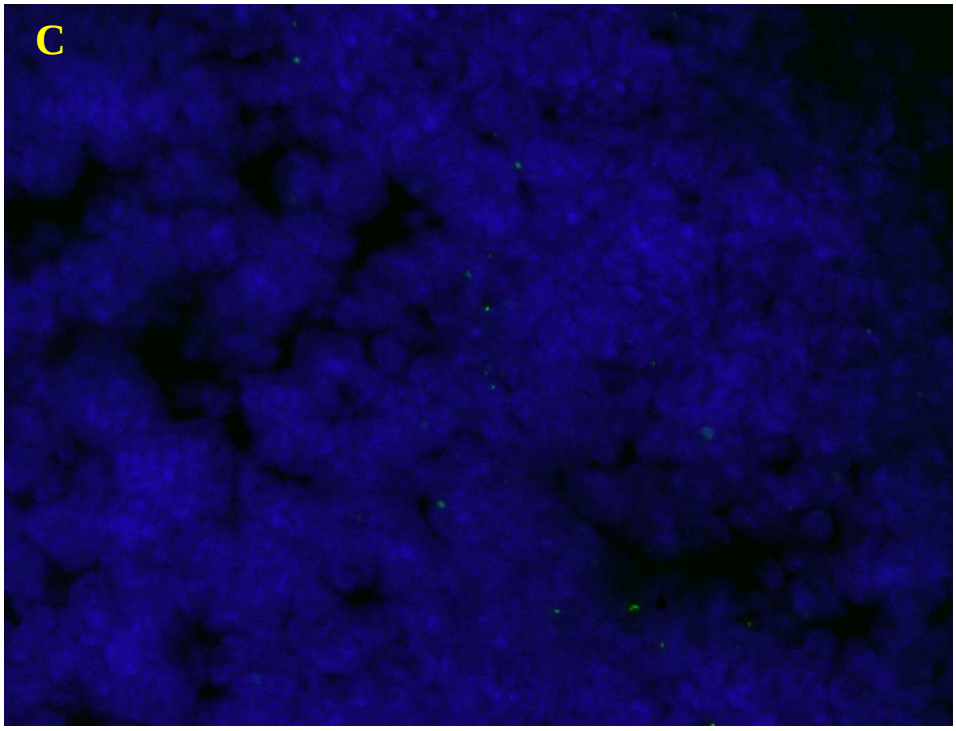

Original magnification x60

Figure 2-7: Representative pictures of the white pulp area of properdin-deficient and wild type mouse spleen sections. A: wild type mouse spleen section stained with DAPI (blue) and immunostained with the FITC-labelled goat anti-human properdin antibody (green); B: wild type mouse spleen section stained with DAPI (blue) and immunostained with the FITC-labelled goat anti-human properdin antibody that had first been pre-absorbed with the properdin antigen (green); C: properdin-deficient mouse spleen section stained with DAPI (blue) and immunostained with the FITC-labelled goat anti-human properdin antibody (green).

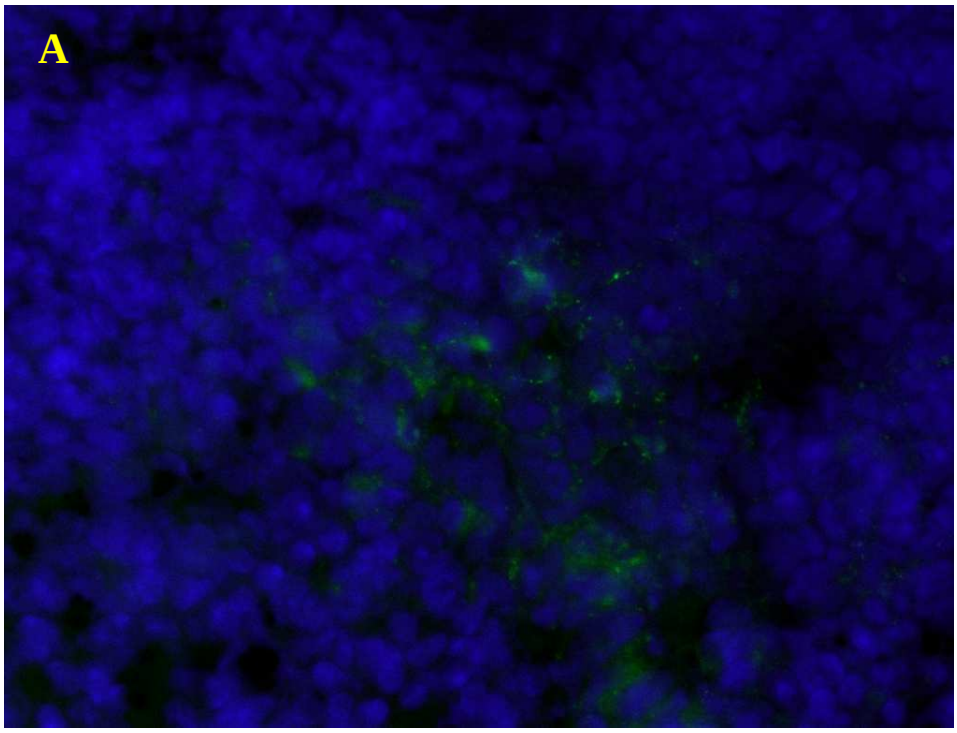

Original magnification x60

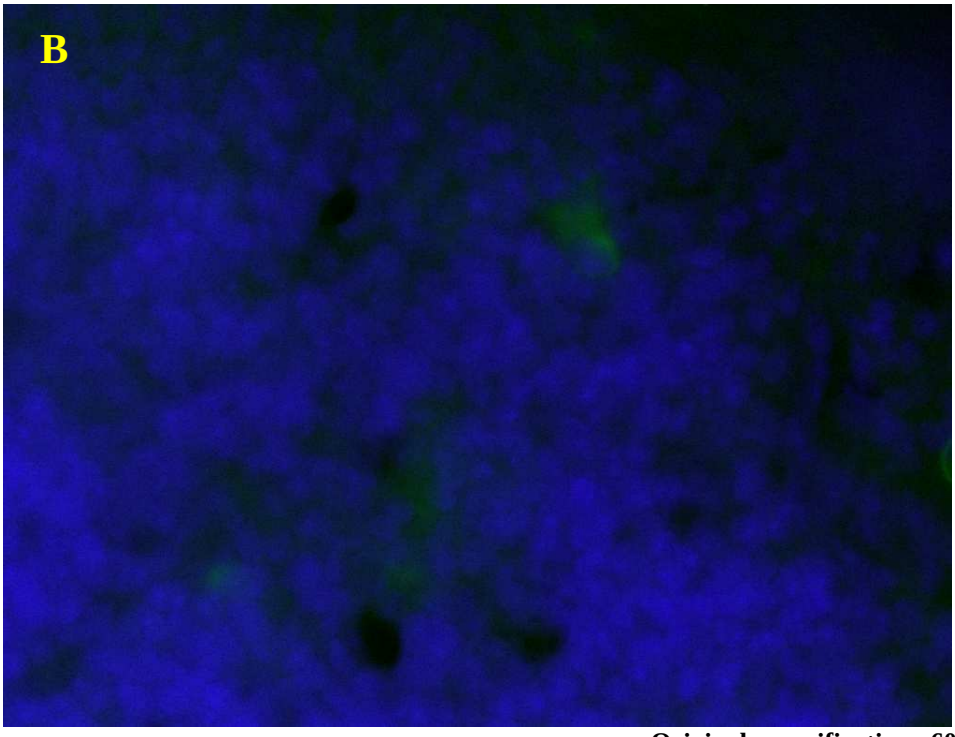

Original magnification x60

Figure 2-8: Representative pictures of the white pulp area of a mouse spleen section stained with DAPI (blue) and immunostained with the FITC-labelled goat anti-human properdin antibody (green). A: Wild type spleen; B: Properdin-deficient spleen. A longer exposure time was applied to the properdin-deficient spleen section to allow the visualisation of the FITC background. Representative observations made from spleen sections obtained from more than 3 different mice.

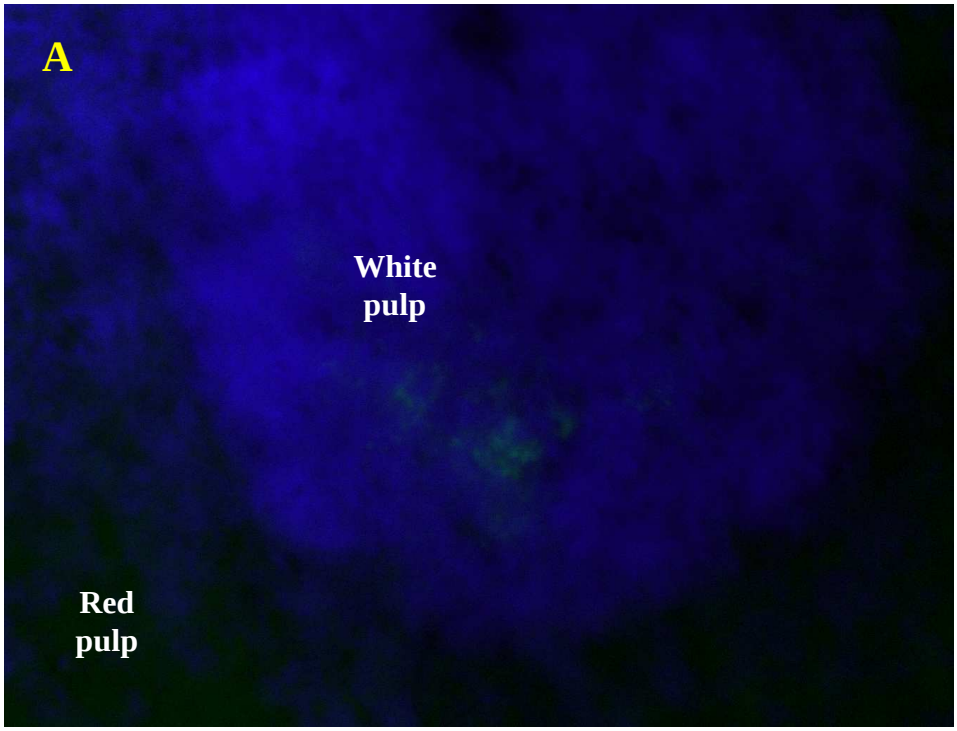

Original magnification x10

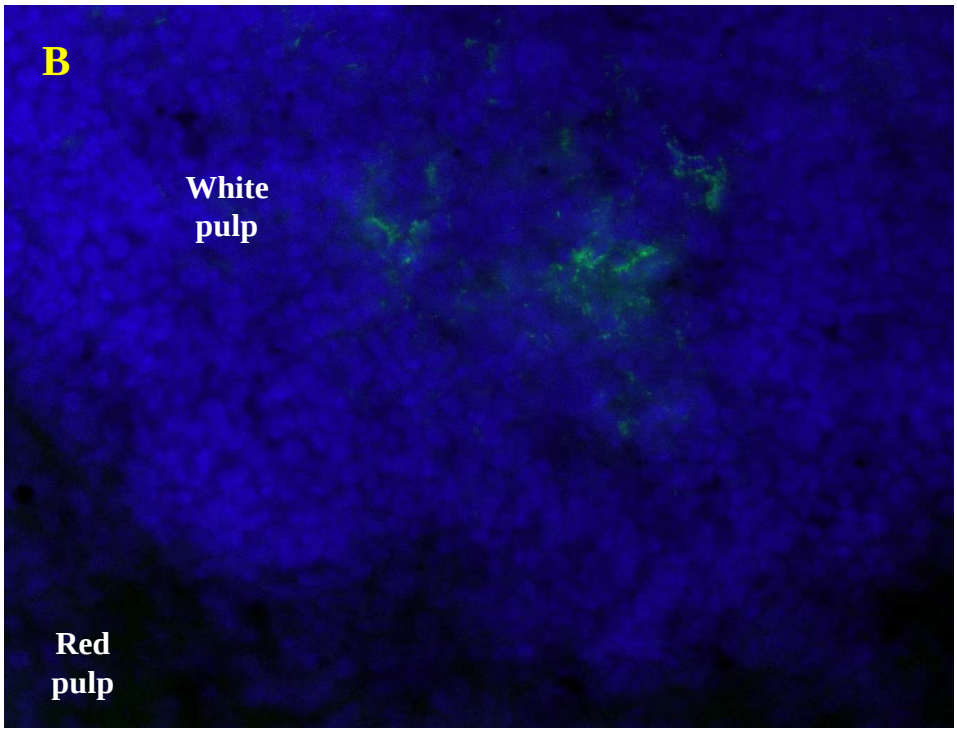

Original magnification x40

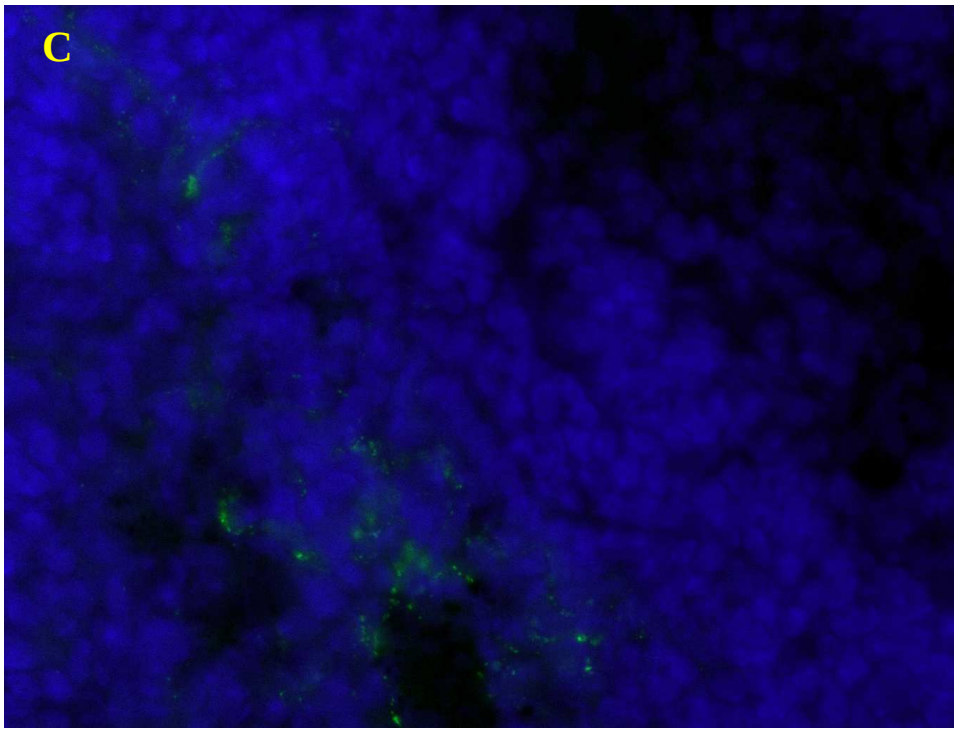

Original magnification x60

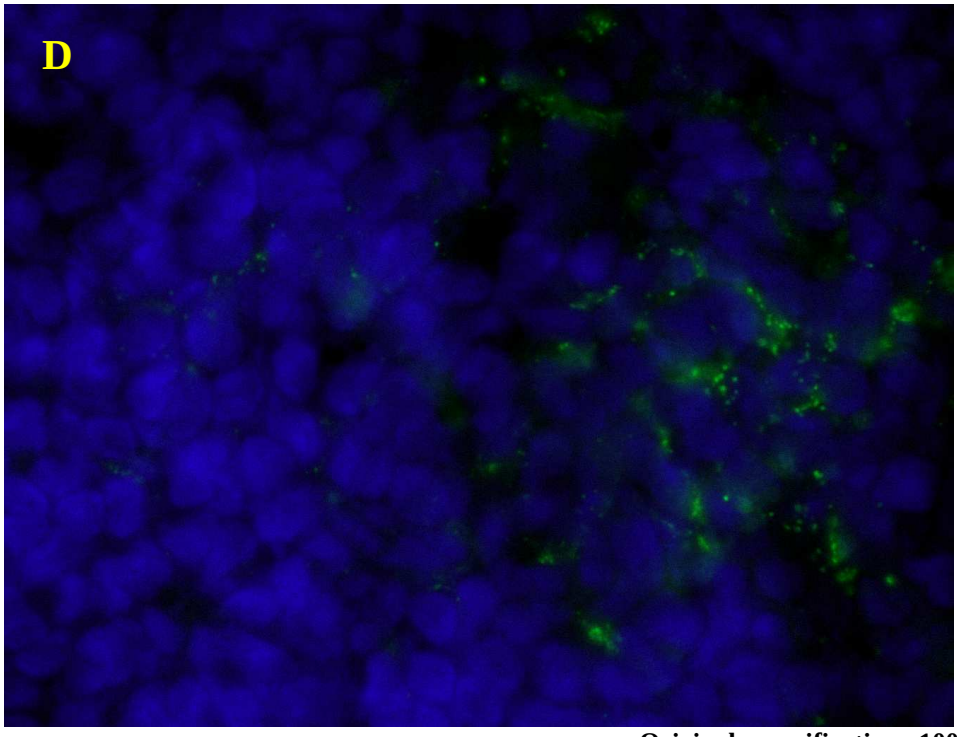

Original magnification x100

Figure 2-9: Representative pictures of mouse spleen sections stained with DAPI (blue) and immunostained with the FITC-labelled goat anti-human properdin antibody (green). Original magnifications were A: x10; B: x40; C: x60 and D: x100. A and B showed both the white and the red pulp, while C and D concentrated on the white pulp compartment of the spleen. Representative observations made from spleen sections obtained from more than 3 different mice.

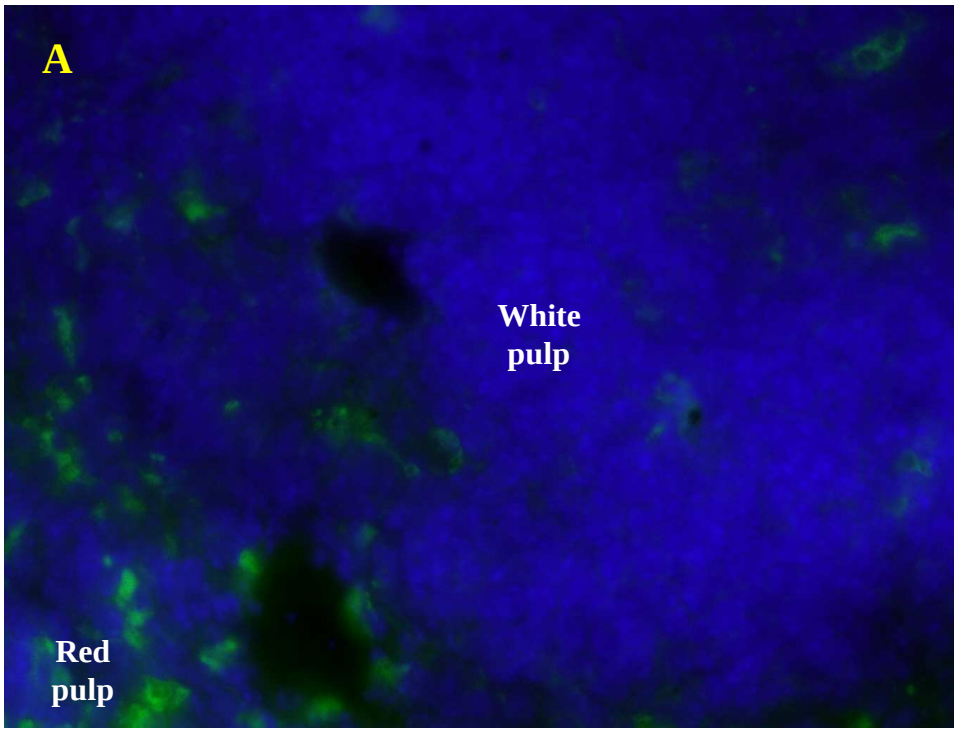

Original magnification x60

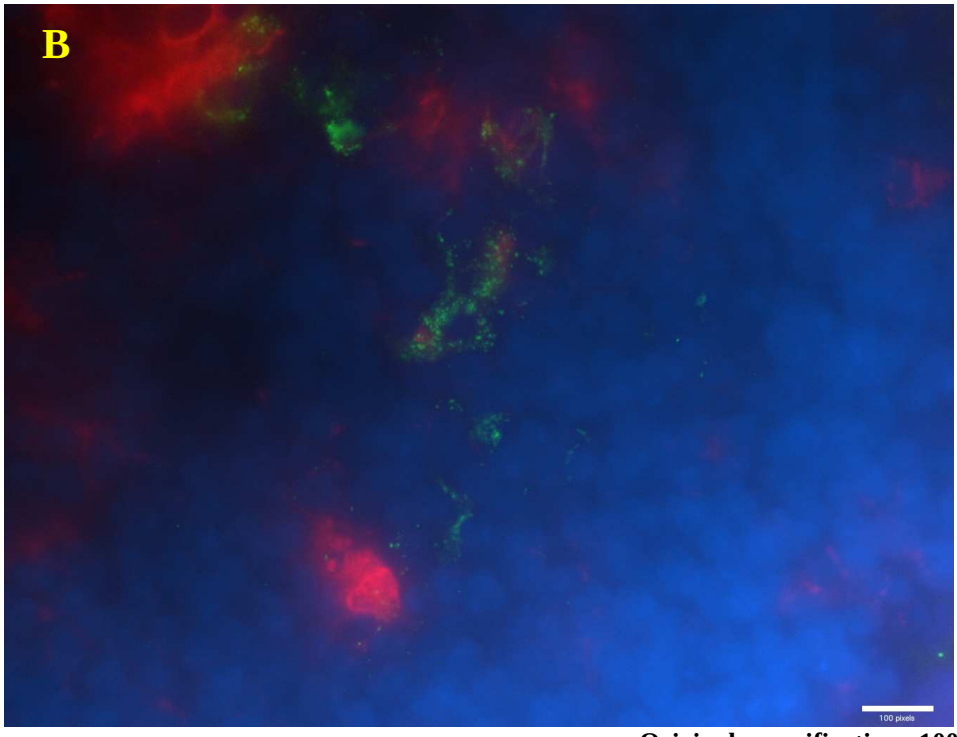

Original magnification x100

Figure 2-10: Representative pictures of mouse spleen sections stained with DAPI (blue) and immunostained A: with the rat anti-mouse CD68 antibody (and detected via the use of a FITC-labelled anti-rat IgG (green)); B: simultaneously with the rat anti-mouse CD68 antibody (and detected via the use of a TRITC-labelled donkey anti-rat IgG (red)) and the FITC-labelled goat anti-human properdin antibody (green). Representative observations made from spleen sections obtained from more 2 different mice.

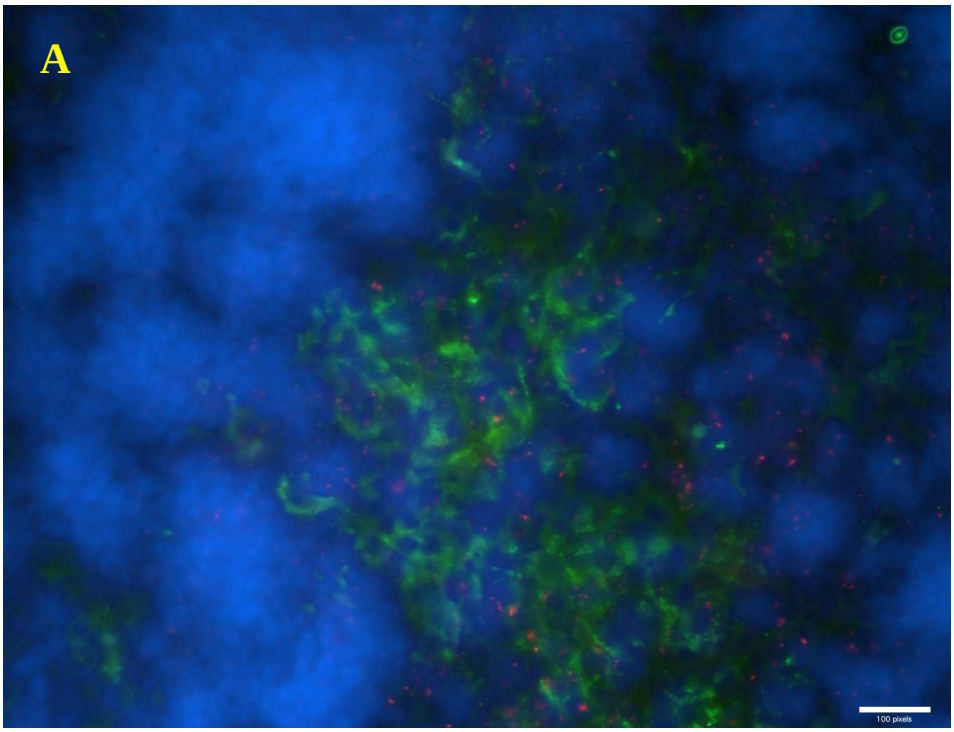

Original magnification x40

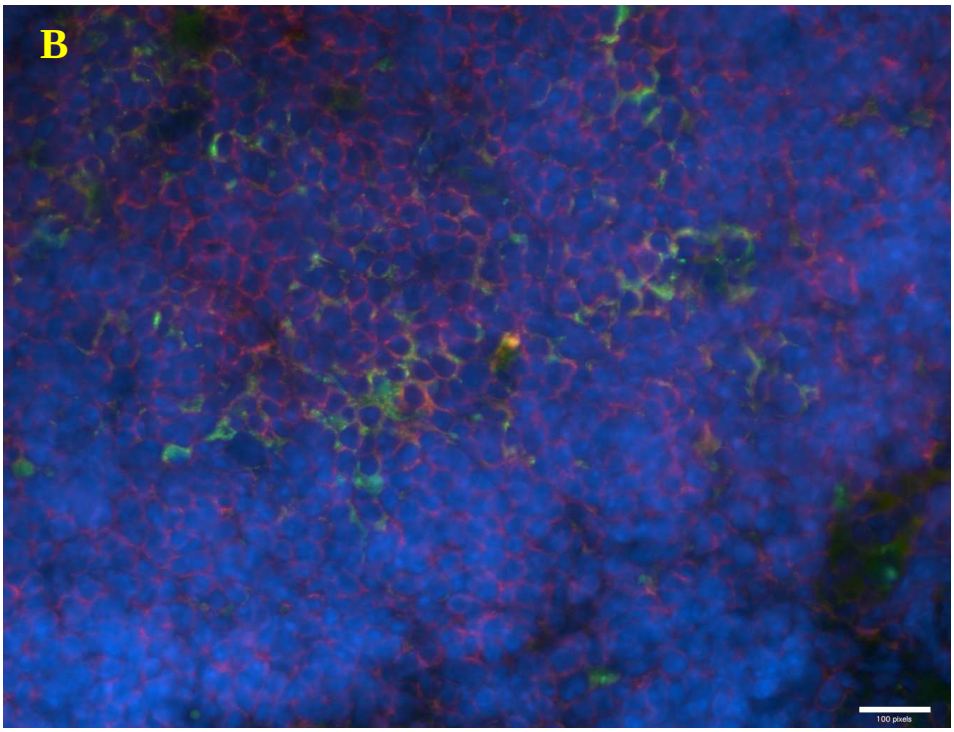

Original magnification x 40

Figure 2-11: Representative pictures of the white pulp area of mouse spleen sections stained with DAPI (blue) and immunostained A: simultaneously with the rat anti-mouse FDC-M1 antibody (and detected via the use of a TRITC-labelled donkey anti-rat IgG (red)) and the FITC-labelled goat anti-human properdin antibody (green); B: simultaneously with the rat anti-mouse CD45R/B220 antibody (and detected via the use of a TRITC-labelled donkey anti-rat IgG (red)) and the FITC-labelled goat anti-human properdin antibody (green). Representative observations made from spleen sections obatined from one single mouse.

2.3.2.3 Properdin deposition on platelets

A recent publication by Del Conde and collaborators has shown that the complement system was activated on the surface of platelets. The level of complement activation was shown to be dependent on the level of platelets activation and on the presence of factor B (Del Conde et al., 2005). It was therefore suggested that platelets were activating more specifically the alternative complement pathway. The ability of properdin, positive regulator of the alternative pathway, to bind to the surface of human platelets was therefore checked by flow cytometry using human whole blood (in an attempt to avoid the unwanted platelets activation that can occur during platelets purification) (see chapter 2.1.8).

The platelet population was identified in the whole blood sample according to its size (forward scatter) and its granularity (side scatter) as shown on figure 2-12A. The four populations observed on the dot blot corresponded, from the bottom left to the top right, to dust, platelets, red blood cells and leukocytes (Chronos et al., 1993; Goodall and Appleby, 2004). The population corresponding to the platelet population was gated (a) and 5000 events belonging to this population were analysed. The detection limit for positive events was set by measuring the signal obtained for the 1 to 2% of platelets with the highest level of fluorescence while staining with the isotype control. This percentage of positive events was then compared to the one obtained using the FITC-labelled mouse anti-human properdin antibody while using exactly the same settings. Thus, for the unstimulated platelets, when only 1.8% of the platelets stained with the isotype control were considered as positive events, 6.6% of the platelets stained with the properdin antibody were positive, meaning that 3.7 times more positive events were detected when the platelets were stained for properdin than for the isotype control (figure 2-12B and table 2-4). This showed that properdin was detected on the surface of unstimulated platelets.

The deposition of properdin on the surface of activated platelets was then assessed using the same technique. The agonists used in this study – namely ADP, TRAP and CRP – were all known to activate platelet degranulation. The percentages of positive cells were measured again for each condition (figures 2-12C, 2-12D and 2-12E). As summarised in table 2-4, properdin was found to be detected on 7.3% of the platelets activated with ADP, 10.1% of the platelets activated with TRAP and 15% of the platelets activated with CRP. In addition of that, platelets activated with TRAP

and CRP presented a median fluorescence intensity for properdin respectively 2 and 3 fold higher than non-activated platelets or platelets activated with ADP. This meant that, not only properdin was found to be detected on a higher percentage of platelets when activated with strong agonists (CRP, TRAP), but also the intensity of properdin deposition on platelets was higher when the platelets were activated with these strong agonists.

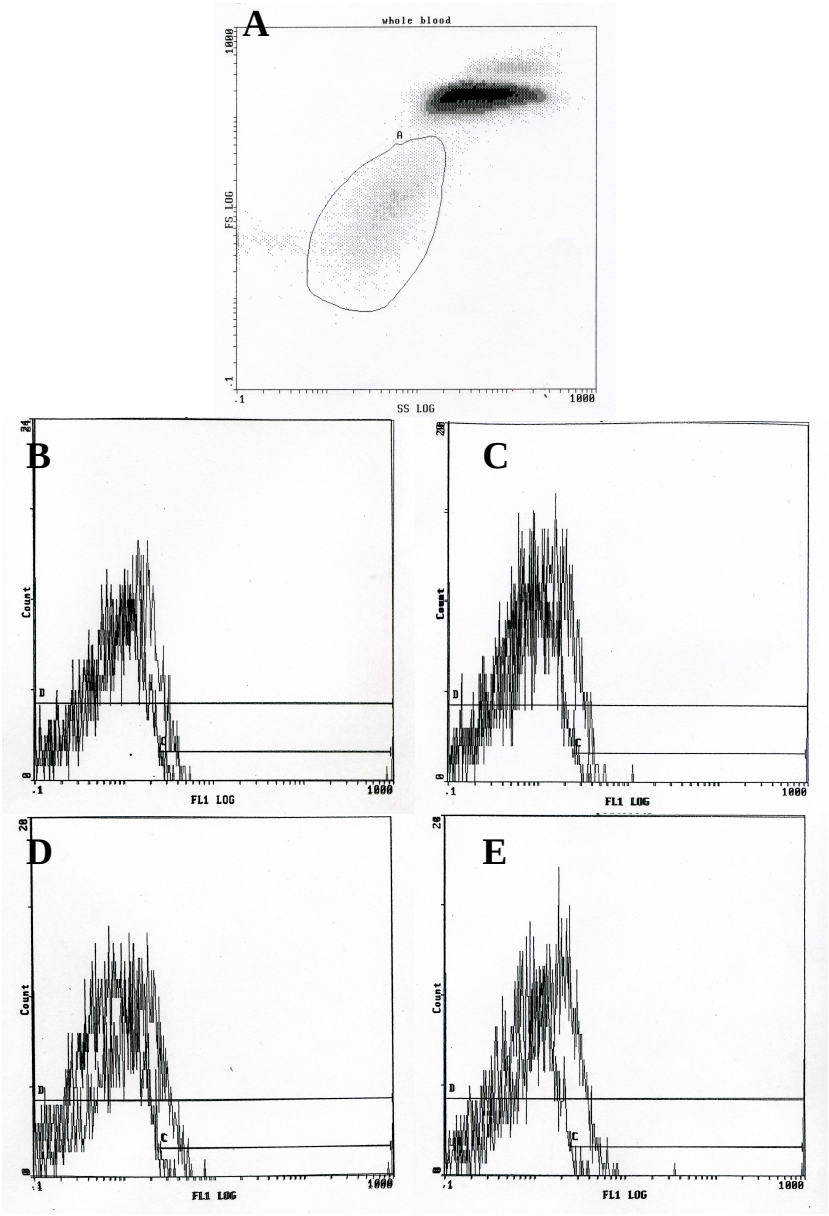

Figure 2-12: Flow cytometric analysis on human whole blood platelets. A: representative whole blood flow cytometric dot blot showing the platelet population (gate a). B-E: Representative histograms obtained for the platelet population after staining with the FITC-labelled mouse anti-human properdin antibody (right peak) and the isotype control (left peak). B: unstimulated platelets; C: ADP-activated platelets; D: TRAP-activated platelets; E: CRP-activated platelets. Each graph is representative of one out of two experiments using a same blood sample.

Agonist	Control	ADP	TRAP	CRP
% of positive cells using the isotype control	1.77	1.22	1.11	1.27
% of positive cells using the properdin antibody	6.61	7.34	10.15	15.05
Median Fluorescence Intensity for the isotype control	0.103	0.103	0.105	0.108
Median Fluorescence Intensity for properdin	0.245	0.257	0.528	0.786

Table 2-4: Summary of the results obtained by flow cytometry.

2.4 Discussion

As mentioned in the introduction, properdin has already been shown to be expressed by a multitude of cell types. However, only few studies have looked at properdin expression at a tissue level. Only spleen, liver, adipose tissue, sinonasal tissue and mammary glands have been investigated in the literature and they all showed different levels of properdin expression (Avery et al., 1993; Choy and Spiegelman, 1996; Maves and Weiler, 1992; Nakamura et al., 2006; Vandermeer et al., 2004).

The first project of my PhD was therefore to investigate the expression of properdin by different types of organs and cells at both a transcriptional and a translational level. In order to accomplish this task, I first screened RNA prepared from a panel of mouse tissues using different molecular biology techniques – namely Northern blotting, PCR and real-time PCR – and then compared my results to the information available on internet using bioinformatics' tools.

2.4.1 Properdin is expressed by lymphoid organs

In order to investigate by Northern blot the expression of properdin by different mouse organs, I constructed a radioactive-labelled probe specific for properdin. Properdin cDNA was obtained by RT-PCR using spleen RNA as a template and primers specifically designed to amplify the whole open reading frame of the properdin gene. After successfully cloning this cDNA into a vector, confirming its identity by sequencing and radioactively labelling the specific fragment, this probe was applied against a membrane containing RNAs obtained from 3 sets of mouse organs. A positive signal corresponding to properdin was, as expected, observed for the spleen sample. The only other organ showing properdin expression was the thymus. No signal was observed for the heart, kidney, brain, lung, gut and even for the liver, an organ known to express properdin (Avery et al., 1993). This illustrated the limits of the Northern blot technique as its sensitivity was low. To summarise, in all the sets of mouse organs tested, properdin expression could only be detected in the two lymphoid organs (the spleen and the thymus).

By comparing the intensity of the signal obtained for properdin with the concentration of total RNA present in each sample (information given by the picture under UV light of the agarose gel), it was evident that properdin was expressed at a

higher level in the spleen of both the "LPS-treated" and "eye-infected" animals compared to the healthy unchallenged control. Unfortunately, more samples to study this in more details were not available and the Home Office Licence at this time did not cover experiments to provide further samples. However, it is still worth mentioning properdin expression could potentially be upregulated during bacterial infection.

In spite of the lack of information concerning properdin expression in mouse tissues in the literature, information could be obtained on the National Center for Biotechnology Information (NCBI) website. Two of its resources – namely GEOprofile and Unigene – offer expression profiles for a wide variety of genes in different species. This includes properdin expression by numerous mouse tissues. GEOprofiles data showing properdin expression (http://www.ncbi.nlm.nih.gov/geo/gds/gds_browse.cgi?gds=182) illustrate the microarray results obtained by Su and collaborators using the Affymetrix Genechip MG-U74A and RNAs isolated from various C57Bl/6L mouse tissues (Su et al., 2002). The properdin GEOprofile showed that the spleen had the greatest abundance of properdin mRNA, and it was followed by two other lymphoid organs – namely lymph node and bone marrow –, adipose tissue and mammary gland (figure 2-13). The thymus was shown to express properdin as well but its expression level was lower, similar to the one observed in the liver.

Unigene – its expression profiles for properdin can be found at http://www.ncbi.nlm.nih.gov/UniGene/ESTProfileViewer.cgi?uglist=Mm.3064 – corresponds to a "digital Northern blot". It presents EST (Expressed Sequence Tag) profiles and is expressed in TPM (Transcript Per Million). ESTs are small portions of the coding region of a gene made of cDNA and the digital properdin expression profiles presented on Unigene are calculated, for each tissue, by dividing the number of ESTs specific for properdin by the total number of ESTs present in the pool of cDNA libraries used. The results given by this resource should, however, be taken with care and only be used as preliminary data needed to be confirmed as no selection criteria are used to obtain these results (Wang and Liang, 2003). This could explain for example the unexpectedly low expression level of properdin found in the spleen using this resource. In fact, ESTs counted in the spleen dataset came from various sources, such as enriched spleen cells cDNA libraries, normalised cDNA libraries and

cDNA libraries containing only few hundred ESTs entries, all of that resulting in a bias. Nevertheless, the results presented by Unigene were suggesting that lymph node, adipose tissue and bone may have a higher properdin expression level than other tissues, as it was previously observed with GEOprofiles (figure 2-13).

As properdin expression in adipose tissue and mammary gland, two tissues supposedly expressing higher level of properdin, has already been investigated in the literature, I then decided to concentrate my work on a specific category of organs presenting elevated level of properdin expression: the lymphoid organs.

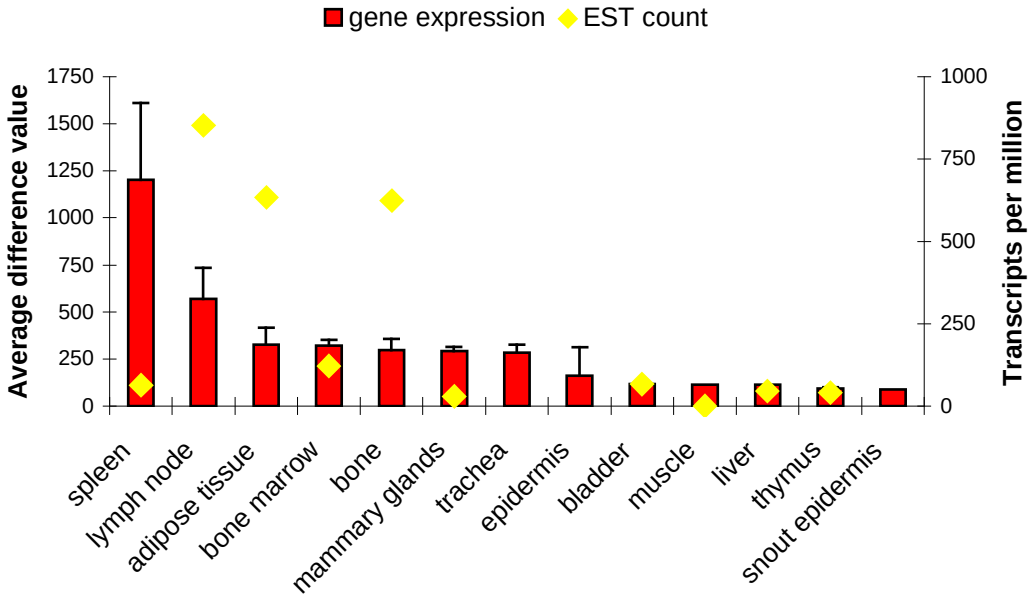

Figure 2-13: Expression profiles of properdin according to GEOprofile (red, left axis) and Unigene (yellow, right axis).

The expression of properdin by mouse thymus was confirmed by PCR using the same conditions as the one used to generate the Northern blot's probe. However, this technique did not allow the detection of properdin in lymph nodes. In order to quantify the level of properdin expression by these three lymphoid organs, a real-time PCR was conducted using these spleen, thymus and lymph node RNAs and primers specific for both the properdin gene and the housekeeping gene GAPDH. Despite its frequent use as an internal control for quantitative PCR, the ability of GAPDH to be used as a reference control has been challenged in recent publications where the level of expression of GAPDH was shown to differ in various mouse organs (Guo et al., 2002; Prieto-Alamo et al., 2003). The GEOprofile resource was therefore used to

check the level of GAPDH expression in spleen, thymus and lymph node and this level was shown to be similar in these three lymphoid organs, confirming the fact that GAPDH could be used as a reference control in this particular experiment. The three properdin expression profiles obtained by real-time PCR were in concordance with findings published on the GEOprofile website. Properdin was expressed at the highest abundance in mouse spleen, with an expression level 6 times higher than that observed for lymph node and 11 times higher than that observed for thymus.

All the results previously discussed proved the importance of the lymphoid organs to synthesise properdin. Moreover, the expression of properdin was more elevated in the spleen and the lymph nodes – two secondary lymphoid organs – than in the thymus and the bone marrow (according to GEOProfile data) – two primary lymphoid organs. This suggested that properdin was most needed where antigen-cell interactions and antibody production occured than where lymphocyte maturation took place. Being secondary lymphoid organs, spleen and lymph nodes possess quite a similar architecture and function. In fact, while the spleen was specialised in trapping blood-borne antigens, the lymph node's main function was to trap tissue-based and lymph-based antigens (Kindt et al., 2007).

2.4.2 Where is properdin expressed in spleen?

In order to understand better the function of properdin in secondary lymphoid organs, its localisation inside the spleen was investigated by immunofluorescence. The localisation of various complement components, including properdin, in three human lymphoid organs (spleen, lymph node and tonsil) has already been examined by Zwirner and coworkers in 1989. At this time, however, properdin was detected in none of these organs, in contrary to other components belonging to the classical pathway of complement (Zwirner et al., 1989).

To visualise properdin on frozen mouse spleen section, a fluorescent-labelled anti-properdin antibody was used. Unfortunately, due to the absence of anti-mouse properdin antibody on the market, the antibody used here was actually raised against human properdin. After proving that this anti-human properdin antibody could specifically recognise mouse properdin (by using the pre-absorbed antibody and properdin-deficient mouse section as negative controls), my attention focused on the localisation of the properdin signals detected on spleen sections.

The spleen is composed of two morphologically and functionally distinct compartments: the red pulp and the white pulp, and both are separated by a thin layer of cells known as the marginal zone. Blood enters the spleen via the splenic artery that gives rise to trabecular arteries and then to central arteries. When the latter enters the red pulp, it quickly gets surrounded by white pulp, where it divides into smaller branches. As the white pulp consists mainly of B lymphocytes, T lymphocytes, macrophages and dendritic cells, an immune response is initiated at this stage against the antigens carried by blood-borne pathogens. The blood carried by these small branches of central arteries then runs towards the marginal zone or towards the red pulp before entering the cords and venous sinuses of the red pulp compartment. Red pulp mainly consists of red blood cells and macrophages. At this stage, old and damaged erythrocytes present in the blood are phagocytised by macrophages. The red pulp can contain as well few plasmoblasts that migrate from the white pulp after antigen-specific differentiation and lead to the production of antibodies which can then quickly be released into the bloodstream via the collecting vein (figure 2-14) (Cesta, 2006; Mebius and Kraal, 2005).

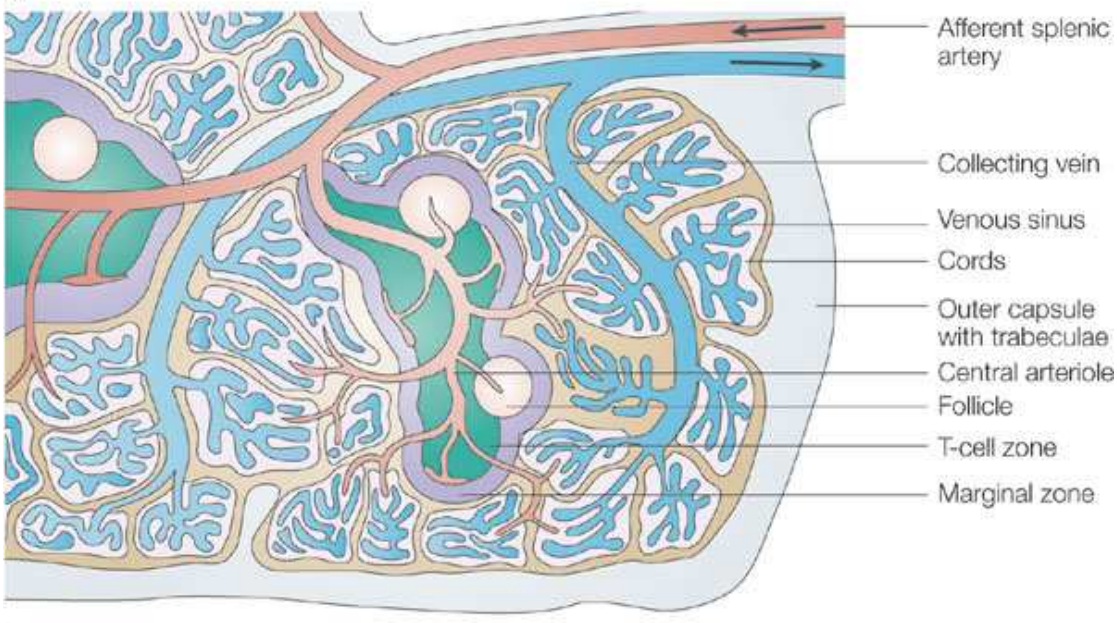

Figure 2-14: Schematic representation of the structure of the spleen (from Mebius and Kraal, 2005)).

Immunostained mouse spleen sections showed specific positive signals for properdin only in one particular area of the splenic white pulp. These signals were localised at the periphery of the white pulp, in follicle-like structures. Splenic

follicles, as lymphoid follicles, are mainly formed by B cells, specific macrophages known as tingible body macrophages, and follicular dendritic cells (Veerman and van Ewijk, 1975). At higher magnification, pictures of spleen sections showed properdin signals were actually observed in only a few cells inside these follicles. As tingible body macrophages and follicular dendritic cells are both found in small numbers in these follicles, I hypothesised that properdin positive cells could be one of them. This hypothesis was reinforced by the fact that properdin seemed to be detected on long cytoplasmic extensions interdigitating between other cells, this description corresponding to the morphology of both tingible body macrophages and follicular dendritic cells. As properdin has already been shown to be expressed by macrophages and dendritic cells, both cells could in principle be the ones carrying properdin.

To begin, I first looked at tingible body macrophages. CD68, or macrosialin, is a cell marker specific for tissue macrophages, including tingible body macrophages (Taylor et al., 2005). In the spleen, this cell marker is found on red pulp macrophages as well as on macrophages from the marginal zone and, in the white pulp compartment, on tingible body macrophages. Thus, staining of mouse spleen sections by this antibody, in addition to enabling the visualisation of tingible body macrophages in the white pulp, allowed distinguishing better the two compartments of the spleen. Analysis of spleen sections co-stained with both anti-properdin and anti-CD68 antibodies confirmed the presence of properdin inside the white pulp compartment of the spleen. Importantly, no colocalisation of CD68-positive cells and properdin-positive cells was observed, proving tingible body macrophages were not the cells carrying properdin antigen in the spleen. However, both CD68 and properdin-positive cells were situated close to each other, supporting the hypothesis that the cells carrying the properdin antigen were part of the splenic follicles. Similar experiments using FDC-M1 antibody, an antibody that specifically recognises follicular dendritic cells gave the same results, it is to say properdin-positive cells and FDC-M1-positive cells did not colocalise, but here again, both cell types were found in close vicinity. Finally, an antibody raised against CD45R/B220, a B-cell specific marker, was used. As expected, positive signals were detected all over the white pulp, B-cells being the major cell type in this compartment. However, the properdin-positive cells were not CD45R-positive. These experiments therefore showed that the properdin-positive cells present in the white pulp of mouse spleen were not $CD68^{+}$

(tingible body macrophages), FDC-M1$^+$ (follicular dendritic cells), nor CD45R$^+$ (B cells). Further experiments using different antibodies, including anti-MIDC8 antibody (interdigitating cells), should allow the identification of the properdin-positive cell population of the spleen. Once splenic properdin-positive cells will be identified, the logical next step would consist of looking at properdin expression on mouse lymph node sections, as both organs share a close architecture and both presents a high level of properdin expression.

2.4.3 Properdin binds to platelets

After studying properdin expression from an organ-point-of-view, properdin was investigated from a cellular perspective. As detailed in the introduction, properdin has been shown to be expressed or synthesised by a multitude of cells, including cells of the immune system (lymphocytes, granulocytes, monocytes and macrophages), but has not been examined yet on the auxiliary cells of the immune system, such as mast cells and platelets. These cells play an important role in inflammation, mainly by releasing the mediators contained inside their granules during activation, leading to the attraction of immune cells and mediators towards the site of infection. The study of properdin expression by mast cells is detailed in chapter 3.

Platelets are anuclear disc-shaped cells circulating in blood that are derived from megakaryocytes. They contain three types of granules – namely lysosomes, dense bodies and alpha granules – which contain various mediators used during blood clot formation and inflammation processes. Numerous studies have already linked platelet activation with complement activation (Del Conde et al., 2005; Peerschke et al., 2006). Lately, del Conde and coworkers have found that C3b could bind to activated platelets via the surface protein P-selectin, and that complement activation could occur as C3a was produced and MAC formed on platelet's surface upon activation (Del Conde et al., 2005). The C3 convertase found on activated platelets was formed using factor B, meaning complement activation occurred via the alternative pathway. The ability of properdin, positive regulator of the alternative complement pathway, to associate with resting and activated platelet's surfaces was therefore investigated. Flow cytometric analysis showed properdin was detected on the surface of resting platelets. The binding of properdin to the platelet's surface was seen to increase when the platelets were activated and more properdin was detected

on platelets activated with strong agonists (TRAP and CRP), where more degranulation occurs, than on platelets activated with weak agonist (ADP). This was consistent with the C3b-binding intensity observed on activated platelets by other groups, this C3b-binding pattern being itself related to the highest expression of P-selectin on platelets activated by strong agonists (Del Conde et al., 2005; Goodall and Appleby, 2004). This increase of properdin-binding to platelet's surface during activation may be linked to the increased number of C3b molecules binding to platelet's surface, the binding of properdin to C3b allowing to amplify the alternative complement pathway C3 convertase activity.

3 Properdin synthesis in mast cells

3.1 Introduction

3.1.1 Mast cells

3.1.1.1 General features

Mast cells (or mastocytes) are auxiliary cells of the immune system. They have first been described in 1878 in the doctoral thesis of Paul Ehrlich (mast cells being the English translation of the German term “Mastzellen”, meaning “well-fed cells”) as aniline-reactive granular cells of the connective tissue (Crivellato et al., 2003). They are detected in the vicinity of blood vessels throughout the body, but mainly in the skin and the mucosa of gut and airways and mature mast cells are not physiologically found in the blood (Metz and Maurer, 2007).

Mast cells arise from bone marrow $CD34^+$ progenitors, either from the common myeloid progenitors (CMP) together with monocytes and granulocytes, or directly from multipotential progenitors (MPP) (Rosenbauer and Tenen, 2007). Their precursors circulate in the blood and the lymph, before entering a tissue mucosa where they differentiate into long-lived mature mast cells under the action of Stem Cell Factor (SCF) and various cytokines. SCF, the mast cell growth factor, is mainly produced by fibroblasts and endothelial cells and acts on mast cells by binding to their c-kit receptors (Broudy, 1997; Metz and Maurer, 2007).

Mast cells are 8 to 20µm ovoid cells with short cytoplasmic extensions, containing a large monolobed nucleus, a multitude of large dense metachromatic cytoplasmic granules, few lipid bodies and numerous mitochondria (Dvorak, 2005). Their granules contain different substances called mediators, the best-known being histamine, serine proteases (chymase, tryptase and carboxypeptidase A) and proteoglycans (heparin and chondroitin sulfate E) (Prussin and Metcalfe, 2006). Mast cells are divided into two subtypes according to the presence in their granules of both tryptase and chymase (MC_{TC}), or tryptase alone (MC_T). Another classification divides mast cells into two sub-populations according to their localisation. Actually, mast cells found in connective tissue (CTMC) (skin, airways) do not possess the same granule content as mast cells found in mucosa (MMC) (gastrointestinal muscosa).

CTMCs are more likely to be MC_{TC} whereas MMCs are more likely to be MC_T (Feger et al., 2002; Metcalfe et al., 1997; Prussin and Metcalfe, 2006).

Mast cell's mediators are divided into two categories: the pre-formed mediators (histamine, proteoglycans, neutral proteases and cytokines), which are stored inside the granules, and the *de novo*-synthesised mediators (cytokines, chemokines and lipid mediators).

3.1.1.2 Mast cell activation

Activation of mast cells results in the release of different pre-formed mediators and/or newly synthesised mediators. Two kinds of mast cell activation have been described: the anaphylactic degranulation and the piecemeal degranulation. The so-called "allergic activation", or anaphylactic degranulation, occurs mainly after stimulation by IgE and results in the release of the granules contained in the cytoplasm of the cells. The other type of mast cell activation, known as piecemeal degranulation, results in the release of the electron dense granules' content with the retention of the empty granules' containers inside the cytoplasm of the cell (Theoharides et al., 2007).

The pattern of degranulation taking place in mast cells actually depends on the molecule responsible for the activation. Numerous molecules are known to activate mast cells, such as IgE, complement anaphylatoxins C3a and C5a, TLR (Toll Like Receptor) ligands, IgG, bacterial products and various cytokines (Galli and Tsai, 2008).

3.1.1.3 Roles of mast cells

For many years, mast cells were only seen as "allergy cells". During type I hypersensitivity reactions, allergens bind to sensitised mast cells coated with IgE via their highly expressed FcεRI receptors and this leads to an anaphylactic activation of mast cells and the release of their granules' content, creating an immunological response in the surrounding tissue that is responsible of the allergic symptoms (Bischoff, 2007).

In the past decade, mast cells have emerged as being much more than just allergy cells, showing various physiological and pathophysiological functions, mainly because of the quick differential release of the various mediators present in their granules upon stimulation, and because of their location within tissues with direct

contact with the external environment and the blood vessels. Thus, mast cells are now known to be involved as well in both innate and acquired immunity. One of the first lines of evidence showing the implication of mast cells during bacterial infection was brought by Echtenacher and coworkers in 1996. They observed that, following caecum ligation and puncture (CLP), a model of acute septic peritonitis, the development of an immune response was less effective and the mortality rate was higher in mast cell-deficient mice than in their wild type littermates, proving the importance of mast cells in this specific model (Echtenacher et al., 1996). Other studies have since confirmed the key role played by mast cells during bacterial and parasitic infections (Malaviya et al., 1996; Siebenhaar et al., 2007). In addition to these roles, mast cells by interacting with immune cells, such as dendritic cells or lymphocytes, are able to induce the acquired immune system as well (Metz and Maurer, 2007). Mast cells play their protective immune role against pathogens by quickly recruiting various inflammatory cells to the site of infection and by enhancing the vascular permeability, activating inflammatory cells and direct killing of the micro-organisms, either via their proteases and anti-microbial peptides, or by phagocytosis (Lin et al., 1999; Marshall and Jawdat, 2004). Mast cells have been shown to be involved as well in various autoimmune diseases, such as multiple sclerosis, rheumatoid arthritis and bullous pemphigoid (Benoist and Mathis, 2002).

Finally, mast cells have been shown to play an important role in tissue remodelling. Tissue remodelling is essential for the healing process observed after injury, but can be responsible as well for the deposition of exaggerated amount of extracellular matrix (ECM) collagen, leading to the development of fibrosis. Mast cell plays its role in this process via the release of its mediators, mainly tryptase, as this protease has been shown to be involved in both collagen synthesis and degradation, and fibroblast and epithelial cells' proliferation (Cairns, 1998; Okayama et al., 2007).

3.1.1.4 Mast cells and complement

As mentioned in the general introduction, C3a and C5a molecules are two strong mast cell activators that lead to the anaphylactic degranulation of serosal mastocytes. In addition to this stimulatory role, another role was attributed to C3a, but only in mucosal mast cells this time. In these cells, C3a, by binding to the β-chain of the FcεRI present on the surface of mast cells, prevents the activation of mast cells by IgE (Erdei et al., 2004). C3a molecules are therefore able to have both a stimulatory

and an inhibitory effect on mast cell activation. C1q, component of the classical complement pathway, was shown to play an important role too in mast cell activation during infection, as its presence altogether with the one of the α2β1 integrin on the mast cell's surface was required for mast cell activation and cytokine secretion (Edelson et al., 2004; Edelson et al., 2006).

Moreover, CR2 and CR3, both present on the membrane of mast cells, were shown to be important during infection using CR2- and CR3-deficient mice in a CLP model, a mast cell-dependent model of acute septic peritonitis (Gommerman et al., 2000; Rosenkranz et al., 1998).

Another line of evidence for the importance of the complement system in mast cells is illustrated by the fact that C3-deficient, C4-deficient and properdin-deficient mice are all more sensitive than their wild-type littermates to CLP (Prodeus et al., 1997; Stover et al., 2008).

Finally, the binding of complement opsonins present on the bacterial surface to CR1 and CR3 present on mast cells' surface enhanced their phagocytic function (Andrasfalvy et al., 2002).

3.1.1.5 Mast cell lines used in this study

Both mast cell lines used in this study were isolated from patients with mastocytosis, a pathology where mast cells accumulate in different organs as well as in peripheral blood and bone marrow (Horny et al., 2007).

The HMC-1 (Human Mast Cell-1) cell line was established by Butterfield and collaborators in 1988 (Butterfield et al., 1988). It became the first mast cell line available and is nowadays a widely used cell line (Drexler and MacLeod, 2003). This cell line derives from the peripheral blood of a 52-year-old woman with mast cell leukemia. HMC-1 cells are immature mast cells belonging to the MC_T type. They possess 2 point mutations in their c-kit gene, that lead to a constitutive activation of the Kit protein and, therefore, HMC-1 cells do not require the presence of SCF to proliferate (Furitsu et al., 1993). The major disadvantage of this cell line is its lack of a functional FcεR (Drexler and MacLeod, 2003).

The LAD 2 (Laboratory of Allergic Diseases 2) cell line was established by Kirshenbaum and collaborators in 2003. This cell line derives from bone marrow aspirates of a 44-year-old male with mast cell sarcoma/leukemia. In contrast to

HMC-1 cells, LAD 2 cells respond to SCF and have functional FcεRI. They are tryptase positive and 37% are chymase positive (Kirshenbaum et al., 2003).

LAD 2 cells could not be used in all the following experiments due to their slow doubling rate (2 to 3 weeks in comparison to the 80 hours for HMC-1 cells) and their need of SCF, which make them expensive to maintain in culture for a prolonged period of time (Drexler and MacLeod, 2003).

3.1.2 Exocytosis

Exocytosis is an event performed in a calcium-dependent or calcium-independent manner by all eukaryotic cells allowing the release of different populations of vesicles into the external micro-environment. Two kinds of vesicles released during exocytosis – namely microvesicles and exosomes – have been shown to be specifically involved during immune responses, by mediating cell-to-cell communication. Both of these vesicles are produced by mast cells.

Microvesicles are 100nm to 1µm-diameter vesicles derived from the shedding of the cell plasma membrane (Ratajczak et al., 2006). They are mainly released by leukocytes, platelets, erythrocytes and neoplastic cells and are normal constituents of the plasma (Gasser et al., 2003; Gasser and Schifferli, 2005; Heijnen et al., 1999; Ratajczak et al., 2006). Their proteins' content differs according to their cellular origin.

Exosomes, as for them, are 40 to 90nm small round membranous vesicles contained in multivesicular bodies (MVB) and released after the fusion of these MVB with the cell plasma membrane (Keller et al., 2006). They derive from cultured hematopoietic cells and have already been isolated from B lymphocyte, reticulocyte, platelet, dendritic cell and mast cell's culture supernatant, as well as from plasma (Caby et al., 2005; Heijnen et al., 1999; Skokos et al., 2001; Thery et al., 2001; Wubbolts et al., 2003).

3.1.3 Aim of the study

Mast cell is the only cell type of the immune system that has not been examined yet for properdin synthesis. However, mast cells are tissue-based cells that can trigger a quick immune response during infection by releasing the mediators present in their granules. The production of properdin by mast cells could potentially

amplify complement activation in no time at the site of the infection and could therefore confer a better immune response to the host. This response could even be more important if mast cells could, like neutrophils, release properdin via their granules during activation.

The aim of this project was therefore to investigate whether mast cells could produce properdin, and if they did, to characterise properdin synthesis and secretion by mast cells.

3.2 Material and methods

3.2.1 Cells and media

The two mast cell lines used in this study, HMC-1 and LAD 2, were provided by Prof. Peter Bradding (University of Leicester).

HMC-1 cells were grown in Iscoves media (Gibco) supplemented with 10% iron supplemented FCS (Gibco; Fisher, Loughborough, UK) and 1.2mM monothioglycerol (Sigma-Aldrich). Cells were maintained in a humidified incubator at 37°C at 5% CO_2 for 3 days. Then, the cell culture medium was removed and cells were resuspended in an appropriate volume of fresh cell media to maintain a cell density between $5x10^5$ and $1x10^6$ cells/ml (Butterfield et al., 1988). When needed, HMC-1 cells were frozen in 10% DMSO-FCS in a freezer at -80°C for 2 days and then stored in liquid nitrogen.

The HMC-1 serum-free media used for the exosome extraction consisted of Iscoves media supplemented with 1.2mM monothioglycerol and 0.1% ITS-G (Gibco), a synthetic medium supplement containing insulin, transferrin and selenium, and used as a substitute for serum in cell culture.

LAD 2 cells were grown in Stem-pro SFM medium (Gibco) supplemented with 2mM L-glutamine (Gibco) and 100ng/ml of recombinant human Stem Cell Factor (rhSCF) (R&D Systems, Abingdon, UK). Cells were maintained in a humidified incubator at 37°C at 5% CO2. Every week, half of the cell culture medium was removed and cells were resuspended in an appropriate amount of fresh medium to maintain the cell density between $5x10^5$ and $1x10^6$ cells/ml in the flask (Kirshenbaum et al., 2003).

Aliquots of HL-60, K562 and Jurkat cells in culture were kindly provided by Dr Mike Browning (University of Leicester).

3.2.2 Mast cell stimulation

Four millilitres of fresh HMC-1 cell medium and 1ml of HMC-1 cells suspension containing $2x10^5$ cells/ml were placed into the wells of 6-well plates (Nunc; Scientific Lab Supplies, Wilford, UK). Five microlitres of either HMC-1 cell medium, IL1β (Sigma-Aldrich, 10ng/µl), TNFβ (Sigma-Aldrich, 10ng/µl), TGFβ

(Sigma-Aldrich, 10ng/µl), IFNγ (Sigma-Aldrich, 10ng/µl), GM-CSF (Sigma-Aldrich, 10ng/µl), or LPS (Sigma-Aldrich, 1µg/µl) were addedinto each well and plates were incubated for 24 hours at 37°C at 5% CO_2. Each condition was performed in 2 separate wells.

The next day, the wells containing HMC-1 cells cultivated under the same conditions were pooled together. Cells were spun down at 250g for 5 minutes. RNAs were extracted from each cell pellet using TRIzol reagent (see chapter 3.2.4.1), while proteins were 10-times concentrated by passing down 2ml of the cell culture supernatant through a Centricon YM-30 column (Amicon; Millipore, Watford, UK) for 2 hours at 400g. The liquid remaining into the Centricon was therefore containing no proteins with a molecular weight of less than 30KDa. The protein concentration in each sample was then measured by the 2-D Quant kit assay (see chapter 3.2.7.1) and the volume of each sample was adjusted with sterile PBS (Oxoid) to ensure all the samples had the same final concentration of total protein.

3.2.3 Exosome extraction

Exosome extraction was performed as described by Al-Nedawi and collaborators and is illustrated in figure 3-1 (Al-Nedawi et al., 2005). HMC-1 cells were harvested in an exosome-free medium for three days before to extract the exosomes, as FCS is known to contain exosomes (Wubbolts et al., 2003). This exosome-free medium consisted in fact of the supernatant obtained after ultracentrifugation of the HMC-1 cell's medium at 70,000g for 2 hours that was then filtered using 0.22µm Acrodisc filters (PALL corporation; Fisher, Loughborough, UK) (Caby et al., 2005). This ensured that no vesicle was present in the media before adding the HMC-1 cells. Twenty four hours before exosome extraction, HMC-1 cells (10^7 cells/ml) were transferred into serum-free media (see chapter 3.2.1).

Exosomes were then extracted from the cell culture supernatant by differential centrifugation at 4°C. First, the medium was centrifuged at 300g for 5 minutes to pellet the cells. The supernatant was then depleted from any cell debris by spinning it down at 1200g for 20 minutes. Big vesicles were removed by ultracentrifuging the supernatant at 10,000g for 30 minutes (Ultracentrifuge TL-100, Beckman Coulters) and exosomes were finally extracted after ultracentrifugation at 70,000g for 2 hours (Skokos et al., 2001). The pellets obtained at each centrifugation steps were all

washed twice in PBS and centrifuged at their isolation speed. They were then resuspended in an appropriate volume of PBS and kept in the freezer until further use.

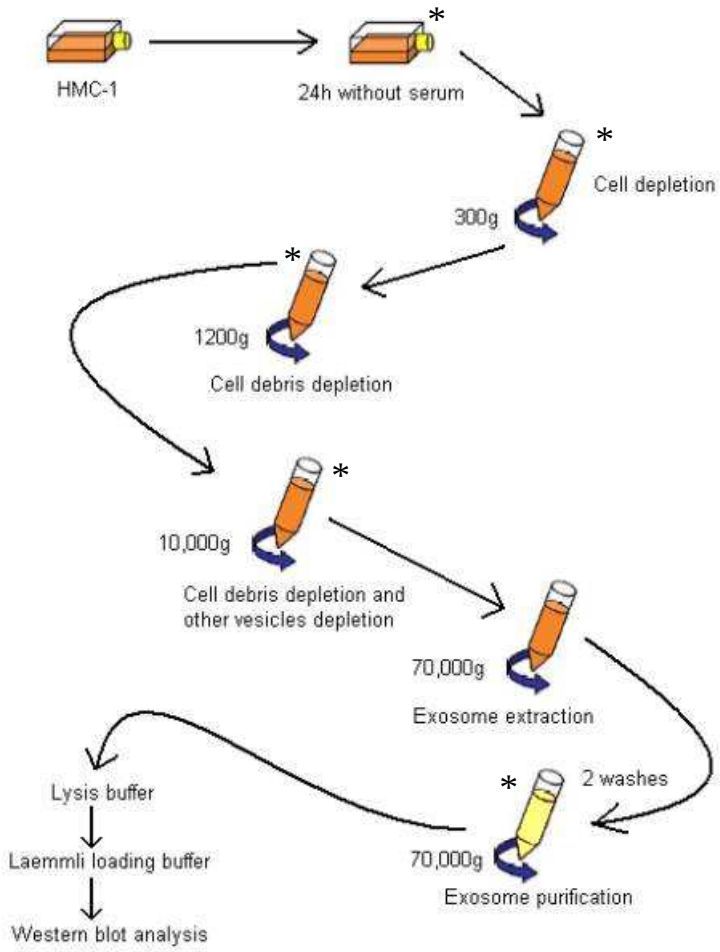

Figure 3-1: Exosome purification (adapted from Quah and O'Neill, 2005). Asterisks represent the fractions which were analysed by Western blot.

3.2.4 Reverse Transcriptase Polymerase Chain Reaction

3.2.4.1 RNA extraction and cDNA synthesis

Total RNAs were extracted from HMC-1 and LAD 2 cells using TRIzol reagent following the manufacturer's instructions. Five hundred microlitres of TRIzol reagent were added to each cell pellet and then mixed with 100µl of chloroform. The same protocol as the one used to extract RNAs from mouse tissues was then followed (see chapter 2.1.2). Next, the concentration of DNase I-treated RNAs was measured and first strand cDNAs were synthesised (see chapters 2.1.3 and 2.1.4.1).

3.2.4.2 Polymerase Chain Reaction

3.2.4.2.1 PCR specific for the ORF of the human properdin gene

Touch-down PCR is more specific than a classical PCR as it begins with an annealing temperature far higher than the optimal Tm, allowing a very specific amplification of poorly-represented DNA. The annealing temperature then decreases of one increment at each cycle to allow the amplification of the specific fragment created (as this fragment is getting more abundant at each cycle).

The reaction was performed by mixing the following reagents in a 0.5ml PCR reaction tube: 0.2mM of each dNTPs (PCR Nucleotide Mix, Promega), 2.5mM of $MgCl_2$ (ABgene), the 10x reaction buffer IV (ABgene) appropriately diluted in DEPC-treated H_2O, 4µM of each primer (forward and reverse HumPN primers (table 2-1)), 40µl/ml of template cDNA (obtained in chapter 3.2.4.1) and 40U/ml of Thermoprime plus DNA polymerase (ABgene). The final volume of each PCR reaction was of 25µl.

The tube was then pulse-centrifuged and placed into a thermocycler (Gene Amp PCR System 9700, PE Applied Biosystems). The following touch-down program was finally applied to the machine. At the step 2 of this touch-down PCR program, the annealing temperature decreases by 0.8°C increment at each cycle and reaches the temperature of 60°C after the 15 first cycles. It then continues for 25 more cycles at the step 3 with this annealing temperature of 60°C.

Step	Temperature (°C)	Time (sec)	Number of cycles	Increment	Function
1	95	90	1		Initial denaturation
2	95 **72** 68	45 45 180	15	-0.8°C/cycle	Denaturation Annealing Extension
3	95 **60** 68	45 45 180	25		Denaturation Annealing Extension
4	68 4	420 ∞	1		Final extension

The PCR products were analysed by agarose gel electrophoresis (see chapter 3.2.5).

3.2.4.2.2 PCR specific for the primers used in real-time PCR

The primers used in real-time PCR were HumPNsh1, HumPNsh2, HumPNsh3, HumPNsh4, HumGAPDH and MouGAPDH (see table 2-1). The reaction was performed by mixing the following reagents in a 0.5ml PCR reaction tube: 0.2mM of each dNTPs (PCR Nucleotide Mix, Promega), the 10x polymeric DNA buffer (Promega) appropriately diluted in DEPC-treated H_2O, 4µM of each primer (forward and reverse), 40µl/ml of HMC-1 cDNA and 40U/ml of Taq DNA polymerase (Promega). The concentration of $MgCl_2$ used for each reaction is specified further down in the text (see chapter 3.3.3.1.1), as the optimal magnesium concentration was different for each pair of primers.

The tube was then pulsed-centrifuged and placed into a T1 plus thermocycler (Biometra). The following programme was applied to the machine, except when notified differently:

Step	Temperature (°C)	Time (sec)	Number of cycles	Function
1	95	90	1	Initial denaturation
2	95 60 72	10 10 25	40	Denaturation Annealing Extension
3	72 4	180 ∞	1	Final extension

The PCR products were then analysed by agarose gel electrophoresis (see chapter 3.2.5).

3.2.5 Agarose gel electrophoresis

Agarose gel electrophoresis was performed as explained in chapter 2.1.4.3. Different percentages of gel were made according to the length of the expected PCR product. Generally, small fragments (below 300bp) were separated using 1.2% (w/v) agarose gel, whereas bigger fragments (above 1kb) were run into 0.8% agarose gel. Fragments having a size comprised between 300bp to1kb were visualised using 1% agarose gel.

DNA samples were mixed either with a 6x bromophenol blue loading dye, or with a 5x orange G loading dye (50% (v/v) glycerol, 50% (v/v) TAE, 1% (w/v) orange G), again according to the size of the expected product. Bromophenol blue overlaps the 300bp DNA double stranded fragment when migrated through agarose gel, whereas Orange G migrates as a 50bp DNA double stranded fragment. Thus, every time 300bp PCR fragments were expected, the orange G loading dye was used.

Ladders used in this study were either the benchtop PCR Markers (Promega), the low DNA Mass Ladder (Invitrogen, previously mixed 1:4 in loading dye), or the 1kb DNA Ladder (Promega).

3.2.6 Real-time PCR

cDNAs were synthesised from RNAs extracted from stimulated HMC-1 cells and from mouse organs and these cDNAs were used as templates for the real-time PCR. Real-time PCR was performed using the SYBR Green Taq Ready/Mix for quantitative PCR, capillary formulation (Sigma-Aldrich) and HumPNsh4 primers were used to quantify properdin expression whereas primers specific for GAPDH (Glyceraldehyde-3-phosphate dehydrogenase) were used as a control reference (HumGAPDH for mast cells experiments and MouGAPDH for mouse experiments). GAPDH was used as a reference because the expression of this housekeeping gene stays constant upon stimulation. The reaction was performed by mixing 10µl of SYBR Green with 7.2µl of H_2O, 2µl of each cDNA (previously diluted 1:10 in DEPC-H_2O) and 4µM of each primer (forward and reverse). As the SYBR green mix contained already a substantial amount of $MgCl_2$, no magnesium chloride was added to the reaction mix this time. In addition to that, 2µl of different dilutions of the cDNA extracted from non-stimulated HMC-1 cells (previously diluted 1:2, 1:4, 1:20, 1:40 and 1:200 in DEPC-H_2O) were used to construct the standard curve. A negative control sample (with dH_2O instead of the cDNA template) and a positive control sample (using the plasmid prep obtained in chapter 3.3.2 as a template) were also prepared for each run.

All samples were then transferred into a 20µl LightCycler capillary (Roche). Capillaries were loaded into a carousel, which was itself inserted into the LightCycler (Roche). The following programme was applied to the machine via the LightCycler software version 3 (Roche). The first, second and last step of the programme were the same as the ones of a classical PCR, while the third step was a slow denaturing step from the primers Tm (65°C) to 95°C. The fluorescence was measured in each capillary at the end of each cycle and recorded during all the denaturing process of the third step. The fluorescence values obtained were then used by the computer to generate a melting curve using the LightCycler software version 3 (Roche). The analysis of this melting curve allowed checking whether any contaminants or primer dimers were among side the amplicon. The melting curve showed only one peak for each sample with every primer as illustrated on figure 3-2. The amplicon obtained using HumPNsh4 primers had a Tm of 90°C (expected Tm: 91.8°C, using the formula

Tm=0.41x(GC%)+69.3-(650/length product)), whereas the amplicon obtained using GAPDH primers presented a Tm close to 82°C (expected Tm: 82.9°C).

Once the melting curve confirmed that only one product was amplified, data were analysed using the LightCycler software version 3 (Roche). First, the baseline was adjusted using the arithmetic option. The level of non-specific background was then set up by dragging the noise band and the data were analysed using the fit points analysis method. The best fit of the curve was calculated using 3 points in the log-linear part of each curve. The crossing point (expressed in cycle number) represented by the interaction between the sample curve and a crossing line (previously defined) was then measured. The crossing points obtained for each of the standard sample were used to build a standard curve representing the relationship between the DNA concentration and the number of cycles (see figure 3-3). The relative expression of each sample was finally calculated based on this standard curve.

Step	**Temperature (°C)**	**Time (sec)**	**Slope (C°/sec)**	**Number of cycles**	**Acquisition mode**	**Function**
1	95	900	20	1	None	Denaturation
2	95 **T** 72	15 15 25	20 20 20	40	None None Single	Cycling
3	95 65 95	2 10 0	20 1 0.1	1	None None Continuous	Melting curve
4	4	∞		1	None	Cooling

T was 60°C for HumPNsh4 and 57°C for HumGAPDH and MouGAPDH.

A

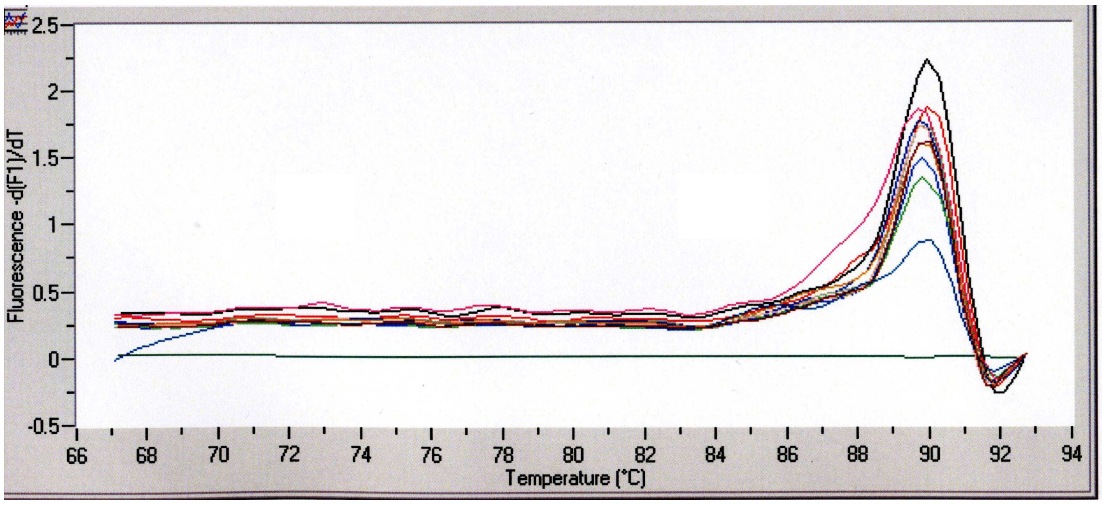

B

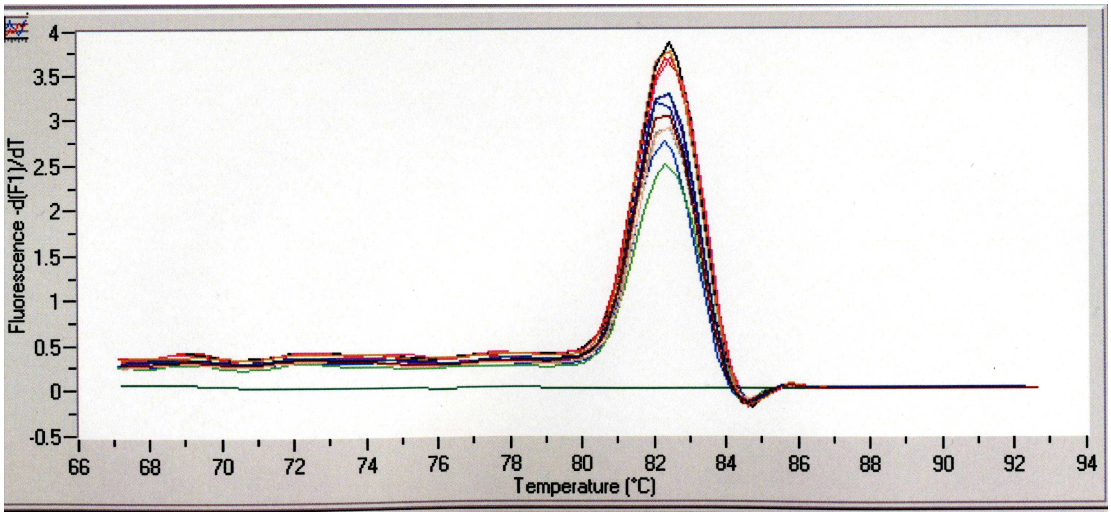

Figure 3-2: Representative melting curves obtained by real-time PCR. A: using HumPNsh4 primers; B: using HumGAPDH primers. The green line corresponds to the negative control.

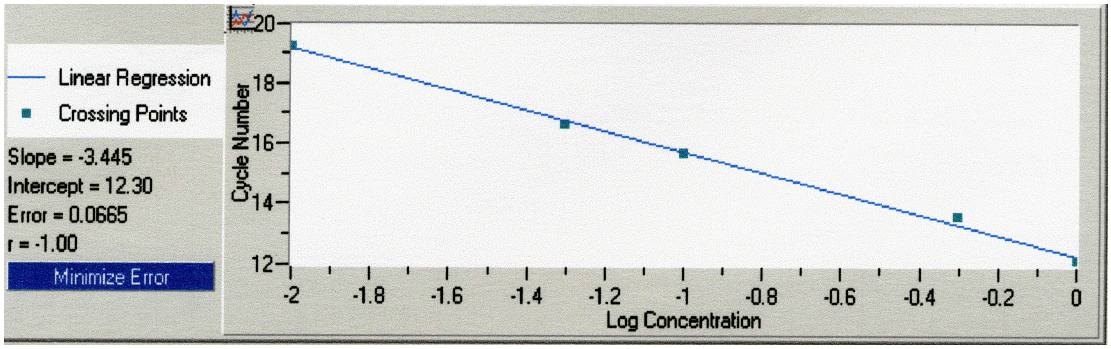

Figure 3-3: Representative standard curve obtained by real-time PCR using HumGAPDH primers. The DNA concentrations of the standards were plotted against the number of cycles to create the standard curve.

3.2.7 Determination of the protein concentration

In order to compare the properdin concentration between different samples, the total protein content of each sample was measured using either the 2-D Quant Kit (Amersham Biosciences), or the Bradford protein assay (Bio-Rad), both following the manufacturer's instructions.

3.2.7.1 2-D Quant Kit

Briefly, each sample and each standard (BSA) were mixed with a precipitant and a co-precipitant solution and all the precipitated material, including the protein, was then spun down and the pellet was resuspended in a copper-containing solution. Copper ions are known to bind specifically to proteins. Therefore, as they bound to the protein present in each sample, the cupric ions (Cu^{2+}) present in the copper solution were reduced to cuprous ions (Cu^{+}). To determine the concentration of protein present in each sample, the amount of cupric ions left in each solution was measured. This was done by adding a colour reagent solution into the mixture for 15 minutes and by measuring the absorbance at 480nm using a 50 BIO UV-visible spectrophotometer (Varian). A standard curve was then built and the total protein concentration of each sample was determined by plotting their OD value against the standard curve, the quantity of protein present in each sample being inversely proportional to the quantity of cupric ions left in solution. This protocol was used to measure the total protein concentration of the "stimulated-cell culture samples".

3.2.7.2 Bradford protein assay

A protein standard curve was constructed by diluting 2, 4, 6, 8 and 10µg of BSA into 800µl of H_2O. Each sample was appropriately diluted as well into H_2O to obtain a final volume of 800µl. Two hundred microlitres of the dye reagent (Bio-Rad) were then added to each sample and standard, mixed by vortexing and transferred into a plastic cuvette. This dye (that is, in fact, a Coomassie brilliant blue G-250 dye) changed colour (red to blue) when binding to protein occured and this was visualised after 15 minutes of incubation at room temperature by measuring the absorbance at 595nm in each cuvette using a 50 BIO UV-visible spectrophotometer (Varian). A standard curve was then built and the total protein concentration of each sample was determined by plotting their OD value against the standard curve. This protocol was used to measure the total protein concentration of the "ultracentrifuged cell and vesicle samples".

3.2.8 Western blot

3.2.8.1 Preparation of the gel

The mini-Protean II system (Bio-Rad) was used to mould the acrylamide gels. Ten or twelve percent SDS-PAGE resolving gels were first prepared by mixing together the components listed in table 3-1. Four and a half millilitres of the mixture were then poured between the glass plates of the mini-Protean II system and water was added on top of the gel to prevent its desiccation. The gel was left to polymerise at room temperature for 20 minutes. During this time, the stacking gel was prepared by mixing together 1.4ml of H_2O, 330µl of acrylamide/bis-acrylamide 30% solution (Sigma-Aldrich), 250µl of 1M Tris-HCl (pH 6.8), 20µl of 10% (w/v) SDS (Fisher), 20µl of 10% (w/v) ammonium persulfate (Fisher) and 2µl of TEMED (Bio-Rad). After removing all the water present on top of the resolving gel, the stacking gel was poured until the top of the glass plates and a comb was inserted to create the wells. The gel was finally left to polymerise at room temperature for at least 1 hour 20 minutes.

Gel percentage	**10%**	**12%**
H_2O	1.9ml	1.6ml
Acrylamide/bis-acrylamide 30% solution	1.7ml	2.0ml
1.5 M Tris (pH 8.8)	1.3ml	1.3ml
10% SDS	50µl	50µl
10% Ammonium Persulfate	50µl	50µl
TEMED	2µl	2µl

Table 3-1: Composition of SDS-PAGE resolving gels.

3.2.8.2 Samples preparation

For “cell culture samples”, 4µl of the adjusted cell supernatants were mixed with 15µl of 2x SDS-PAGE sample buffer (10% (v/v) glycerol (Sigma-Aldrich), 50mM Tris-HCl (pH 6.8), 4% (w/v) SDS, 4% (v/v) β-mercaptoethanol (Sigma-Aldrich) and 0.2% (w/v) bromophenol blue) and 11µl of PBS and boiled for 10 minutes. After chilling on ice for 1 minute, 20µl of each sample and 5µl of the broad

range prestained SDS-PAGE standards (Bio-Rad) were loaded into the wells of a 12% SDS-PAGE gel.

For "purified cell and vesicle" samples, an appropriate volume of each sample was first mixed with a lysis buffer (2% Nonidet P-40 (BDH; VWR International, Lutterworth, UK), protease inhibitors (Sigma-Aldrich) in PBS) for 20 minutes at 4°C (Caby et al., 2005). Total protein concentration inside each sample was then measured using the Bio-Rad protein assay (see chapter 3.2.7.2) and various amounts of total protein from each sample were mixed with PBS to obtain a final volume of 12µl. Four microliters of 5x SDS-PAGE sample buffer (0.25M Tris, 50% (v/v) glycerol, 5% (w/v) SDS, 0.25M DTT, 1% (w/v) bromophenol blue) were then added to the mix. Samples and 8µl of the prestained Precision plus protein standards (Bio-Rad) were boiled for 10 minutes, chilled on ice for 1 minute, and loaded into the wells of a 10% SDS-PAGE gel.

3.2.8.3 Western blotting

Gel electrophoresis was performed in running buffer (25mM Tris, 190mM glycine (Fisher), 0.1% (w/v) SDS, pH 8.3) for 1.5 hours at 90V. The gel was then blotted onto a nitrocellulose membrane (TransBlot, Bio-Rad) in ice-cold transfer buffer (50mM Tris, 40mM glycine, 10% methanol, 0.03% SDS) for 1 hour at 250mA. After transfer, the nitrocellulose membrane was stained with Red Ponceau (0.1% (w/v) Ponceau S (Sigma-Aldrich), 5% (v/v) acetic acid) for 5 minutes to visualise the efficiency of the transfer, washed 3 times 5 minutes in PBS and blocked overnight at 4°C in a blocking solution under agitation.

The next day, the membrane was incubated for 2 hours with a solution containing the primary antibody at room temperature under agitation. After 4 washes in a washing solution, the membrane was incubated for 1 more hour with a solution containing the HRP-labelled secondary antibody at room temperature under agitation. The membrane was washed 4 more times in the washing solution. The detection of the HRP-labelled antibody bound to the membrane was done using an ECL kit, following the manufacturer's instructions. The ECL-treated membrane was next wrapped in cling film and exposed to an X-ray film in a cassette for 30 seconds to 5 minutes. The film was finally developed manually as explained in chapter 2.1.6.5.

The availability of new antibodies and reagents on the market during the time of my PhD allowed me to improve the detection limit and the quality of the technique, explaining why different conditions were used to detect properdin on "cell culture samples" and "purified cells/vesicles samples". These conditions are summarised in table 3-2.

3.2.9 Properdin ELISA

This was done using the properdin ELISA kit (Antibody Shop) by Kathryn Staley (University of Leicester) following the manufacturer's instructions. Briefly, 100µl of appropriately diluted "purified cell/particle samples" and of each calibrator were incubated for 1 hour at room temperature inside the pre-coated wells of the ELISA plate. After 3 washes in the washing solution, 100µl of the biotinylated properdin antibody were added to each well and let to stand for 1 hour. Three more washes were applied before incubating the plate for 1 hour with the HRP-Streptavidin-conjugated antibody. The plate was washed 3 last times before adding the TMB substrate and, 15 minutes later, the stop solution. The absorbance across the plate was measured at 450nm using a microplate reader (Model 680, Bio-Rad) and analysed using the microplate manager software, version 5.2.1 (Bio-Rad). The standard curve was generating using a five-parameter logistic curve fitting (type Rodbard).

Samples	« Cell culture samples »	« Purified cells/vesicles samples »
Blocking solution	5% (w/v) skimmed milk-PBS	5% (w/v) BSA-TBS
Antibody solution	1% (w/v) skimmed milk-PBS	3% (w/v) BSA-TBS
Primary antibody	Polyclonal rabbit anti-human properdin antibody (provided by Prof. W. Schwaeble, University of Leicester [from Prof. K. Reid, University of Oxford]) diluted 1:1000 in the antibody solution	Monoclonal mouse anti-human properdin HYB 039-06 antibody (Antibody Shop) diluted 1:1000 in the antibody solution
Washing solution	0.05% Tween 20 (Sigma-Aldrich)-PBS	0.05% Tween 20-TBS
Secondary antibody	HRP-labelled goat anti-rabbit IgG antibody (Sigma-Aldrich) diluted 1:2500 in the antibody solution	HRP-labelled goat anti-mouse IgG antibody (Sigma-Aldrich) diluted 1:6000 in the antibody solution
ECL kit	ECL Western Blotting kit (Amersham Biosciences)	Supersignal West Dura Extended Duration substrate (Pierce; Perbio Science, Cramlington, UK)
X-ray film	Super RX (Fuji Medical; Genetic Research Inst., Braintree, UK)	Hyperfilm ECL (Amersham Biosciences)

Table 3-2: Western blot conditions used for "cell culture samples" and "purified cells/vesicles samples".

3.2.10 Flow cytometry

3.2.10.1 Indirect immunofluorescence staining of cells

Mast cells were pelleted at 300g for 5 minutes and resuspended in PBS to obtain a concentration of $1x10^6$ cells/ml. One hundred microlitres of this cell suspension were blocked in 3% BSA-PBS for 30 minutes at 4°C, stained for 30 minutes at 4°C with 100µl of 1% BSA-PBS containing 5µg of the primary antibody or of its isotype control (see table 3-3). After three washes in the washing solution (1% BSA-PBS), cells were then incubated for 30 minutes in the dark with 100µl of a solution containing the secondary antibody (table 3-3) diluted 1:10 in the washing solution. The cells were washed three more times in the washing solution, resuspended in 500µl of PBS and data were acquired by the FACSCalibur Instrument (Becton Dickinson) and finally analysed using the CellQuest Pro Software (Becton Dickinson).

Target	Primary antibody	Isotype control	Secondary antibody
Properdin	Mouse anti-human properdin antibody HYB 039-06 (Antibody Shop)	Mouse anti-EcoRI antibody HYB 098-08 (Antibody Shop)	Goat $F(ab')_2$ fragment anti-mouse PE-labelled (Beckman Coulter)
Tryptase	Mouse anti-human tryptase antibody (AbD Serotec)	Mouse IgG1 negative control (AbD Serotec)	Goat $F(ab')_2$ fragment anti-mouse PE-labelled (Beckman Coulter)

Table 3-3: Antibodies used in flow cytometry to detect properdin and tryptase on mast cells.

3.2.10.2 Permeabilisation of cells

Three different methods were tested to permeabilise the mast cells.

First, the commercial Cytofix/Cytoperm kit (BD Biosciences) was used following the manufacturer's instructions. Mast cells ($1x10^5$ cells) were resuspended into 250µl of Cytofix and left to stand for 20 minutes at 4°C. Cells were then washed in 1ml of Perm/Wash buffer for 5 minutes and stained for 30 minutes at 4°C with 100µl of Perm/Wash buffer containing 5µg of the primary antibody or of its isotype control. After three washes in Perm/Wash buffer, cells were incubated for 30 minutes in the dark at 4°C with 100µl of a solution containing the secondary antibody (table 3-

3) diluted 1:10 in the Perm/Wash buffer. Cells were washed three more times in the Perm/Wash buffer, resuspended in 500µl of PBS and data were acquired by the FACSCalibur Instrument and finally analysed using the CellQuest Pro Software.

The second method used was a mixture of the two methods previously explained. Cells were first stained using the protocol for indirect immunofluorescence staining of cells (see chapter 3.2.10.1) and then cells were permeabilised and stained for a second time using the permeabilisation protocol described above. This ensured the binding of the antibody to the cell surface before that the cell permeabilisation occurred.

The third protocol used was inspired by the one developed by Grützkau and collaborators (Grutzkau et al., 1997). Cells ($1x10^5$) were fixed in a solution containing 4% paraformaldehyde and 0.1% glutaraldehyde for 30 minutes at 4°C. Cells were then washed three times in a washing solution (0.5% BSA-0.03% saponin-PBS) for 5 minutes and stained for 30 minutes at 4°C with 100µl of the washing solution containing 5µg of the primary antibody or of its isotype control. After three washes in the washing solution, cells were incubated for 30 more minutes in the dark at 4°C with 100µl of a solution containing the secondary antibody (table 3-3) diluted 1:10 in the washing solution. Cells were finally washed 3 last times, resuspended in 500µl of PBS and data were acquired by the FACSCalibur Instrument and finally analysed using the CellQuest Pro Software.

3.2.11 Microscopy

3.2.11.1 Cytospin

A cytospin cuvette, a thick filter card (Shandon Scientific, Runcorn, UK) and a microscopic slide (Histobond, Lamb) were held together by a cytospin slide holder. Mast cells in culture were pelleted at 300g for 5 minutes prior to being resuspended in PBS at a concentration of $1x10^6$ cells/ml. Two hundred microlitres of this cell suspension were put into the cytospin cuvette and the slide holder was inserted into a cytospin 2 centrifuge (Shandon Scientific). Samples were then cytospun at 1500rpm for 5 minutes and fixed in methanol for 10 minutes.

3.2.11.2 Toluidine blue staining

Mast cells were stained using toluidine blue, a stain able to detect metachromasia typical of mucins, cartilages and mast cell granules. This stain therefore specifically stains the cytoplasmic granules of mast cells in purple.

The protocol used to stain mast cells was taken from the IHC World website (http://www.ihcworld.com/_protocols/special_stains/toluidine_blue.htm). Mast cells, either cytospun onto a microscopic slide (see chapter 3.2.11.1), or deparaffinised microsections of embedded cells (obtained during the preparation of the sample for electron microscopy, see chapter 3.2.11.3.2), were rehydrated in water and stained with the toluidine blue solution (0.1% (w/v) Toluidine blue O (Sigma), 0.9% (w/v) NaCl, 7% (v/v) ethanol, pH 2.3) for exactly 3 minutes. Slides were then washed 3 times in distilled water, dehydrated once in 95% ethanol and twice in 100% ethanol, cleared in xylene and mounted with DPX Mountant (Fisher). Slides were then observed and pictured using an optic microscope (Prior) equipped with a Coolpix digital camera (Nikon).

3.2.11.3 Electron microscopy

All the electron microscopy experiments were performed by Stefan Hyman and Natalie Allcock at the Electron Microscopy Laboratory, School of Biological Sciences (University of Leicester). Different techniques were used according to the purpose of the study.

3.2.11.3.1 Ultrastructural observations

Fixing cells with a combination of glutaraldehyde and osmium tetroxide allows good preservation of the tissue (because of the glutaraldehyde) and acts as an electron stain (because of the osmium tetroxide), making it one of the best fixative combinations to study the ultrastructure of cells (Hayat, 1981).

HMC-1 and LAD 2 cells, harvested as described in chapter 3.2.1, were spun down at 250g for 5 minutes and washed twice in PBS prior to being pelleted. An amount of pelleted cells corresponding to approximately the 100µl graduation of an Eppendorf tube was then sent to the Electron Microscopy Laboratory.

There, cells were fixed in 2% glutaraldehyde-PBS for 1 hour. After 3 washes in PBS, cells were post-fixed in 1% osmium tetroxide-PBS for 1 hour, thoroughly washed with PBS and then embedded in warm 2% Agar-PBS. The agar was chilled to

4°C and then cut into small cubes. These were then dehydrated by being passed through an alcohol dehydration series (70%, 90%, and 100% ethanol), washed twice in propylene oxide and finally infiltrated with Spurr's epoxy resin (Spurr, 1969). The resin-infiltrated samples were transferred to BEEM capsules (Agar Scientific, Stansted, UK) and polymerised at 70°C for 16 hours to produce a solid block for ultrathin sectioning. The embedded cells were then cut into ultrathin (70-90nm) sections using either a Leica Ultracut S or Reichert Ultracut E ultramicrotome (Leica Microsystems). Sections were collected onto copper mesh electron microscope grid (Athene, Agar Scientific), stained with 2% aqueous uranyl acetate followed by Reynolds' lead citrate (Reynolds, 1963). After washing and drying, the grids were observed and recorded using a JEOL 1220 Transmission Electron Microscope. Images were digitally recorded at various magnifications using a SIS Megaview III Digital Camera (Olympus-SIS).

3.2.11.3.2 Immunogold staining of cells

This technique gives less information about the ultrastructure of the cell, but allows the localisation of protein using specific antibodies coupled with gold particles.

HMC-1 and LAD 2 cells, harvested as described in chapter 3.2.1, were spun down at 250g for 5 minutes and washed twice in PBS prior to be pelleted. An amount of pelleted cells corresponding to approximately the 100µl graduation on an Eppendorf tube was then resuspended in 4% formaldehyde-PBS and sent to the Electron Microscopy Laboratory.

There, cells were left to stand in the formaldehyde solution for 1 hour, washed 3 times in PBS and embedded in warm 2% Agar-PBS. The agar was chilled to 4°C and then cut into small cubes. These were then dehydrated by being passed through an alcohol dehydration series (70%, 90% and 100% ethanol). During the dehydration, the temperature was progressively lowered to reach -35°C at the 100% stage. The samples were then infiltrated with Lowicryl K4M acrylic resin (Polysciences, Agar Scientific) as follows: 1:1 resin:ethanol, 2:1 resin:ethanol and finally 100% Lowicryl K4M resin. The samples were then loaded into gelatine capsules and UV-polymerised at -35°C for 24 hours, followed by 48 hours at room temperature. The embedded cells were then cut into ultrathin (70-90nm) sections using either a Leica Ultracut E or a Reichert Ultracut E ultramicrotome. Sections were collected onto gold mesh electron microscope grid (Agar Scientific), and stored for immunostaining. Sections were

blocked in 1% BSA-PBS-Tween 20, stained either with the mouse anti-human properdin HYB 039-06 antibody (Antibody Shop) or with the FITC-labelled goat anti-human properdin antibody (Nordic Immunology), both diluted 1:100 in 1% BSA-PBS-Tween 20, washed in 1% BSA-PBS-Tween 20 and stained again either with an anti-mouse IgG antibody coupled with gold particle (British Biocell, Cardiff, UK) or an anti-goat IgG antibody coupled with gold particle (British Biocell) diluted 1:100 in 1% BSA-PBS-Tween 20. Sections stained only with the gold-labelled anti-mouse IgG antibody without being previously incubated with the anti-properdin antibody solution were used as negative controls. Samples were then post-fixed in 0.5% glutaraldehyde-PBS-Tween 20, rinsed in distilled deionised water and then stained with 2% aqueous uranyl acetate, followed by Reynolds lead citrate (to enhance the contrast). After washing and drying, the grids were observed and recorded using a JEOL 1220 Transmission Electron Microscope. Images were digitally recorded at various magnifications using a SIS Megaview III digital camera (Olympus-SIS).

3.2.11.3.3 Negative staining

This technique allows the observation of the fine structure of a sample by staining all around the particle of interest rather than the sample. This renders the background electron dense as compared to the sample, thus unveiling the sample in “negative” contrast.

Three to five microlitres of the fractions extracted after ultracentrifugation at 10,000g and 70,000g (and washing to remove any traces of phosphate salts) were applied to the surface of a freshly glow-discharged carbon-coated piotoform-covered electron microscope grid. This was left for 2 to 5 minutes to allow the sample to adsorb onto the surface. Excess sample was then removed from the grid to only leave a very thin layer. The grid was next covered with a drop of aqueous 1 to 2% uranyl acetate, an electron opaque metal salt which will cover the grid, but will not interfere with the sample, creating a contrast between the sample and the background. This solution should be applied and removed quickly. After removing the excess stain, samples were air-dried, observed and recorded on the JEOL 1220 Transmission Electron Microscope as described previously.

3.2.11.3.4 Immunogold staining of vesicles

Different techniques were used to detect properdin antigens on 10,000g and 70,000g fraction vesicles. Extra steps were added to the negative staining method previously explained (see chapter 3.2.11.3.3).

Briefly, after adsorption of the sample onto the grid, grids were pre-fixed, immersed into a blocking solution, rinsed in a washing solution, incubated with the mouse anti-human properdin antibody HYB 039-06 (Antibody Shop) diluted 1:100 into the first antibody solution, rinsed in the washing solution and finally stained with the anti-mouse IgG antibody coupled with gold particles (British Biocell) diluted 1:100 into the secondary antibody solution. The composition of all the solutions just mentioned is indicated in table 3-4. Grids stained only with the gold-labelled anti-mouse IgG antibody without being previously incubated with the anti-properdin solution were used as negative controls.

Samples were then rinsed once in 1% BSA-PBS, three times in PBS, post-fixed in 0.5% glutaraldehyde-PBS and finally rinsed in double distilled H_2O before to be stained with 2% uranyl acetate/Reynolds lead citrate as previously described (see chapter 3.2.11.3.3).

Experiment	**1**	**2**	**3**	**4**	**5**
Pre-fixation	None	None	None	None	10% formal saline
Blocking solution	1% BSA-0.1% Tween 20-PBS	1% BSA-0.1% Tween 20-PBS	1% BSA-0.02% Triton X100-PBS	1% BSA-0.02% Triton X100-PBS	0.02% Triton X100-PBS
1st antibody solution	1% BSA-0.1% Tween 20-PBS	1% BSA-0.02% Triton X100-PBS	1% BSA-PBS	1% BSA-PBS	1% BSA-PBS
Washing solution	1% BSA-0.1% Tween 20-PBS	1% BSA-0.1% Tween 20-PBS	1% BSA-PBS	1% BSA-PBS	1% BSA-PBS
2nd antibody solution	1% BSA-0.1% Tween 20-PBS	1% BSA-0.1% Tween 20-PBS	1% BSA-PBS	1% BSA-PBS	1% BSA-PBS
Size of the gold particle	15nm	15nm	15nm	5nm	15nm

Table 3-4: Conditions used to detect properdin on 10,000g and 70,000g-fraction particles.

3.2.11.4 Immunohistochemistry

3.2.11.4.1 Paraffin embedding

This work was done by Irina Elliott (University of Leicester). Tissue samples were immersed in a 10% formal saline solution immediately after dissection and left in the fridge until further treatment. Tissues were next dehydrated using the Citadel 2000 tissue processor (Shandon): samples were first immersed into successive solutions of IMS (with an increasing percentage of IMS), then into a chloroform solution and finally into some polywax (TCS Biosciences, Buckingham, UK).

Paraffin blocks were then cut into 4µm-thick sections using a microtome (Leitz Wetzlar). Sections were then immersed in dH_2O and picked up on a microscope slide (Histobond, Lamb) and slides were stored in a slide box at room temperature until further use.

3.2.11.4.2 Blood smear preparation

One droplet of human blood freshly collected from a healthy adult volunteer was applied on top of a microscopic slide (Histobond, Lamb). Blood was then evenly distributed on the slide using the slide of another microscope slide by applying low pressure and finally left to dry on the bench.

3.2.11.4.3 Immunostaining

Slides containing cytospun cells or human blood smear were left to dry at room temperature for 30 minutes prior to be fixed for 10 minutes in methanol. The protocol described in chapter 2.1.7.2 was then followed using the FITC-labelled goat anti-human properdin antibody (Nordic Immunology).

Paraffin-embedded sections of mouse ear skin were deparaffinised in xylene (Fisher) for 10 minutes and rehydrated by being immersed into successive IMS solutions (twice in 100% IMS and once in 95% IMS, 5 minutes each) and finally rinsed under running tap water for 5 minutes and buffered in 1x TBS for 10 minutes. Slides were then treated with 1x trypsin (Sigma-Aldrich) at 37°C for 20 minutes to digest any putative protein crosslinking formed during the formal saline fixation. Next, the slides were rinsed under running tap water for 20 minutes and the protocol described in chapter 2.1.7.2 was followed (ignoring the methanol fixing step), using the FITC-labelled goat anti-human properdin antibody (Nordic Immunology).

3.3 Results

The aim of this part of my work was to investigate whether mast cells, auxiliary cells of the immune system, produce properdin. As explained in chapter 3.1.1.5, HMC-1 and LAD 2 cells were the two mast cell lines used in this study. However due to their slow doubling rate (2 to 3 weeks), LAD 2 cells were only used in some of the following experiments.

3.3.1 Identification of the mast cell lines

Before looking at properdin production by mast cells, I first verified the purity of the two mast cell lines used in this study. Both HMC-1 and LAD 2 cells were regularly stained with toluidine blue (see chapter 3.2.11.2), a mast cell-specific stain, and observed by light microscopy to ensure the homogeneity of the cell culture. As seen on figure 3-4, both HMC-1 and LAD 2 cell populations were homogeneous and all the cells presented numerous purple granules inside their cytoplasm after toluidine blue staining.

Flow cytometry analyses were performed only on HMC-1 cells using a mast cell-specific anti-tryptase antibody (see chapter 3.2.10.1). The data obtained showed one population of tryptase-positive cells, as expected (figure 3-5) (Nilsson et al., 1994).

Both HMC-1 and LAD 2 cells were next fixed using both osmium and glutaraldehyde treatment to preserve their ultrastructure, and their morphology was examined using transmission electron microscopy (TEM) (see chapter 3.2.11.3.1). As previously described in the literature, HMC-1 cells appeared to be 10-15µm ovoid cells with a large nucleus, few electron dense granules, lots of mitochondria and some lipid bodies (figure 3-6A), while LAD 2 cells were circular cells (10-15µm diameter) with a large nucleus, numerous cytoplasmic projections, lots of mitochondria and granules (figure 3-6B) (Grutzkau et al., 1997; Kirshenbaum et al., 2003). It is worth mentioning the granules found inside the cytoplasm of LAD 2 cells did not appear electron dense.

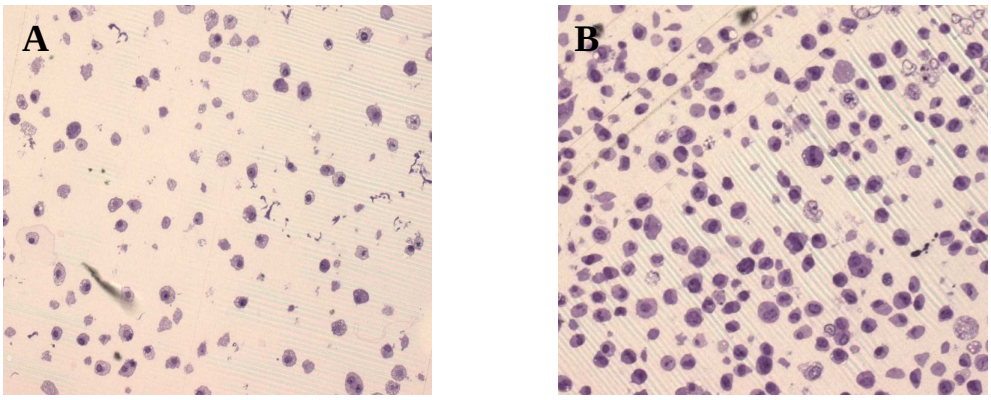

Figure 3-4: Representative pictures of sections of paraffin-embedded mast cells stained with Toluidine blue. A: HMC-1 cells, B: LAD 2 cells. Original magnification x10.

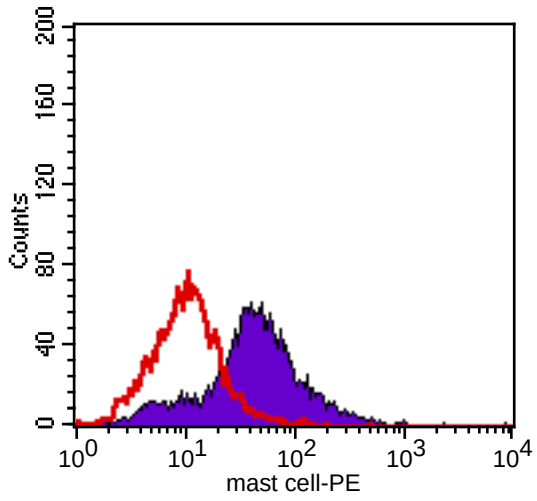

Figure 3-5: Flow cytometric analysis on HMC-1 cells. Representative histogram of these cells after staining with the mouse anti-human tryptase antibody (blue) and its isotype control (red). The detection of both antibodies was done via the use of goat anti-mouse IgG PE-labelled.

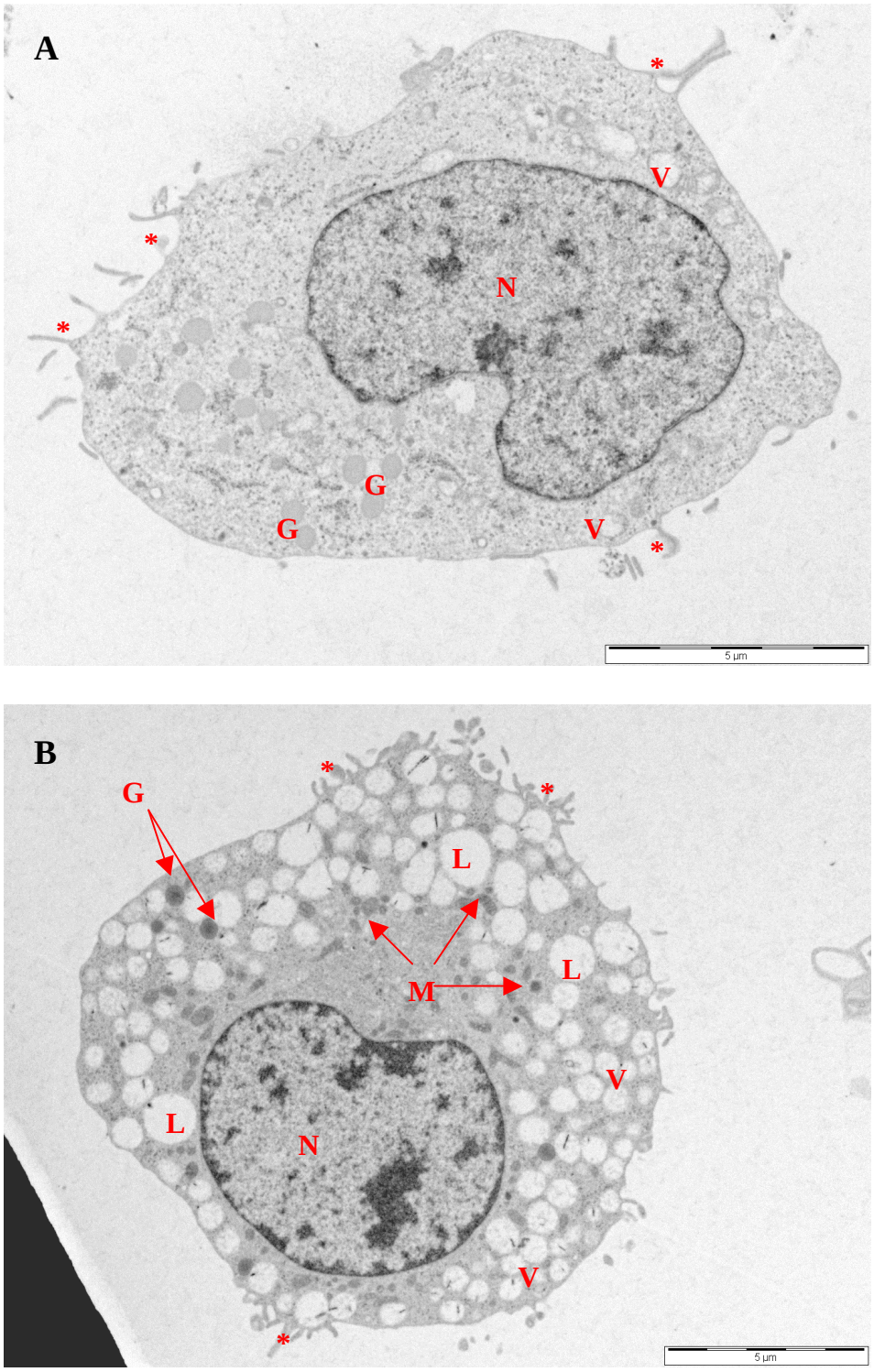

Figure 3-6: Representatives transmission electron micrographs of both mast cell lines that have been fixed using a glutaraldehyde-osmium tetroxide solution. A: HMC-1 cells; B: LAD 2 cells. N: nucleus; G: electron-dense granules; V: non-electron dense vesicles; M: mitochondria; L: lipid bodies; *: cytoplasmic extensions.

3.3.2 Properdin expression in mast cells

To investigate whether properdin was expressed in mast cells, RNAs were isolated and purified from both HMC-1 and LAD 2 cells and these RNAs were used as templates to synthesise single-stranded cDNAs (see chapter 3.2.4.1). PCRs were then performed using these freshly-synthesised cDNAs and a pair of primers specific for the human properdin gene as described in chapter 3.2.4.2.1. These primers called "HumPN" were designed to obtain a PCR product that included the all ORF of the human properdin gene (table 2-1). Human properdin ORF has a length of 1410bp and the PCR product obtained using these primers was expected to be 1451bp long.

As shown on figure 3-7, a band with the expected size of 1451bp was visualised on the 0.8% agarose gel for both HMC-1 (lane 1) and LAD 2 cells (lane 3). In order to confirm the identity of the product, six others PCRs were performed using exactly the same conditions as previously but by using only the HMC-1 cDNA as a template. These PCR reactions were run into an agarose gel, the PCR products obtained at 1451bp were all excised from the gel, pooled together, and the DNA was extracted from the gel using the Sephaglas BandPrep kit (see chapter 2.1.5.1). The DNA concentration was estimated and this 1451bp fragment was cloned into a PGEM-T easy vector (see chapter 2.1.5.4). The plasmid obtained was then used to transform Top 10F' competent cells (see chapter 2.1.5.5) and the transformed bacteria were plated onto LB agar plates supplemented with ampicillin, X-Gal and IPTG. Six white single colonies were selected, picked up individually and grown overnight before to be submitted to a plasmid extraction (see chapter 2.1.5.6). This was followed by a screening of the plasmid by restriction digest using *EcoR*I (see chapter 2.1.5.7). Bioinformatics analysis using Gene Tool Lite 1.0 showed that two restriction sites for *EcoR*I were present on the vector but none on the insert. As observed on figure 3-8A, one out of the six plasmids digested by *EcoR*I (lane 4) gave the two expected fragments of 3000bp (linearised PGEM-T easy vector) and 1469bp (properdin ORF insert), suggesting that the properdin fragment was successfully inserted into the plasmid for this sample. This plasmid was then submitted to more restriction digests using three different restriction enzymes – *EcoR*I, *Kpn*I and *Pst*I – to confirm the identity of its insert before sequencing. Bioinformatics analyses showed that the PGEM-T easy vector possessed no restriction site for *Kpn*I and one for *Pst*I, while the properdin insert possessed one restriction site for both *Kpn*I and *Pst*I. Therefore, after

restriction digest, one band was expected to be visualised for *Kpn*I, and two for both *Pst*I and *EcoR*I. As seen on figure 3-8B, *EcoR*I cut again the plasmid into the two expected fragments of 3000bp and 1469bp (lane 1). After restriction digest with *Kpn*I, a single band with a size of approximately 5500bp was observed (lane 2). However, PGEM-T easy vector containing the properdin insert should have a size of 4469bp. The product obtained using *Kpn*I actually had the apparent size of the non-linearised plasmid (data not shown). Further tries to linearise the plasmid using this specific restriction enzyme all failed. Concerning *Pst*I, the expected 4289bp fragment was clearly present, whereas the 180bp fragment was barely visible, probably due to its small size (lane 3). All these results taken together confirmed that the insert carried by the plasmid was of the expected size of 1451bp. This plasmid was finally sent for sequencing to PNACL to confirm the identity of its insert (see chapter 2.1.5.8). This was done using primers specific for both the T7 and the SP6 promoter regions that flanked the insert region of the PGEM T-easy vector. The sequence obtained using the T7 promoter primer and the complementary sequence of the one obtained using the SP6 promoter primer were then aligned with the known sequence of the Homo sapiens complement factor properdin mRNA (EMBL accession number: NM_002621) using the multi-align editor function of the Gene Tool Lite 1.0 software (figure 3-9).

From the 957bp of the insert sequenced using the T7 promoter primer, 875bp matched the human properdin sequence. However, 52 of the bases which did not match the properdin sequence were “no call” (meaning they could not be identified by the sequencer) and were found at the very end of the sequence, way after the first 500bp of best quality sequence (see note in chapter 2.2.1.1). Thus 97% of the identified nucleotides sequenced from the T7 promoter site side matched the human properdin sequence. The sequence obtained using the SP6 promoter primer, as for it, showed 93% identity with the human properdin gene, when excluding the abundant “no call” observed at the very end of the sequence. Thus, more than 95% of the identified bases of my insert were identical to the sequence of the human properdin gene. These results taken together therefore showed that the product previously obtained by RT-PCR using cDNA extracted from HMC-1 cells was indeed properdin and strongly suggested that the one observed for the LAD 2 cell line was properdin as well.

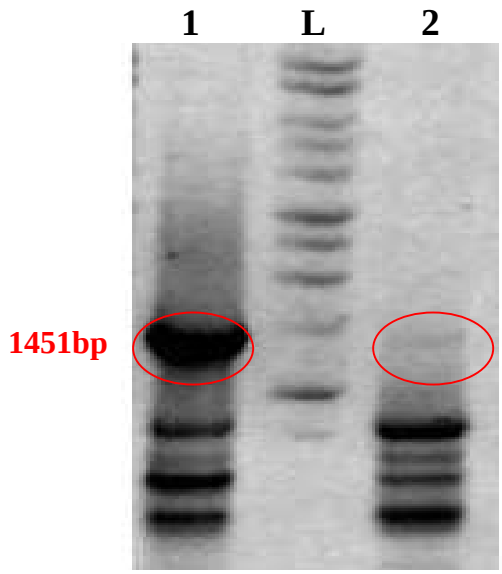

Figure 3-7: Representation of the PCR products obtained using mast cell cDNA and the HumPN primers pair after migration into a 0.8% agarose gel. Lane 1: using HMC-1 cell cDNA, lane 2: using LAD 2 cell cDNA. L: benchtop 1kb DNA ladder (Promega).

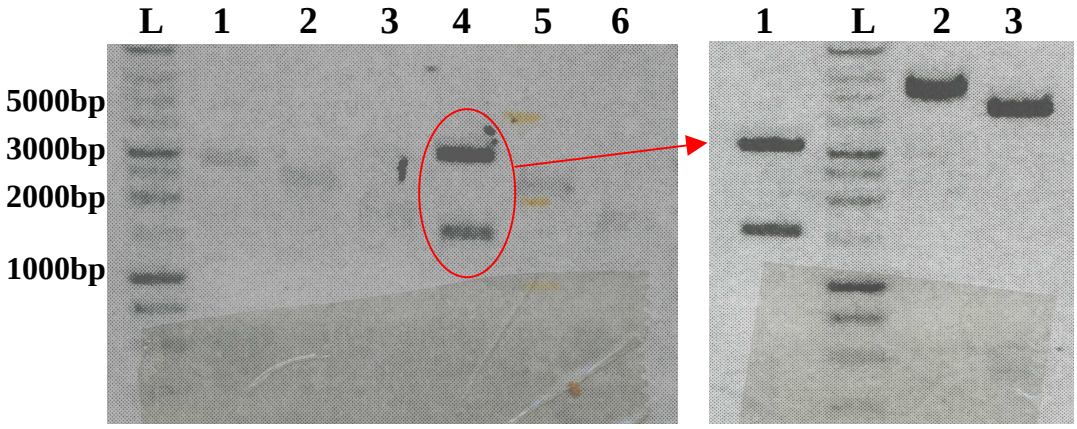

Figure 3-8: Representation of the products obtained after restriction digest run into a 1% agarose gel. A: Restriction digests by *EcoR*I of the plasmids extracted from TopF10' cells transformed with the PCR product obtained using HMC-1 cell cDNA and the HumPN primers pair. L: Benchtop 1kb DNA ladder, lane 1, 2, 3, 4, 5, 6: different clones; B: Restriction digests of the clone 4 by 3 different restriction enzymes. L: Benchtop 1kb DNA ladder, lane 1: using *EcoR*I, lane 2: using *Kpn*I and lane 3: using *Pst*I restriction enzyme.

A

```
Consensus  ATGATCACAG AGGGAGCGCA ----C-T--A ---TG-TGCT GCCGCCGCTG CTCCTGCTGC
Properdin  ATGATCACAG AGGGAGCGCA GGCCCCTCGA ---TGTTGCT GCCGCCGCTG CTCCTGCTGC 300
Insert T7  ATGATCACAG AGGGAGCGCA CCTNCTTNAA AANTGNTGCT GCCGCCGCTG CTCCTGCTGC 60

Consensus  TCACCC---- A---ACAGGC TCAGACCCCG TGCTCTGCTT CACCCAGTAT GAAGAATCCT
Properdin  TCACCCTGCC AGCCACAGGC TCAGACCCCG TGCTCTGCTT CACCCAGTAT GAAGAATCCT 360
Insert T7  TCACCCNTTN AAAAACAGGC TCAGACCCCG TGCTCTGCTT CACCCAGTAT GAAGAATCCT 120

Consensus  CCGGCAAGTG CAAGGGCCTC CT--GGGG-G GTGTCAGCGT GGAAGACTGC TGTCTCAACA
Properdin  CCGGCAAGTG CAAGGGCCTC CTGGGGGGTG GTGTCAGCGT GGAAGACTGC TGTCTCAACA 420
Insert T7  CCGGCAAGTG CAAGGGCCTC CTNCGGGGNG GTGTCAGCGT GGAAGACTGC TGTCTCAACA 180

Consensus  CTGCCTTTGC CTACCAGAAA CGTAGTGGTG GGCTCTGTCA GCCTTGCAGG TCCCCACGAT
Properdin  CTGCCTTTGC CTACCAGAAA CGTAGTGGTG GGCTCTGTCA GCCTTGCAGG TCCCCACGAT 480
Insert T7  CTGCCTTTGC CTACCAGAAA CGTAGTGGTG GGCTCTGTCA GCCTTGCAGG TCCCCACGAT 240

Consensus  GGTCCCTGTG GTCCACATGG GCCCCCTGTT CGGTGACGTG CTCTGAGGGC TCCCAGCTGC
Properdin  GGTCCCTGTG GTCCACATGG GCCCCCTGTT CGGTGACGTG CTCTGAGGGC TCCCAGCTGC 540
Insert T7  GGTCCCTGTG GTCCACATGG GCCCCCTGTT CGGTGACGTG CTCTGAGGGC TCCCAGCTGC 300

Consensus  GGTACCGGCG CTGTGTGGGC TGGAATGGGC AGTGCTCTGG AAAGGTGGCA CCTGGGACCC
Properdin  GGTACCGGCG CTGTGTGGGC TGGAATGGGC AGTGCTCTGG AAAGGTGGCA CCTGGGACCC 600
Insert T7  GGTACCGGCG CTGTGTGGGC TGGAATGGGC AGTGCTCTGG AAAGGTGGCA CCTGGGACCC 360

Consensus  TGGAGTGGCA GCTCCAGGCC TGTGAGGACC AGCAGTGCTG TCCTGAGATG GGCGGCTGGT
Properdin  TGGAGTGGCA GCTCCAGGCC TGTGAGGACC AGCAGTGCTG TCCTGAGATG GGCGGCTGGT 660
Insert T7  TGGAGTGGCA GCTCCAGGCC TGTGAGGACC AGCAGTGCTG TCCTGAGATG GGCGGCTGGT 420

Consensus  CTGGCTGGGG GCCCTGGGAG CCTTGCTCTG TCACCTGCTC CAAAGGGACC CGGACCCGCA
Properdin  CTGGCTGGGG GCCCTGGGAG CCTTGCTCTG TCACCTGCTC CAAAGGGACC CGGACCCGCA 720
Insert T7  CTGGCTGGGG GCCCTGGGAG CCTTGCTCTG TCACCTGCTC CAAAGGGACC CGGACCCGCA 480

Consensus  GGCGAGCCTG TAATCACCCT GCTCCCAAGT GTGGGGGCCA CTGCCCAGGA CAGGCACAGG
Properdin  GGCGAGCCTG TAATCACCCT GCTCCCAAGT GTGGGGGCCA CTGCCCAGGA CAGGCACAGG 780
Insert T7  GGCGAGCCTG TAATCACCCT GCTCCCAAGT GTGGGGGCCA CTGCCCAGGA CAGGCACAGG 540

Consensus  AATCAGAGGC CTGTGACACC CAGCAGGTCT GCCCCACACA CGGGGCCTGG GCCACCTGGG
Properdin  AATCAGAGGC CTGTGACACC CAGCAGGTCT GCCCCACACA CGGGGCCTGG GCCACCTGGG 840
Insert T7  AATCAGAGGC CTGTGACACC CAGCAGGTCT GCCCCACACA CGGGGCCTGG GCCACCTGGG 600

Consensus  GCCCCTGGAC CCCCTGCTCA GCCTCCTGCC ACGGTGGACC CCACGAACCT AA-GAGACAC
Properdin  GCCCCTGGAC CCCCTGCTCA GCCTCCTGCC ACGGTGGACC CCACGAACCT AAGGAGACAC 900
Insert T7  GCCCCTGGAC CCCCTGCTCA GCCTCCTGCC ACGGTGGACC CCACGAACCT AANGAGACAC 660

Consensus  -AAGCCGCAA GTGTTCTGCA CCTGAGC-CT CCCA-AAACC -CCTGGGAAG CCCTG-CCGG
Properdin  GAAGCCGCAA GTGTTCTGCA CCTGAGCCCT CCCAGAAACC TCCTGGGAAG CCCTGCCCGG 960
Insert T7  NAAGCCGCAA GTGTTCTGCA CCTGAGCTCT CCCANAAACC NCCTGGGAAG CCCTGNCCGG 720

Consensus  GGCTAGCCTA CGA-CAGCGG A-GTGCACCG GCCTGCCACC CTGCCCAGTG GCTGGGGG-C
Properdin  GGCTAGCCTA CGAGCAGCGG AGGTGCACCG GCCTGCCACC CTGCCCAGTG GCTGGGGG-C 1019
Insert T7  GGCTAGCCTA CGANCAGCGG ANGTGCACCG GCCTGCCACC CTGCCCAGTG GCTGGGGGGC 780

Consensus  TGGGGG-CCT TGGGGCCCTG -GA-CCCCTG CCCTG-GACC TG-GG-C-GG G-CA-A-CA-
Properdin  TGGGGG-CCT TGGGGCCCTG TGAGCCCCTG CCCTGTGACC TGTGGCCTGG GCCAGACCAT 1078
Insert T7  TGGGGGNCCT TGGGGCCCTG NGANCCCCTG CCCTGNGACC TGGGGNCNGG GNCANANCA- 839

Consensus  GGAACAA-GG A-G-GCAATC ACCC-G-GCC CCA--A-GGG GG-CCC-T-- G-G--GG-G-
Properdin  GGAACAACGG ACGTGCAATC ACCCTGTGCC CCAGCATGGG GGCCCCTTCT GTGCTGGCG- 1137
Insert T7  GGAACAANGG ANGNGCAATC ACCCNGGGCC CCANNANGGG GGNCCCNTNN GGGGNGGGGG 899

Consensus  A-G-C-CCCG G--CC--A-- -G-AA-A--- --G--CCC-G -CC-G-G-A- GGGGAG-GGG
Properdin  ATGCCACCCG GACCCACATC TGCAACACAG CTGTGCCCTG CCCTGTGGAT GGGGAGTGGG 1197
Insert T7  ANGNCNCCCG GNACCNNANN NGNAAAAANN NNGGNCCCNG NCCGGGGAAG GGGGAGGGGG 959
```

B

```
Consensus  --AAACCTTC CAGTCCCCCG AGTCTCACCT CCTCTCTTCA C----TC--G GAGAAGGAGT
Properdin  CCAAACCTTC CAGTCCCCCG AGTCTCACCT CCTCTCTTCA CAATCTCAAG GAGAAGGAGT 1634
Insert SP6 NAAAACCTTC CAGTCCCCCG AGTCTCACCT CCTCTCTTCA CNNNATCNNG GAGAAGGAGT 60

Consensus  CCCAGAAACG TTCGTCCGTG CACATCTGTA CCAGCAAAGA GGAGGTGGTG GTCGAAGACG
Properdin  CCCAGAAACG TTCGTCCGTG CACATCTGTA CCAGCAAAGA GGAGGTGGTG GTCGAAGACG 1574
Insert SP6 CCCAGAAACG TTCGTCCGTG CACATCTGTA CCAGCAAAGA GGAGGTGGTG GTCGAAGACG 120

Consensus  GGAACATCGA GGAGTGTGGC ACCGTCGCCA GAGGGGGTCT TCCAGTG-AA GAAGAGCGGG
Properdin  GGAACATCGA GGAGTGTGGC ACCGTCGCCA GAGGGGGTCT TCCAGTGCAA GAAGAGCGGG 1514
Insert SP6 GGAACATCGA GGAGTGTGGC ACCGTCGCCA GAGGGGGTCT TCCAGTGTAA GAAGAGCGGG 180

Consensus  ACTGGAAGCT GGTACCTTTG CCACCCGCCC ATGAACCCCT CGTTCCCACA CGTCTCCGCG
Properdin  ACTGGAAGCT GGTACCTTTG CCACCCGCCC ATGAACCCCT CGTTCCCACA CGTCTCCGCG 1454
Insert SP6 ACTGGAAGCT GGTACCTTTG CCACCCGCCC ATGAACCCCT CGTTCCCACA CGTCTCCGCG 240

Consensus  ACCGCCCGTG CCCATCCTAA TCCAGGTGTC CCCCCGTACG -GT-GGGGGT CCATGAGGTG
Properdin  ACCGCCCGTG CCCATCCTAA TCCAGGTGTC CCCCCGTACG TGTCGGGGGT CCATGAGGTG 1394
Insert SP6 ACCGCCCGTG CCCATCCTAA TCCAGGTGTC CCCCCGTACG CGTNGGGGGT CCATGAGGTG 300

Consensus  AGACTGGTAC TAGGAAAGTT CCCCGTCACG ACCTACGACA TCGTCACG-C CTATAGGACG
Properdin  AGACTGGTAC TAGGAAAGTT CCCCGTCACG ACCTACGACA TCGTCACGGC CTATAGGACG 1334
Insert SP6 AGACTGGTAC TAGGAAAGTT CCCCGTCACG ACCTACGACA TCGTCACGNC CTATAGGACG 360

Consensus  ACAACGGGCC -TGTAGCTAC AGG-A-TTT- AAC---CG-G GGAC-T-CAG GAGGG---C-
Properdin  ACAACGGGCC GTGTAGCTAC AGGCAGTTTG AACGC-CG-G GGACGTCCAG GAGGG-CGCA 1277
Insert SP6 ACAACGGGCC NTGTAGCTAC AGGTAATTTN AACNNTCGNG GGACNTTCAG GAGGGGNNCN 420

Consensus  CTG-CGAC-- GGG-CCTAAA G-AACT--TC GA-CT-C-CT GA-AGT-ACA A-GG-A---C
Properdin  CTGACGACC- GGGCCCTAAA G-AACTG-TC GA-CTAC-CT GA-AGT-ACA A-GGCA--GC 1227
Insert SP6 CTGNCGACNN GGGNCCTAAA GNAACTNNTC GANCTTCTCT GANAGTCACA ANGGNATTNC 480

Consensus  CT-TGTC--- CGA-GT-AGG GGG--TGCT- AG-GT-G--- G-G--A-G-- -CCC-T---C
Properdin  CTATGTCC-C CGAGGTGAGG GGGG-TGCTC AGGGT-G--A GGGGTAGGTG TCCCGTC-CC 1173
Insert SP6 CTNTGTCNTN CGANGTNAGG GGGNATGCTN AGTGTTGTTN GNGNNANGCN NCCCCTNTNC 540

Consensus  --GT--A--- --C--CTA-- ------
Properdin  GTGTCGACAC AACGTCTACA CCCAGG                                    1147
Insert SP6 NNGTTNATGN N-CN-CTATN NNNNTN                                    564
```

Figure 3-9: Comparaison of the sequence of the cloned insert (lane 3) sequenced from the T7 promoter site (A) and the SP6 promoter site (B) with the sequence of the human complement factor properdin mRNA (EMBL accession number NM_002621) (lane 2). The consensus sequence (lane 1) was constructed from the alignment of the reference sequence (lane 2) with the sequence of the cloned insert (lane 3) using the multi-align editor function of the Gene Tool Lite1.0 software. Identities between both sequences are represented in black, mismatches in red, no call bases in blue, gap in green. Lane 1: consensus sequence, lane 2: properdin sequence, lane 3: cloned insert sequence. A: Adenine, C: Cytosine, G: Guanine, T: Thymine, N: No call.

3.3.3 Effect of different stimuli on properdin synthesis by mast cells

After proving properdin was expressed by both HMC-1 and LAD 2 cells, I then studied the regulation of properdin expression and synthesis by HMC-1 cells upon stimulation by different molecules.

3.3.3.1 At a molecular level

To study the regulation of properdin expression in HMC-1 cells upon stimulation at a transcriptional level, a real-time PCR technique had to be developed.

3.3.3.1.1 Optimisation of the real-time PCR

According to the manufacturer's instructions, small amplicons (less than 800bp) were needed in order to perform real-time PCRs. Two pairs of specific primers, chosen to anneal small regions of the human properdin gene containing an intron (to ensure no DNA contamination would interfere with the quantification of the gene), were designed. These pairs of primers named "HumPNsh1" and "HumPNsh2" were then tested by RT-PCR using the conditions described in chapter 3.2.4.2.2 (table 2-1). One PCR product obtained using HumPNsh1 primers and HMC-1 cDNA as a template had the expected size of 451bp on an agarose gel (figure 3-10B). However, primer dimers were visualised as well. Despite the use of different concentration of $MgCl_2$ in the PCR master mix, the formation of these primer dimers could not be prevented (figure 3-10B). Three amplicons were visualised on the agarose gel when the PCR was performed using HumPNsh2 primers, including one of the expected size of 220bp and one corresponding to primer dimers (lane 3, figure 3-10C). The amplicon of the expected size disappeared when different concentrations of magnesium chlorate were used (figure 3-10C).

I hypothesised that the formation of unexpected primer dimers for both pairs of primers was due to some cross-reactions between the two primers of a same pair. As no primer dimer formation could be allowed in real-time PCR, two other pairs of primers were tested: "HumPNsh3" and "HumPNsh4". "HumPNsh3" is composed in fact the forward primer of "HumPNsh1" and the reverse primer of "HumPNsh2", whereas "HumPNsh4" consists of the forward primer of "HumPNsh2" with the reverse primer of "HumPNsh1". Using these two new pairs of primers with low concentration of $MgCl_2$ in the PCR master mix, PCR products of the expected sizes of respectively 451bp and 311bp were visualised on an agarose gel (lane 1, figure 3-10A and lane 2, figure 3-10D). As no extra band was observed on the agarose gel in these

specific conditions, these two new pairs of primers could therefore potentially be used in real-time PCR. As shorter amplicons were obtained with “HumPNsh4” primers, this pair of primers was chosen for all the further real-time PCR experiments. The PCR conditions for “HumPNsh4” primers were then optimised: an annealing temperature of 60°C and an $MgCl_2$ concentration of 1.5mM were found to be optimum.

HumGAPDH and MouGAPDH primers, specific for the human and for the mouse housekeeping gene GAPDH, respectively, were then tested by PCR. Amplicons of the expected sizes of respectively 148bp and 180bp were observed using the recommended annealing temperature of 57°C and an added $MgCl_2$ concentration of 1.5mM (Guo et al., 2002; Zhang and Insel, 2004).

3.3.3.1.2 Results

HMC-1 cells were either grown under normal conditions or stimulated by different cytokines (TNFβ, TGFβ, IL-1β, IFNγ, GM-CSF) or LPS (see chapter 3.2.2). RNAs were extracted from cells cultivated for 24 hours under each of these conditions and cDNAs were synthesised as previously described (see chapter 3.2.4.1). Using the real-time PCR technique previously developed (see chapter 3.2.6), the expression of the properdin gene was then quantified and compared to the expression of the housekeeping gene GAPDH. The relative expression obtained for the properdin gene for each sample was divided by the one obtained for the GAPDH gene and results were expressed as percentage. The Il-1β-stimulated HMC-1 cells sample was given the arbitrary value of 100. The expression ratios obtained are summarised in figure 3-11. A problem occurred during the RNA extraction of the unstimulated HMC-1 cells in the second experiment, while properdin expression for LPS-stimulated HMC-1 cells was not assessed in the first experiment, explaining the lack of data for these two particular samples.

As seen on figure 3-11, no significant difference in properdin expression was observed between unstimulated and stimulated HMC-1 cells ($p=0.705$).

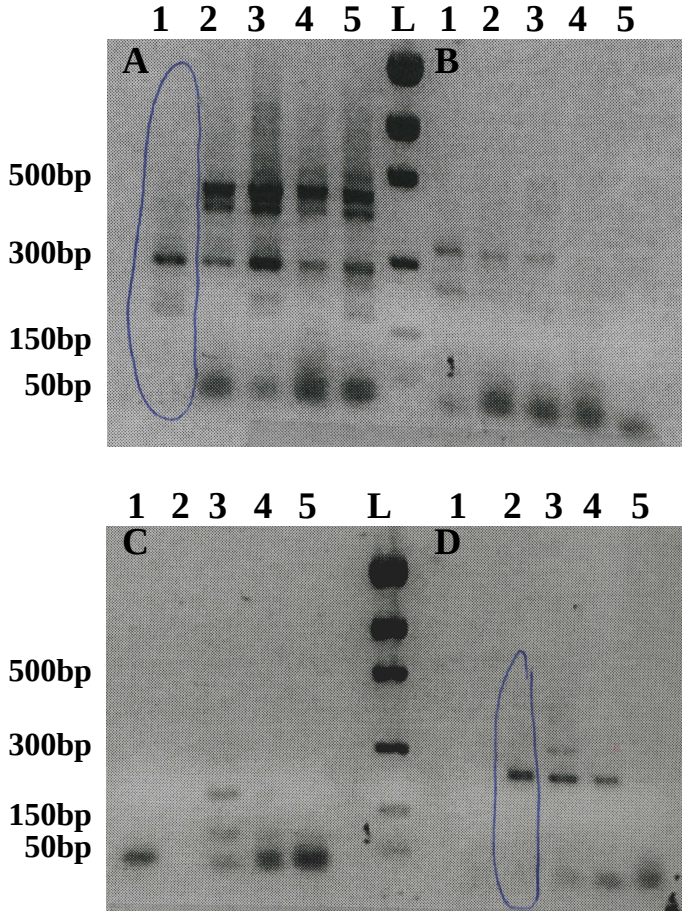

Figure 3-10: Representation of the PCR products obtained using HMC-1 cells cDNA after migration on a 1.5% agarose gel. The pair of primers used were A: "HumPNsh3"; B: "HumPNsh1"; C: "HumPNsh2" and D: "HumPNsh4". For each figures, the concentration of $MgCl_2$ added to the PCR master mix was: lane 1: 0.5mM; lane 2: 1.5mM; lane 3: 2.5mM; lane 4: 4.5mM and lane 5: 5.5mM; L: benchtop PCR markers (Promega).

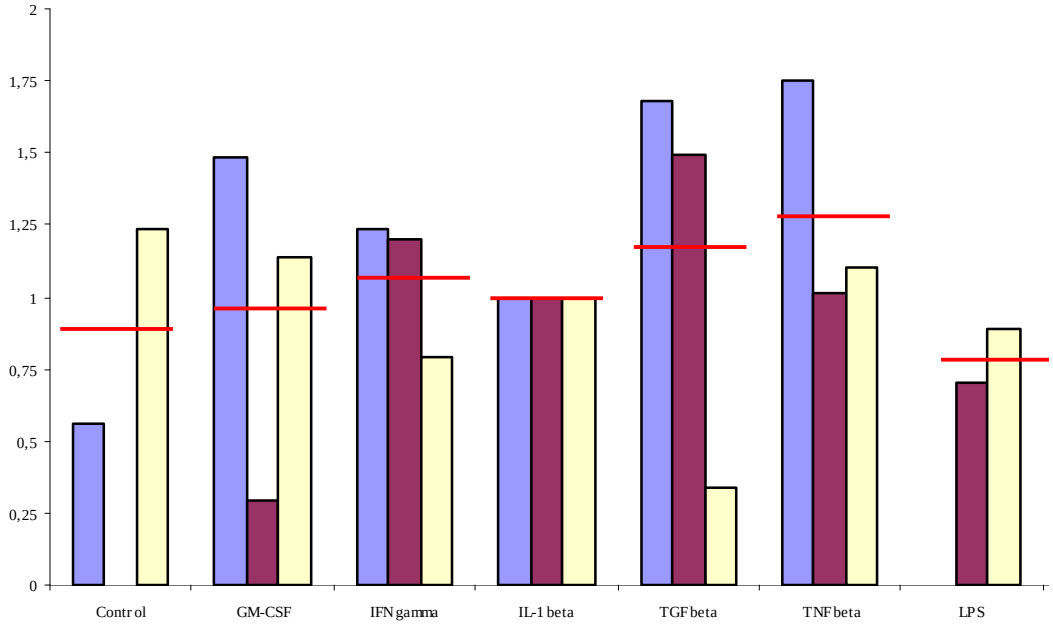

Figure 3-11: Analysis of the real-time PCR results showing properdin expression by stimulated HMC-1 cells. Properdin levels were measured by dividing the normalised expression value obtained for the GAPDH gene by the normalised expression value obtained for the properdin gene. The IL-1β-stimulated samples have been given arbitrary the value of 1AU. In blue, results of the first experiment; in purple, results of the second experiment; in cream: results of the third experiment; red bars: means of the three experiments. One single real-time PCR was carried out each time. p=0.705 [Kruskal-Wallis test].

3.3.3.2 At a protein level

The effect of these molecules on properdin release by mast cells was then investigated. The concentration of properdin present in the supernatant of different HMC-1 cell cultures after stimulation was therefore assessed by Western blot,.

As explained in chapter 3.2.2, cell culture media were collected 24 hours after stimulation and concentrated by centrifugation through a protein cutting membrane. The amount of total proteins in these enriched supernatants was measured, adjusted (see chapter 3.2.7.1) and analysed by Western blot using a polyclonal rabbit anti-human properdin antibody and a HRP-labelled goat anti-rabbit IgG (see chapter 3.2.8).

Figure 3-12 shows representative X-ray films of the three stimulation experiments performed. On figure 3-12A, the expected 53KDa band corresponding to a monomer of properdin was observed on the film for all but the non-stimulated HMC-1 cell sample. The intensity of this band was higher for both IFNγ and TNFβ-stimulated HMC-1 cell samples than it was for the others samples. However, as observed on figure 3-12B, in the two subsequent experiments performed, the signal detected at the expected size of 53KDa became really faint, even with longer exposure of the X-ray film. Moreover, for each sample, the intensity of the 53KDa band was different within the three independent experiments and, in the two last experiments, in addition to the loss of intensity of the 53KDa band, extra bands of high molecular weights reactive with the polyclonal antibody were visualised on the X-ray film (figure 3-12B). It is worth mentioning that for the experiment corresponding to figure 3-12A, red Ponceau staining of the membrane was regrettably not performed, meaning there was no evidence that the same amount of protein was transferred to the membrane for each sample for this specific experiment. It was therefore not possible to compare the concentration of properdin present in the different samples.

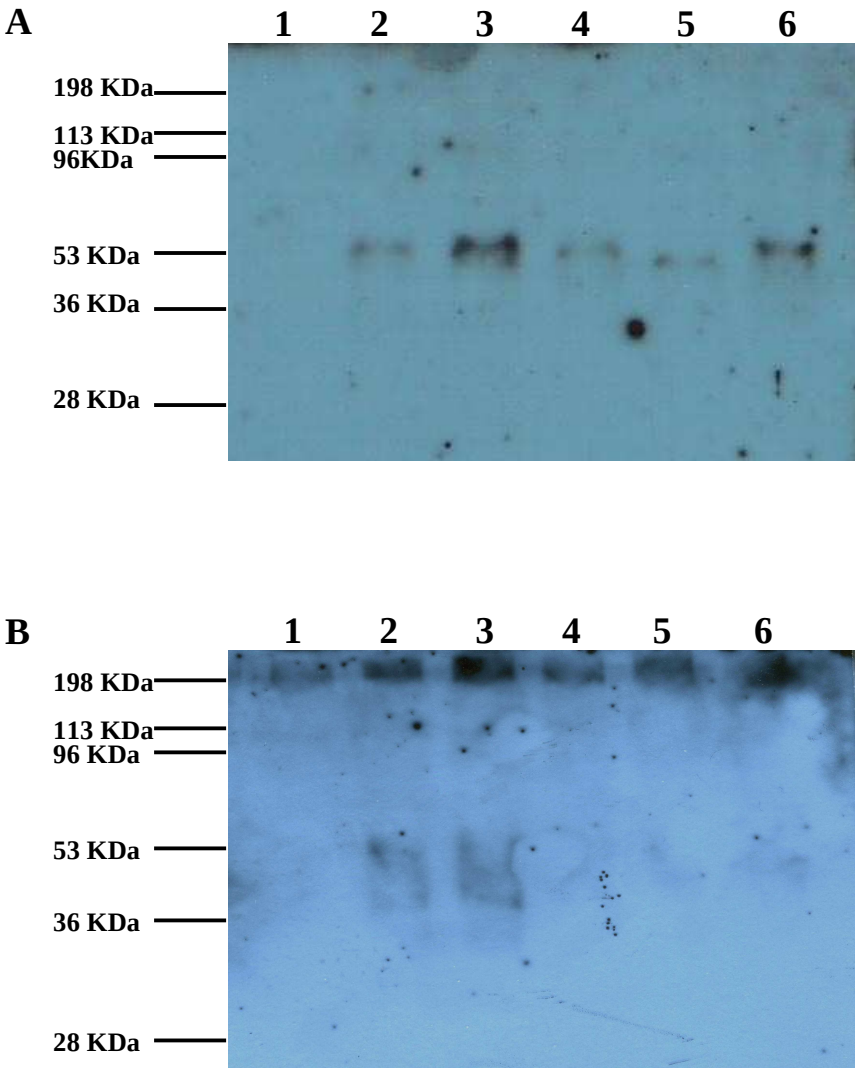

Figure 3-12: Western blot analysis of the cell media of cultures of HMC-1 cells stimulated for 24 hours by various molecules. The detection of properdin was done using a rabbit anti-human properdin antibody followed by the use of the HRP-labelled goat anti-rabbit IgG. X-ray films shown are representatives of A: one out of the three experiments performed; B: the two others experiments. Lane 1: Non-stimulated cells; lane 2: GM-CSF-stimulated cells; lane 3: IFNγ-stimulated cells; lane 4: IL-1β-stimulated cells; lane 5: TGFβ-stimulated cells; lane 6: TNFβ-stimulated cells.

3.3.4 Localisation of properdin on mast cells

After looking at properdin secretion by HMC-1 cells under the influence of different stimuli, my work focused on the localisation of properdin inside mast cell and I investigated the putative storage compartment of properdin in mast cells.

Flow cytometry, a technique that allows the detection of specific antigen present on the surface of cells, was used to assess the presence of properdin antigen on the surface of mast cells (Wirthmueller et al., 1997). Mast cells were specifically stained using a mouse anti-human properdin antibody and detected via the use of a Phycoerythrin (PE)-conjugated rat anti-mouse IgG antibody (see chapter 3.2.10.1). Flow cytometry was performed as well on three other cell lines – namely the myelomonocytic cell line HL-60, the myelogenous leukemia cell line K562 and T cell line Jurkat – that are more or less known to express properdin (both HL-60 and Jurkat cells synthesis and secrete properdin, while properdin expression by K562 has never been reported in the literature (Farries and Atkinson, 1989; Schwaeble et al., 1993; Schwaeble et al., 1994)). The results obtained for these three controls were compared to the one obtained for HMC-1 and LAD 2 cells.

As seen on the figures 3-13A and 3-13B, a fluorescent signal was detected on the surface of both mast cell lines. The intensity of this signal was higher than the one obtained using the appropriate isotype control: HMC-1 presented a geometric MFI (Mean Fluorescence Intensity) 1.36 fold higher for properdin than for its isotype control, while LAD 2 cells had a geometric MFI 1.5 fold higher for properdin than for its isotype control. No shift of the fluorescence signal was detected for Jurkat (figure 3-13C) and for K562 cells (figure 3-13D) compared to their isotype controls, whereas HL-60 cells had a positive shift compared to its isotype control (geometric MFI of HL-60 1.9 fold higher for properdin than for the isotype; figure 3-13E).

The presence of properdin inside the cell was further investigated, still using flow cytometry, but this time cells were first permeabilised. Different treatments were applied to the cells in order to permeabilise them (as listed in chapter 3.2.10.2). However, a same pattern was obtained whether cells were treated with saponin or with a commercial detergent solution: no properdin signal was detected inside HMC-1 cells as illustrated by the fact that more fluorescence was observed on cells stained with the isotype control than on cells stained with properdin. A histogramm representative of the results obtained using the three different permeabilisation treatment is shown on

figure 3-13F. The loss of the fluorescent signal for permeabilised cells compared to non-treated cells suggested that properdin was not stored inside the mast cell's intracellular compartment.

To confirm this interpretation, microscopic analyses of mast cells were performed. For this purpose, HMC-1 and LAD 2 cells were fixed in formaldehyde and embedded in agar. Ultrathin sections of embedded cells were then stained with a mouse anti-human properdin antibody and with anti-mouse IgG coupled to gold particles and examined by electron microscopy. As illustrated on figures 3-14 and 3-15, gold particles were only detected around the cytoplasmic membrane of both HMC-1 and LAD 2 cells. No antigen-antibody complex was observed inside the cytoplasm of both cell lines confirming the flow cytometric result. In the vicinity of the cell membrane, properdin was seen to be present either in clusters of two to eight molecules attached to cytoplasmic extensions (circles), or alone dispersed all around the cell surface of both mast cell lines (small arrow). A similar pattern was obtained with the polyclonal goat anti-human properdin antibody (data not shown).

The availability of this new polyclonal FITC-labelled goat anti-human properdin antibody on the market allowed investigating further the localisation of properdin in mast cells. This same antibody was previously used to characterise properdin localisation on mouse spleen sections (see chapter 2.1.7.2). In addition to mast cells, immunofluorescence analyses were performed on human blood smears (peripheral blood T cells have been shown to synthesise and secrete properdin while peripheral blood granulocytes have been shown to secrete properdin (Schwaeble et al., 1993; Wirthmueller et al., 1997)). Slides containing cytospun HMC-1 cells or human blood smears were stained with the FITC-labelled goat anti-human properdin antibody as described in chapter 3.2.11.4.3 and observed under a fluorescence microscope. The use of the Vectashield Hard Set mounting medium with DAPI allowed the visualisation of the cell nuclei as DAPI emits at a wavelength of about 460nm when bound to double-stranded DNA (manufacturer datasheet). It therefore helped to identify the different cell types present in blood according to their nuclear morphology. As shown on figure 3-16A, red blood cells, granulocytes and lymphocytes could easily be differentiated: red blood cell were DAPI-negative due to the absence of nucleus in these cells, whereas granulocytes nuclei appeared multilobed and lymphocytes presented a round-shaped nucleus. As expected, positive

properdin signals were observed inside the cytoplasm of granulocytes, while no signals were seen for both red blood cells and lymphocytes (see figure 3-16B).

Concerning HMC-1 cells, a weak signal was observed all around the cell surface and positive fluorescent signals were seen as well close to the cell nuclei (figure 3-17). However, the experiment did not allow seeing clearly whether the signal seen close to the nuclei came actually from inside the cell or was due to the detection of properdin on top of the cell. Bright green spots (open arrows) corresponding to non-specific binding of the FITC antibody to bacteria and/or dust particles deposited on top of the slides were visualised, but could easily been differentiated from specific staining under the microscope. It is worth mentioning that due to time restriction this experiment was performed only once and more experiments would need to be conducted. It is important to note that the fluorescence intensity of the signal detected in mast cells was lower than the one observed in the granulocytes.

Next, the localisation of properdin on murine tissue-based mast cells was assessed, still using immunofluorescence. Paraffin-embedded sections of mouse ear skin, a tissue expressing plenty of mast cells, were used as good quality frozen sections of this tissue could not been obtained due to the texture of the tissue. These sections of paraffin-embedded mouse ear skin were first investigated for the presence of mast cells using the mast cell-specific staining toluidine blue (see chapter 3.2.11.2). As seen on figure 3-18A, toluidine blue-positive cells presenting numerous purple granules were found throughout the sections. Sections consecutives to the toluidine blue ones were next immunostained using the FITC-labelled goat anti-human properdin antibody. As seen on figure 3-18B, numerous FITC positive signals were detected on wild type mouse skin sections. However, a similar staining pattern was observed too on properdin-deficient mouse skin sections (figure 3-18C), giving evidence that the FITC-positive signals previously observed on the wild type mouse ear skin sections were most likely unspecific. The technique would therefore need to be improved to ensure a specific detection of the properdin antigen in paraffin-embedded tissues, more particularly in paraffin-embedded ear skin, in order to see if properdin can be visualised on tissue-based murine mast cells.

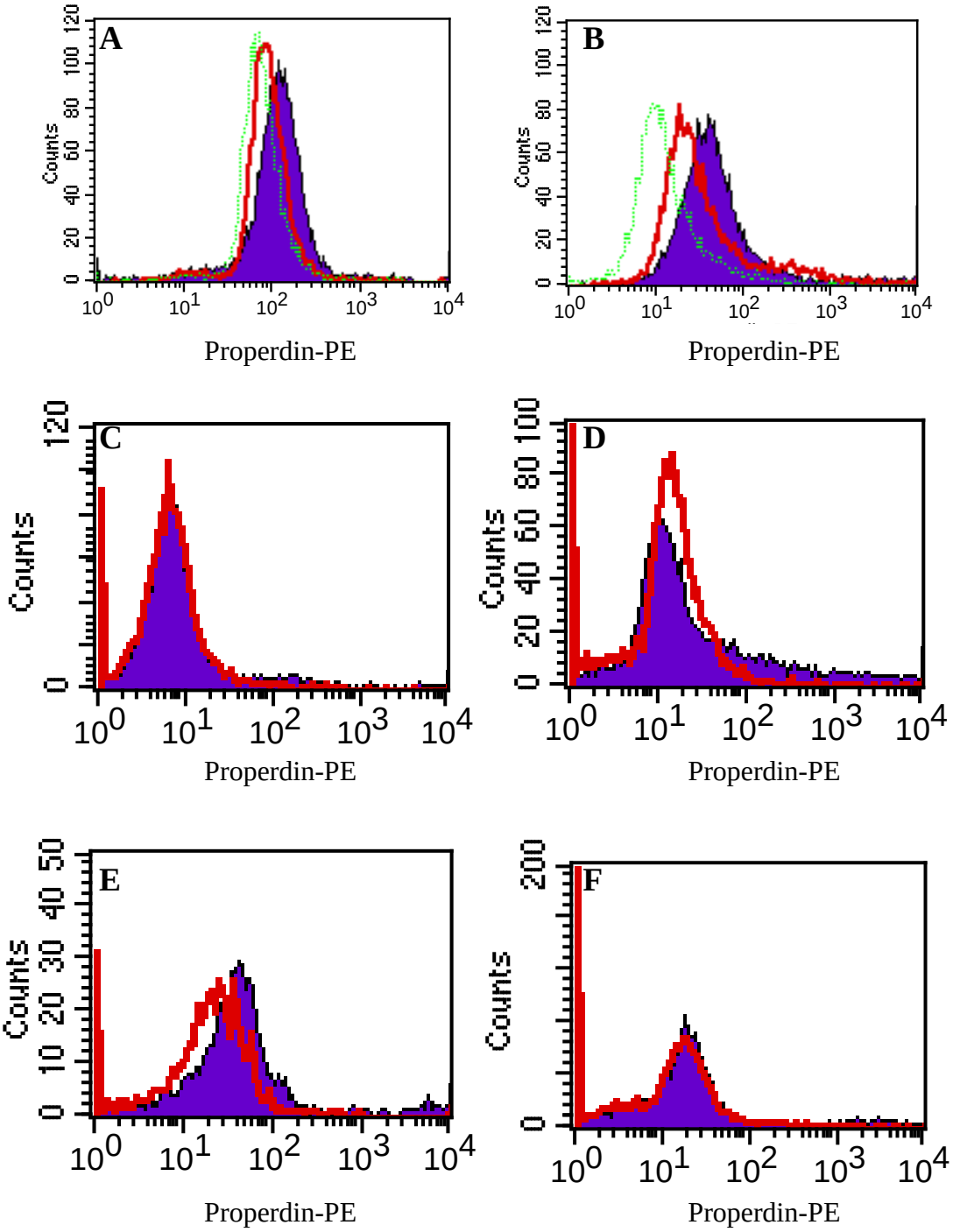

Figure 3-13: Flow cytometric analyses on various cell lines stained with the mouse anti-human properdin antibody (blue) or its isotype control (red). The detection of both antibodies was done via the use of the goat anti-mouse IgG PE-labelled. Representative histograms of A: HMC-1 cells, B: LAD 2 cells; C: Jurkat cells; D: K562 cells; E: HL-60 cells and F: permeabilised HMC-1 cells are shown. The green curve represents a negative control (secondary antibody only was added to the cells).

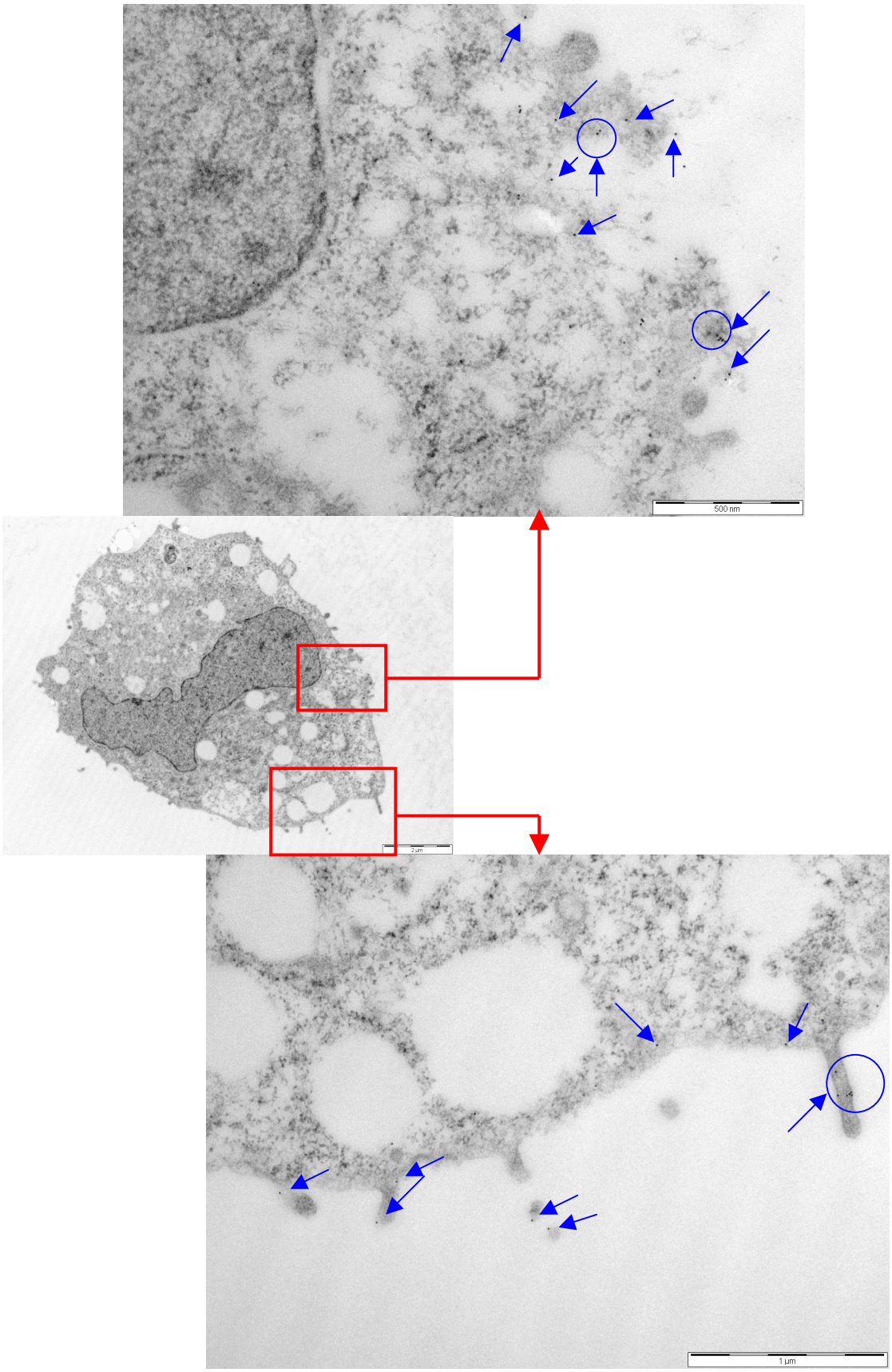

Figure 3-14: Representative electron micrographs of HMC-1 cells immunostained with the mouse anti-human properdin antibody and IgG coupled to gold particles. Arrows point at gold particles. Circles represent clusters of gold particles. Representative observations made from 2 different mast cell preparations.

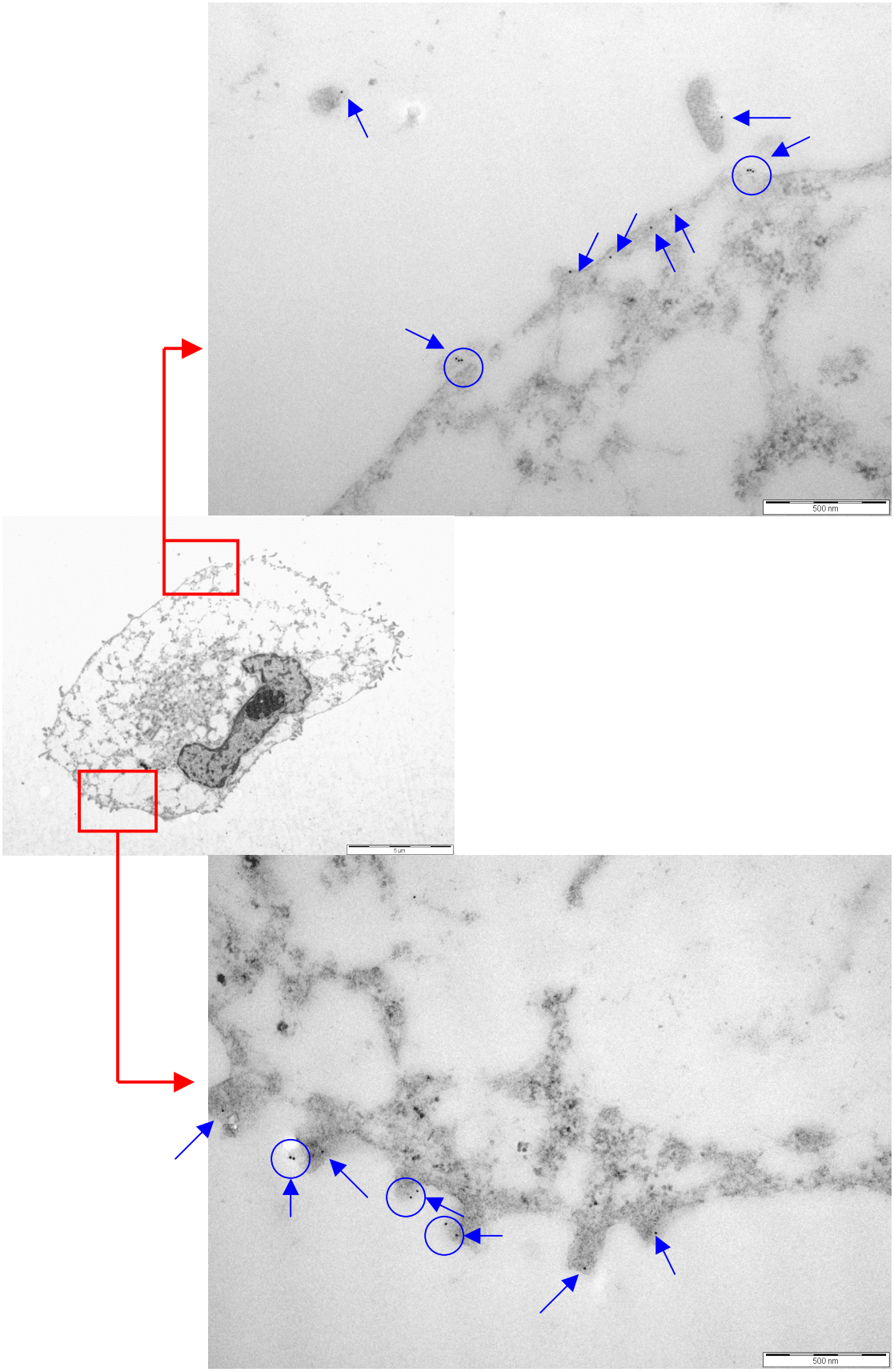

Figure 3-15: Representative electron micrographs of LAD 2 cells immunostained with the mouse anti-human properdin antibody and IgG coupled to gold particles. Arrows point at gold particles. Circles represent clusters of gold particles. Representative observations made from 2 different mast cell preparations.

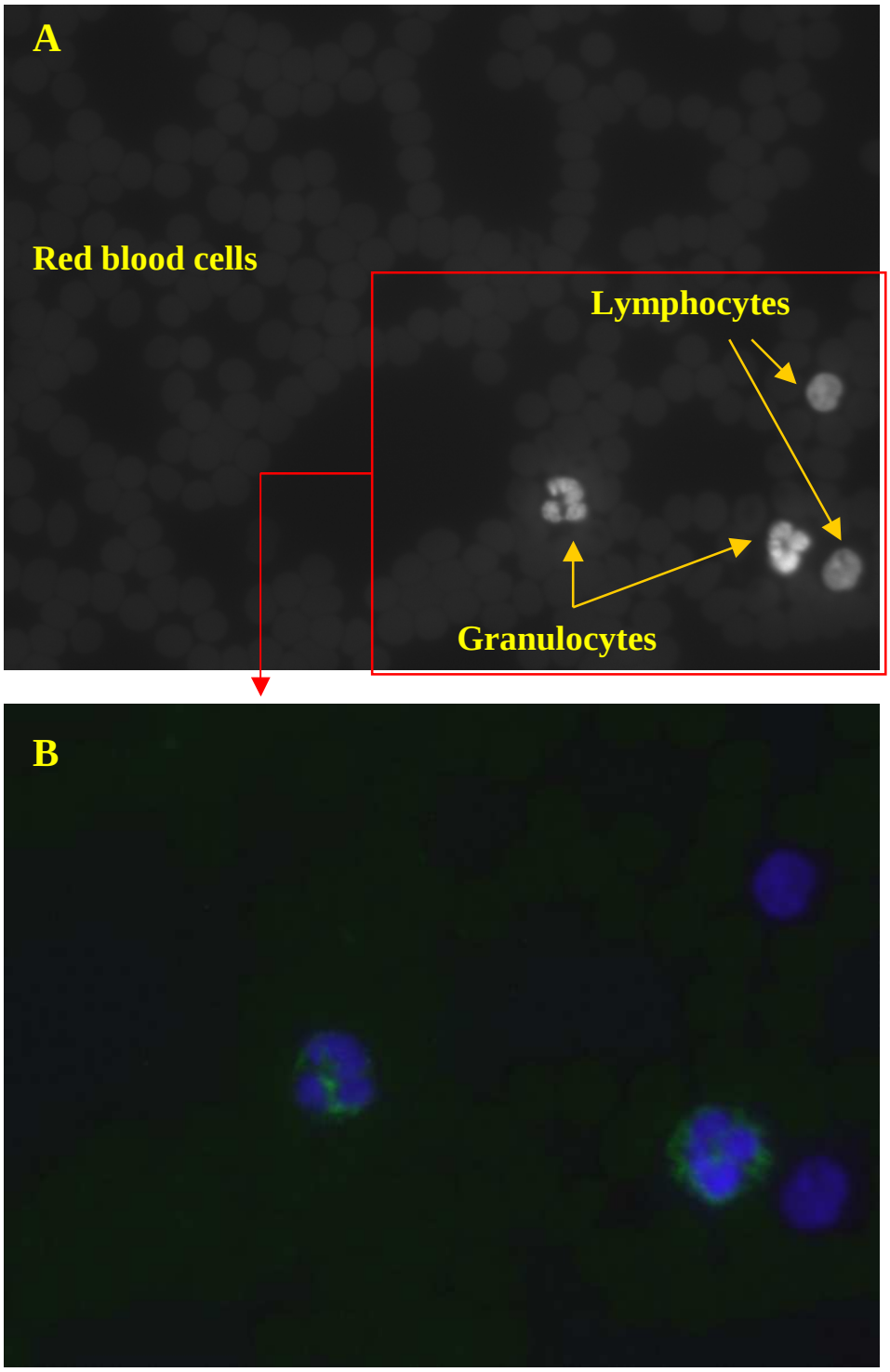

Original magnification x40

Figure 3-16: Representative picture of human blood smear stained with DAPI and immunostained with the FITC-labelled goat anti-human properdin antibody. A: using the DAPI filter and without background correction and artificial colouring; B: merge picture of the one obtained using the DAPI filter and the one obtained using the FITC filter and after background correction (DAPI in blue and FITC in green). Representative observations made with the blood of one single individual.

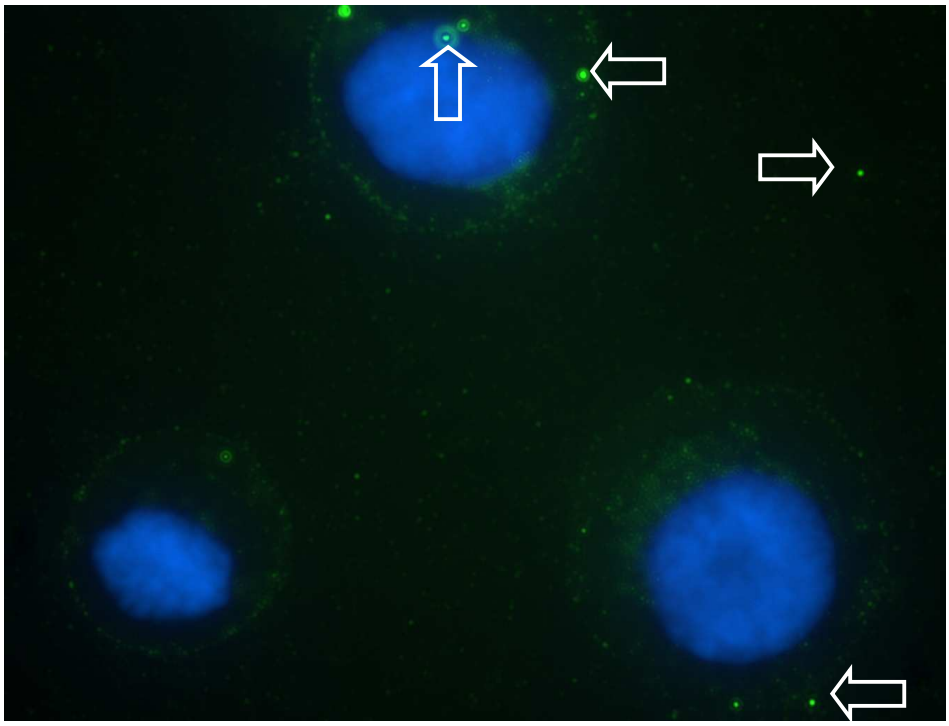

Original magnification x100

Figure 3-17: Representative picture of cytospun HMC-1 cells stained with DAPI (blue) and immunostained with the FITC-labelled goat anti-human properdin antibody (green). Bright green spots corresponded to non-specific binding of the FITC-labelled antibody to bacteria or dust present on the specimen (open arrows). Representative observation made from one single mast cell preparation.

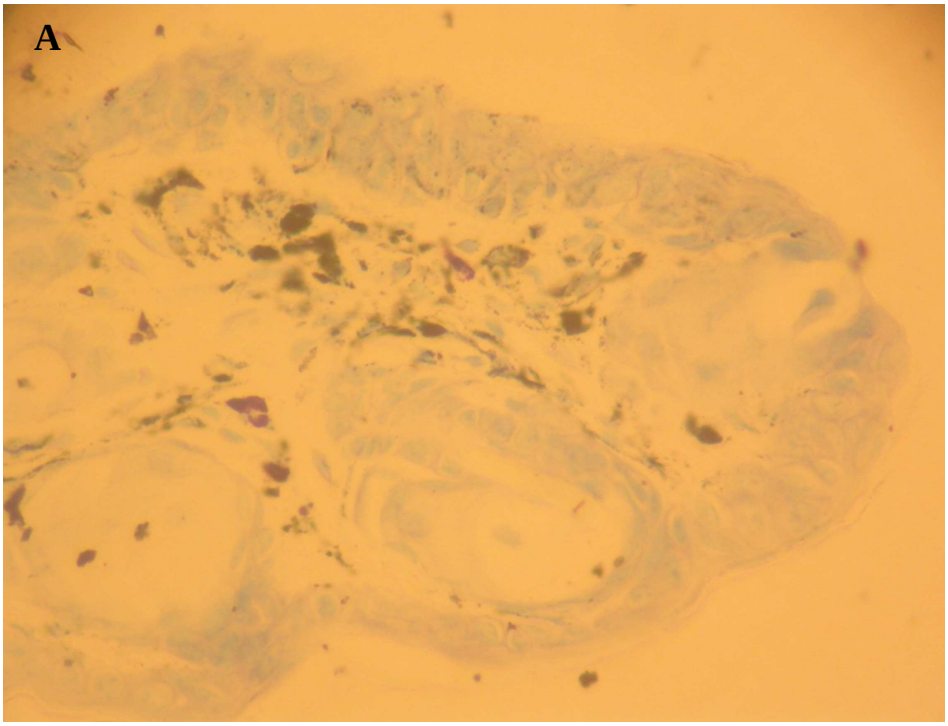

Original magnification x40

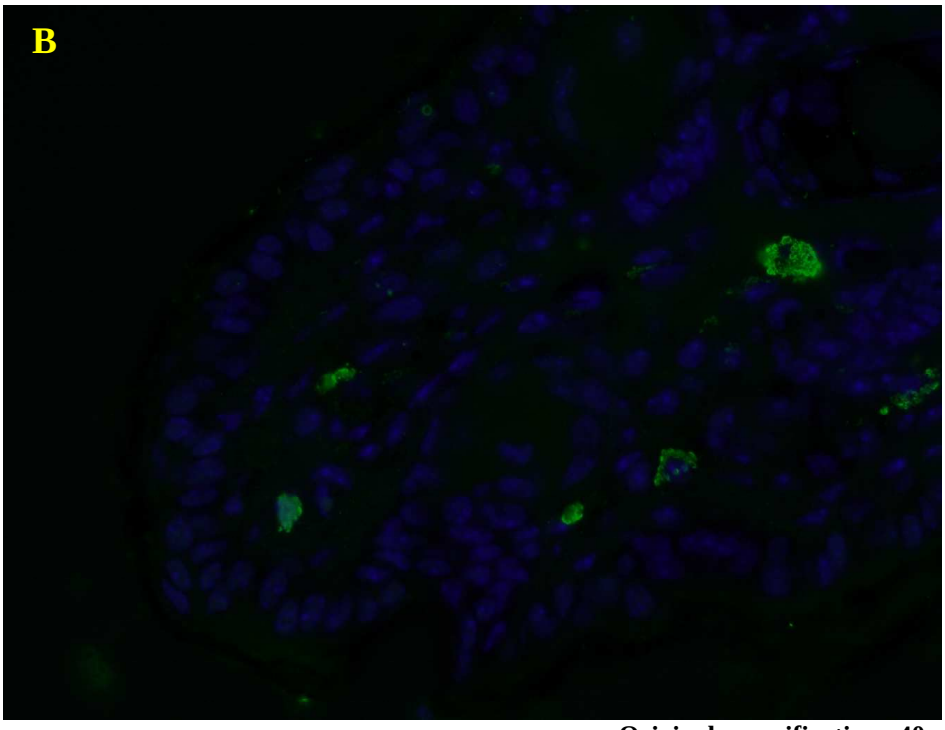

Original magnification x40

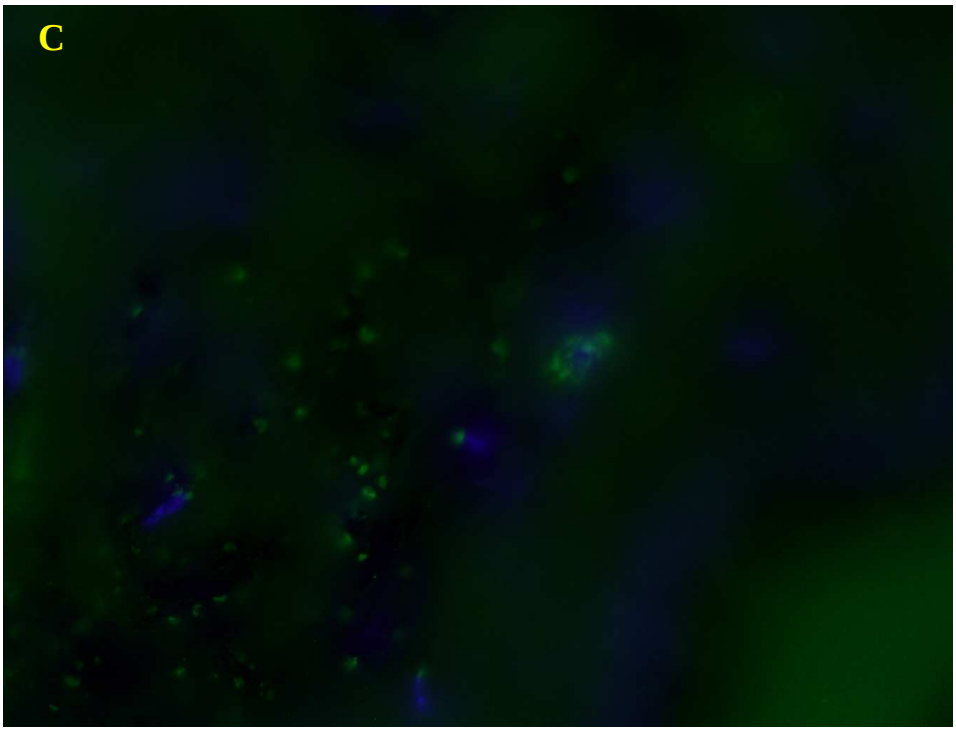

Original magnification x40

Figure 3-18: Representative pictures of mouse skin ear sections A: wild type mouse skin section stained with toluidine blue; B: wild type mouse skin section stained with DAPI (blue) and immunostained with the FITC-labelled goat anti-human properdin antibody (green); C: properdin-deficient mouse skin section stained with DAPI (blue) and immunostained with the FITC-labelled goat anti-human properdin antibody (green). Representative observations made with skin sections obtained from more than 3 different mice.

3.3.5 Secretion of properdin by mast cells

The previous results suggested that properdin was associated with the mast cell's membrane, especially with some structures similar to vesicles in process to be released. The last aim of this project consisted of verifying whether properdin was secreted, as suggested by the electron microscopic pictures, via membrane vesicles.

In order to confirm the mode of secretion of properdin by mast cells, membrane particles were isolated by differential ultracentrifugations of the HMC-1 cell culture media (see chapter 3.2.3). Two kinds of vesicles were collected. Negatively stained electron micrographs of the material collected at 10,000g showed round-shaped vesicles with a diameter varying from 50nm to 1µm. The majority of the vesicles observed in this fraction had a diameter close to 100nm (figure 3-19A). The material extracted after ultracentrifugation at 70,000g was more homogenous. The negatively stained vesicles observed by electron microscopy had a smaller diameter, mainly oscillating from 40 to 100nm, although few vesicles with a diameter exceeding 100nm could be spotted in this fraction (figure 3-19B).

The presence of properdin on these two types of vesicles was then assessed using the monoclonal mouse anti-human properdin antibody. First, 300g fractions corresponding to cells, 1200g fractions corresponding to cell debris, 10,000g fractions and 70,000g fractions were lysed (see chapter 3.2.8.2) and the total protein content of each fraction was measured by Bradford assay (see chapter 3.2.7.2). Properdin concentration (for two different dilutions of each fraction) was assessed using a commercial properdin ELISA kit (see chapter 3.2.9.3). Properdin could be detected in the two different dilutions of both the 300g and 1200g fractions. Both dilutions of a same sample gave a similar final concentration (table 3-5). Concerning the 10,000g fraction, properdin was only detected in the least diluted sample, whereas properdin was not detected in both dilutions of the 70,000g fraction. Due to the restricted amount of samples available for both the 10,000g and the 70,000g fractions, lower dilutions of these samples could not be tested.

Different amounts of total protein from each fraction were then loaded onto a 10% SDS-PAGE gel and developed by Western blot using the mouse anti-human properdin antibody (see chapter 3.2.8). Properdin was eventually detected in all the fractions by Western blot (figure 3-20). However, two different patterns of bands were

observed: properdin was either detected as a 53 KDa band corresponding to a monomer of properdin (figure 3-20A) or as the 53KDa monomeric band and a 106KDa band, the latter corresponding to a dimer of properdin (figure 3-20B). However, in all cases, properdin was detected with the highest intensity in the 10,000g fraction, whereas the 70,000g fraction was showing the lowest concentration of properdin, these being consistent with the previous ELISA results.

Finally, after detecting properdin in both kinds of vesicles, the last experiment of this project consisted of localising properdin on both vesicles using an electron microscopic approach. In order to do that, the mouse anti-human properdin antibody and the anti-mouse IgG coupled with gold particles used previously to detect properdin on mast cells were used. Despite the use of different techniques to detect the antigen (permeabilisation of the vesicles with Triton X-100 (as, this time, it was not sections of sample, but the whole sample which was present on the grid), use of smaller gold particles to ensure they could penetrate the permeabilised vesicles and fixation of the vesicles before to treat them (see chapter 3.2.11.3.4)), properdin could not be detected on the surface or inside both the 10,000g fraction and the 70,000g fraction vesicles (data not shown).

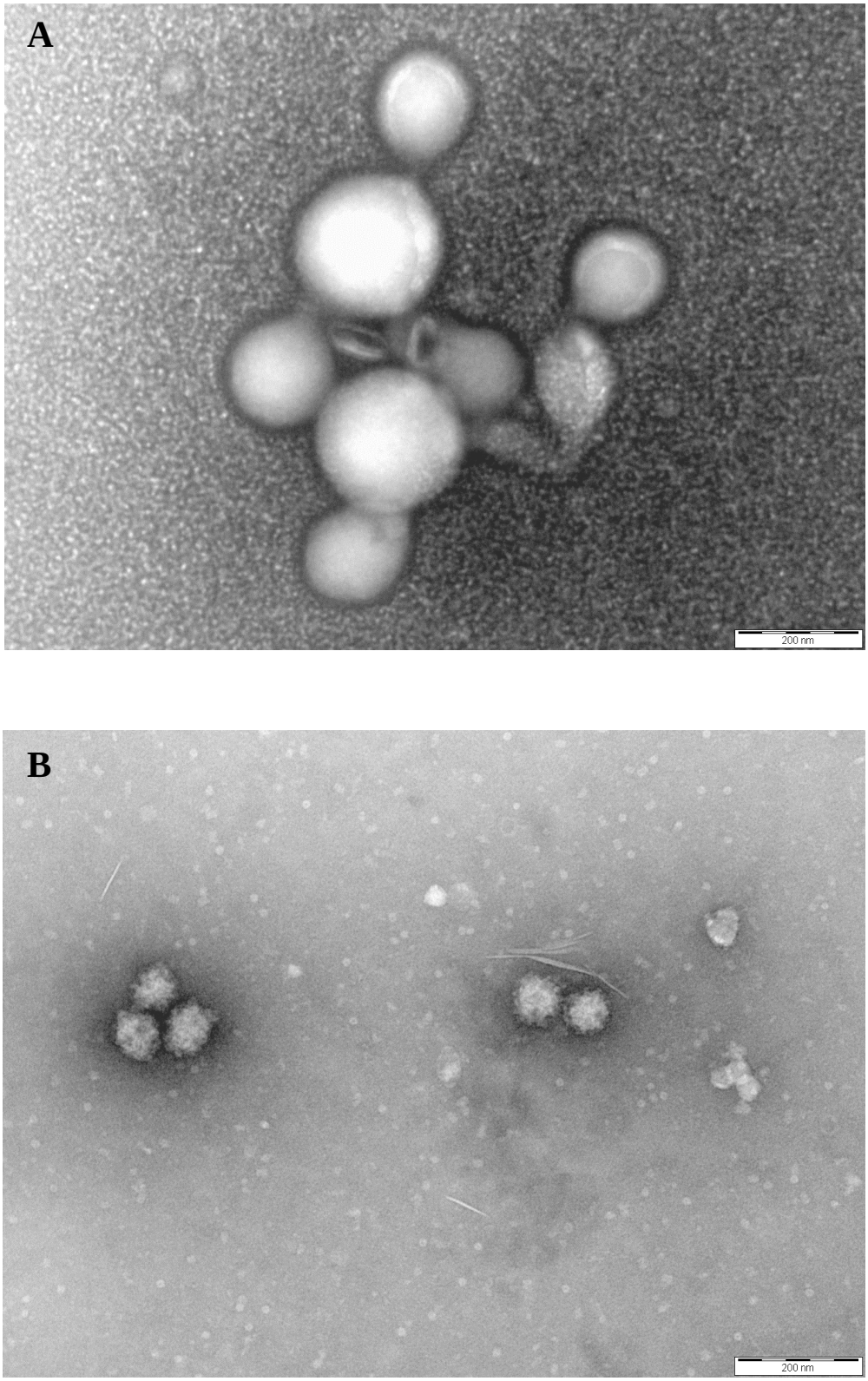

Figure 3-19: Representative transmission electron micrographs of the negatively stained vesicles extracted from HMC-1 cell culture medium after ultracentrifugation at A: 10,000g and B: 70,000g. Representative observations made using, for both fractions, two different vesicle preparations.

Fraction	300g fraction (cells)	1200g fraction (cell debris)	10,000g fraction (microvesicle-like vesicles)	70,000g fraction (exosome-like vesicles)
Concentration (ng/µg of total protein)	22.2	72.5	106.0	Non detected

Table 3-5: Properdin concentration of the various fractions obtained after ultracentrifugation of HMC-1 cell culture, measured by ELISA. Results obtained from duplicates obtained from one single vesicle preparation.

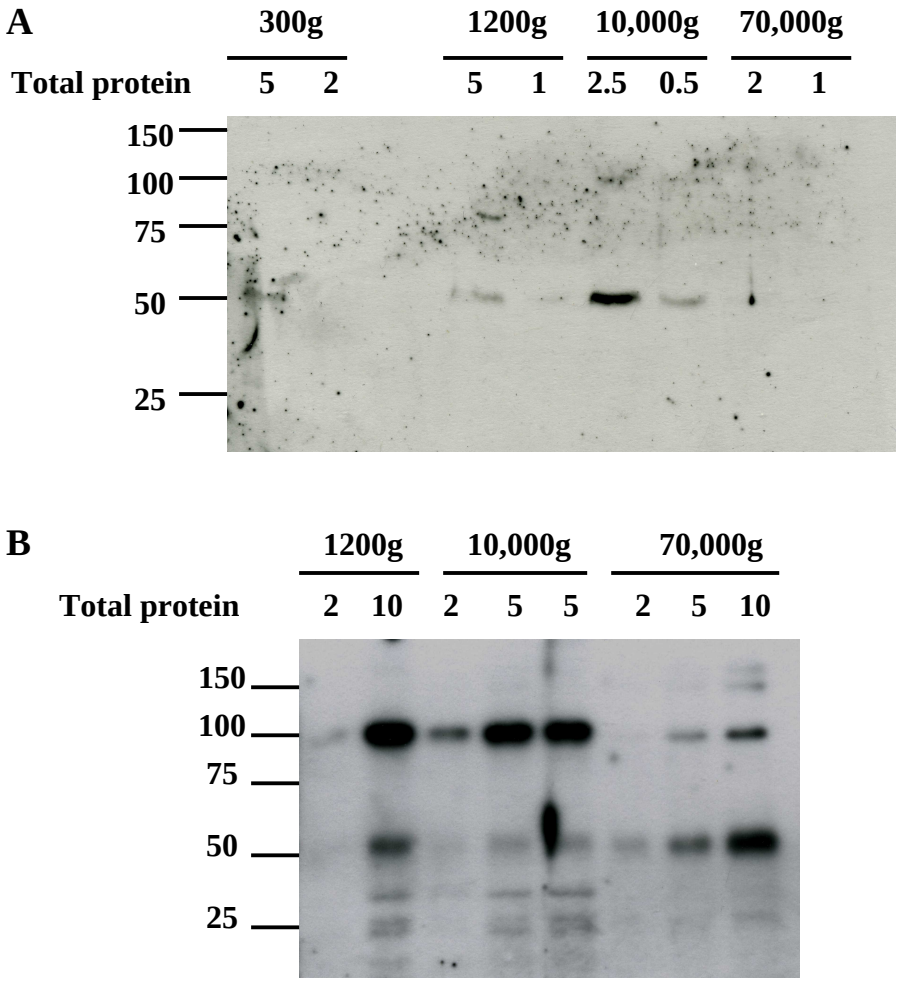

Figure 3-20: Western blot analyses of the 300g, 1200g, 10,000g and 70,000g fractions extracted from HMC-1 cell culture after ultracentrifugation. The detection of properdin was done using a monoclonal mouse anti-human properdin antibody followed by the use of HRP-labelled goat anti-mouse IgG. A: using material from the first vesicles extraction; B: using material from the second vesicles extraction.

3.4 Discussion

As mentioned in the introduction, properdin, the only positive regulator of the alternative complement pathway, is synthesised by a wide range of cells, including cells of the immune system such as lymphocytes, granulocytes, monocytes, macrophages and dendritic cells. Mast cells, another cell type belonging to the immune system, play major roles in immunity by triggering hypersensitivity reactions when activated by some allergens, or by regulating the specific immune response observed after infection (Bischoff, 2007). The aim of this project was to investigate whether mast cells produced properdin, and, if they did, to characterise further the synthesis and secretion of properdin by this cell type.

This work was done using two well characterised human mast cell lines: HMC-1 and LAD 2 cells. The purity of these cell lines was regularly verified using toluidine blue, a mast cell-specific histological stain (Drexler and MacLeod, 2003). Both HMC-1 and LAD 2 cells were reactive with Toluidine blue as shown by the staining of their metachromatic granules in purple. Further investigations indicated that, as expected, a majority of the HMC-1 cell population was positive for tryptase, a major constituent of mast cells (Nilsson et al., 1994). Electron microscopic observations of HMC-1 cells after osmium fixation showed that this cell line appeared, as usually described in literature, with numerous electron-dense granules in their cytoplasm (Alexandrakis et al., 2003; Grutzkau et al., 1997; Kandere-Grzybowska et al., 2003). Concerning LAD 2 cells, usual characteristics were observed as well, except for the appearance of their granules (Theoharides et al., 2007). LAD 2 cell granules actually appeared empty following osmium fixation, as they usually appeared after piecemeal degranulation (Dvorak, 2005; Theoharides et al., 2007). This suggested that the LAD 2 cells may have undergone degranulation while processed for electron microscopic analyses.

3.4.1 Properdin is expressed by mast cells

Using different approaches, properdin expression was then detected in both cell lines. Using the RNA isolated from both HMC-1 and LAD 2 cells as templates and specifically designed primers, a product of the expected size of 1451bp corresponding to the open reading frame of the human properdin gene was detected by reverse transcriptase-PCR. The RT-PCR product obtained with HMC-1 RNA was

then successfully cloned into PGEM-T easy vector, analysed by restriction digests and sequenced. Its sequence showed almost 89% identity with the known sequence of the Homo sapiens complement factor properdin mRNA (accession number: NM_002621). However when not taking into account the high proportion of bases not identified by the sequencer (no call) at the very beginning and at the very end of the sequence (this was probably due to technical reasons, the best quality sequence with this technique being usually observed between 50bp and 500bp after the sequencing primer (PNACL DNA sequencing service, personal communication)), the percentage of identity between this sequence and the published sequence of human properdin exceeded 95%.

Properdin expression by HMC-1 (stimulated or not) and LAD 2 cells (non-stimulated, data not shown) was then confirmed by real-time PCR using a different pair of primers specific for properdin. Various molecules, namely GM-CSF, IFNγ, IL-1β, TGFβ, TNFβ and LPS were used to stimulate HMC-1. Stimulation of neutrophils and monocytes by various cytokines has been shown to affect the release of properdin. Schwaeble and collaborators investigations concluded that properdin expression and secretion by the monocytic cell line Mono Mac 6 was up-regulated by LPS, PMA and TNF-α, whereas Wirthmueller and collaborators showed that TNF-α, GM-CSF, G-CSF, IL-1β, IL-8 and C5a enhanced properdin release by neutrophils (Schwaeble et al., 1994; Wirthmueller et al., 1997). Properdin expression by stimulated mast cells was therefore investigated. All molecules used to stimulate HMC-1 cells, except for TNF-β (Tumor Necrosis Factor β), were already reported in the literature as affecting mast cell's functions. In HMC-1 cells, TGF-β (Transforming Growth Factor β) has been shown to induce cell migration and to inhibit cell growth, IL-1β (Interleukin 1β) to induce the production of various pro-inflammatory cytokines, IFNγ (Interferon γ) to induce the expression of cytokines/chemokines, and GM-CSF (Granulocyte-Macrophage Colony-Stimulating Factor) to downregulate the expression of several mast cell's characteristics (tryptase, FcεRIα) (Chi et al., 2004; Gilchrist and Befus, 2007; Olsson et al., 2001; Welker et al., 2001). Concerning LPS (Lipopolysaccharide), it has been shown to induce both piecemeal and anaphylactic degranulation (Yang et al., 2005). This last phenomenon was observed only when cells were stimulated by both LPS and LBP (LPS Binding Protein), while, here, HMC-1 were only stimulated by LPS. However, the 10% FCS present in the culture media can substitute for LBP and therefore degranulation should occur after stimulation with LPS (Lee et al., 1992).

In my study, the expression of properdin by stimulated or native HMC-1 cells was analysed by real-time PCR and found to be similar 24 hours after stimulation. Low values were observed for two individual samples (GM-CSF and TGFβ-stimulated cells) while their replicates using the same conditions showed a similar expression level. This variation of expression level obtained for these particular samples was thought to be due to the presence of more heparin in these samples during the RNA extraction, as this mast cell mediator has been shown to interfere with reverse transcriptase-PCR (Glaum et al., 2001).

Properdin concentration in the culture medium of cytokine-stimulated or LPS-stimulated HMC-1 cells 24 hours after stimulation was then measured by Western blot and ELISA. Difficulties to detect properdin by Western blot were encountered. The polyclonal anti-human properdin antibody used for this experiment gave non-reproducible results as it showed different band patterns on the X-ray film for the three different experiments performed. The expected 53 KDa band was observed at different intensities in my first attempt for all samples, but the unstimulated cells. However, as no red Ponceau staining of the membrane was performed for this particular experiment, it was impossible to prove that the same amount of protein was transferred from the gel to the membrane during the blotting. When trying to reproduce this result, the 53 KDa band on the X-ray film was shown to become fainter each time and bands with higher molecular weight could be observed too on the gel, suggesting the antibody could have been affected during the time of the experiment (probably during the multiple freeze/thaw of the antibody aliquot). This antibody being not manufactured, another aliquot could not be obtained. This made the quantification of properdin in the cell media of HMC-1 cells impossible by this technique at the time of this experiment.

Finally, the origin of properdin in these samples was confirmed to be cellular as no properdin could be detected in cell-free medium by ELISA.

3.4.2 Localisation of properdin in mast cells

After showing that properdin was expressed and secreted by two mast cell lines, its localisation and putative storage inside these cells was then investigated. First, flow cytometric analysis of permeabilised and non-permeabilised cells was performed using a properdin-specific monoclonal antibody and a PE-labelled

secondary antibody. Different detergents were used to create pores in the cell membrane, allowing antibodies to penetrate the cell and therefore allowing the detection of intracytoplasmic antigens. Properdin could be detected on non-permeabilised HMC-1, LAD 2 and HL-60 cells, whereas no signal was observed on permeabilised HMC-1 cells and non-permeabilised Jurkat cells. The fact that the properdin positive signal was lost after detergent treatments on HMC-1 cells suggested that cell permeabilisation actually occurred and membrane-bound properdin was lost during pore formation. This implied that properdin protein was not stored inside the cytoplasm of HMC-1 cells, but was associated to the mast cell membrane.

HL-60, K562 and Jurkat cells were used as positive and negative controls in this experiment. HL-60 is a human promyelocytic leukaemia cell line that predominantly contains in culture neutrophilic promyelocytes and can differentiate toward granulocyte-like cells after treatment with DMSO (Dimethylsulfoxyde) (Farries and Atkinson, 1989; Gallagher et al., 1979). Properdin has been shown to be expressed at the same level by both unstimulated and DMSO-treated HL-60 cells (Schwaeble et al., 1994). At a protein level, properdin could be detected only in the cell supernatant of DMSO-treated HL-60 cells and not in the supernatant of unstimulated HL-60 cells (Farries and Atkinson, 1989). Jurkat, an immortalised T lymphocyte cell line, is known as well to both express and secrete properdin (Schwaeble et al., 1993). However, the level of properdin found in the cell medium after 3 days of culture was relatively low (0.12ng of properdin/10^6 cells) compared to, for example MonoMac 6 cells (1.21ng of properdin/10^6 cells after 24 hours of culture), a monocytic cell line (Schwaeble et al., 1994). Nothing has been published yet concerning the expression or the secretion of properdin by the human chronic myelogenous leukemia cell line K562. Flow cytometric analysis of these three cell lines suggested that properdin was found at a higher level on undifferentiated HL-60 cells than on Jurkat and K562 cells, as no signal was detected on Jurkat and a low partial signal was seen on K562 cells. The absence of signal for properdin on Jurkat cells, despite knowing this cell line secretes properdin, may be due to the fact that the amount of properdin present was below the detection limit of the technique. To conclude, all these results taken together suggested that properdin was not stored intracellularly, but present at the surface of mast cells, and that less properdin was

bound on the surface of the HMC-1 and LAD2 mast cell lines than on the promyelocytic cell line HL-60.

The presence of properdin at the surface of mast cells was then confirmed by electron microscopy using a properdin-specific antibody coupled to gold particles. Properdin was detected on the cell membrane of both HMC-1 and LAD 2 cells. This was observed all over the cell surface. Properdin was present either alone, or in clusters of 2 to 8 molecules. Isolated properdin reactivities were mainly localised on the cell membrane by itself, while clusters were more often found on cytoplasmic extensions. No signal was seen inside the cytoplasm of both cell lines, neither inside their cytoplasmic granules. On these pictures, HMC-1 and LAD 2 cells granules did not appear electron dense as, for this experiment, the cells were not fixed with osmium tetroxide, but with formaldehyde, which is not an electron stain (Hayat, 1981). However some material could be seen inside their granule compartments suggesting that, this time, no piecemeal degranulation or anaphylactic degranulation occurred for the LAD 2 cells.

Fluorescence microscopy was the last technique used to locate properdin in mast cells. Only preliminary results were obtained and more experiments would need to be performed. A polyclonal anti-properdin antibody FITC-conjugated was applied on slides containing cytospun HMC-1 cells and blood smears. Positive signals were here again detected all around the membrane of HMC-1 cells. However, positive signals were detected as well around the cell nuclei. As cells were cytospun to the slide, it was difficult to say if this signal actually corresponded to properdin molecules present inside the cytoplasm of these cells or if properdin was present on the top surface of the cells. This would need to be investigated further.

Concerning the human blood cells, properdin could only be detected inside the granules of cells morphologically identified as granulocytes. No signal was seen on red blood cells, lymphocytes, or monocytes (all identified according to the shape of their nucleus). These results were in accordance with what has been published in the literature as, even if properdin was known to be expressed by these three cell types, neutrophil was the only cell type known to store properdin inside their granules (secondary granules) (Schwaeble et al., 1993; Schwaeble et al., 1994; Soderstrom et al., 1991; Truedsson et al., 1990; Wirthmueller et al., 1997). Moreover, this was consistent with the fluorescence microscopic results obtained previously on mouse

spleen sections (see chapter 2.2.2.2), where no signal was detected inside the red pulp of the spleen, a reservoir for red blood cells, and no intensive signals were observed inside the white pulp, mainly composed of lymphocytes.

The non-detection of properdin inside the cytoplasm of mast cells in this study was thought to be potentially due to a conformational matter. In fact, properdin is subjected to several post-translational modifications (N-glycosylation, C-mannosylation and O-fucosylation) and is always found in an oligomeric form in extracellular media (Farries and Atkinson, 1989; Gonzalez de Peredo et al., 2002; Hartmann and Hofsteenge, 2000). The epitope recognised by the monoclonal anti-human properdin antibody was not known, but could be masked on the monomeric or non-glycosylated forms of properdin putatively present intracytoplasmically. However, the use of the polyclonal anti-properdin antibody FITC-conjugated for the analysis of mast cells by electron microscopy showed the same pattern as the one observed using the monoclonal antibody (no properdin detected inside the cytoplasm). Further analyses of HMC-1 cells by fluorescence microscopy using this polyclonal antibody should be performed in the future to elucidate this point.

In the same way, the unspecific detection pattern observed with paraffin-embedded mouse skin sections may be explained by the incompatibility of the polyclonal FITC-labelled anti-properdin antibody with formalin-fixed tissues as this antibody has never been tested for paraffin sections (according to the manufacturer) and as formaldehyde treatment has already been associated with high level of background.

3.4.3 Secretion of properdin by mast cells

As mentioned earlier, properdin was detected on the surface of both HMC-1 and LAD 2 cells on structures similar to vesicles ready to be excreted. This kind of structure has already been described in the literature (Kandere-Grzybowska et al., 2003). Properdin seems to be attached to round shaped vesicles with a diameter comprised between 100 and 200nm. This could correspond to either exosomes, or microvesicles, two types of vesicles known to be excreted by mastocytes in general, HMC-1 cells in particular, which play a role in cell-to-cell communication (Ratajczak et al., 2006). The last part of this project was thus to investigate the putative presence of properdin inside vesicles secreted by mast cells.

Vesicles were first extracted from HMC-1 cell culture supernatant by using a differential ultracentrifugation technique broadly used in the literature (Al-Nedawi et al., 2005; Caby et al., 2005). Electron micrographs of the material extracted showed that the 10,000g fraction was similar in size and in shape (100 to 400nm round vesicles) to microvesicles (and was thus named microvesicle-like vesicles), whereas the vesicles isolated after the 70,000g step had a smaller diameter (40-100nm) and were sharing similarity with exosomes (and were therefore called exosome-like vesicles). Analysis of these vesicles using a different Western blot approach than the one previously used to detect properdin on stimulated HMC-1 cells showed that properdin was present on both types of vesicles. Moreover, properdin was shown to be expressed at a higher concentration on the microvesicle-like vesicles compared to the exosome-like vesicles or to the cell and the cell debris fractions. This result, confirmed by ELISA, suggested that microvesicle-like vesicles were in fact a properdin-enriched sub-population of vesicles secreted by mast cells.

Using the same electron microscopic approach as the one used for HMC-1 and LAD 2 cells, both exosome-like and microvesicle-like vesicles were immunostained for properdin. Unfortunately, despite various modifications of the protocol – pre-fixation, use of detergents and use of smaller gold particles – properdin could not be visualised on either type of vesicles. It would however be interesting to know whether properdin is localised inside or on the surface of these vesicles as this could give valuable information to determine the role played by properdin in these vesicles.

4 Characterisation of the properdin-deficient mouse line during pneumococcal pneumonia

4.1 Introduction

4.1.1 *Streptococcus pneumoniae*, complement attack and evasion

Streptococcus pneumoniae is an encapsulated alpha hemolytic cocci-shaped Gram positive bacterium. It is an important human pathogen causing bacterial pneumonia, meningitis, otitis media and septicaemia. It affects mainly infants, elderly and immunocompromised individuals. Despite the availability of antibiotics, *S. pneumoniae* still causes 10 million deaths per year worldwide (WHO, 1998).

Streptococcus pneumoniae is a commensal of the normal human upper respiratory tract. At any time, it asymptomatically colonises the nasopharynx of up to 20% and 50% of healthy adults and children, respectively (Lanie et al., 2007). However, when colonisation of the lower respiratory tract occurs, it becomes pathogenic and it generates an innate immune response and an inflammatory reaction with, among others, an important influx of neutrophils and the activation of the complement system (Reviewed in Jarva et al., 2003; Kadioglu et al., 2000; Kadioglu and Andrew, 2004). According to the structure of their capsular polysaccharide, more than 90 different serotypes of pneumococci have already been identified, all of them showing considerable differences in virulence as the capsule is a major virulence factor for pneumococci (Kadioglu et al., 2008). *S. pneumoniae* produces several other factors that are involved in its pathogenicity, such as pneumolysin, PspA, PspC (Jedrzejas, 2001).

Humans with a deficiency in complement as well as complement-deficient mice (C3-, C4-, C1qa-, factor B-, factor D-, CR1/2-, CR3- and CR4-deficient mice) have been shown to be more susceptible to pneumococcal infection, emphasing the fact that complement plays a crucial role in protection against *S. pneumoniae* (Janoff and Rubins, 2000; Brown et al., 2002; Kerr et al., 2005; Ren et al., 2004). Using complement-deficient mice, it has been shown that both the alternative pathway and

the classical pathway play a major role in the innate immunity to pneumococci, while the lectin pathway seems to have only a minor role (Brown et al., 2002; Ren et al., 2004). The classical pathway, activated immediately after infection via natural IgM antibodies or via C-reactive proteins, plays its role by initiating bacterial opsonisation and therefore depositing C3b fragments onto the surface of pneumococci. Some of this C3b-bound molecules then binds to Bb to create alternative pathway C3 convertases and, via its amplification loops, the alternative pathway then amplifies the formation and allows the deposition of more C3b molecules onto the bacterial surface (Brown et al., 2002; Xu et al., 2001; Yuste et al., 2005).

Kerr and collaborators have shown, in a model of pneumococcal pneumonia, that C3 or C5 were not required to attract inflammatory cells at pulmonary infection sites (via their anaphylatoxin fragments C3a and C5a). Instead, opsonophagocytosis (via C3b, C4b and iC3b) and anti-bacterial activities (via C3a and its inactive form C3a-desArg, which can act as antimicrobial peptides) are the main complement activities occurring during pneumococcal infection (Kerr et al., 2005; Nordahl et al., 2004).

Streptococcus pneumoniae has developed several strategies to evade the complement system, mainly via its various virulence factors. The pneumococcal capsule, pneumolysin (a major streptococcal cytotoxin), PspA (Pneumococcal surface protein A) and PspC (Pneumococcal surface protein C) all interfere with complement deposition on pneumococci and therefore reduce the opsonic complement activity of the host (table 4-1) (Jarva et al., 2003; Kadioglu et al., 2008).

Virulence factors	**Role against complement**
Capsule	Inhibits effective opsonophagocytosis
Pneumolysin	Activates C3 in absence of specific anti-capsular antibodies
PspA	Interferes with C3 deposition and with the formation of the alternative pathway C3 convertase
PspC	Binds to factor H and degrades C3

Table 4-1: Role of the main pneumococcal virulence factors against complement.

4.1.2 Infection model

The strain used in this study – *S. pneumoniae* D39 – is a serotype 2 encapsulated strain. It was isolated from a patient in 1916 and has been used by Avery and collaborators in 1944 to show that genes are made of DNA. This strain has since been widely used in mouse infection models (Lanie et al., 2007).

Two different infection models were used during this study: mice were infected either intranasally with a high dose of *S. pneumoniae* D39 (from 0.5 to $1.5x10^6$ pneumococci/mouse; gives an intermediate phenotype for susceptibility to infection) or intravenously with a lower dose of *S. pneumoniae* D39 ($1x10^5$ pneumococci/mouse) (Gingles et al., 2001). Only *S. pneumoniae* D39 that have been passaged in animals were used to infect the mice in this study as passaging enhances the virulence of pneumococci by stimulating capsule synthesis (Saladino et al., 1997). Moreover, in order to ensure a certain consistency between the different preparations of *S. pneumoniae*, the viability and the virulence of each bacterial stock were always checked (by plating serial dilutions and infecting MFI mice) and aliquots of bacteria were never kept more than 3 months at -80ºC.

4.1.3 Properdin-deficient mouse line

Mouse susceptibility to pneumococcal disease varies according to the genetic background of mouse strains (Kadioglu and Andrew, 2005). The wild type C57Bl/6 mouse strain is known to possess an intermediate phenotype for susceptibility to infection following infection with D39 pneumococci, as shown by the analysis of their survival time and blood clearance 24 hours post-infection (Gingles et al., 2001). Because the properdin-deficient mouse is on a C57Bl/6 background, it constitutes a good choice to investigate the role of properdin during pneumococcal infection.

The properdin-deficient mouse line used in this study was generated by Dr. Cordula Stover (University of Leicester). This line was developed to deduce the functions of properdin as, at the start of this project, the function of properdin seemed restricted to providing host-immunity to Neisseria meningitidis only. The properdin gene was disrupted by homologous recombination that leads to the elimination of the part of the properdin gene coding for TSR2 to TSR5. This was then microinjected to C57Bl/6 blastocysts. Two chimeric mice were derived, their offsprings intercrossed and one of the heterozygous female obtained was then backcrossed with a C57Bl/6

male to obtain properdin-deficient males and wild-type littermates (figure 4-1A) (Stover et al., 2008). Studies of this mouse line have shown these mice effectively lack properdin in their serum and have an impaired alternative pathway activity (figure 4-1B) (Stover et al., 2008). Unchallenged, these properdin-deficient mice are not immunocompromised, however they have been shown to be impaired in their survival compared to their wild type littermates following sublethal caecal ligation and puncture and in non-septic shock models (LPS and zymosan-induced) (Ivanovska et al., 2008; Stover et al., 2008).

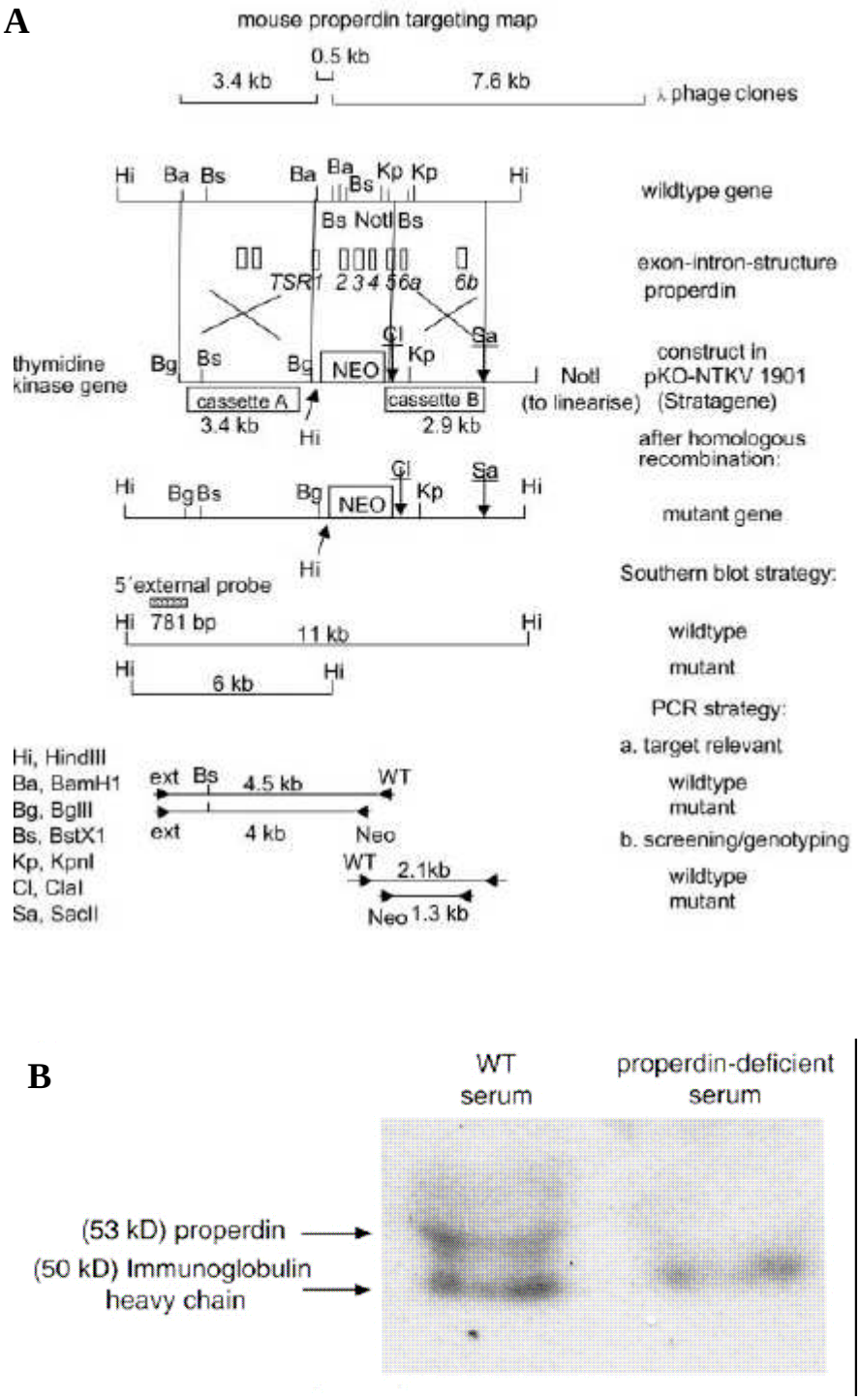

Figure 4-1: The properdin-deficient mouse line. A: Strategy used to generate the properdin-deficient mouse line. B: Western blot analysis of properdin-deficient and wild type serum using an anti-properdin antibody (from Stover et al., 2008).

4.2 Material and methods

4.2.1 Mice and bacteria

Eight to 20 weeks-old male properdin-deficient mice and wild type littermates (called "gold line", a C57Bl/6 line developed from Charles Rivers breeders at the University of Leicester Transgenic Unit) were used in these studies. Mice were maintained in a barrier unit and health screened regularly as part of the institutional guidelines. Ethical approval was obtained for all the animal experiments. Experiments were carried out in accordance with Home Office regulations. The genotyping of the mice used in this study was done by Dr. Cordula Stover as previously described (Stover et al., 2008).

Streptococcus pneumoniae serotype 2, strain D39 (NCTC 7466) was obtained from the National Collection of Type Cultures (London, UK) by Dr. Aras Kadioglu (University of Leicester). *S. pneumoniae* recovered from mouse blood (called "passaged") are more virulent than non-passaged bacteria, therefore, passaged *S. pneumoniae* D39 were used to challenge the mice *in vivo* (Saladino et al., 1997). *S. pneumoniae* were passaged by Luke Richards (University of Leicester) as described by Canvin et al. (Canvin et al., 1995). Briefly, MF1 mice were intraperitoneally infected with *S. pneumoniae*. 24 hours post-infection, mice were culled and *S. pneumoniae* were recovered from their blood, grown overnight in BHI medium, aliquoted in BHI medium containing FCS and stored in the freezer at -80°C until further use. The viability of the suspension was determined by plating serial dilutions onto blood agar and counting CFUs as explained in chapter 4.2.7. The virulence of the stock was finally assessed by infecting intranasally MF1 mice with 10^6 *S. pneumoniae*. Only bacteria from a stock able to induce severe septicaemia in less than 48 hours in all of the infected MF1 mice were used in this study.

For *in vitro* analyses, fresh stocks of non-passaged *S. pneumoniae* were used. *S. pneumoniae* were plated onto a blood agar plate and grown overnight. A single colony was then picked and grown in BHI medium. The next day, cells were spun down at 3000g for 5 minutes and the pellet was resuspended into 15ml of serum broth (80% BHI, 20% FCS) and incubated at 37°C for 5 hours before aliquoting and freezing at -80°C. The viability of the suspension was determined by plating serial dilutions onto blood agar and counting CFUs as explained in chapter 4.2.7. When

needed, an aliquot was either grown in BHI or in vegetable special infusion medium, or pelleted and resuspended at an adequate concentration in PBS.

Escherichia coli DH5α was provided by Dr. Richard Haigh (University of Leicester).

4.2.2 *In vitro* analysis

4.2.2.1 Preparation of human serum and plasma

In order to obtain human serum, blood was withdrawn from a superficial arm vein of a healthy female volunteer and left to coagulate on ice. After coagulation occurred, the blood sample was spun down at 1000g for 5 minutes and the supernatant was collected, aliquoted and stored at -20°C until further use.

Concerning the plasma, blood was withdrawn from a superficial arm vein of a healthy female volunteer and mixed with either EDTA (5mM) or heparin (5U/ml). The blood sample was then spun down at 1000g for 5 minutes and the supernatant was collected, aliquoted and stored at -20°C until further use.

4.2.2.2 Isolation of human polymorphonuclear cells (PMN) and human peripheral blood mononuclear cells (PBMC)

PMN cells were isolated from whole human blood using dextran sedimentation followed by Histopaque® density gradient centrifugations (Kouoh et al., 2000). Blood was withdrawn from a superficial arm vein of a healthy female volunteer and anticoagulated with heparin (5U/ml) and spun down at 1550g for 5 minutes. The plasma was removed and the cell pellet was resuspended in a same volume of a 0.9% (w/v) NaCl solution. ¼ volume of a dextran/saline solution (5% (w/v) dextran (MW 150,000-200,000), 0.7% (w/v) NaCl) was then added and the mixture was let to settle at room temperature for 30 minutes. The supernatant was then carefully removed without disturbing the red blood cell layer and pelleted at 1500g for 2 minutes. This leukocyte pellet was resuspended in PBS and carefully layered on top of a layer of Histopaque-1077 (Sigma-Aldrich), itself layered on top of a layer of Histopaque-1119 (Sigma-Aldrich) before to be centrifuged at 700g for 30 minutes. The middle opaque layer containing the granulocyte fraction was finally cautiously aspirated and resuspended in PBS.

PBMC were isolated using Histopaque® density gradient centrifugations following manufacturer's instructions. Heparinised human blood was, as previously

described, layered on top of layers of Histopaque-1077 and Histopaque-1119 and centrifuged at 700g for 30 minutes. The top opaque layer containing the mononuclear cell fraction was then cautiously aspirated and resuspended in PBS.

4.2.2.3 Serum bactericidal assay

Two different approaches have been used to obtain the mouse serum used in this assay.

At first, blood was taken by cardiac puncture from properdin-deficient and wild type mice after culling (this work was done by Jane Brown, University of Leicester). This blood was left to clot for 30 minutes on ice, pelleted by centrifuging it at 1250g for 20 minutes and the serum was finally collected, aliquoted and stored at -20°C until further use.

In the second set of experiments, properdin-deficient and wild type mice were deeply anaesthetised with 5% (v/v) fluothane (AstraZeneca, Macclesfield, United Kingdom) over oxygen (1.5 to 2 litres/min) and blood was taken by cardiac puncture from mice under terminal anaesthesia (this work was done by Dr Aras Kadioglu) and immediately incubated at 37°C (wet bath) for 30 minutes. After clotting the blood and pelleting it at 4°C by spinning it down at 1250g for 20 minutes, the serum was collected and used immediately for the bactericidal assay (Mueller-Ortiz, S.L., personal communication).

Ninety microlitres of these sera were then mixed with 10µl of either a non-passaged stock of *S. pneumoniae* D39 ($1x10^7$ pneumococci/ml PBS), or a fresh culture of *E.coli* DH5α ($1x10^7$ *E. coli*/ml PBS) in a 96 well plate and incubated for 1 hour in an incubator at 37°C. Then, 60µl of this culture media were plated to determine the number of pneumococci present in each sample (see chapter 4.2.7) (Mueller-Ortiz et al., 2004).

4.2.2.4 Splenocytes bactericidal assay

Properdin-deficient and wild type mice were sacrificed and their spleen was removed aseptically and immediately placed into sterile PBS. Splenocytes isolation was then performed in a tissue culture hood using a modified version of the protocol used by Derrico and collaborators (Derrico and Goodrum, 1996). Spleens were mashed using a scalpel blade and resuspended into 1ml of sterile PBS. This suspension was then filtered through a 100µl Nylon Cell Strainer (BD Falcon) and the

filtrate was collected. Red blood cells were then lysed using a red blood cell lysis buffer (eBiosciences; Insight biotechnology, Wembley, UK). The reaction was stopped by adding 2 to 3 volumes of PBS into this preparation and the cells were finally resuspended into RPMI media supplemented with 10% FCS (Gibco) and cultivated in a humidified incubator at 37°C at 5% CO_2. After 48 hours, the splenocytes were finally divided into 2 subpopulations: the adherent cells and the non-adherent cells. The proportion of adherent cells being low, only the non-adherent cell population was used for the analysis.

Fifty microlitres of the non-adherent cell population ($2x10^6$ cells/ml) were incubated with 50µl of a non-passaged stock of *S. pneumoniae* D39 ($2x10^3$ or $2x10^6$ pneumococci/ml) in a humidified incubator at 37°C at 5% CO_2 for 10 hours. Then, 60µl of each culture medium were used to determine the number of pneumococci present in each sample (see chapter 4.2.7).

4.2.2.5 Peripheral Blood Mononuclear Cells bactericidal assay

PBMC were isolated from human blood as described in chapter 4.2.2.2.

Non-passaged *S. pneumoniae* D39 were grown overnight in vegetable special infusion medium (Fluka; Sigma-Aldrich, Gillingham, UK). This medium is a replacement for BHI of a vegetal origin (while BHI is from animal origin) and was used here as a complement source-free growing medium. The next day, bacteria were spun down at 700g for 5 minutes and resuspended either in PBS, or opsonised for 30 minutes at 37°C in 20% human plasma-PBS to obtain a final concentration of $4x10^6$ bacteria/ml. Opsonised and non-opsonised bacteria were then mixed with a same volume of PBMC ($5x10^6$ cells/ml PBS) and placed in a humidified incubator at 37°C at 5% CO_2.

After 30, 60 and 120 minutes of incubation, 20µl of each sample were plated on blood agar (see chapter 4.2.7). At each time point, gentamicin (100µg/ml) and penicillin (100U/ml) were added to another 200µl of each sample and incubated at 37°C at 5% CO_2 for 2 more hours in order to kill any extracellular pneumococci present in the cell culture medium. Then, the cells were washed twice in PBS, resuspended into 1% saponin-PBS for 10 minutes and 20µl of each sample were plated on blood agar to enumerate the intracellular bacteria present (Segura et al., 1998).

4.2.2.6 Polymorphonuclear cells bactericidal assay

PMN cells were isolated from human blood as described in chapter 4.2.2.2.

Pneumococci were prepared as explained in chapter 4.2.2.5 and were then resuspended either in PBS, or opsonised for 1 hour at 4°C in 50% human serum-PBS to obtain a final concentration of $5x10^6$ bacteria/ml. Two volumes of opsonised and non-opsonised bacteria were then mixed with 1 volume of PMN ($2x10^6$ cells/ml PBS) and placed in a humidified incubator at 37°C at 5% CO_2 (Benton et al., 1995; Letiembre et al., 2005)

After 30 and 90 minutes of incubation, 20µl of each sample were plated on blood agar (see chapter 4.2.7).

4.2.3 Mice infection

4.2.3.1 Intranasal challenge

Properdin-deficient and wild type mice were lightly anaesthetised with 2.5% (v/v) fluothane over oxygen (1.5 to 2 litres/min) and 50µl of a suspension of passaged pneumococci ($1x10^7$ *Streptococcus pneumoniae* D39/ml PBS for the experiment using the mice from the seventh backcrossing stage, $3x3.10^7$ *Streptococcus pneumoniae* D39/ml PBS for the experiment using the mice from the tenth and higher backcrossing stage) were applied to the nostrils of the mice (this work was done by Dr. Aras Kadioglu as previously described (Manco et al., 2006). The number of bacteria injected was confirmed by plating serial dilutions of the inoculum on blood agar. Mice were monitored and severity recorded twice a day during the whole time of the experiment.

Approximately 30 minutes (referenced hereafter as “time 0”), 6, 24, 48 and 72 hours after infection, properdin-deficient and wild type mice were sacrificed. They were deeply anaesthetised with 5% (v/v) fluothane over oxygen (1.5 to 2 litres/min) and blood was taken by cardiac puncture from mice under terminal anaesthesia (this work was done by Dr. Aras Kadioglu as previously described (Jounblat et al., 2005). Lungs were collected as well and placed immediately into sterile PBS.

4.2.3.2 Intravenous challenge

Properdin-deficient and wild type mice were lightly anaesthetised with 2.5% (v/v) fluothane over oxygen (1.5 to 2 litres/min) and $1x10^5$ CFUs of passaged *S. pneumoniae* D39 were administered via the dorsal tail vein (this work was done by

Dr. Aras Kadioglu as previously described (Manco et al., 2006)). The number of bacteria injected was confirmed by plating serial dilutions of the inoculum on blood agar. Mice were monitored and severity recorded twice a day during the whole time of the experiment.

Twenty four, forty eight and seventy two hours after infection, properdin-deficient and wild type mice were lightly anaesthetised with 2.5% (v/v) fluothane over oxygen (1.5 to 2 litres/min) and blood was taken by tail bleeds (this was done by Dr. Aras Kadioglu).

4.2.4 Survival curve

Properdin-deficient and wild type mice were infected intranasally with 50µl of a suspension of passaged *S. pneumoniae* D39 ($2x10^7$ pneumococci/ml PBS). The number of bacteria injected into the mice was confirmed by plating serial dilutions of the inoculum on blood agar. Mice were health-checked and monitored three times a day during the 7 days of the experiment and culled when presenting signs of lethargy in accordance to the Home Office regulations.

4.2.5 Blood preparation

Three hundred and fifteen microlitres of the freshly withdrawn blood were immediately put into an Eppendorf containing anti-coagulant for thromboelastography experiments (see chapter 4.2.8.2) while 20µl of the blood were used to determine the number of viable pneumococci recovered (see chapter 4.2.7). The rest of the blood was clotted on ice, spun down at 13,000g for 5 minutes and serum was then removed, aliquoted and stored at -20°C until further use.

4.2.6 Lung preparation

Lungs were collected, weighed and placed into universal tubes containing 10ml of PBS. Lungs were homogenised using an Ultra-Turrax T8 homogeniser (IKA-Werke). Twenty microlitres of these homogenates were used to determine the number of viable pneumococci present in each sample (see chapter 4.2.7), 500µl were kept for Western blot analysis (see chapter 4.2.10) and the rest was cytospun onto microscope slides for differential analysis of the leukocyte populations present (see section 4.2.11).

For the Western blot, 5µl of protease cocktail inhibitor (Sigma-Aldrich) were added to the 500µl of lung homogenate and spun down at 8,100g for 30 minutes at 4°C. The supernatant was then collected, aliquoted and stored at -20°C until further use.

4.2.7 Determination of viable pneumococci

Both lung homogenates and blood were serially diluted 1:10 in PBS and six 10µl drops of each dilution (from 10^{-1} to 10^{-6}) were plated onto blood agar. Plates were incubated overnight at 37°C in an anaerobic jar. The next day, CFUs were counted from the dilution showing between 10 to 100 colonies per 10µl.

This same technique was used to determine the viability of all stocks of pneumococci and for all the *in vitro* experiments.

4.2.8 Rotational thromboelastography (ROTEG®)

4.2.8.1 Principle

Thromboelastography (TEG) was originally developed by Hartert in 1948 (Hartert, 1948). This technique gave information about both the thrombosis and the fibrinolysis by measuring the viscoelastic properties of whole blood in real time. Citrated whole blood is placed into a cup pre-warmed at 37°C containing calcium ions to reverse the calcium chelation obtained with the citrate. A pin suspended to a torsion wire is introduced into a cup oscillating with a 4.45° angle. When coagulation begins, formed fibrin strands attach the cup to the pin and the oscillations of the cup lead to the oscillations of the pin. The pin's motions are recorded as a TEG's trace (Mallett and Cox, 1992).

Rotational thromboelastography (ROTEG®) has the same basic principle as TEG, except for the fact that here the pin is the oscillating part and the cup is fixed, making the ROTEG® system less susceptible to vibrations and therefore more reliable. Briefly, a plastic pin is fixed on the tip of a rotating axis and a light is sent on to the reflective surface of this axis. The mirror reflects the light onto a detector and thus allows recording the motion of the pin. When coagulation occurs, the pin's movements are restricted by the fibrin strands and the detector translates the change of light displacement into a trace similar to the one obtained by TEG (see figure 4-2; from *http://www.pentapharm.de*).

The TEG's trace enables the determination of the kinetics of the clot's formation, strength and stability. From this cigar-shaped graph, four major parameters of thrombosis can be obtained as outlined by Senzolo and collaborators (figure 4-3) (Senzolo et al., 2007):

- The reaction time (r), which is the period of time from the beginning of the test until a clot begins to form (when it reaches the amplitude of 2mm). It represents the rate of the initial fibrin formation.
- The clotting time (k), which is the period of time from the beginning of the clot formation until the thromboelastogram reaches an amplitude of 20mm. It represents the time needed to reach the standard clot firmness.
- The alpha angle (α), which is the angle formed by the 0mm amplitude line and a tangent of the curve through the 2mm amplitude point. It represents the rate of clot's growth.
- The maximum amplitude (MA), which is the maximum firmness the clot reaches. It represents the clot's strength.

4.2.8.2 Experimental procedure

Blood freshly withdrawn by cardiac puncture was directly mixed with anti-coagulant. Two methods were used to anti-coagulate the blood:

- Method 1: Three hundred microlitres of freshly withdrawn blood were added into an Eppendorf containing 50µl of ACD buffer (140mM sodium citrate/72mM citric acid:7% dextran T500 (1:1)).
- Method 2: Three hundred and fifteen microlitres of freshly withdrawn blood were added into an Eppendorf containing 35µl of a 3.8% trisodium citrate solution.

ROTEG® was performed as described by Landskroner and collaborators using a ROTEG® thombelastograph (Pentapharm, Munich, Germany) in collaboration with Prof. Alison Goodall (University of Leicester) (Landskroner et al., 2005). Briefly, 20µl of 200mM $CaCl_2$ were put into a ROTEG® plastic cup and 300µl of anti-coagulated blood were added. As soon as the blood was added to the cup, the thromboelastograph began to record the different parameters. No exogenous tissue factor was added to the blood.

As only four samples could be run at the same time, the accuracy of the technique over a period of 6 hours post-blood collection was tested by running blood samples obtained from a same mouse 0, 2 and 6 hours after the blood was withdrawn. Similar r, k, α and MA values were obtained during this 6 hours time period (data not shown).

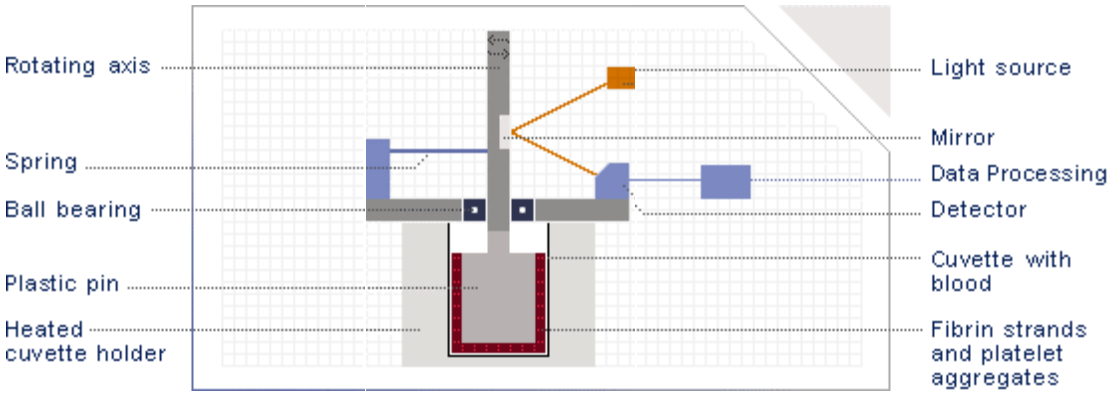

Figure 4-2: Schematic representation of a rotational thromboelastograph (ROTEG®) (from *http://www. pentapharm.de*).

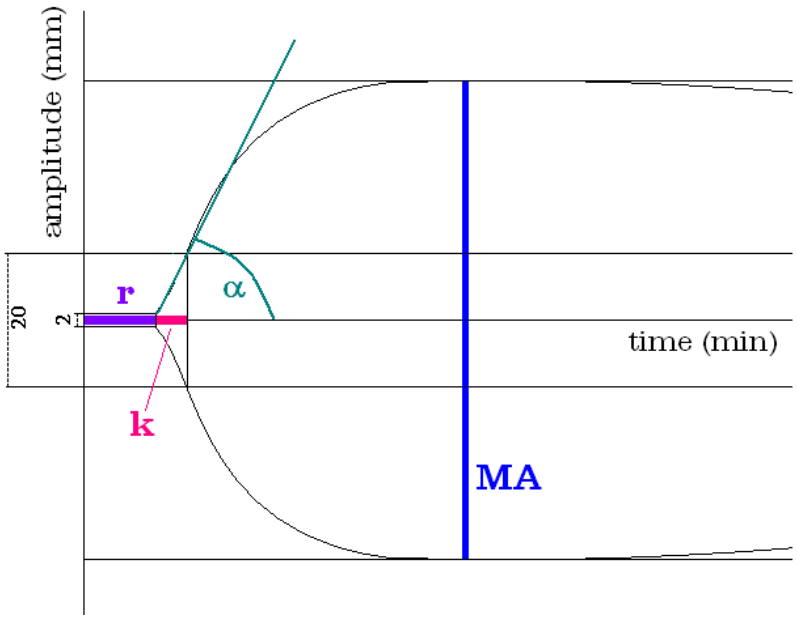

Figure 4-3: Graphic representation of the different thromboelastographic variables (r, k, *a* and MA) obtained by ROTEG® analysis.

4.2.9 ELISA

Different ELISA techniques were used to measure the immunoglobulin M (IgM), immunoglobulin G (IgG) and C3 concentrations present in the serum of unchallenged and challenged properdin-deficient and wild type mice.

4.2.9.1 Indirect IgG and IgM ELISA

In order to compare the IgG and IgM serum levels of unchallenged properdin-deficient and wild type mice, an indirect ELISA technique was developed.

Three microlitres of each serum sample, previously diluted 1:100 in PBS, were mixed with 300µl of coating buffer (35mM $NaHCO_3$, 15mM Na_2CO_3, pH 9.6). Each sample was then serially diluted six times 1:1 in coating buffer and 100µl of each dilution were transferred to an ELISA plate (F96 Maxisorp Nunc-Immuno plates, Nunc) and incubated overnight at 4°C. The next day, the plate was washed 3 times in a washing solution (0.05% Tween 20-PBS) prior to being blocked 1 hour at 37°C with 200µl of a blocking solution (5% (w/v) skimmed milk-PBS). After 3 additional washes, 100µl of a HRP-labelled goat anti-mouse IgG antibody (Sigma-Aldrich) diluted 1:10,000 in 1% (w/v) skimmed milk-PBS were added to each well and incubated for 2 hours at room temperature. The plate was next rinsed 3 more times and 100µl of the single component TMB peroxidase EIA substrate kit (Bio-Rad) were added to the plate. The reaction was stopped few minutes after by adding 100µl of a stopping solution (0.18M H_2SO_4) to each well. The absorbance across the plate was measured at 450nm using a microplate reader.

The same technique was applied to compare the IgM serum levels of properdin-deficient and wild type mice. In this case, 10µl of each serum sample, previously diluted 1:100 in PBS, were mixed with 300µl of coating buffer. The antibody used to detect IgM was the goat anti-mouse IgM antibody AP-conjugated (Sigma-Aldrich) diluted 1:10,000 in 1% (w/v) skimmed milk-PBS. As the antibody was labelled with alkaline phosphatase, a different detection technique was used. Two 5mg pNPP (para-nitrophenyl phosphate) tablets (Sigma-Aldrich) were dissolved into 10ml of pNPP buffer (0.1M glycine, 1mM $MgCl_2$, 1mM $ZnCl_2$, pH 10.4) and, after the final three washes, 100µl of this solution were added to each well. The plate was then incubated at 37°C in the dark until a yellow coloration developed and the absorbance across the plate was measured at 405nm using a microplate reader.

4.2.9.2 Commercial IgM ELISA

IgM serum concentration of challenged and unchallenged mice was determined using the mouse IgM ELISA quantitation kit (Bethyl Laboratories; Universal Biol., Cambridge, UK) according to manufacturer's instructions. All steps were performed at room temperature. The wells of an ELISA microplate (F96 Maxisorp Nunc-Immuno plates, Nunc) were coated for 1 hour with 100µl of coating buffer (0.05M carbonate-bicarbonate, pH 9.6) containing a 1:100 dilution of the goat anti-mouse IgM antibody. The plate was then washed 3 times in a washing solution (1x TBS, 0.05% Tween 20, pH 8.0) and blocked for 30 minutes with 200µl of a blocking solution (1x TBS, 1% BSA, pH 8.0). After 3 additional washes, 100µl of each standard and of each serum diluted 1:300 in sample diluent (1x TBS, 1% BSA, 0.05% Tween 20, pH 8.0) were added to the plate and incubated for 1 hour. The plate was next washed 3 more times and incubated for another hour with the goat anti-mouse IgM HRP-conjugated antibody diluted 1:75,000 in sample diluent (100µl/well). Five last washes were performed and 100µl of TMB substrate (Single component TMB peroxidase EIA substrate kit, Bio-Rad) were added to the plate. The reaction was stopped approximately 6 minutes later by adding 100µl of a stopping solution (0.18M H_2SO_4) to each well. The absorbance across the plate was measured at 450nm using a microplate reader (Model 680, Bio-Rad) and analysed using the microplate manager software, version 5.2.1 (Bio-Rad). The standard curve was generated using a five parameter logistic curve fitting (type Rodbard).

4.2.9.3 C3 ELISA

Serum C3 levels were measured using the mouse C3 ELISA kit (Immunology Consultants Laboratory, Newberg, USA) following manufacturer's instructions. The wells of a microplate pre-absorbed with anti-mouse C3 antibody were loaded with 100µl of each standard or mouse serum diluted 1:50,000 in sample diluent and the plate was incubated for 20 minutes at room temperature. After 4 washes in washing buffer, the plate was incubated for 20 minutes with the enzyme-antibody conjugate. The plate was then washed 4 times with washing buffer and 100µl of the TMB substrate solution were added into each well. The reaction was stopped 10 minutes after by adding 100µl of the stop solution. At the end of the assay, the absorbance across the plate was measured at 450nm using a microplate reader (Model 680, Bio-Rad) and analysed using the microplate manager software, version 5.2.1 (Bio-Rad).

The standard curve was generated using a five parameter logistic curve fitting (type Rodbard).

4.2.10 Western blot

4.2.10.1 Determination of the total protein concentration

To ensure that the same amount of total protein was loaded in each case, the protein concentration of each sample was measured using the Bradford protein assay (Bio-Rad) as explained in chapter 3.2.7.2. The assay was performed using 5µl of lung homogenate.

4.2.10.2 Preparation of the gel

Acrylamide gels were prepared as explained in chapter 3.2.8.1. Ten percent SDS-PAGE resolving gels were used for this experiment.

4.2.10.3 Samples preparation

Twenty four microlitres of lung homogenate (appropriately diluted to contain 20µg of total protein) were mixed with 8µl of 4x SDS-PAGE sample buffer and boiled for 10 minutes. After chilling on ice for 1 minute, samples and 8µl of the prestained Precision plus standards (Bio-Rad) were loaded into the wells of the SDS-PAGE gel. One well of each gel was loaded with an internal reference sample.

4.2.10.4 Western blotting

Electrophoresis was performed as explained in chapter 3.2.8.3. The particular conditions used for this Western blot are summarised in table 4-2.

Blocking solution	5% (w/v) skimmed milk-PBS
Antibody solution	5% (w/v) skimmed milk-PBS
Primary antibody	HRP-conjugated polyclonal goat anti-mouse C3 antibody (ICN pharmaceuticals, Inc.) diluted 1:5000 in the antibody solution
Washing solution	0.05% Tween 20-PBS
Secondary solution	None
ECL kit	ECL Western blotting substrate (Pierce)
X-ray film	Hyperfilm ECL (Amersham Biosciences)

Table 4-2: Conditions used for the C3 Western blot on lung homogenate.

4.2.11 Differential leukocytes analysis of lung tissue

This work was done by Dr. Hannah Brewin (University of Leicester). Briefly, 50µl of lung homogenate were cytospun onto a cytospin slide (Shandon) in a cytocentrifuge (Cytospin 2, Shandon) at 100g for 3 minutes. Slides were then briefly air-dried, fixed in 100% methanol for 10 min and stained with Giemsa stain (BDH) (Kadioglu et al., 2000). Alveolar macrophages, monocytes, lymphocytes and polymorphonuclear leukocytes on each slide were identified according to their morphology and quantified. At least 200 cells in total were counted on two different slides for each sample. The relative percentage of each types of leukocyte was then calculated. All slides were read by an investigator blinded to their identity.

4.2.12 Statistical analysis

In general, arithmetic means (referred as “means”) were used for the analysis of data presented on a linear scale (e.g. C3 serum concentration), while geometric means were applied to data collected on a logarithmic scale (e.g. cfu, flow cytometry).

To compare the numbers of blood and lung CFUs between properdin-deficient and wild type mice, the two-tailed Mann-Whitney U test was applied as non-parametric (transformed) data were used. To compare the survival curve of properdin-deficient and wild type mice, the log rank test and the chi square goodness-of-fit test were applied; while the first test takes into account the survival rate of both groups at each time point, the second only compares the outcome (dead/alive) at the end of the 7-days experiment. To compare the level of serum IgM and serum C3 at different time intervals post-infection, the two-tailed T-test was applied as parametric data with a normal distribution were used. To compare the leukocyte counts between wild type and properdin-deficient, the two-tailed Mann-Whitney U test was applied with Bonferroni correction, as non-parametric multiple data were analysed.

4.3 Results

In this chapter, I examined the importance of properdin during bacterial infection in an *in vivo* infection model using *Streptococcus pneumoniae* D39.

4.3.1 *In vitro* analysis

Before studying the role of properdin during pneumococcal infection *in vivo*, the ability of phagocytic cells and/or serum to kill *S. pneumoniae* D39 *in vitro* was investigated.

4.3.1.1 Serum bactericidal assay

Frozen aliquots of properdin-deficient and wild type mouse serum were incubated with a suspension of non-passaged *S. pneumoniae* D39 for 1 hour at 37°C before being plated onto blood agar and counted (see chapter 4.2.2.3). The same amount of bacteria was recovered from the culture media whereas the bacteria were incubated with or without serum (both properdin-deficient and properdin-sufficient sera), meaning no bactericidal effect was observed with both types of serum in these conditions (data not shown).

This same experiment was repeated using fresh mouse and human serum with both *S. pneumoniae* and *E. coli* DH5α. *E. coli* DH5α being known to be serum-sensitive (to human serum), this strain was used as a positive control in this experiment (Aguilar et al., 1999; Mueller-Ortiz et al., 2004). Here again, no pneumococcal serum killing was observed using both mouse and human sera, while, for DH5α, a significant reduction of bacteria was observed after incubation with the human serum, but none was spotted with both kinds of mouse sera (see figure 4-4). This latter result suggested that the sensitivity of *E. coli* DH5α to mouse serum differed from the one of the *E. coli* HB101 used in my reference study (Mueller-Ortiz et al., 2004). The resistance of DH5α to mouse serum has been confirmed the same year by another study (Anisimov et al., 2005).

4.3.1.2 Splenocytes bactericidal assay

In this experiment, the non-adherent splenocyte population obtained from properdin-deficient and wild type splenocytes after 2 days of culture was incubated with different concentrations of *S. pneumoniae* D39. After 10 hours, phagocytosis was

measured by counting the number of bacteria recovered from the cell culture media (see chapter 4.2.2.4).

As seen in figure 4-5, the same amount of bacteria was recovered from the properdin-deficient and wild type splenocyte culture media after 10 hours of incubation. Moreover, this number was the same whether the pneumococci were cultivated alone or in presence of splenocytes. This suggested that these splenocyte sub-populations obtained from both properdin-deficient and wild-type mice were unable to phagocytose *S. pneumoniae* D39 under these experimental conditions.

4.3.1.3 Opsonophagocytosis assays

As serum alone and cells alone were not sufficient to induce a bactericidal effect on *S. pneumoniae* serotype 2 D39 in the previous assays, several bactericidal assays involving both humoral and cellular components were then performed. For practical reasons, human samples were used instead of murine samples in the following experiments.

4.3.1.3.1 Peripheral Blood Mononuclear Cells killing assay

Human PBMC were incubated with opsonised and non-opsonised pneumococci and, after defined periods of time, extracellular and intracellular pneumococci present in each sample were counted (see chapter 4.2.2.5). As seen in figure 4-6, the same amount of *S. pneumoniae* was recovered from the cell culture after both the 30 minutes and the 1 hour incubation period, and that whether pneumococci had been cultivated alone or in presence of PBMC, and whether they had been pre-opsonised or not. After 2 hours of incubation, differences were spotted between the different samples. More bacteria were present in the cell culture media when pneumococci had been pre-opsonised and incubated with PBMC than when they had been cultivated alone without pre-opsonisation. Concerning the intracellular bacteria, none could be recovered from any of the cell preparations after saponin treatment (data not shown). These results showed that phagocytosis of *S. pneumoniae* by PBMC did not occur in these conditions. The higher number of pneumococci recovered from samples cultivated in presence of plasma for 2 hours was explained by the fact pneumococci are able to grow in plasma.

4.3.1.3.2 PMN killing assay

The same experiment was reproduced using PMN cells instead of PBMC as human PMN cells have previously been shown to kill *S. pneumoniae* D39 in presence of normal human serum (see chapter 4.2.2.6) (Benton et al., 1995). As seen on figure 4-7, the same amount of pneumococci was recovered from the cell culture media whether pneumococci had been cultivated alone or in presence of PMN cells, suggesting that no phagocytosis of pneumococci by human PMN cells happened in these conditions. Pneumococci, here again, used serum to proliferate when they were cultivated in presence of serum.

These preliminary results were contradicting published data showing important phagocytosis of opsonised pneumococci D39 by human PMN in 30 minutes (Benton et al., 1995). I hypothesised that the neutrophils used may have been activated during their preparation as one drawback of the sedimentation method that had to be used to isolate sufficient numbers of neutrophils is the length of time the neutrophils spend in a sub-optimal environment. As phagocytosis could not be observed in these conditions using human material (knowing that mice have significantly less neutrophils than men (http://www.jax.org)) and as more experiments could not be performed to improve this technique due to a lack of time, this technique was not transcribed to mouse and therefore did not allow the comparison of the phagocytosis' efficiency between properdin-deficient and wild type neutrophils.

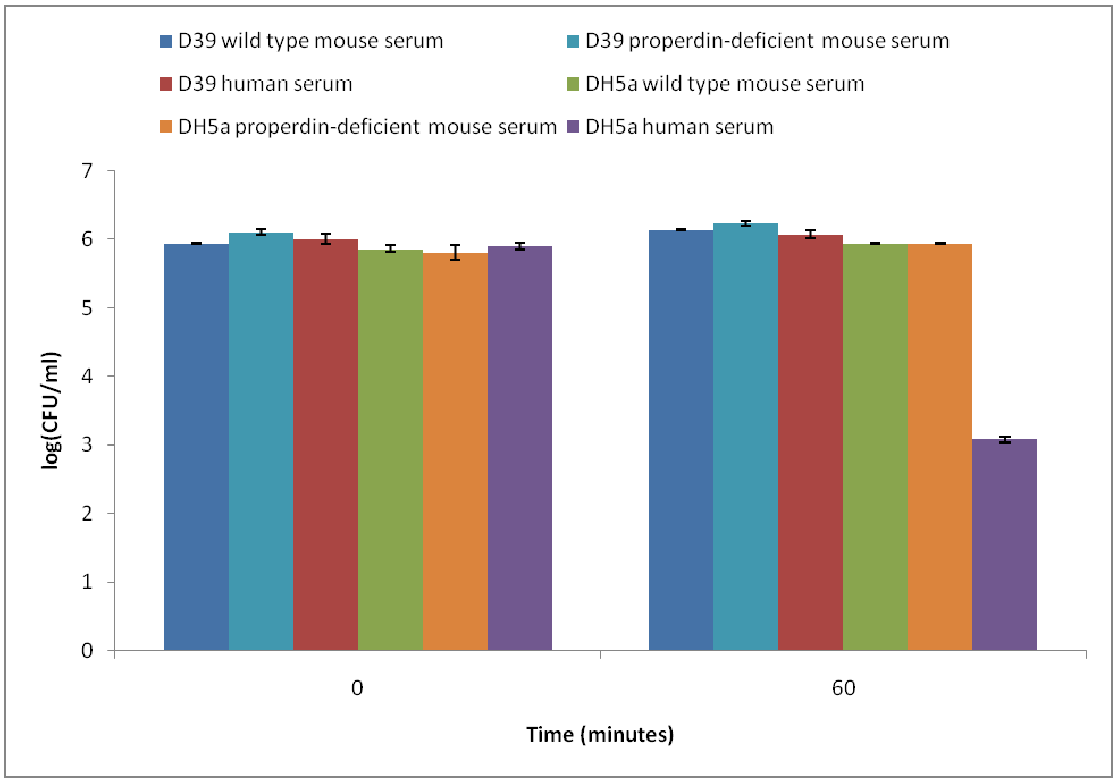

Figure 4-4: Serum bactericidal assay. Properdin-deficient mouse serum, wild type mouse serum and normal human serum were incubated with *S. pneumoniae* D39 or *E. coli* DH5α for 1 hour at 37°C. Log of mean values +/- SD obtained with 2 different mouse sera are given. Representative results obtained from one out of two independent experiments are shown.

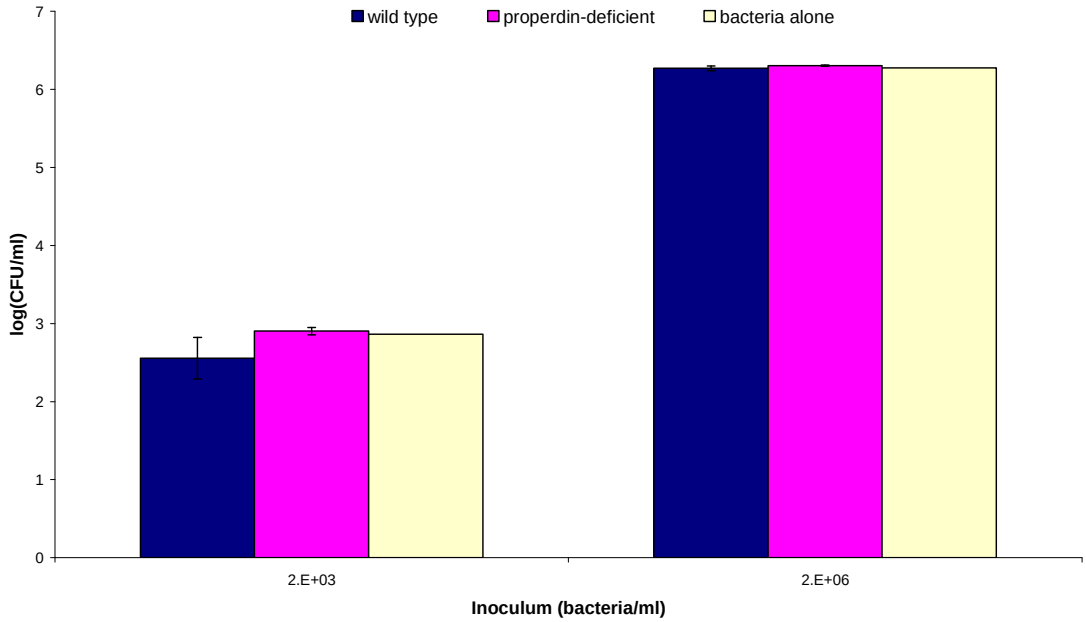

Figure 4-5: Splenocytes bactericidal assay. Properdin-deficient and wild type splenocytes were incubated with non-opsonised *S. pneumoniae* D39 at a MOI of 0.001 and 1 for 10 hours at 37°C at 5% CO_2. Log of mean values +/- SEM from 2 samples obtained from a same mouse are given. Representative results obtained from one out of two independent experiments are shown.

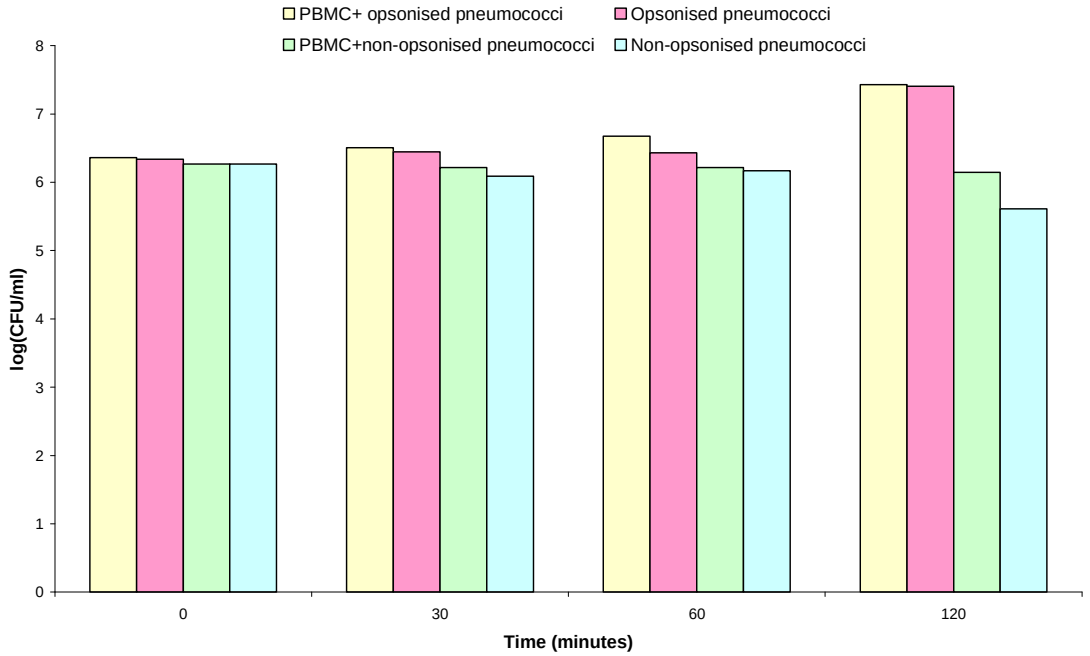

Figure 4-6: PBMC bactericidal assay. PBMC were incubated with opsonised and non-opsonised *S. pneumoniae D39* at a MOI of 0.8 for various amounts of time at 37°C at 5% CO_2.

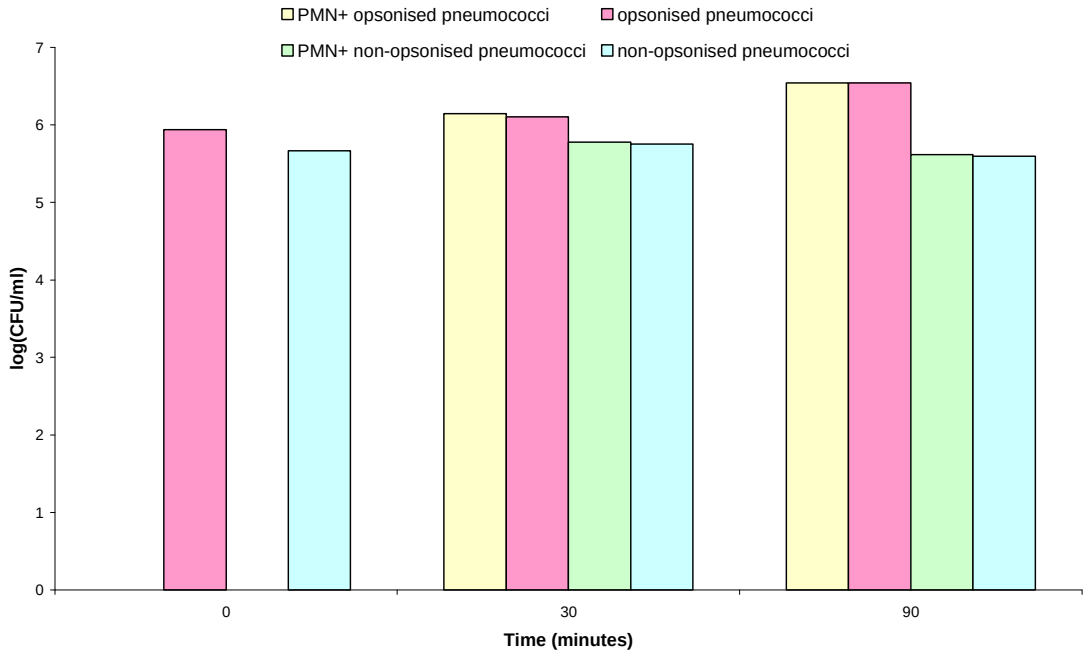

Figure 4-7: PMN cells bactericidal assay. PMN cells were incubated with opsonised and non-opsonised *S. pneumoniae* D39 at a MOI of 5 for various amounts of time at 37°C at 5% CO_2. Representative results obtained from one out of two experiments are shown.

4.3.2 Progression of streptococcal infection in properdin-deficient and wild type mice

Complement playing an important role during infection, including pneumococcal infection, and properdin being a key regulator of the alternative pathway, the role played by properdin during infection with *S. pneumoniae* D39 was investigated using a properdin-deficient mouse line.

4.3.2.1 Intranasal infection

Properdin-deficient and wild type mice from the seventh backcrossing stage were infected intranasally with a suspension of passaged *Streptococcus pneumoniae* D39 ($5x10^5$ pneumococci/mouse) (see chapter 4.2.3.1). Twenty four and forty eight hours post-infection, lung homogenate and blood obtained from each mouse were serially diluted, plated onto blood agar and CFUs were enumerated (see figure 4-8).

The amount of pneumococci found in the lungs of both wild type and properdin-deficient animals was relatively similar 24 hours post-infection, whereas an important difference between both groups was measured 48 hours post-infection. From 24 to 48 hours post-infection, a 10-fold decrease of pneumococci recovered from the lungs of wild type mice was observed, whereas at the same time, a 100-fold increase in bacterial count was detected in the lungs of properdin-deficient mice, resulting in the fact that 500 times more pneumococci were recovered from the lungs of properdin-deficient mice 2 days after infection (see figure 4-8A). A similar pattern was observed in the blood of these mice. While no major difference in the bacterial load was observed in the blood of properdin-deficient and wild type mice one day after infection, a 20-fold decrease of the blood pneumococci content in wild type animals was associated with an 80-fold increase in the blood of properdin-deficient mice at 48 hours post-infection (figure 4-8B).

These early data using mice of the seventh backcrossing stage showed a significant difference between properdin-deficient and wild type mice for both their blood and lung bacterial loads 48 hours after infection with *S. pneumoniae* D39. These preliminary results suggested that, in this intranasal infection model, properdin did not play a determinant role in the early phase following the infection, but showed its contribution at 48 hours post-infection.

A

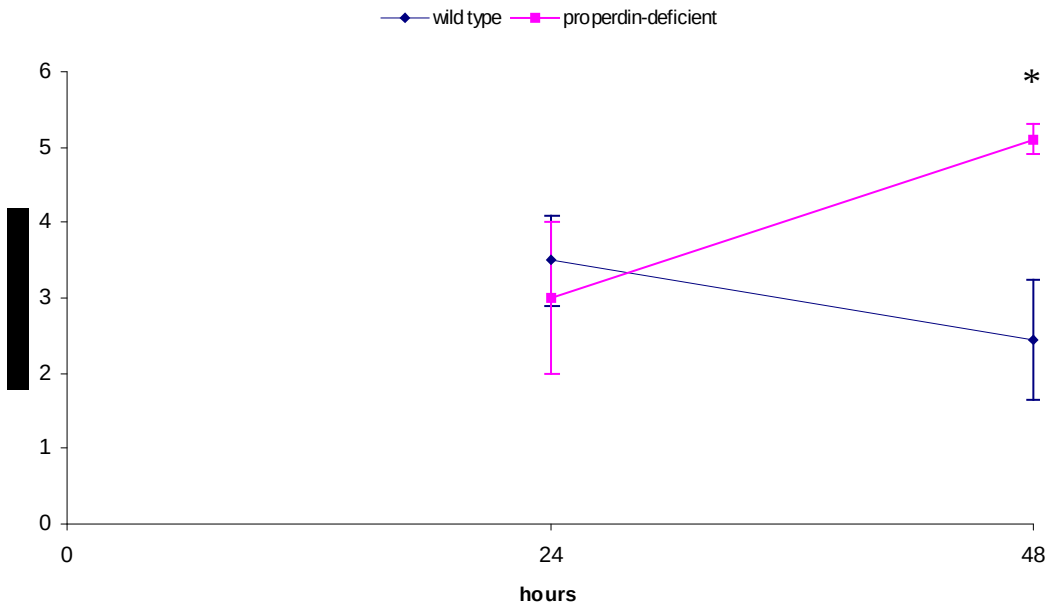

B

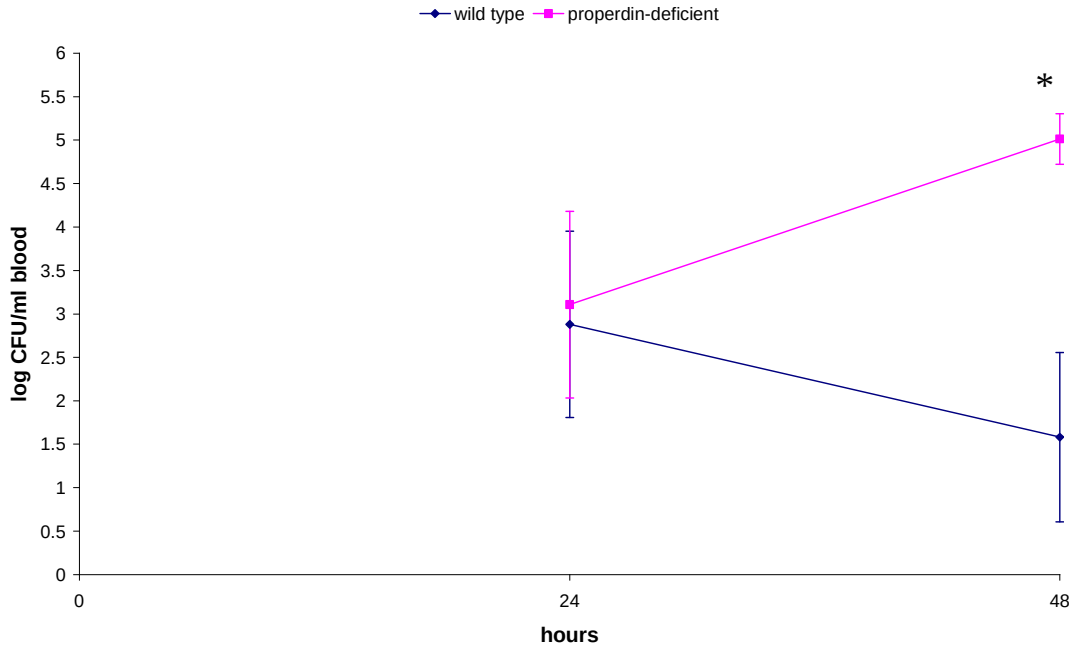

Figure 4-8: Time course of the pneumococci recovered from the lungs and the blood of 7-generation backcrossed properdin-deficient and wild type mice infected intranasally with $5x10^5$ *S. pneumoniae* D39. A: from the lungs; B: from the blood (n=4). The detection limit for the lung homogenate was 50 CFU/mg lung. Results are presented as geometric mean of the log(CFU)/ml +/- SEM and were obtained from one single experiment. *, $p<0.05$ [two-tailed Mann-Whitney U test].

4.3.2.2 Intravenous infection

Properdin-deficient and wild type mice from the tenth backcrossing stage were infected intravenously with a suspension of passaged *Streptococcus pneumoniae* D39 ($1x10^5$ pneumococci/mouse) (see chapter 4.2.3.2). Twenty four, forty eight and seventy two hours post-infection, blood was obtained via tail bleeds, serially diluted, plated onto blood agar and CFUs were counted.

As early as 24 hours post-infection, the quantity of pneumococci recovered from the blood of properdin-deficient mice was significantly higher than what was recovered from the blood of wild type animals. The amount of bacteria present in the blood of these two groups of mice then increased at the same rate from 1 to 3 days after infection, meaning the 2-log difference observed 24 hours post-infection was still observed 72 hours post-infection (see figure 4-9).

The fact that the difference observed between both populations of mice stayed constant from 24 to 72 hours post-infection, together with the fact that the 2-log difference for the blood bacterial load was already present as early as 24 hours post-infection, suggested that, in contrary to what was observed in the intranasal infection model, properdin played a major role in the early phase of the infection in this particular model of intravenous infection.

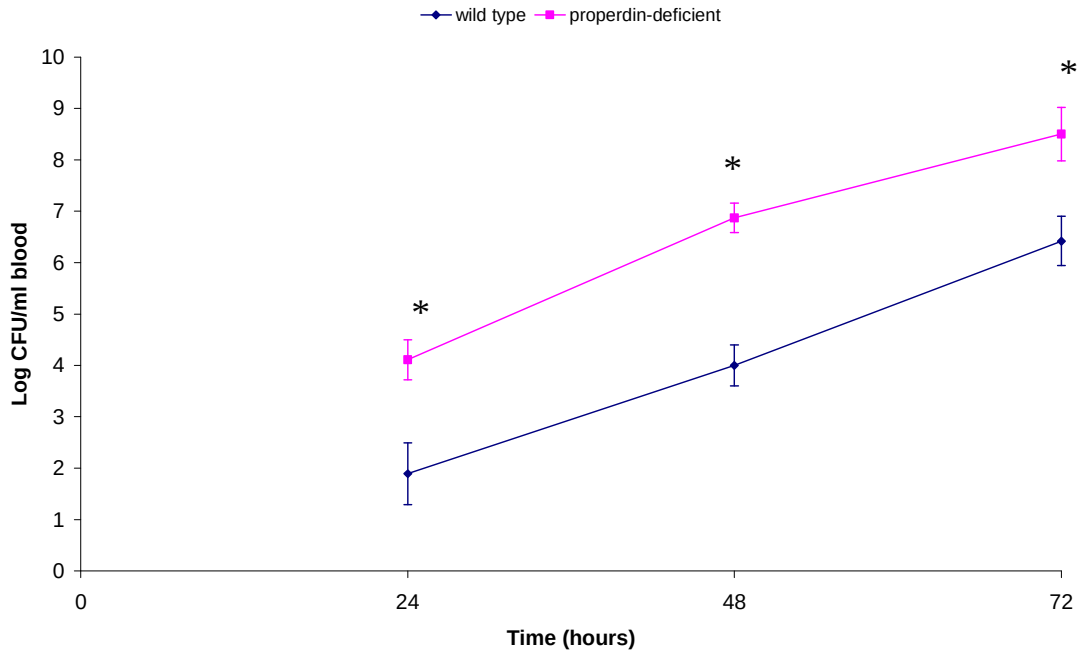

Figure 4-9: Time course of the pneumococci recovered from the blood of 10-generation backcrossed properdin-deficient and wild type mice infected intravenously with $1x10^5$ *S. pneumoniae* D39 (n=5). Results are presented as geometric mean of the log(CFU)/ml +/- SEM and were obtained from one single experiment. *, $p<0.05$ [two-tailed Mann-Whitney U-test].

4.3.3 Intranasal infection model

In order to understand better what happened in properdin-deficient mice infected intranasally with *S. pneumoniae*, this experiment was repeated with fully backcrossed properdin-deficient mice. Thus, mice of the tenth or higher backcrossing generation stage were used for the following experiments. Both properdin-deficient and wild type mice were infected intranasally with $1.5x10^6$ *S. pneumoniae* D39. Infected mice were monitored twice a day and, at chosen time post-infection, mice were culled and their blood and lungs were taken for analysis (see chapter 4.2.3.1). Different parameters such as C3 and immunoglobulin M levels, blood clotting kinetics and percentage of leukocytes present in the lung tissue of these infected animals were measured and compared.

4.3.3.1 Progression of streptococcal infection in properdin-deficient and wild type mice

Lung homogenates and blood from properdin-deficient and wild type mice 0, 6, 24 and 48 hours after infection were serially diluted and plated onto blood agar. CFUs on the plates were counted the next day (see chapter 4.2.7).

The number of bacteria present in the lungs of wild type mice decreased massively from 0 to 6 hours after infection. This was followed by a marked increase at 24 hours post-infection and then the number of bacteria in lung tissue stayed relatively stable from 24 to 48 hours post-infection. Concerning the properdin-deficient mice, the same pattern was observed 6 hours after infection. Nevertheless, there was no increase in bacterial number from 6 to 24 hours, but a substantial increase occurred from 24 to 48 hours post-infection. Twenty four hours after infection with *S. pneumoniae*, 10 times more bacteria were counted in the lung tissue of wild type mice than in the lungs of their properdin-deficient littermates and this trend reversed at 48 hours where 4 times more bacteria were observed in properdin-deficient lung tissue (figure 4-10A).

In the blood, CFUs were counted only at 24 and 48 hours post-infection. Both properdin-deficient and wild-type mice had the same number of bacteria present in their blood 24 hours post-infection. From 24 to 48 hours post-infection, the same pattern as the one observed previously in the lungs was seen for both properdin-deficient and wild type mice. Therefore during this time frame, the number of bacteria present in the blood of wild type mice slightly decreased whereas, in properdin-

deficient mice, this number increased. Twenty four hours post-infection, almost 4 times less bacteria were recovered from properdin-deficient blood than from wild type blood, whereas 48 hours after infection, 31 times more bacteria were counted in the properdin-deficient mouse blood than in the wild type blood (figure 4-10B).

These results showed again that properdin-deficient mice had a markedly higher bacterial load in both their lungs and blood 48 hours after intranasal infection with *S. pneumoniae* D39 than their wild type littermates. The fact that no significant difference was obtained at this time point for the blood CFUs was easily explained by the presence of one outlier in our properdin-deficient population (one properdin-deficient mouse completely cleared the infection 48 hours post-infection) and by the low number of samples tested.

4.3.3.2 Survival of challenged properdin-deficient and wild type mice

Ten properdin-deficient and wild type mice were intranasally challenged with *S. pneumoniae* and monitored for 7 days (see chapter 4.2.4). All the mice survived the first two days of the experiment. At 3 days post-infection, an important death rate was observed in wild type animals (4 mice out of 10 died), whereas only one properdin-deficient mouse succumbed. At the end of the one-week experiment, 8 out of the 10 properdin-deficient mice survived, whereas only 4 out of the 10 wild type did (figure 4-11). This experiment therefore showed that, while the critical point for mice to succumb pneumococcal infection (2-5 days) was the same in both group, there was a significant advantage for properdin-deficient mice to survive pneumococcal pneumonia and sepsis.

A

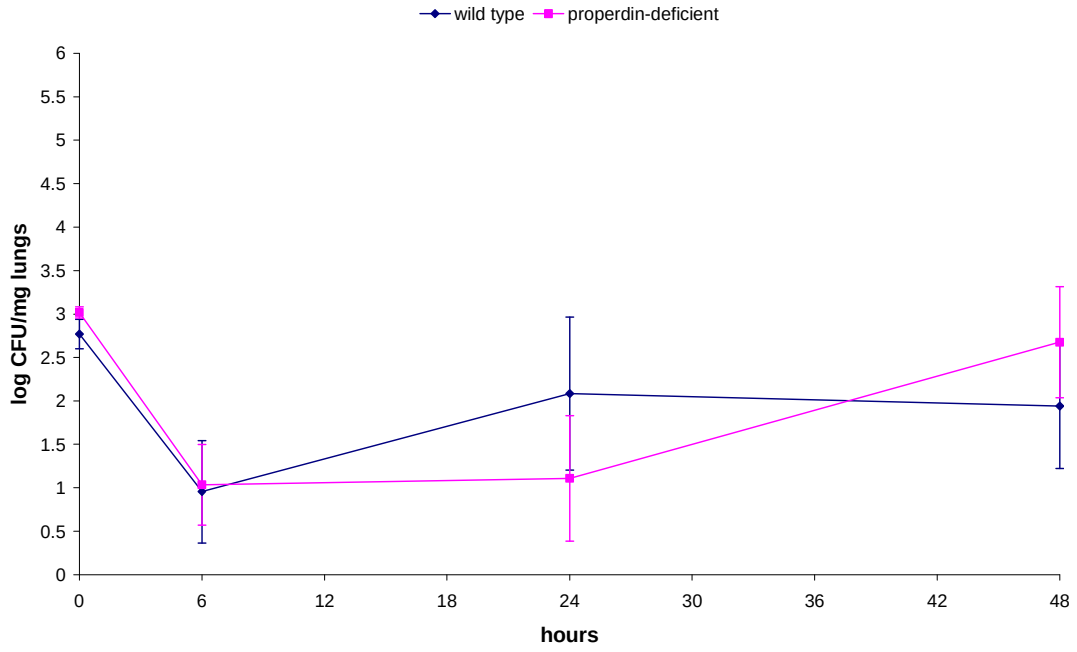

B

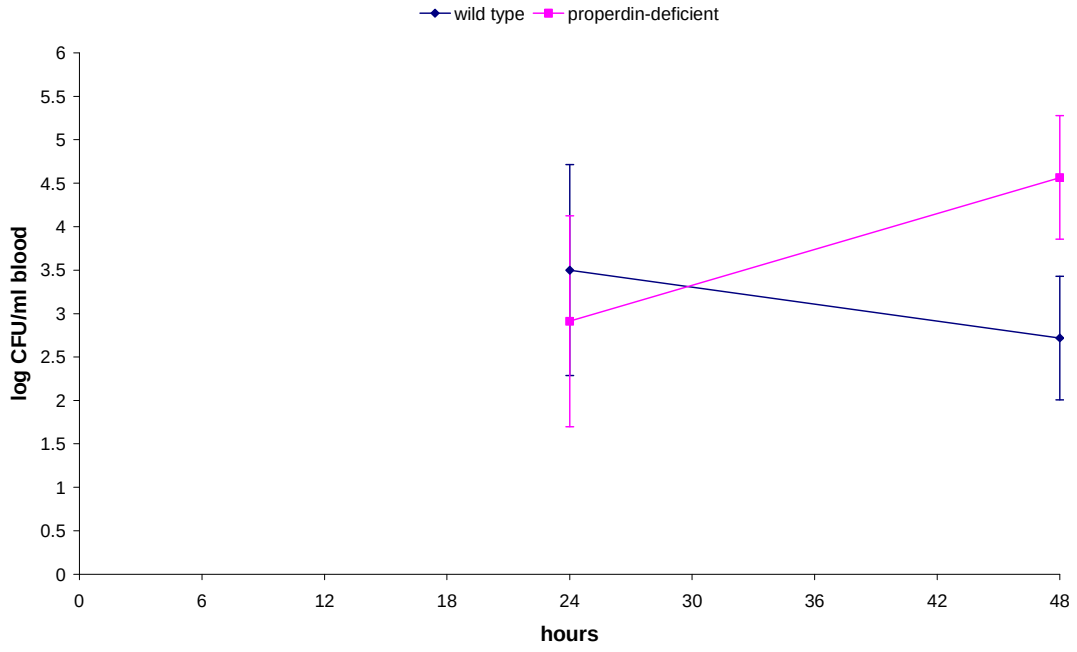

Figure 4-10: Time course of the pneumococci recovered from the lungs and the blood of 10-generation or more backcrossed properdin-deficient and wild type mice infected intranasally with $1.5x10^6$ *S. pneumoniae* D39. A: from the lungs; B: from the blood (n=2 (t0), n=5-6 (t6) and n=8-10 (t48)). The detection limit for the lung homogenate was 50 CFU/mg lung. Results are presented as geometric mean of the log(CFU)/ml +/- SEM and were obtained from two independent experiments. $p>0.2$ [two-tailed Mann-Whitney U test].

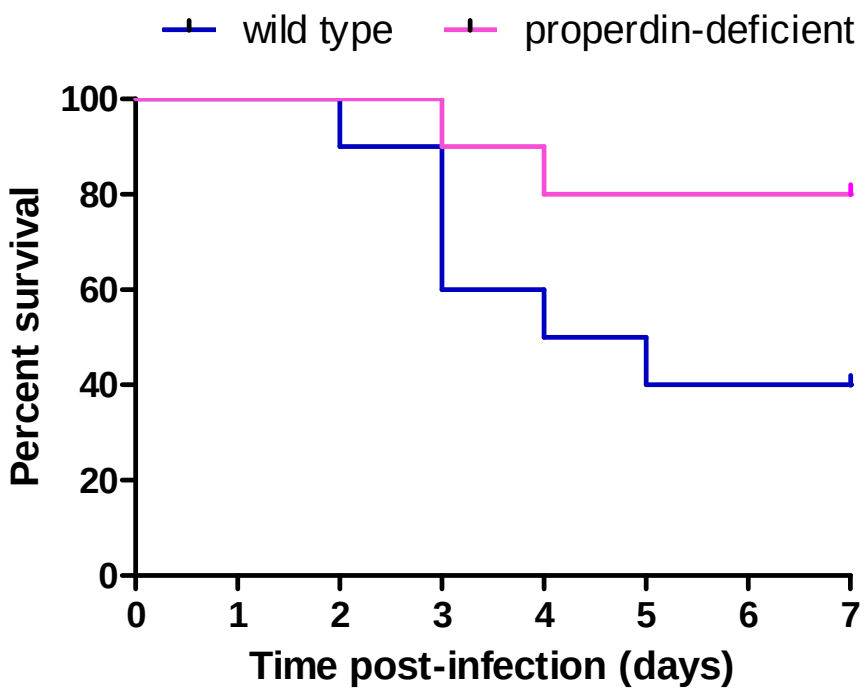

Figure 4-11: Kaplan-Meier survival curves of properdin-deficient (pink line) and wild type (blue line) mice challenged intranasally with $1.5x10^6$ *S. pneumoniae* D39 for 7 days (n=10). Results were obtained from one single experiment. p=0.068 [log Rank test]. p=0.01 [chi square goodness-of-fit test].

4.3.3.3 Baseline level of various markers in unchallenged mice

Blood clot formation, serum levels of IgM and C3 are important markers that can vary during infection. In order to study these parameters in properdin-deficient and wild type mice during infection, it was fundamental to investigate first their baseline levels in unchallenged mice in order to ensure that the absence of properdin did not affect them.

4.3.3.3.1 Coagulation time

The initiation clotting time of mouse blood was measured using rotational thromboelastography (ROTEG®). ROTEG® was performed first using whole blood anti-coagulated with ACD buffer (see method 1, chapter 4.2.8.2). Clotting was induced by adding calcium ions to the samples and r, k, α and MA values were measured for properdin-deficient and wild type blood (see table 4-3).

The reaction time (r), clotting time (k) and growth rate of the blood clot (α) were found to differ importantly between different mice with the same phenotype. As duplicates were always showing high reproducibility (data not shown), the variations observed for these parameters were thought to be due to a problem during the sampling of the blood. It is worth mentioning that blood samples were withdrawn from more mice for this experiment, but these samples could not be used as the blood was already beginning to clot before even the addition of the calcium ions. Tissue factor, a protein playing a crucial role in blood coagulation, by catalysing the formation of a thrombus and thus decreasing the initiation time of the clot formation and increasing its growth, is expressed in sub-endothelial tissues (Nielsen and Crow, 2004). A little amount of this tissue factor is always taken altogether with the blood during the cardiac puncture as the needle has to go through layers of tissue. During this first set of experiments, few punctures were sometimes performed to maximise the quantity of blood withdrawn from one single mouse and this may be responsible for the variabilities observed between samples.

Therefore, for the next set of experiments, extra cautions were taken when performing the cardiac puncture (only one puncture of the cardiac tissue was performed per mouse to withdraw the blood) to minimise any variation of the concentration of endogenous tissue factor taken with each sample and the anti-coagulation buffer used was changed as well (see method 2, chapter 4.2.8.2)

(Landskroner et al., 2005). A typical ROTEG® tracing obtained under these conditions is shown in figure 4-12.

In this second set of experiments, the ranges of values for the 4 parameters measured were close within a same group as shown with the low standard deviation obtained (table 4-4). This technique was thus used for all the future ROTEG® experiments performed. Morever, these results were in concordance with the ones obtained by Landskroner and coworkers when using wild type C57Bl/6 mouse blood (r=4.5min +/-0.7; k=0.8min +/-0.1 and a=81° +/-1.7), the lowest value for r in our case being explained by the fact that more tissue factor was taken when withdrawing the blood by cardiac puncture (the bleeding was done via the inferior vena cava in Landskroner's experiments) (Landskroner et al., 2005).

No difference in clotting time (r, k), kinetics of clot formation (α) and clot strength (MA) was observed between unchallenged properdin-deficient and wild type blood.

4.3.3.3.2 Serum concentration of total immunoglobulins

The level of IgG and IgM present in the serum of unchallenged properdin-deficient and wild type mice was investigated using different ELISA techniques. First, the levels of both immunoglobulins in the serum of properdin-deficient (n=4 for IgG, n=6 for IgM) and wild type mice (n=4 for IgG, n=6 for IgM) from the third to the seventh backcrossing stage were analysed using an indirect ELISA technique (see chapter 4.2.9.1). Similar ODs were obtained for both phenotypes, with a similar OD increment following serial dilutions of the samples (data not shown). These early data suggested both phenotypes had a same level of IgG and IgM. The exact serum IgM concentration of properdin-deficient and wild type mice from the tenth or higher backcrossing stage was then determined using a commercial IgM ELISA (see chapter 4.2.9.2). No significant difference in the total IgM level was observed between properdin-deficient (84.1 ng/µl +/-47.9 (mean+/-SD), n=10) and wild type (88.1 ng/µl +/-42.4, n=19) mouse sera.

4.3.3.3.3 Serum concentration of the C3 component

The level of C3 present in the serum of unchallenged properdin-deficient and wild type mice from the tenth or higher backcrossing stage was measured using a commercial ELISA kit (see chapter 4.2.9.3). No significant difference in serum C3

was observed between properdin-deficient (0.75mg/ml +/-0.22 (mean +/-SD), n=5) and wild type (0.69 mg/ml +/-0.19, n=5) mouse sera.

Parameters	Wild type mice	Properdin-deficient mice
r (min)	8.5+/-5.7	6+/-2.1
k (min)	5.6+/-3.2	3.6+/-0.1
α (°)	44.3+/-17	53.5+/-0.7
MA (mm)	64+/-3.6	66.5+/-7.8

Table 4-3: Thromboelastographic parameters (mean+/-SD) obtained by ROTEG® analysis for wild type and properdin-deficient mouse blood anti-coagulated with ACD buffer (n=3 wild type and n=2 properdin-deficient mice).

Parameters	Wild type mice	Properdin-deficient mice
r (min)	3.5+/-0.4	3.3+/-0.1
k (min)	1+/-0.4	0.9+/-0.1
α (°)	78.5+/-3.6	79+/-1.4
MA (mm)	69+/-7.1	68.5+/-2.1

Table 4-4: Thromboelastographic parameters (mean+/-SD) obtained by ROTEG® analysis for properdin-deficient and wild type mouse blood anti-coagulated with citrate buffer (n=2).

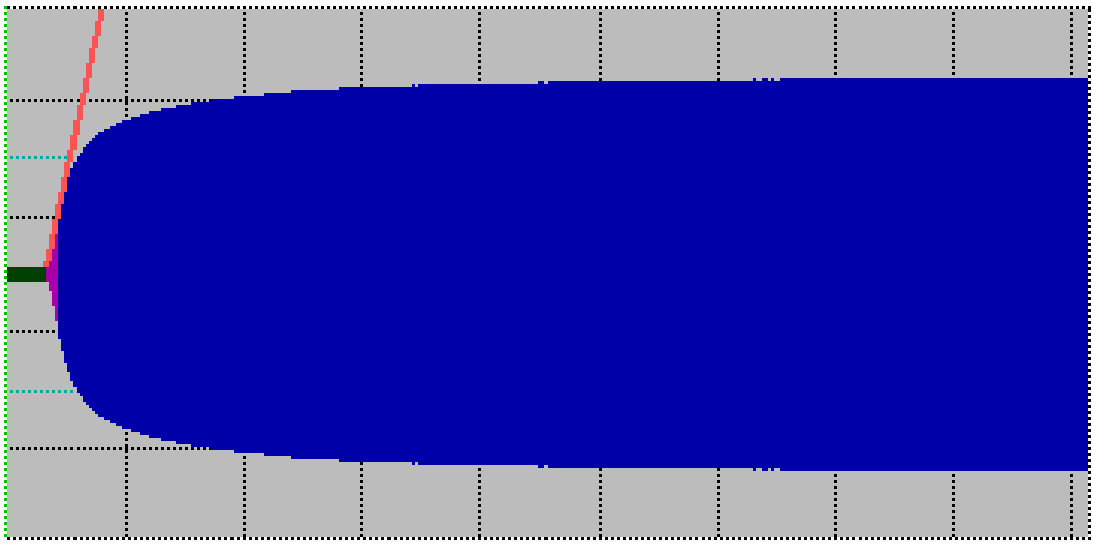

Figure 4-12: Typical ROTEG® tracing obtained for mouse blood anti-coagulated with the citrate buffer. In green: r (reaction time); in purple: k (clotting time); in red: α (alpha angle).

4.3.3.4 Characterisation of blood clot formation in properdin-deficient and wild type mice challenged with *S. pneumoniae*

As complement and coagulation are connected and as the coagulation pathway is known to be modified during the different phases following bacterial infection, the kinetics of clot formation using blood obtained from challenged properdin-deficient and wild type mice was investigated (Esmon, 2004; Guckian, 1975; Markiewski et al., 2007). Blood samples withdrawn from animals 0, 24 and 48 hours after intranasal infection with *S. pneumoniae* D39 were analysed by rotational thromboelastography (see chapter 4.2.8.2). The results obtained are summarised in table 4-5 and figure 4-13.

Table 4-5A presents the mean values obtained for both the properdin-deficient and the wild type population. Twenty four hours after infection, the different parameters measured (r, k, α, MA) were similar for both properdin-deficient and wild type mice (figure 4-13A). Moreover, these values were comparable as well to the ones observed with unchallenged mice, meaning there was no actual difference in clot initiation time and clot dynamics from 0 to 24 hours post-infection.

Forty eight hours after infection, the clot initiation time (r) of wild type mice showed a slightly higher value compared to the properdin-deficient one and compared to the results obtained at 0 and 24 hours post-infection (figure 4-13A). The other parameters measured at 48 hours were similar to the ones observed at 0 and 24 hours post-infection, except for the MA value (strength of the clot) that was slightly higher for properdin-deficient mouse blood, suggesting that a stronger blood clot was formed in properdin-deficient mice 48 hours after the challenge with *S. pneumoniae*.

Then, when analysing further the data obtained from each single mouse, some differences could be detected inside a same group of mice. I thus divided the mice into two new groups, one called “bacteraemia” and the other “no bacteraemia”, the bacteraemia state being defined as the presence of bacteria in the blood of the animal at the culling time (table 4-5B and figures 4-13B and 4-13C). Twenty four hours post-infection, the four coagulation parameters were similar in both bacteraemia and no bacteraemia groups for the wild type blood. Concerning the properdin-deficient mice, at this same time point, all parameters but the clot initiation time (r) were similar. In general, the blood of properdin-deficient mice showing bacteraemia needed less time

than the unchallenged blood to begin to clot, whereas the blood of properdin-deficient mice with no sign of bacteraemia had a markedly prolonged clot initiation time.

The pattern just described for the properdin-deficient sub-groups at 24 hours post-infection was observed as well for the wild type mouse blood at 48 hours post-infection (table 4-5B and figures 4-13B and 4-13C). The r value was markedly lower in the blood of mice with bacteraemia than in the one of non-infected mice, whereas mice with no evidence of bacteraemia had a prolonged clot initiation time. In addition to that, the k value (clotting time) of mice showing no sign of bacteraemia was twice as high than the k value of mice with bacteraemia, enhancing even more the kinetic difference in clot formation between blood of animal with bacteraemia and blood of animal without bacteraemia. The α value (clot growth) being related to the k value, a difference between both groups of wild type mice was observed for this value as well. Concerning the properdin-deficient mice, differences were observed too between the bacteraemia group and the no bacteraemia group at this time point. Again, the differences mainly concerned the clot initiation time (r), but this time, the presence of bacteria in the blood of the mice was a factor that prolonged the time required for a clot to form. In addition to that, mice showing signs of bacteraemia 48 hours after infection with *S. pneumoniae* had a remarkably higher MA value than any other samples, meaning the clot formed under these conditions was stronger.

A last parameter obtained from the ROTEG® tracing that has not been discussed yet is fibrinolysis. Effectively, if fibrinolysis occurs, it will be specified by the ROTEG®, and after the 120 minutes of analysis, only two blood samples began to show signs of fibrinolysis detectable by the system (data not shown). Both blood samples came from properdin-deficient mice presenting evidence of bacteraemia 48 hours after infection with *S. pneumoniae*, meaning the clot formed with the properdin-deficient blood taken 48 hours after infection with *S. pneumoniae* was the least stable.

A

t=0 hour	Wild type mice	Properdin-deficient mice
r (min)	3.5+/-0.4	3.3+/-0.1
k (min)	1+/-0.4	0.9 +/-0.1
α (°)	78.5+/-3.6	79+/-1.4
MA (mm)	69+/-7.1	68.5 +/-2.1

t=24 hours	Wild type mice	Properdin-deficient mice
r (min)	3.1+/-1.6	3.1+/-1.2
k (min)	1.1+/-0.3	1.3+/-0.6
α (°)	76.5+/-3.3	74.8+/-6.6
MA (mm)	68.7+/-7.5	69.4+/-7.4

t=48 hours	Wild type mice	Properdin-deficient mice
r (min)	**4.3+/-2.2**	3.7+/-2.5
k (min)	1.4+/-0.6	1.3+/-0.5
α (°)	74.2+/-6.6	76+/-6.2
MA (mm)	70.2+/-9.4	**75+/-14**

B

Parameters	Wild type mice		Properdin-deficient mice	
t= 24 hours	No bacteraemia	Bacteraemia	No bacteraemia	Bacteraemia
r (min)	3+/-1.6	3.1+/-2.3	**4.1+/-0.1**	**2.3+/-0.9**
k (min)	0.9+/-0	1.3+/-0.2	1.1+/-0.1	1.5+/-0.8
α (°)	79+/-0	74+/-2.8	77.5+/-2.1	73+/-8.6
MA (mm)	71+/-1.4	66.5+/-12	71.5+/-5	68+/-9.5
t=48 hours	**No bacteraemia**	**Bacteraemia**	**No bacteraemia**	**Bacteraemia**
r (min)	**6.1+/-1.3**	**2.5+/-0.1**	1.6	**4.7+/-2.4**
k (min)	**1.8+/-0.4**	0.9+/-0.5	1.4	1.2+/-0.6
α (°)	70+/-4.2	78.5+/-6.4	74	77+/-8.5
MA (mm)	68.5+/-3.5	72+/-15.6	59	**83+/-2.8**

Table 4-5: Thromboelastographic parameters obtained by ROTEG® analysis for properdin-deficient and wild type mouse blood at different time intervals after infection with *S. pneumoniae*. A: for the wild type and properdin-deficient populations considered as a whole (n=2 at t=0 hours; n=4-5 at t=24 hours and n=3-5 at t=48 hours) and B: by taking into account the number of bacteria recovered from the blood of the mice at the culling time (n=2-3 at t=24 hours and n=1-3 at t=48 hours). Results are presented as mean+/-SD.

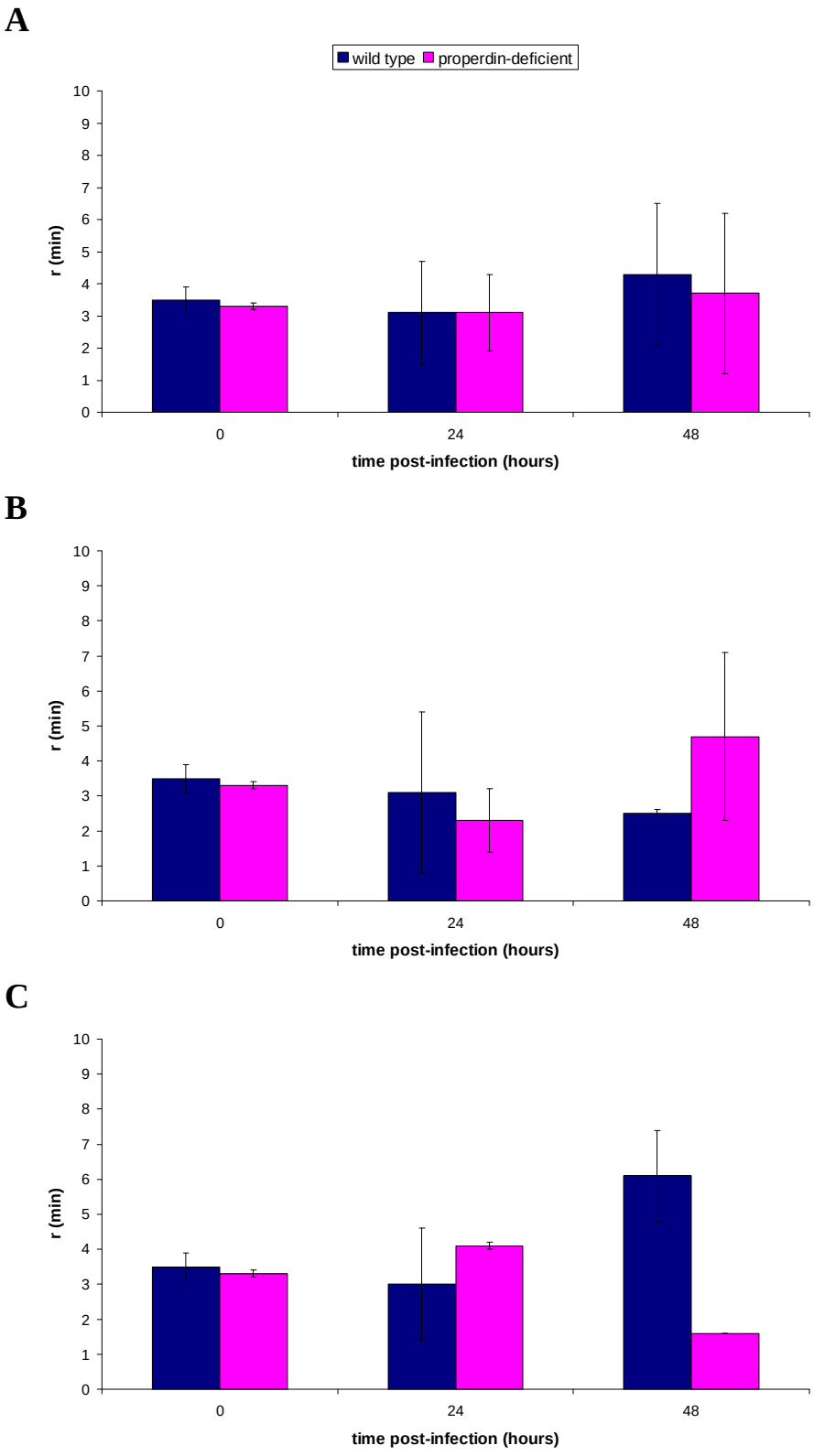

Figure 4-13: Evolution of the clotting reaction time (r) measured by ROTEG® analysis during the time course of the infection. A: using wild type and properdin-deficient populations considered as a whole (n=3-5); B: using only wild type and properdin-deficient mice showing signs of bacteraemia at the culling time (n=2-3) and C: using only wild type and properdin-deficient mice showing no sign of bacteraemia at the culling time (n=1-2). Results are expressed as mean+/-SD.

4.3.3.5 Serum concentration of IgM in properdin-deficient and wild type mice challenged with *S. pneumoniae* D39

Natural antibodies of the IgM type play an important role in the first innate immune defence against bacterial infection (Boes et al., 1998). Because complement activation requires 2 Fc portions in close vicinity and because of the pentameric structure of IgM, IgM is also better than any other immunoglobulin to initiate the classical complement pathway (Brown et al., 2002). To ensure that the same level of IgM was present in both properdin-deficient and wild type mouse serum at various time intervals after infection, its concentration was measured by ELISA (see chapter 4.2.9.2). As seen on figure 4-14, the total IgM level measured at each time point showed no difference between properdin-deficient and wild type sera. Nevertheless, IgM levels in both properdin-deficient and wild type mouse sera were seen to have decreased significantly at 24 and 48 hours post-infection when compared to the zero time point, suggesting serum IgM should have bound to the pathogens to initiate immune defences.

4.3.3.6 Serum concentration of C3 component in properdin-deficient and wild type mice challenged with *S. pneumoniae* D39

The concentration of C3, an acute phase reactant and the central component of the complement system, was measured by ELISA in both properdin-deficient and wild type mouse serum at various time intervals after infection (see chapter 4.2.9.3). As seen on figure 4-15, the same amount of serum C3 was observed in the serum obtained from properdin-deficient and the one obtained from wild type mice at 0 and at 6 hours after infection with *S. pneumoniae*. A slight increase of the C3 level was observed 24 hours post-infection in the sera of both groups of mice, the concentration of serum C3 in both cases staying inside the normal range for mouse serum C3 concentration (data sheet of the mouse C3 ELISA kit, ICL). Forty eight hours after infection, a significant increase was observed, the serum level of C3 in wild type mice being elevated 2-fold compared to the one observed in unchallenged animals, whereas the concentration of C3 in properdin-deficient sera reached more than 1.55 mg/ml, this is to say three times more than the one of unchallenged animals and two times more than the level observed 24 hours post-infection. Thus, while the serum concentration of C3 was still inside the normal range for wild type animals 48 hours

post-infection, the one of properdin-deficient mice was not included in this range anymore.

Importantly the mice with a serum C3 level above the normal range 48 hours after infection (for both properdin-deficient and wild type animals) had as well the highest amount of *S. pneumoniae* recovered from their blood and lungs, whereas the mice showing a normal C3 level 48 hours post-infection with *S. pneumoniae* presented no or few sign of bacteraemia. As seen on figure 4-16, the level of serum C3 seemed to be related to the amount of bacteria recovered from the blood of mice 48 hours post-infection with *S. pneumoniae*, and this independently of the phenotype. Unfortunately, the number of samples used was small and therefore more samples would need to be analysed to confirm this trend.

4.3.3.7 C3 cleavage in properdin-deficient and wild type mouse lung tissue during infection with *S. pneumoniae* D39

In order to determine the extent of complement pathway activation in both properdin-deficient and wild type mice challenged intranasally with *S. pneumoniae*, the level of the C3 activation products present in mouse lung tissue, the place where the infection actually begins, was investigated by Western blot analysis at different time points post-infection (see chapter 4.2.10). The polyclonal anti-C3 antibody used in this experiment (ICN Pharmaceuticals, Inc.) allowed the detection of the α chain C3 fragments C3b (104 KDa), iC3b (63 and 41KDa), C3dg (40 KDa) and C3d (35KDa), with the small fragment of iC3b and C3dg appearing as a single band as seen on figure 4-15 (see chapter 1.2.7.1 and figure 1-3). The β chain of C3 could not be visualised under these conditions.

The quantity of C3-derived opsonin molecules present in lung homogenates (including therefore both soluble and membrane-bound C3b and iC3b) was similar in both groups from 0 to 24 hours post-infection, the C3b level being higher than the iC3b one (figures 4-17A and 4-17B). At 48 hours post-infection, a different densitometric pattern was observed: properdin-deficient mice had a higher level of iC3b than their wild type littermates as seen with the intensity of the 63KDa band, while, at the same time, the level of C3b stayed similar (figure 4-17C). Here again, properdin-deficient and wild type mice could be grouped according to the presence of bacteria in their blood at the time of culling. C3b was found at a higher concentration in the lungs of mice presenting no or little sign of bacteraemia compared to mice

presenting signs of bacteraemia, and that independently of the presence or absence of properdin, while, in mice presenting signs of bacteraemia, the band corresponding to "iC3b and C3dg" (40KDa) was more intense. In this sub-group of mice, it was evident that the band corresponding to the "iC3b+C3dg" fragments was denser in properdin-deficient mice than in their wild type littermates despite the fact that the level of the 63KDa band corresponding to the other fragment of iC3b was similar in both groups. This difference of intensity between the two bands corresponding to the two fragments of the iC3b molecule suggested that C3dg could actually be detected in this case. In fact, in every other sample, both fragments of the iC3b molecules were detected with the same intensity, meaning the "iC3b+C3dg" band in these cases was mainly representing iC3b. However, the fact that the C3dg molecule is issued from the degradation of the 63KDa fragment of the iC3b molecule and the intensity of the 63KDa fragment of the iC3b molecule was expressed at a similar level in properdin-deficient and wild type animals 48 hours post-infection meant that the increase in intensity for the "iC3b+C3dg" band observed in properdin-deficient animals was partly due to the presence of C3dg and partly due to a higher level of iC3b in properdin-deficient lungs.

It is worth noting that an extra band of 35KDa corresponding to the C3d fragment could be observed in one properdin-deficient and one wild type mouse lung tissue 48 hours after infection (figure 4-17C).

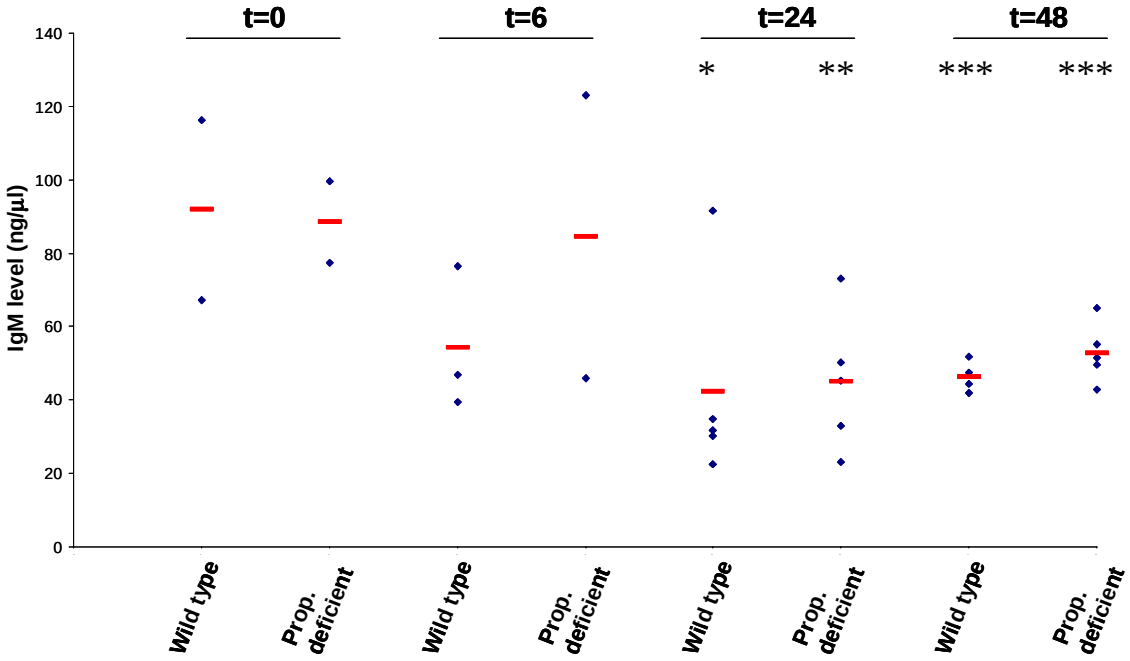

Figure 4-14: Concentration of total serum IgM (ng/µl), measured by ELISA, in properdin-deficient and wild type mouse sera at different time points after intranasal infection with *S. pneumoniae* D39. Results were obtained from one single infection experiment. *, $p<0.03$; **, $p<0.02$; ***, $p<0.01$ [Two-tailed T-test against [properdin-deficient and wild type levels at t=0]].

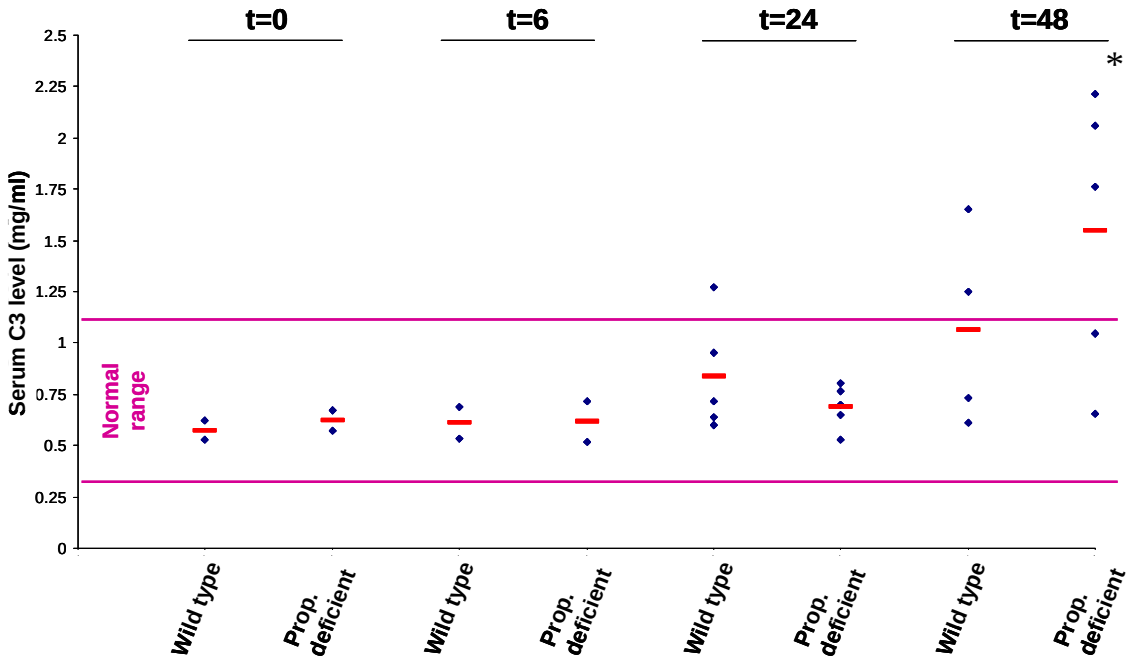

Figure 4-15: Concentration of serum C3 (mg/ml), measured by ELISA, in properdin-deficient and wild type mouse sera at different time points after intranasal infection with *S. pneumoniae* D39. The two violet lines delimit the normal range of serum C3 in mice. Results were obtained from one single infection experiment. *, $p<0.03$ [Two-tailed T-test against [properdin-deficient and wild type levels at t=0]].

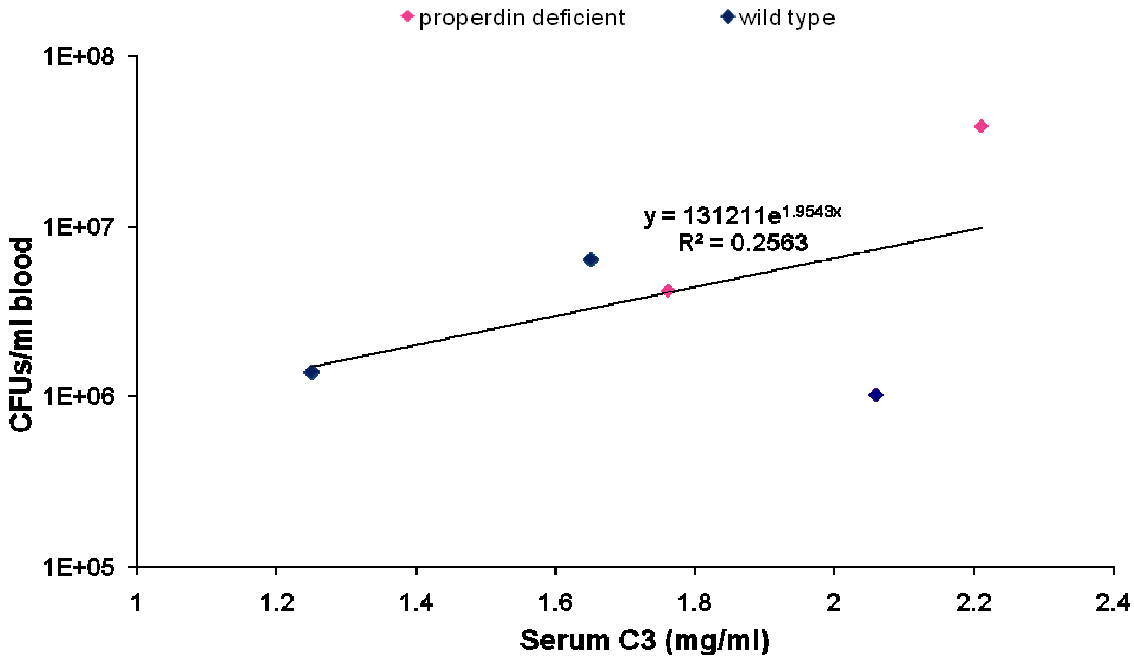

Figure 4-16: Graph plotting the serum C3 level against the number of pneumococci recovered from the blood of properdin-deficient (pink) and wild type (blue) mice showing out-of-range C3 concentrations 48 hours after intranasal infection with *S. pneumoniae* D39.

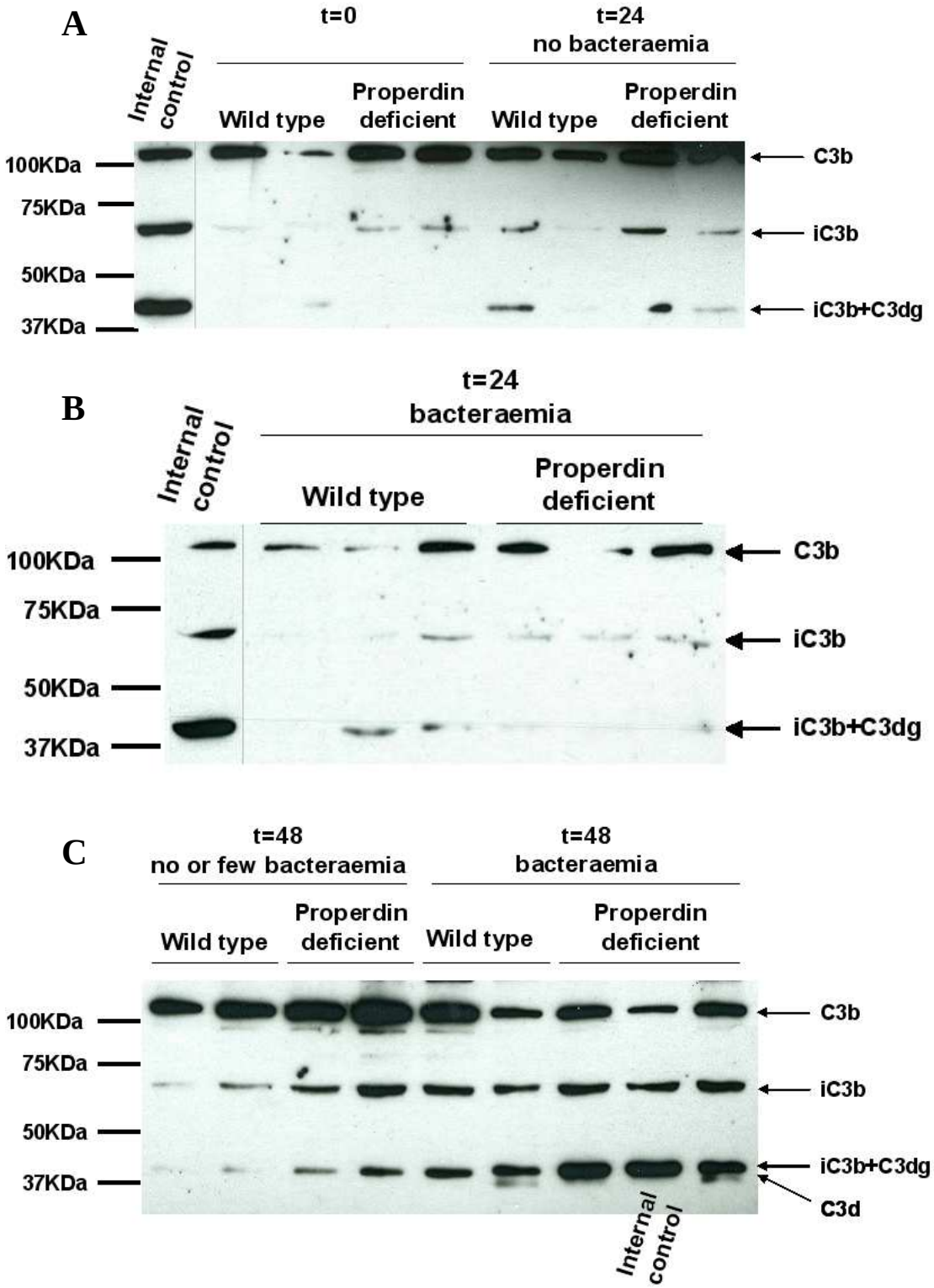

Figure 4-17: Western blot analysis of C3 activation products present in mouse lung tissues obtained from properdin-deficient and wild type mice at chosen time intervals post-infection. C3 activation products were detected via the use of the polyclonal HRP-labelled goat anti-mouse C3 antibody. A: at 0 and 24 hours post-infection; B: at 24 hours post-infection and C: at 48 hours post-infection. Representative results obtained from two independent Western blots using samples obtained from one single infection experiment.

4.3.3.8 Differential leukocyte analysis of cytospun lung homogenate

A differential analysis of pulmonary leukocytes was performed by cytospinning the lung homogenates obtained from infected properdin-deficient and wild type mice and by staining those with Giemsa stain (see chapter 4.2.11). Each type of leukocyte present on the microscope slide was then easily identified according to their morphology. As seen on figure 4-18, alveolar macrophages, monocytes, leukocytes and granulocytes could easily be distinguished according to their specific characteristics. The distribution of each leukocyte population at each time point post-infection was then calculated and the results obtained are presented on figure 4-19.

At the very beginning of the experiment (time point 0), a similar proportion of neutrophils (22-25%), lymphocytes (35-36%), alveolar macrophages (35-36%) and monocytes (4-8) was found in the lungs of properdin-deficient and wild type mice.

No major difference was seen from 0 to 6 hours post-infection in wild type animals, while in properdin-deficient mice, almost 50% of the leukocytes present in the lungs of these mice were macrophages by that time.

At 24 hours post-infection, the proportion of monocytes present in the lungs of both properdin-deficient and wild type animals considerably dropped. The majority of white blood cells in properdin-deficient infected lungs were therefore neutrophils.

Two days post-infection, it was then the turn of the lymphocytes to be the most represented leukocyte population in the lungs of wild type animals. At each time-point (from 0 to 48 hours), lymphocytes always represented around 35 to 40% of the leukocytes present in the lung of wild type animals. In properdin-deficient mice, the dominant population 48 hours post-infection was the neutrophils one (representing 60% of the leukocytes present in the lungs), the lymphocyte being represented in this case by only 22% of the leukocytes.

Three days after infection, while for the wild type mice, the lymphocyte population was still the most represented (57%), for the properdin-deficient mice, both the neutrophils (43%) and the lymphocytes (37%) were highly represented. Concerning the other leukocyte populations, their relative expression stayed relatively stable compared with the 48 hours time point.

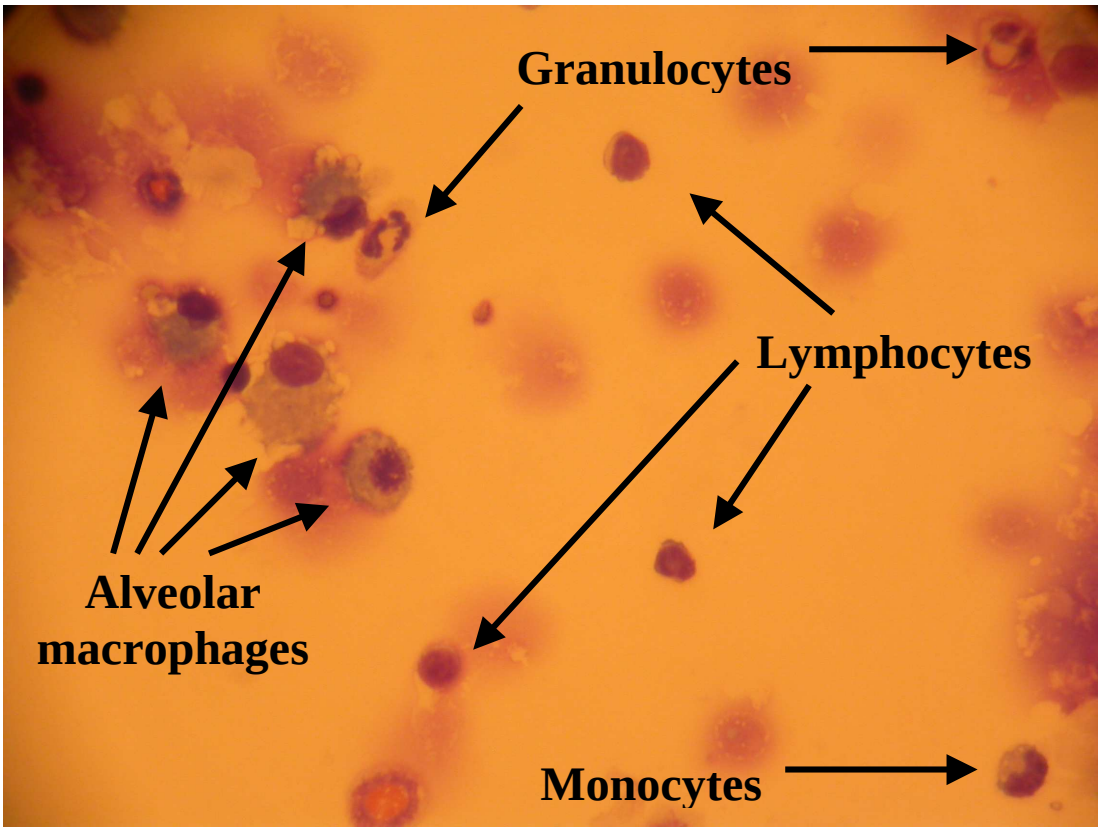

Figure 4-18: Representative picture of lung homogenate cytospun onto a microscope slide and stained with Giemsa. Lymphocytes, monocytes, granulocytes and alveolar macrophages could easily be distinguished according to their morphological characteristics.

A

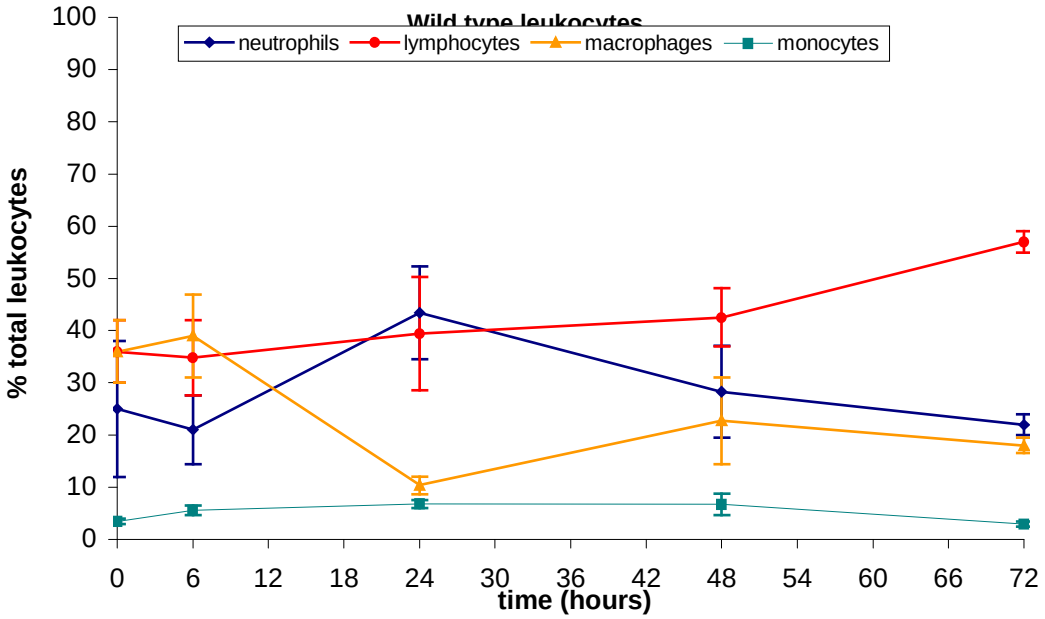

B

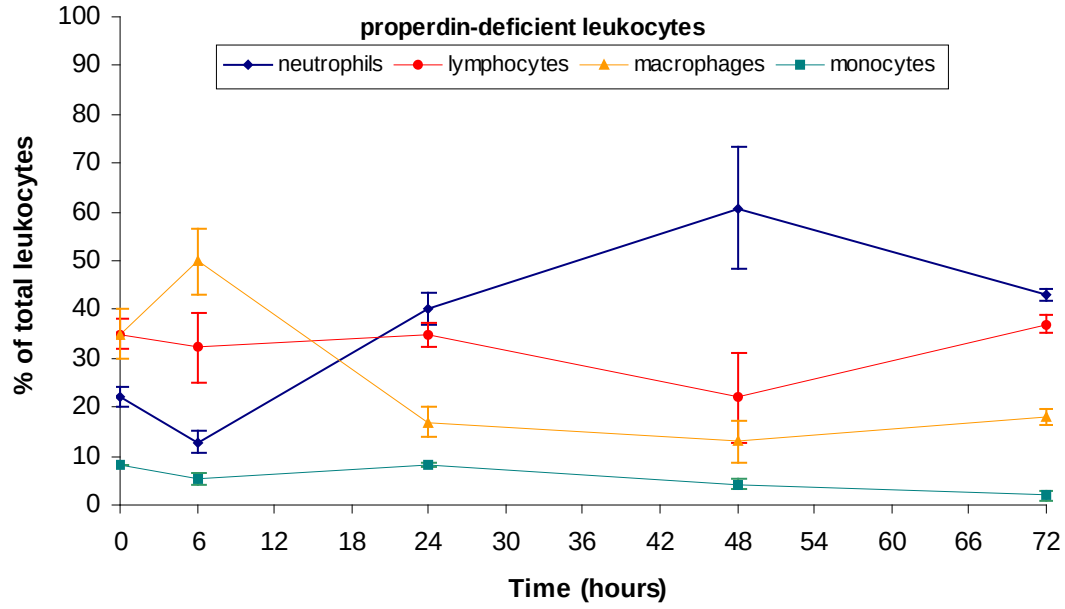

Figure 4-19: Differential analysis of the neutrophil, lymphocyte, macrophage and monocyte populations in mouse lung tissue obtained from properdin-deficient and wild type mice at defined time intervals after intranasal infection with *S. pneumoniae* D39. A: for wild type mice and B: for properdin-deficient mice (n=2 at t=0 hour; n=4-5 at 48 hours and n=5 at t=6, t=24 and n=2-3 at t=72 hours post-infection). $p>0.1$ [two-tailed Mann-Whitney U test].

4.4 Discussion

The complement system plays a key role during innate immune response towards pathogens, including *Streptococcus pneumoniae*. Different investigators have studied the role played by the complement system during pneumococcal infection using complement-deficient mice and concluded that both the alternative complement pathway and the classical complement pathway were of major importance to clear the infection and to reduce the mortality (Brown et al., 2002; Xu et al., 2001). In order to study the specific role played by properdin during streptococcal infection, a model using *S. pneumoniae* serotype 2 strain D39 and properdin-deficient and properdin-sufficient mice (on C57Bl/6 background) was developed. Importantly, the mere absence of properdin did not influence baseline coagulation kinetics, IgM, IgG or C3 serum level, supporting the fact that this mouse line (maintained in a barrier unit) did not seem immunocompromised when unchallenged.

4.4.1 Properdin seems to play a sepsis-limiting role at a late stage (48 hours) following streptococcal infection…

In the first day following intranasal infection with *S. pneumoniae*, the presence or absence of properdin did not seem to impact on pneumococcal clearance, as similar bacterial loads were found in the lungs of both properdin-deficient and wild type mice 6 hours after infection. In another infection study using similar conditions (intranasal infection of C57Bl/6 mice with $1x10^6$ *S. pneumoniae* D39), at the same time post-infection, the effect of the absence of the C3 component could already be measured (higher bacterial loads in the lung tissue), suggesting that, in contrast to properdin, this component was of major importance at an early stage following the infection (Kerr et al., 2005). However, here, the absence of properdin was noticeable at a latter stage (from 24 to 48 hours post-infection): properdin-deficient mice were unable to contain the pneumococcal infection 48 hours post-infection, as seen with the higher bacterial loads in the blood and in the lungs of these animals.

Other parameters such as blood coagulation kinetics and C3 levels tended to confirm the fact that properdin's contribution appeared at a late stage (2 days post-infection) in this model. In fact, when grouping properdin-deficient and wild type mice according to the presence or absence of pneumococci in their blood at the time of culling, differences in blood coagulation parameters were observed. The quicker

blood clot's formation in wild type animals presenting signs of bacteraemia 48 hours post-infection was most likely due to the initiation of the pro-coagulant cascade in an attempt to restrain the dissemination of the bacteria in these animals, while the slower formation of the blood clot observed using the blood of wild type mice showing no signs of bacteraemia confirmed the fact these mice were recovering from an infection (Geelen et al., 1992; Guckian, 1975). Concerning properdin-deficient mice presenting signs of bacteraemia, the time required to induce the formation of a blood clot was slightly reduced 24 hours post-infection, suggesting that septicaemia was developing earlier in these mice than in their wild type littermates. The initiation of the coagulation was slower at 48 hours post-infection, suggesting that the sepsis was more severe in these mice than in the wild types as this anti-coagulant phenomenon is usually observed at a later stage during septicaemia, when there is a limitation of the pro-coagulant factors (coagulopathy). This idea is reinforced by the fact that the properdin-deficient blood clot was less stable than the one obtained with wild type blood 48 hours post-infection. In conclusion, the properdin-deficient mice seemed to reach a sepsis state quicker than their properdin-sufficient littermates.

C3 is a positive acute phase protein, meaning its serum concentration increases during infection. In this model, C3 serum concentration was shown to be stable during the day following the pneumococcal challenge, but was markedly higher 48 hours post-infection for both properdin-deficient and wild type groups. This result was in concordance with those obtained by different groups recently: one study showed that the serum C3 level stayed constant in a mouse model 24 hours after infection with *S. pneumoniae* and another study demonstrated that this level was increasing only at the late stage of an induced sepsis in a rat model (Kerr et al., 2005; Kulah et al., 2006). In my study, even if serum complement 3 protein concentration was found to be higher in both properdin-deficient and wild type mice 48 hours post-infection, the rise was significantly more pronounced in properdin-deficient animals. This observation suggested again that the absence of properdin was linked with a more severe septicaemia 48 hours after infection with *S. pneumoniae*.

Taken together, the higher bacterial loads in lungs and blood, the changes in blood kinetics and the higher systemic C3 level gave evidence that properdin-deficient mice encountered a more severe septicaemia than their wild type littermates 2 days post-infection, and that was probably due to the fact that the induction of the septic

stage happened earlier in properdin-deficient than in wild type mice. This may be explained by the fact that, properdin being a humoral component, the complement activation in the blood of properdin-deficient mice was reduced due to the absence of the alternative pathway's activation loop, resulting in a poorer clearance of the pneumococci after their passage from the lungs to the blood and, therefore, leading afterwards to the re-seeding of more bacteria into the lungs and logically to a higher infection state. C3 serum level and blood coagulation pathway activation, being dependent of the level of the infection, were thus higher in properdin-deficient animals. The essential role played by properdin in the blood to limit the bacterial count was highlighted in my intravenous infection model. In this case, the systemic bacterial load was always found to be higher in properdin-deficient mice than in their wild type littermates and that as early as 24 hours post-infection. Properdin seemed therefore to reduce the number of pneumococci in the blood at an early stage post-infection. And when the number of *S. pneumoniae* present in the blood became too important, the influence of properdin became minimal as shown by the similar rate of bacterial growth from 24 to 72 hours post-infection in both groups of mice.

4.4.2 … but the presence of properdin leads to an increased mortality

However, despite the fact that properdin-deficient mice seemed to develop septicaemia earlier than the wild type mice and did not seem able to contain the infection, the survival rate of these mice was twice as high following intranasal infection with *S. pneumoniae* (survival rate of 80%) than that of their wild type littermates (survival rate of 40%). For both phenotypes, the critical point was 2 to 5 days post-infection. The results obtained for the wild type mice were in concordance with what has already been published in the literature for C57Bl/6 mice intranasally infected with D39 pneumococci (survival rates from 37.5% to 50%, succumbing time from 48 to 96 hours post-infection) (Brown et al., 2002; Gingles et al., 2001; Kerr et al., 2005). However, it was the first time that the absence of a complement component – properdin – did increase the survival chance of the infected animals as all complement-deficient mice already tested – C1qa-, factor B-, C3- and C4-deficient mice (of a C57Bl/6 background) – always had a higher mortality rate than their wild type littermates one week after intranasal infection with a similar dose of *S. pneumoniae* D39 (Brown et al., 2002; Kerr et al., 2005). Similarly, factor D-, CR1/2-,

CR3- and CR4-deficient mice (of a C57Bl/6 background as well) infected intranasally with a similar dose of serotype 3 pneumococci (WU2) had a lower survival rate than their wild type littermates (Ren et al., 2004). The absence of properdin only partially impaired the alternative complement pathway, therefore, the expectation was that properdin-deficient mice would have a better survival than factor B-, factor D- or C3-deficient mice as, in these complement-deficient mice, the ability to activate the alternative complement pathway was completely abolished. However, properdin-deficient mice were not expected to survive better the infection than properdin-sufficient mice. This gave evidence that properdin was playing a detrimental role in this model.

At this point, it is worth mentioning that, after intranasal infection, 37.5% of the wild type mice had completely cleared the infection in both their lungs and blood by 48 hours post-infection, whereas only 10% of the properdin-deficient mice had cleared the infection in both their lungs and blood at this same time-point (the presence of mice that cleared the infection and mice that did not clear the infection explain the important standard error of the mean reported earlier). Therefore, I just showed that, in one set of experiments, 40% of the wild type mice survived the week's experiment while, in another set of experiments, 37.5% of the mice cleared the infection by 48 hours post-infection. It is easy to suppose that the mice that cleared the infection after 48 hours were probably the ones which survived in the survival experiment. Concerning the properdin-deficient mice, only 10% of the mice had cleared the infection by 48 hours, but 80% of the mice survived the week's experiment. This showed that, in the case of properdin-deficient mice, animals that did not clear the infection by 48 hours post-infection could still overcome the infection and survive. Therefore, it seemed that properdin was playing its essential humoral activity via its complement activation loop to limit the bacterial count in the blood of wild type mice during the first two days post-infection. And if the system had failed to clear the infection by this crucial point, the pneumococci could be re-seeded into the lungs via the blood circulation and, at this stage, the presence of properdin appeared to be detrimental.

4.4.3 What is the role played by properdin in this model?

To investigate the influence that properdin could have in the lungs during pneumococcal infection, the different leukocyte populations present in the lungs of

both groups of animals were analysed and compared. Here again, the results obtained for the wild type mice were as expected: an influx of neutrophils was observed 24 hours post-infection, followed by a macrophage infiltration 48 hours post-infection, while at 72 hours post-infection, the proportion of lymphocytes present in the lungs of these mice was increasing (Bergeron et al., 1998; Gillespie and Balakrishnan, 2000; Kadioglu et al., 2000). Thus, in wild type animals, the neutrophil migrated massively to the lungs at 24 hours post-infection when the bacterial load was at its maximum and then, at 48 hours post-infection, the monocytes travelled to the lungs to clear the debris and the apoptotic cells (Bergeron et al., 1998). Concerning the properdin-deficient mice, a similar increase was observed for the neutrophil population at 24 hours post-infection, but this influx lasted longer, reaching its maximum 48 hours post-infection, and the proportion of neutrophils was still important 72 hours post-infection. No particular change was observed for the three other leukocyte populations present in the lungs of properdin-deficient animals at any time point post-infection (the rise and fall of the curves observed on the graph being relative, due to the variation of the neutrophil population). However, despite the important proportion of neutrophils present in the lung tissue 48 hours post-infection, no pneumococcal decline was observed in both the lungs and the blood of properdin-deficient mice 2 days after infection. These results suggested that the phagocytic function of the neutrophils could be altered by the absence of properdin in these mice. When looking only at the mice that did not clear the infection by 48 hours post-infection in both groups, the importance that the neutrophils could have in this model was reinforced: in this case, the percentage of neutrophils was markedly higher in the properdin-deficient sub-population (representing 73% of total leukocytes) than in the wild type sub-population (representing 40% of total leukocytes), despite both sub-populations having a relatively similar level of pneumococci in their blood and lungs at this time-point. As properdin has been shown to be stored in the secondary granules of neutrophils and could be secreted upon stimulation with various chemotactic agonists, I hypothesised that properdin may play a role during neutrophil activation and its absence in properdin-deficient mice may affect some neutrophil's functions, which could explain the behaviour observed for properdin-deficient mice during pneumococcal pneumonia (Wirthmueller et al., 1997).

This putative impairment of the neutrophil's function in properdin-deficient mice did not seem to be due to a chemotactic problem. In fact, the proportion of neutrophils in infected properdin-deficient lungs was higher than in infected wild type lungs and their influx lasted longer in the absence of properdin. Even so, as we are speaking about relative percentages, no indication about the actual number of neutrophils migrating into the lungs was given; my data highly suggested that high numbers of properdin-deficient neutrophils were attracted to the infection site, the other explanation for the high proportion of neutrophils in infected properdin-deficient lungs (the actual number of neutrophils stayed stable and the three other leukocytes population decreased tremendously) appearing less plausible. Moreover, an agarose-droplet migration assay using neutrophils from properdin-deficient and wild type mice showed that properdin-deficient neutrophils were not impaired in their ability to migrate towards fMLP, a pro-inflammatory bacterial peptide known for its strong neutrophil chemoattracting and activating properties (Stover, C., personal communication).

After considering the migratory function of the properdin-deficient neutrophils, their phagocytic activity was investigated. Using Western blot, I looked at the level of opsonins present in the lungs of both groups of infected animals to ensure that if there was any defect in phagocytosis, it was not due to a different level of complement activation leading to a difference of opsonin concentration in the lungs. The alternative complement pathway is responsible for the formation of two kinds of opsonins: C3b and its inactivation product iC3b that the particular anti-C3 antibody used in this study was able to detect in parallel. This Western blot showed that, at 48 hours post-infection, C3b was the predominant form of C3 activation products in the lungs of mice that clear the infection, while C3b and iC3b fragments were both present in comparable quantities in the lungs of mice that did not clear the infection. In the bacteraemia sub-group, iC3b was present at a higher level in properdin-deficient lungs and was as well seen to be further degraded (into C3dg), a fact that was not observed in the wild type lungs. This higher level of C3 activation products in properdin-deficient mice 48 hours post-infection was relative as it was probably linked with the higher level of C3 previously found in the serum of these mice (Ekdahl et al., 2007). It cannot be excluded though that some of the C3 got cleared outside the complement system, via the C3-degrading activity of the pneumococci

(Angel et al., 1994). These results therefore showed that the absence of properdin, despite impairing partially the alternative complement pathway, did not affect the concentration of C3-related opsonin molecules in the lungs of properdin-deficient mice. The similar decrease in IgM serum concentration observed for both properdin-deficient and sufficient mice during the time course of the infection suggested that the impairment of the alternative complement pathway was not compensated by an overactivation of the classical pathway, IgM being the main activator of the classical complement pathway in absence of specific antibodies (Boes et al., 1998). Opsonin molecules being present in the lungs, the binding of C3b to CR1 and iC3b to CR3 and/or CR4 on various phagocytic cells including neutrophils should then lead to the phagocytosis of the target in the absence of antibodies (Hostetter, 2000). This result showed that, if properdin-deficient neutrophils were defective in their phagocytic activity, this will not be due to a lack of opsonin molecules in the lungs. Unfortunately, due to the reasons discussed earlier (see chapter 4.3.1.3.2), the phagocytic capabilities of properdin-deficient neutrophils could not be investigated in this study.

As mentioned beforehand, the Western blot analysis showed as well that C3dg, the degradation product of iC3b, was found at a detectable concentration in the lungs of properdin-deficient animals 48 hours after the infection. While C3dg is known to bind CR2 on B lymphocytes and therefore to increase the B cells' immunoglobulin response to the antigen, its presence can as well be the sign of a good regulation of the complement system in properdin-deficient lungs (Lyubchenko et al., 2005). In fact, the inactivation of C3 into C3b and its further degradation into C3dg by factor I and co-factors, at the same time as creating C3dg, decreased the concentration of C3b and iC3b present in the lungs, and therefore may prevent an overactivation of the complement system that could have been detrimental for the host.

To conclude, to explain the lower clearance of pneumococci detected in the lungs and blood of properdin-deficient animals infected intranasally with *S. pneumoniae* D39 48 hours post-infection despite the higher survival rate and the more pronounced neutrophil influx in the lungs, I hypothesised that properdin may play a role affecting the neutrophils' activation. While the migration function of the neutrophils did not seem to be impaired, the absence of properdin could decrease the phagocytotic function of the neutrophils, which will explain the slower clearance of

pneumococci observed in properdin-deficient mice. A lower level of neutrophils' activation in the absence of properdin may be beneficial for the host as important number of activated neutrophils in tissue can result in fatal tissue damage (Ricevuti, 1997). This could as well limit the release of pro-inflammatory cytokines and therefore result in a lower inflammatory response. Moreover, as the presence of a large number of pneumococci in the organism of the mice 48 hours post-infection seemed to be indicative of a fatal outcome in properdin-sufficient mice, but did not seem to influence the survival of properdin-deficient mice, it is legitimate to think that the cause of death, in this infection model, may more be due to an overactivation of the immune system in presence of properdin than to the presence of the pneumococci by itself.

This study therefore showed that properdin, in addition to the beneficial role it played in the blood at the beginning of the infection by limiting the bacterial counts, seemed to possess a detrimental role when organ-specific inflammation occurred, and that this was most likely to be related to the activity of the neutrophils during bacterial infection with Gram positive bacteria.

5 Final conclusion and perspectives

In this thesis, the biology of properdin was studied from different angles, by keeping an open-eye on its putative functions outside its well-known role of positive regulator of the alternative complement pathway.

5.1 Properdin expression in mouse organs

5.1.1 To summarise

In this part (chapter 2), the mouse properdin ORF obtained from mouse spleen mRNA was successfully cloned into a vector, its identity was confirmed by restriction digest and sequencing, and this DNA was then radioactively labelled in order to be used as a probe for Northern blot analysis.

Next, the expression of properdin in different mouse organs was assessed by various more or less sensitive techniques – Northern blotting, RT-PCR, real-time RT-PCR – and using bioinformatics resources. Lymphoid organs such as spleen, lymph node, thymus and bone marrow expressed properdin at a higher level than others organs. The expression of properdin was then examined in more detail for one of these organs – the spleen – using immunofluorescence. Properdin was found only in the white pulp compartment of the spleen. Clusters of properdin signals were observed on cells present inside B cell follicles. The identity of these properdin-positive cells with long cytoplasmic extensions was further investigated using antibodies specific for several splenic cell markers. However, CD68, FDC-M1 and CD45R, which are cell markers specific for tingible body macrophages, follicular dendritic cells and B cells respectively, were found not to colocalise with the properdin-positive cell population of the spleen. More specific cell markers will need to be tested in order to identify the properdin-positive cell population.

5.1.2 Role of properdin in the spleen

Even though the cell population carrying properdin inside the white pulp follicles of the mouse spleen could not yet be identified, the presence of properdin in this specific area of the spleen provided information to theorise on the putative role played by properdin in this organ. Properdin was not detected at all inside the red pulp compartment despite the fact that this compartment is partly made of macrophages, a

cell type known to express and produce properdin (Bentley et al., 1978; Reis et al., 2006). Of course, this may just be due to a detection limit problem. However, this reinforced the importance of detecting properdin at a sufficient concentration inside the white pulp compartment and emphasised the importance of the role played by properdin at this specific location. The spleen's main functions are phagocytosis and antibody production. After the capture of blood-borne antigens by marginal zone B cells in the marginal zone of the spleen, these cells migrate to the white pulp follicles where they deposit the antigens onto follicular dendritic cells. This transfer is essential for the development of an efficient adaptive immune response and has been shown to require an intact complement system (Carroll, 2004; Ferguson et al., 2004; Kraal, 2008). In fact, the use of different deficient mice has shown that C3, CD21 (CR2) and CD35 (CR1) all play key roles during the antigen transfer occurring in the splenic follicles between the marginal zone B cells and the follicular dendritic cells (Ferguson et al., 2004). Follicular dendritic cells possess numerous complement receptors (CR1, CR2 and CR3) and the lack of CD21 and CD35 in mice has been associated with low antibody responses (both T-cell dependent and T-cell independent) (Jacobson et al., 2008; Reynes et al., 1985). The exact role played by the complement system inside the splenic follicles is not known and the importance of the alternative complement pathway during this phenomenon has not yet been explored. However, it seems that the complement breakdown products bind to the antigens and act as a bridge between the antigen and the immune cell. Properdin, by stabilising the C3 convertase complex, could therefore potentially increase this interaction between the antigen and the follicular dendritic cell, and therefore increase the antigen retention in the spleen. This would explain why properdin is expressed at a high level in this part of the spleen and why properdin is expressed at a high level in lymphoid organs in general. Similar analyses would next need to be carried out on lymph node, the other major secondary lymphoid organ, as well as on the primary lymphoid organs.

Another study to perform would be to look at properdin expression in the spleen during bacterial infection. Preliminary data using *Streptococcus pneumoniae* D39 showed that properdin expression was two times higher in the spleen of infected mice compared to the one of their uninfected littermates (chapter 2.2.1.2). It would be interesting to localise properdin inside infected spleens and to determine whether

properdin can still be detected as clusters in splenic follicles (secondary follicles and germinal centres) after pneumococcal infection.

5.2 Properdin in mast cells

5.2.1 To summarise

In this chapter (chapter 3), the expression of properdin by mast cells was examined. HMC-1 and LAD 2 cells, two well-characterised mast cell lines, were shown, for the first time, to express properdin, the identity of the product obtained by RT-PCR being then confirmed by restriction digest and sequencing. Next, the expression of properdin by HMC-1 cells subjected to various stimuli was studied at both a transcriptional level, using a real-time PCR approach, and a translational level, using Western blot analysis. No up- or down-regulation of properdin expression could be observed at both levels 24 hours after stimulation with GM-CSF, IFNγ, IL-1β, TGFβ, TNFβ or LPS. Moreover, ELISA analysis on cell-free medium confirmed the cellular origin of the properdin found in the HMC-1 cell culture medium.

The location of properdin inside mast cell was then investigated. By flow cytometry, properdin could only be detected on the membrane of mast cells, the permeabilisation of the cells leading to the loss of the signal. Electron micrographs of HMC-1 and LAD 2 cells using both monoclonal and polyclonal anti-human properdin antibodies showed as well no properdin inside the cytoplasm of these cells. Properdin could therefore be detected either alone on the cell membrane, or in clusters of 2 to 8 molecules on the cell membrane too, but mainly on membrane extensions similar to vesicles in the process to be released. Fluorescence microscopy confirmed the presence of properdin on the mast cell membrane.

The expression of properdin by mast cells was compared to that of other cell lines such as K562, HL-60 and Jurkat cells. Properdin was found to be expressed on the surface of HMC-1 cells at a higher level than K562 and Jurkat cells, but at a slightly lower level than HL-60 cells.

Finally, the putative excretion of properdin by mast cells via vesicles was examined. Two kinds of vesicles could be identified in the supernatant of HMC-1 cell culture: the so-called “microvesicle-like vesicles” with a diameter of 100 to 400nm

and the “exosome-like vesicles”, smaller in size, with a diameter smaller than 100nm. Properdin was seen to be mainly expressed on the microvesicle-like vesicles fraction.

5.2.2 Role of properdin in mast cells

Properdin being now known to be expressed and secreted by mast cells, hypotheses were formulated to explain the putative roles played by properdin in these cells. Mast cells’ main functions reside in allergy, in innate immunity and in tissue remodelling (Metcalfe et al., 1997). Being one of the first cells to encounter the pathogen, mast cells play a major role during infection as they can phagocytose the pathogen, initiate the immune response via the release of their pro-inflammatory cytokines and attract neutrophils and others immune cells at the site of infection and finally participate in wound healing (Abraham and Malaviya, 1997). Properdin seems to be able to contribute to each of the functions previously mentioned.

In fact, being present in tissues close to the external environment, the expression of properdin by mast cells should ensure that properdin is present in the vicinity of the mast cells in tissue and therefore could lead to an extremely quick activation of the complement system and to a rapid up-take of pathogens by tissue-based phagocytic cells, maybe by mast cells themselves, in case of an infection. In fact, several recent publications showed that properdin was able to bind directly to the bacterial surface, without the need of a pre-formed C3bBb complex, leading to the generation of the complement alternative pathway C3 convertase and the deposition of C3b onto the membrane of the pathogen and thus leading to the pathogen’s phagocytosis (Spitzer et al., 2007; Stover et al., 2008). Kemper and collaborators showed more recently that direct binding of properdin to apoptotic T-cells could even result in the phagocytosis of the cells by phagocytic cells in the absence of complement activation, and that probably via properdin:GAG interactions (Kemper et al., 2008). It would be interesting to see if the direct binding of properdin to pathogen could lead too to its direct phagocytosis without the requirement of other complement molecules.

Mast cells have already been associated with tissue remodelling at different anatomical sites (Galli and Tsai, 2008; Okayama et al., 2007). TSR-containing proteins, such as thrombospondins and connective tissue growth factor, are known to play various roles during tissue remodelling (Bein and Simons, 2000; Robinet et al.,

2008; Tong and Brigstock, 2006). Thus, properdin released by mast cells at the site of infection could putatively play a role in wound healing via the interaction of its TSR modules with extracellular components, properdin being one of the members of the TSR superfamily (Sun et al., 2004).

Finally, the fact that properdin seemed to be concentrated in microvesicle-like vesicles suggested that properdin could be trafficking from mast cells to other cell types. Actually, microvesicles and exosomes have already been implicated in cell-to-cell communication and other immunological mechanisms (Distler et al., 2006). Furthermore, the binding of C1q to some microparticles has been shown to be able to trigger complement activation (Nauta et al., 2002). In this sense, the presence of properdin in these vesicles could play the same role. Moreover, the properdin present in these microvesicle-like vesicles could be as well viewed as an extracellular storage compartment for properdin. In fact, lysis of these vesicles could lead to the release of the "active" form of properdin present inside these vesicles, the detection of properdin inside these vesicles by the monoclonal antibody during Western blot analysis suggesting properdin was present under its final polymer form, and therefore lead to higher complement activation.

5.3 Characterisation of a properdin-deficient mouse line during pneumococcal pneumonia

In this section (chapter 4), the role of properdin during pneumococcal pneumonia was investigated. Properdin-deficient mice infected intranasally with *Streptococcus pneumoniae* serotype 2 strain D39 presented a worse level of infection 2 days post-infection, characterised by a higher serum level of the positive acute phase reactant C3, a change in the blood coagulation kinetics and an impairment to clear the pneumococci from the blood and the lungs of these animals, and was associated with a higher survival rate one week following the challenge. It was shown that these mice could overcome the infection despite the presence of bacteria in their organisms 48 hours after infection, while this condition seemed to be associated with a fatal outcome for a higher proportion of the wild type animals.

In order to explain this, I hypothesised that the absence of properdin could affect the neutrophils' function as a protracted influx of neutrophils into the lungs associated with a poor bacterial clearance was observed in mice deficient in properdin.

The migration function of the neutrophils and the level of opsonin present in the lung tissue of infected animals were shown to not be affected by the absence of properdin.

To conclude, my results suggested that properdin could play a bivalent role in this infection model: first, a beneficial role in the blood via its complement activation loop to control the number of bacteria during the first two days after pneumococcal infection (seen as well during the intravenous infection model); and then, a detrimental role when organ-specific inflammation occurred, probably by over-inducing the inflammatory response. This latter role may be linked with the activation of the neutrophils. This double-edged sword phenomenon has already been widely described for many immunological processes, but it was the first time it was described for properdin.

More work would need to be done to point out the exact role played by properdin in this pneumococcal pneumonia model, including investigating the level of activation of properdin-deficient neutrophils and assessing the exact cause of death of the infected mice.

5.4 Final conclusion

More than fifty years after the discovery and the first analyses of properdin by Pillemer and co-workers, properdin was still until recently only known as being the positive regulator of the alternative pathway that played a beneficial role during infection with rather uncommon serotypes of *Neisseria meningitidis*. This thesis and the many papers published in the past few years (showing the recrudescent interest for properdin) showed that properdin seemed to play a wider role in immunity (Ivanovska et al., 2008; Kemper et al., 2008; Kimura et al., 2007; Spitzer et al., 2007; Stover et al., 2008; Xu et al., 2008). In this work, the descriptions of properdin expression in the lymphoid organs and in mast cells open up new ways to think about properdin and new putative roles for this molecule. Moreover, an association between the development of an infection due to a Gram positive bacteria and the absence of properdin was for the first time seen in this thesis. Besides, the role played by properdin during pneumococcal infection was seen to be dual: in addition to its beneficial role played by amplifying the C3 convertase activity and therefore the immune response towards the pathogen, properdin was seen to play too an unfavourable role when the infection persisted by overwhelming the inflammatory

system. The development of new therapeutics to block properdin activity when its presence becomes detrimental could constitute a new interesting approach to protect the host during bacterial infection.

Appendix A

Bacterium media

Luria-Bertani broth (LB):

- 5g bacto-tryptone (OXOID, Basingstoke, UK)
- 2.5g yeast extract (OXOID)
- 5g NaCl
- 500ml dH2O

The medium was then autoclaved.

Luria-Bertani agar (LB-agar):

- 5g bacto-tryptone (OXOID)
- 2.5g yeast extract (OXOID)
- 5g NaCl
- 7.5g agar (OXOID)
- 500ml dH2O

The medium was then autoclaved, left to cool at 50°C and finally poured onto plates (20ml per plate).

When needed, ampicilin (100µg/ml), X-Gal (80µg/ml) and/or IPTG (0.5mM) were added to the medium just before to be poured into plates.

Brain Heart Infusion (BHI):

- 18.5g Brain Heart Infusion (OXOID)
- 500ml dH2O

The medium was then autoclaved.

Vegetable special infusion medium:

- 18.5g vegetable special infusion medium (Fluka)
- 500ml dH2O

The medium was then autoclaved.

Blood agar:

- 20g Blood agar base (OXOID)
- 500ml dH2O

The medium was then autoclaved and left to cool at 50°C. Twenty five millilitres of horse blood defibrinated (OXOID) were then added to the medium. It was finally mixed and poured onto plates (20ml per plate).

Appendix B

Publication

Properdin Plays a Protective Role in Polymicrobial Septic Peritonitis[1]

Cordula M. Stover,[2]* Jeni C. Luckett,* Bernd Echtenacher,[‡] Aline Dupont,* Sue E. Figgitt,* Jane Brown,[†] Daniela N. Männel,[‡] and Wilhelm J. Schwaeble*

Properdin is a positive regulator of complement activation so far known to be instrumental in the survival of infections with certain serotypes of *Neisseria meningitidis*. We have generated a fully backcrossed properdin-deficient mouse line by conventional gene-specific targeting. In vitro, properdin-deficient serum is impaired in alternative pathway-dependent generation of complement fragment C3b when activated by *Escherichia coli* DH5α. Properdin-deficient mice and wild-type littermates compare in their levels of C3 and IgM. In an in vivo model of polymicrobial septic peritonitis induced by sublethal cecal ligation and puncture, properdin-deficient mice appear immunocompromised, because they are significantly impaired in their survival compared with wild-type littermates. We further show that properdin localizes to mast cells and that properdin has the ability to directly associate with *E. coli* DH5α. We conclude that properdin plays a significant role in the outcome of polymicrobial sepsis. *The Journal of Immunology*, 2008, 180: 3313–3318.

Cecal ligation and puncture (CLP)[3] is a model for acute polymicrobial septic peritonitis following perforated appendicitis or diverticulitis. The severity of this model for the animal varies with length of the ligated cecum, needle size, and number of perforations (1). Complement activation, mast cells, and neutrophils are some of the outcome-determining factors of the host. Blockade of C5a or its receptor C5aR is beneficial for survival of the acute model of CLP in mice (2, 3) by suppression of C5a-mediated functions of peritoneal neutrophils (migration, oxidative burst, phagocytic response) (4). In the subacute model of CLP, however, neutrophil recruitment to the peritoneal cavity (5) and IL-12-mediated, IFN-γ-driven neutrophil phagocytosis (6) are important for survival. During acute CLP, neutrophil migration is effected by TNF, which is produced locally by peritoneal mast cells, which, thereby, are significant players in disease outcome (7). Mast cell degranulation, TNF release, and neutrophil infiltration are significantly impaired in C3-deficient mice during acute CLP, accounting for their high mortality compared with wild-type (WT) mice (8). Properdin is an oligomeric serum protein that amplifies ongoing complement activation. By virtue of each of its monomers to bind to C3b, it acts to extend the half-lives of the C3-converting and C5-converting enzyme complexes (C3bBb and $C3b_nBb$), respectively (9–11). These are generated after activation of the alternative pathway of complement via deposition of C3b to target surfaces by so-called spontaneous tickover of fluid phase C3 or by activation of classical or lectin pathways (via recognition of immune complexes or carbohydrate moieties on microorganisms, respectively). C1q-deficient mice (deficient of the recognition molecule of the classical pathway) and mice with a dual deficiency of factor B and C2 (affecting activities for lectin, classical and alternative pathways) (all on Sv/129 background) have previously been studied in sublethal CLP (12). The study concluded that intact lectin and alternative pathways are important for survival of sublethal CLP; however, it did not allow quantification of the separate contribution of the alternative pathway amplification to this effect. Therefore, the sublethal CLP model seemed a highly suitable model to characterize the phenotype of a properdin-deficient mouse line, which we have developed and describe herewith for the first time. So far, properdin deficiency is known in humans and shows variable penetrance with predilection to succumb to fatal meningococcal disease when infected with uncommon serotypes Y and W-135 (13).

Materials and Methods

Generation of a properdin-deficient mouse line

The mouse properdin gene was isolated from a mouse (129Sv) genomic bacteriophage library (λ2001) using mouse properdin cDNA (European Molecular Biological Laboratory/GenBank accession number X12905) as a probe. λ DNA of three hybridizing clones was purified using a Nucleobond λ phage purification kit (Clontech) (14). *Bam*H1 digest of two overlapping clones yielded 7.6-, 3.4-, and 0.5-kb fragments (corresponding to bp position 10,309–21,407 of the mouse BAC clone, European Molecular Biological Laboratory/GenBank accession number AL671853.7) that were subcloned in pBSKS+ and sequenced. A targeting construct was generated in pKO-NTKV 1901 (Stratagene) designed to contain the 5′ part of the properdin gene (promoter region, exon for thrombospondin repeat (TSR) 1) and the 3′ part of the gene (comprising exons for TSR 5, 6a, and 6b) flanking a positive selection marker gene (*neo*^{r}). Embryonic stem cells derived from male 129/Ola mice (E14.1a) were transfected with the linearized construct by electroporation. Clones were grown in G418 (positive selection for the presence of *neo*^{r}) and gancyclovir (negative selection against random integration, which produces thymidine kinase activity). Homologous recombination of this vector with the WT gene results in a replacement of exons 3–7 (1.6 kb) coding for the TSR 2–4 modules by the

*Department of Infection, Immunity and Inflammation and [†]Biomedical Services, University of Leicester, Leicester, United Kingdom; and [‡]Institute of Immunology, University of Regensburg, Regensburg, Germany

Received for publication August 10, 2007. Accepted for publication December 14, 2007.

The costs of publication of this article were defrayed in part by the payment of page charges. This article must therefore be hereby marked *advertisement* in accordance with 18 U.S.C. Section 1734 solely to indicate this fact.

[1] The work was funded by the Medical Research Council (Grant G0400300 to C.M.S.), the Wellcome Trust (Grant 060574 to W.J.S.), and Deutsche Forschungsgemeinschaft (Grant MA760/10-3 to D.N.M).

[2] Address correspondence and reprint requests to Dr. Cordula M. Stover, Department of Infection, Immunity and Inflammation, University of Leicester, University Road, Leicester LE1 9HN, U.K. E-mail address: cms13@le.ac.uk

[3] Abbreviations used in this paper: CLP, cecal ligation and puncture; TSR, thrombospondin repeat; WT, wild type.

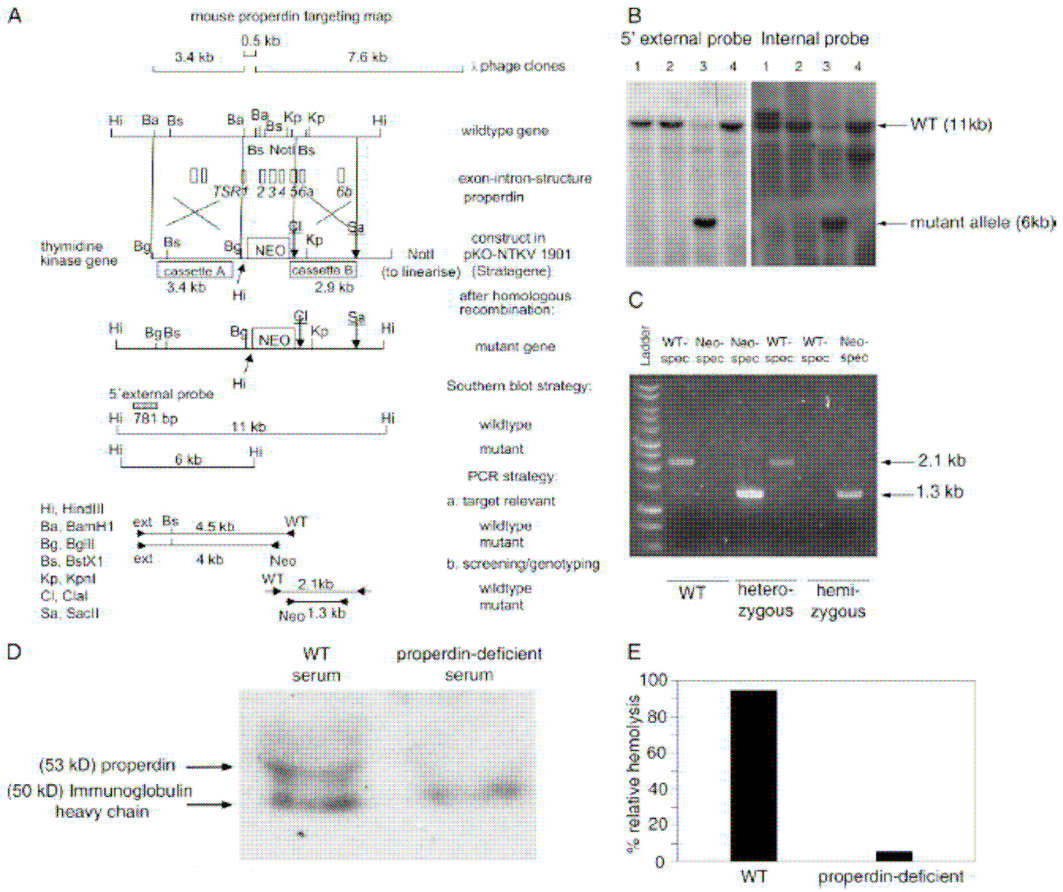

FIGURE 1. Generation of a properdin-deficient mouse line. *A*, Representation of the strategy to target the murine properdin gene, to replace exons 3–7 with a selection marker, and to detect specificity of this event. *B*, Southern blot analysis of *Hin*dIII-restricted genomic DNA prepared from positively and negatively selected embryonic stem cell clones using the external probe of 781 bp (5′ external probe) and the 3.4-kb fragment of cassette A (internal probe), see *A*, as probes. They both hybridize with a 6-kb band as indicated for *lane 3*. The size of the WT gene on *Hin*dIII restriction is 11 kb. The clones in *lanes 1, 2,* and *4* are either negative for any recombination event or nonhomologous recombinants. *C*, Typical agarose gel electrophoresis of PCR products obtained when genotyping offspring (see *A* for location of products). *D*, Verification of the absence of properdin in serum of hemizygous, gene-targeted mice using monoclonal anti-human properdin Ab with cross-reactivity to mouse protein (HYB 039-04, diluted 1/1000; Antibody Shop) by Western blot. (The secondary Ab (rabbit anti-mouse Ig, HRP conjugated) used for detection of the primary (anti-properdin) Ab) reacts with Igs contained in the sera.) *E*, Impairment of alternative pathway-mediated rabbit RBC lysis by properdin-deficient mice in comparison with WT littermate control. One of three representative experiments using two-sera set up in duplicate is shown.

neo^r gene (1.6 kb) of the targeting vector. Positive clones were identified by Southern blotting through the presence of a 6-kb band in *Hin*dIII-digested genomic DNA (an additional *Hin*dIII site is introduced during targeting) using a probe external to the targeted region. One of the 170 embryonic stem cell clones screened contained the disrupted allele of the targeted gene and was microinjected into C57BL/6 blastocysts which were implanted in pseudopregnant mice. Two male chimeras were derived. Germline transmission of the targeted allele was obtained upon mating to C57BL/6 mice (agouti offspring). As expected, all male offspring were WT and all female offspring were heterozygous for the targeting event. Target-specific PCR with restriction mapping of this fragment with *Bst*X1 showed correct replacement in these heterozygotes. Intercrossing resulted in hemizygous males, heterozygous females, and WT offspring, as identified by PCR, at the expected ratio. The properdin-deficient mice appear normal in weight and fertility and are maintained in a barrier unit according to institutional guidelines. The mice used in these experiments were backcrossed onto the C57BL/6 background for 9 and 10 generations. WT littermates were controls.

Rabbit RBC lysis

Target cells were prepared as follows. Rabbit blood (Biomedical Services, University of Leicester, Leicester, U.K.) was collected in Alsever's solution (114 mM sodium citrate, 27 mM glucose, and 72 mM sodium chloride, pH 6.1), spun down at 200 × *g*, washed twice in PBS, and the pellet was resuspended in 1× VBS (727 mM sodium chloride, 16 mM 5,5-diethylbarbituric acid, and 9 mM 5,5-diethylbarbituric acid sodium salt)-20 mM Mg^{2+}-8 mM EGTA (pH 7.4) to where lysis of 50 μl of RBC in 200 μl of water gave an absorption at 413 nm of 1.0–1.2 (positive control). The assay was set up in duplicate, diluting 100 μl of mouse serum (sample and heat-inactivated control) with 100 μl of VBS-Mg^{2+}-EGTA, then adding 50 μl of adjusted rabbit RBC. The cells in 200 μl of VBS-Mg^{2+}-EGTA were the negative control. After 2 h at 37°C, absorptions were read and hemolysis

was expressed as a percentage against the controls (relative hemolysis = [(mean OD sample − mean OD heat inactivated mouse serum)/(mean OD water − mean OD buffer)] × 100%) (15).

C3 activation of WT and properdin-deficient sera

Properdin-deficient or WT mouse sera were diluted 1/20 in either PBS^{++} (with Ca^{2+} and Mg^{2+}), GVB^{++}, GVB/Mg^{2+}-EGTA, or GVB^{++}-EDTA buffers and incubated at 37°C with 1×10^6/ml formalin-fixed (10% formal saline) *E. coli* DH5α. (washed in the respective buffers). After 30 min, the supernatant, that is, activated serum, was removed and separated under reducing conditions (2-ME, boiling) on 10% SDS-polyacrylamide gels. After electrophoretic transfer using cellulose membrane 2micron (Bio-Rad Laboratories), the membrane was incubated with monoclonal biotin-coupled rat anti-mouse C3 (Cedarlane Laboratories), detected with a streptavidin-HRP ABC kit (DakoCytomation), and developed using ECL reagent (Pierce).

IgM and C3 levels in mouse sera

Serum was prepared from mouse blood obtained via the tail vein and frozen in aliquots. Serum levels for IgM and C3 were determined by sandwich ELISAs according to the manufacturers' manuals (Bethyl Laboratories, Universal Biologicals and Immunology Consultants Laboratory, Immune Systems) and analyzed using a five-parameter logistics curve.

Sublethal CLP

Mice were anesthetized by i.p. injection of 75 mg/kg Ketanest (Parke-Davis) and 16 mg/kg Rompun (Bayer). The cecum was exteriorized and the distal end (<30%) was ligated and punctured once with a needle (0.4-mm diameter, 27-gauge) to achieve a sublethal CLP as previously described (16). Mice were observed for 2 wk. Kaplan-Meier survival curves were compared using the log rank test. The experiments were performed in compliance with federal guidelines for animal experimentation (State of Bavaria, Germany).

Immunohistochemical and immunofluorescent analysis of mouse mast cells

Four-micrometer sections were cut from paraffin-embedded connective tissue obtained from the abdominal wall, incubated with proteinase K (2 mg/ml), 3% H_2O_2, and, after blocking with 5% BSA and application of SeroBlock FcR (BUF041A; Serotec) were incubated with goat anti-human properdin IgG (1/100; Nordic Immunology), or as control, goat anti-rabbit IgG (P0448; DakoCytomation), and rabbit anti-goat Igs, HRP-conjugated (1/400, A5420; Sigma-Aldrich). After development with diaminobenzidine tetrahydrochloride (D5637; Sigma-Aldrich), sections were counterstained with toluidine blue. For immunofluorescent analysis, sections were processed as above, incubated with FITC-coupled goat anti-human properdin IgG (1/200; Nordic Immunology) or rabbit anti-human mast cell tryptase Ab (1/400, sc-32889; Santa Cruz Biotechnology) and goat-anti-rabbit IgG, $F(ab')_2$-TRITC (1/400, sc-3841; Santa Cruz Biotechnology). Fluorescence signals were analyzed using a Nikon TE300 wide-field epifluorescence microscope.

Binding of properdin to E. coli *DH5α*

Formalin-fixed *E. coli* DH5α (1×10^6/ml) were incubated with human sera (diluted 1/20 in PBS/Mg^{2+}/5% BSA) of known concentration of properdin (determined using a properdin ELISA kit obtained from Antibodyshop). After washing with PBS, monoclonal anti-human properdin Ab (HYB 039-06, diluted 1/1000; AntibodyShop) was added for 1 h and, after another washing step with PBS, FITC-coupled anti-mouse Fab Igs (Sigma-Aldrich) were added (1/4000). Fluorescence signals were analyzed as above. In parallel, an equal concentration of purified properdin (purity >98%; Europa Bioproducts) was added (diluted in PBS/Mg^{2+}/5% BSA to the predetermined level for the respective sera) and slides were processed as above. Part of this latter incubation, along with a control (*E. coli* without properdin), was used for immunoprecipitation studies, in which the microbes are washed, then lysed in radioimmunoprecipitation assay buffer with protease inhibitors (P8340; Sigma-Aldrich), sheared, precleared with protein G-Sepharose (P3296; Sigma-Aldrich), and incubated with Sepharose-coupled monoclonal anti-human properdin Ab (HYB 039-06; AntibodyShop). The immunoprecipitate was run on a 10% SDS-polyacrylamide gel, blotted, and probed with rabbit anti-human properdin Ab.

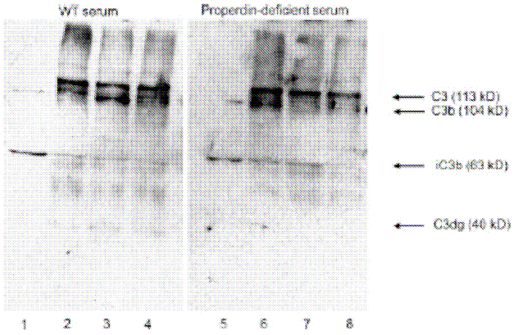

FIGURE 2. C3 activation in properdin-deficient mice. Western blot for C3 activation products in WT and properdin-deficient sera after incubation with *E. coli* DH5α in different buffer conditions (*lanes 1* and *5*: PBS with Ca^{2+} and Mg^{2+}; *lanes 2* and *6*: GVB^{++}; *lanes 3* and *7*: GVB/Mg^{2+}-EGTA; and *lanes 4* and *8*: GVB^{++}-EDTA). One of three experiments is shown using WT and properdin-deficient littermate sera. The band indicated to represent C3dg is seen on longer exposure for the properdin-deficient sera.

Results

Generation of properdin-deficient mice

A properdin-deficient mouse line was generated by specific targeting and disruption of the murine properdin gene, which is located on chromosome X (17). The strategy was to delete those exons coding for thrombospondin repeats (TSR) with importance in binding to C3b and thereby stabilization of the C3bBb complex or for oligomerization of the protein (18) (Fig. 1*A*). Homologous recombination of mouse properdin DNA contained in the targeting vector and segments of the properdin gene in 129/Ola embryonic stem cells was confirmed in 1 of 170 clones (Fig. 1*B*). This clone was microinjected in C57BL/6 blastocysts and two chimeric mice were derived. Both showed germline transmission and produced heterozygous female and WT male offspring. These were intercrossed, obtaining genotypes at the expected Mendelian ratio and X chromosome linkage. Heterozygous mice were backcrossed to C57BL/6 to obtain male WT and properdin-deficient littermates (Fig. 1*C*). The hemizygous properdin gene-targeted mice lack properdin protein in their sera (Fig. 1*D*) and they are grossly impaired in the alternative pathway-dependent diagnostic test of lysing rabbit RBC (19) (Fig. 1*E*). Heterozygous mice showed an intermediate phenotype (data not shown).

C3 activation in sera of WT and properdin-deficient mice

Western blot analysis was performed for different WT and properdin-deficient sera activated by *E. coli* DH5α in four different

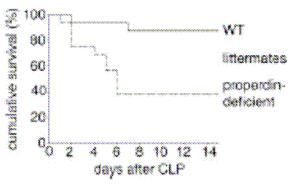

FIGURE 3. Properdin-deficient mice are impaired in their survival after sublethal CLP. Properdin-deficient mice and WT littermates ($n = 16$, each group) were subjected to sublethal CLP and mortality was recorded ($p = 0.003$; log rank statistic).

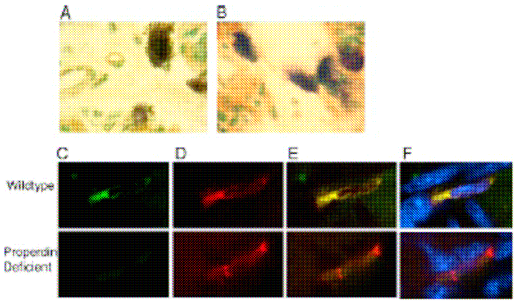

FIGURE 4. Properdin is produced by mast cells. Immunohistochemical analysis of connective tissue mast cells using goat anti-human properdin (*A*) or control Ab (*B*). Both sections were developed with diaminobenzidine tetrahydrochloride (brown stain) and counterstained with toluidine blue (purple stain). Immunofluorescent analysis showing reactivity of properdin (*C*), mast cell marker tryptase (*D*), and overlap (*E*) for gut mucosa (4′,6-diamidino-2-phenylindole stained, *F*) of WT, but not properdin-deficient mice.

buffer conditions. One of three representative experiments is shown (Fig. 2): incubation of serum diluted in PBS/Mg^{2+}/Ca^{2+} with the microbe leads to complete conversion of C3 to C3b and iC3b for both WT and properdin-deficient serum. In buffer conditions that restrict activation of complement, either selectively (GVB^{++}, GVB^{++}EGTA) or globally (GVB^{++}EDTA), by contrast, the uncut 113-kDa C3α chain is seen (*lanes 2–4* and *6–8*, Fig 2). In conditions favoring activation of complement via the alternative pathway (*lanes 3* and *7*, Fig. 2), properdin-deficient serum shows a clear reduction of the 104-kDa activation product C3b. Further degradation of iC3b to the 40-kDa α-chain product occurs in conditions that preclude C3 binding (EDTA) and in those inhibiting assembly of all recognition molecules to surfaces (GVB^{++}/GVB^{++}EGTA), but not in the most physiologic of these conditions (PBS^{++}).

Serum C3 levels of the sera thus analyzed were found to be comparable, as was the range of levels determined for larger numbers of the two groups (properdin-deficient, $n = 14$: 1.19 ± 0.39 mg/ml, and WT, $n = 17$: 0.99 ± 0.30 mg/ml).

Survival of WT and properdin-deficient mice in CLP

The severity of the CLP model was chosen to produce sublethal and prolonged inflammation. In the first 7 days of the observation period, 14 of 16 WT mice survived, whereas only 6 of 16 properdin-deficient mice survived (Fig. 3).

Properdin is produced by mast cells

Sections of connective tissue mast cells of unchallenged WT mice were analyzed for reactivity of properdin by standard immunohistochemistry. Representative figures from two independent experiments clearly demonstrate properdin reactivity localizing to the granules of mast cells (Fig. 4*A*), which compares to the granule-specific metachromatic stain produced by toluidine blue on the control section (Fig. 4*B*). Subsequent immunofluorescence analysis of gut sections from WT and properdin-deficient mice using a mast cell marker, tryptase, confirmed that reactivities of properdin and tryptase overlap for WT, but not properdin-deficient mice (Fig. 4, *C–F*).

Properdin associates directly with E. coli *DH5α*

Incubation of formalin-fixed *E. coli* DH5α with human serum of known properdin concentrations or with the same amount of purified properdin on its own leads to the same patchy reactivity with the monoclonal anti-properdin Ab (Fig. 5, *A–C*). This association is absent on chelation of serum with EDTA (data not shown). There is no detectable C3 in the properdin preparation (Fig. 5*D*). To ascertain the physical association between *E. coli* and properdin, immunoprecipitation was performed using the

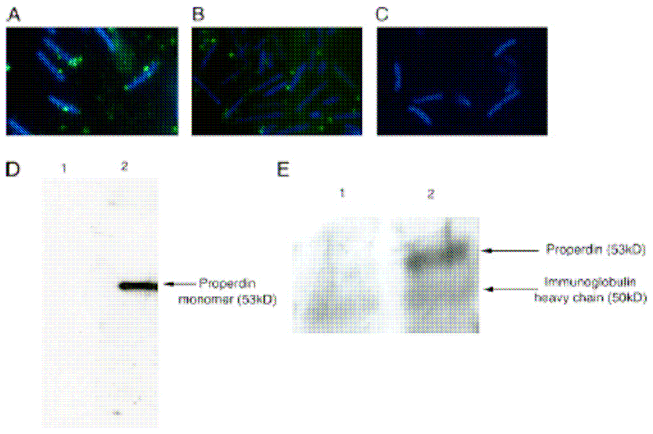

FIGURE 5. Properdin associates with *E. coli* DH5α. *A*, After incubation of *E. coli* DH5α with human serum (determined at 27 μg/ml properdin), properdin was detected using a monoclonal anti-human properdin Ab and FITC-coupled anti-mouse Fab Igs. *B*, After incubation of *E. coli* DH5α with purified properdin (25 μg/ml stock), bound properdin was detected as above. *C*, Negative control (addition of the secondary Ab only). Different sera were used and the amount of exogenous properdin was adjusted to the respective serum concentration. This is a representative figure of three such experiments. *D*, Aliquots of the purified properdin preparation were separated by SDS-PAGE and analyzed for possible C3 content using mouse anti-human C3 (ab11871; Abcam) (*strip 1*). *Strip 2* of the same transfer was developed with mouse anti-human properdin Ab (HYB 039-06; Antibody Shop) and shows the expected 53-kDa band for monomeric properdin. *E*, Immunoprecipitation of properdin bound to *E. coli* DH5α (*lane 2*) and control (*lane 1*) using monoclonal anti-human properdin Ab. Transferred lysates were developed with polyclonal goat anti-human properdin Ab. The 53-kDa band for properdin is indicated. The secondary Ab (rabbit anti-goat Ig, HRP conjugated) reacts with Igs contained in both immunoprecipitates. The H chain of Ig is indicated.

monoclonal anti-properdin Ab or a control Ab followed by Western blot analysis of immunoprecipitates using a polyclonal anti-properdin Ab. A 53- kDa band for monomeric properdin is detected for the specific immunoprecipitate (Fig. 5*E*).

Discussion

DH5α is a nonpathogenic *E. coli* K12 derivative that is able to activate the alternative pathway of complement (20) and was therefore used to test the contribution of properdin toward activation of C3 in properdin-deficient vs WT sera. In conditions using PBS^{++}, the iC3b product seems more abundant in activated WT compared with activated properdin-deficient serum and may reflect the contribution of an intact amplification loop the alternative pathway provides for the activation of classical and lectin pathways. Analysis of C3 activation products in sera of WT and properdin-deficient littermates, using buffer conditions favoring alternative pathway activation, consistently shows impaired processing of C3 in properdin-deficient sera in the 30-min incubation with *E. coli* DH5α. The difference between properdin-deficient and WT sera is less marked on longer incubation times (1h; data not shown). This, along with the fact that Factor B reactivity on Western blot analysis of WT and properdin-deficient sera varies little (data not shown), is consistent with the understanding that properdin provides stabilization of a specific C3-cleaving ability of serum. One variable in this experiment may be the actual serum levels for C3 in properdin-deficient and WT mice, based on a description of elevated C3 levels in heterozygous properdin-deficient persons, due to a proposed lower consumption of C3 (21), but this was not found to be the case.

Properdin-deficient and WT littermates were subjected to sublethal CLP, a model of subacute peritoneal inflammation provoked by polymicrobial leakage from punctured distal cecum after ligation, which develops into sepsis. In this model, severity is measured by mortality (22). The present study finds that in the absence of properdin, survival after sublethal CLP-induced polymicrobial sepsis over an observation period of 14 days is significantly impaired. Natural Abs, germline-expressed Igs of the IgM type, bind to bacterial Ags and are protective in models of septic and endotoxin shock (23, 24). However, there was no difference between properdin-deficient ($n = 4$; 41.9 μg/ml ± 2.45 SD) and WT ($n = 5$; 43.14 μg/ml ± 9.89 SD) mice in their total serum IgM levels.

Mast cells are crucially important to survive CLP, relating to a significant degree to their ability to synthesize TNF-α (7) and this study finds that mast cells express properdin. A direct association of properdin on the surface of fixed *E. coli* DH5α was investigated by incubation with human serum or with purified properdin. Properdin is found associated with *E. coli* DH5α and may thereby provide a scaffold for increased C3b or C3Bb binding as recently proposed (25). The properdin protein contained in the specific immunoprecipitate from *E. coli* after prior incubation with human properdin (Fig. 5*E*) compares to the protein identified as mouse properdin in WT serum (Fig. 1*D*). Our finding that properdin associates directly with *E. coli* DH5α (exhibiting so-called rough LPS) is strongly supported by recently published work showing that properdin binds to rough, not WT, so-called smooth, *E. coli* LPS mutants (26).

Based on the findings obtained for the in vitro and in vivo phenotype of the properdin-deficient mice, the immune response of the WT mice in this model of sublethal CLP is likely to be influenced by these properdin-dependent factors: optimal, i.e., properdin-stabilized, C3b generation is crucial to attract neutrophils to the peritoneal cavity (5, 6) through C3b-mediated TNF-α release by mast cells (27). Neutrophils store, among other factors, properdin in their secondary granules (28) and so do mast cells. On release of properdin, it can associate with, and independent of, C3b to the surface of the microorganism (26). The molecular implications of these modes of properdin binding are currently under investigation.

Acknowledgments

This publication contains a part of Lynda Dupont's doctoral thesis. We are grateful to Prof. K. B. M. Reid (University of Oxford, Oxford, U.K.) for providing the mouse properdin cDNA clone and rabbit anti-human properdin antiserum and to Dr. C. Pritchard (University of Leicester) for advice and for providing the genomic library. We thank Mariya Hristova (University College London, London, U.K.) for helpful advice regarding the hemolysis test, Kathryn Staley (University of Leicester) for performing properdin ELISA measurements, Dr. Rana El-Rachkidy-Lonnen for useful discussions, and Claudia Dembek (Ludwig-Maximilians-University, Munich, Germany) and Irina Elliott (University of Leicester) for technical assistance.

Disclosures

The authors have no financial conflict of interest.

References

1. Ebong, S., D. Call, J. Nemzek, G. Bolgos, D. Newcomb, and D. Remick. 1999. Immunopathologic alterations in murine models of sepsis of increasing severity. *Infect. Immun.* 67: 6603–6610.
2. Riedemann, N., R. F. Guo, T. Neff, I. Laudes, K. Keller, V. Sarma, M. Markiewski, D. Mastellos, C. Strey, C. Pierson, et al. 2002. Increased C5a receptor expression in sepsis. *J. Clin. Invest.* 110: 1010–1108.
3. Riedemann, N., T. Neff, R. F. Guo, K. Bernacki, I. Laudes, J. Sarma, J. Lambris, and P. Ward. 2003. Protective effects of Il-6 blockade in sepsis are linked to reduced C5a receptor expression. *J. Immunol.* 170: 503–507.
4. Huber-Lang, M., N. Riedeman, J. Sarma, E. Younkin, S. McGuire, I. Laudes, K. Lu, R. F. Guo, T. Neff, V. Padgaonkar, et al. 2002. Protection of innate immunity by C5aR antagonist in septic mice. *FASEB J.* 16: 1567–1574.
5. Rios-Santos, F., C. Benjamim, D. Zavery, S. Ferreira, and F. Cunha. 2003. A critical role of leukotriene B4 in neutrophil migration to infectious focus in cecal ligation and puncture sepsis. *Shock* 19: 61–65.
6. Moreno, S., J. Alves-Filho, T. Alfaya, J. da Silva, S. Ferreira, and F. Liew. 2006. IL-12, but not Il-18, is critical to neutrophil activation and resistance to polymicrobial sepsis induced by cecal ligation and puncture. *J. Immunol.* 177: 3218–3224.
7. Echtenacher, B., D. N. Männel, and L. Hültner. 1996. Critical protective role of mast cells in a model of acute septic peritonitis. *Nature* 381: 75–77.
8. Prodeus, A. P., X. Zhou, M. Maurer, S. J. Galli, and M. C. Carroll. 1997. Impaired mast cell-dependent natural immunity in complement C3-deficient mice. *Nature* 390: 172–175.
9. Pillemer, L., L. Blum, I. H. Lepow, O. A. Ross, E. W. Todd, A. C. Wardlaw. 1954. The properdin system and immunity: I. Demonstration and isolation of a new serum protein, properdin, an its role in immune phenomena. *Science* 120: 279–285.
10. Smith, C. A., M. K. Pangburn, C. W. Vogel, and H. J. Müller-Eberhard. 1984. Molecular architecture of human properdin, a positive regulator of the alternative pathway of complement. *J. Biol. Chem.* 259: 4582–4588.
11. Medicus, R. G., O. Götze, and H. J. Müller-Eberhard. 1976. Alternative pathway of complement: recruitment of precursor properdin by the labile C3/C5 convertase and the potentiation of the pathway. *J. Exp. Med.* 144: 1076–1093.
12. Wiedbichler, M., B. Echtenacher, T. Hehlgans, J. C. Jennenius, W. Schwaeble, and D. N. Männel. 2004. Involvement of the lectin pathway of complement activation in antimicrobial immune defense during experimental septic peritonitis. *Infect. Immun.* 72: 5247–5252.
13. Späth, P. J., A. G. Sjöholm, G. N. Fredrikson, G. Misiano, R. Scherz, U. B. Schaad, B. Uhring-Lambert, G. Hauptmann, J. Westberg, M. Uhlen, et al. 1999. Properdin deficiency in a large Swiss family: identification of a stop codon in the properdin gene, and association of meningococcal disease with lack of the IgG2 allotype marker $G2m_n$. *Clin. Exp. Immunol.* 118: 278–284.
14. Lee, S. H., and J. B. Clark. High-yield method for isolation of λ DNA. 1997. *BioTechniques* 23: 598–600.
15. Klerx, J. P., C. J. Beukelman, H. Van Dijk, and J. M. Wilers. 1983. Microassay for colorimetric activity in guinea pig, human and mouse serum. *J. Immunol. Methods* 63: 215–220.
16. Echtenacher, B., W. Falk, D. N. Männel, and P. H. Krammer. 1990. Requirement of endogenous tumor necrosis factor/cachectin for recovery from experimental peritonitis. *J. Immunol.* 145: 3762–3766.
17. Evans, E. P., M. D. Burtenshaw, S. H. Laval, D. Goundis, K. B. Reid, and Y. Boyd. 1990. Localization of the properdin factor complement locus Pfc to band A3 on the mouse X chromosome. *Genet. Res.* 56: 153–155.

18. Higgins, J. M. G., H. Wiedemann, R. Timpl, and K. B. M. Reid. 1995. Characterization of mutant forms of recombinant human properdin lacking single thrombospondin type I repeats: identification of modules important for function. *J. Immunol.* 155: 5777–5785.
19. Austen, K. F., and D. T. Fearon. 1979. A molecular basis of activation of the alternative pathway of human complement. *Adv. Exp. Med. Biol.* 120B: 3–17.
20. Schreiber, R., D. C. Morrison, E. Podack, and H. J. Müller-Eberhard. 1979. Bactericidal activity of the alternative complement pathway generated from 11 isolated plasma proteins. *J. Exp. Med.* 149: 870–882.
21. Davis, C. A., and J. Forristal. 1980. Partial properdin deficiency. *J. Lab. Clin. Med.* 96: 633–639.
22. Buras, J. A., B. Holzmann, and M. Sitkovsky. 2005. Animal models of sepsis: setting the stage. *Nat. Rev. Drug Discov.* 4: 854–865.
23. Reid, R., A. Prodeus, W. Khan, T. Hsu, F. Rosen, and M. Carroll. 1997. Endotoxin shock in antibody-deficient mice: unraveling the role of natural antibody and complement in the clearance of lipopolysaccharide. *J. Immunol.* 159: 970–975.
24. Boes, M., A. P. Prodeus, T. Schmidt, M. C. Carroll, and J. Chen. 1998. A critical role of natural immunoglobulin M in immediate defense against systemic bacterial infection. *J. Exp. Med.* 188: 2381–2386.
25. Hourcade, D. E. 2006. The role of properdin in the assembly of the alternative pathway C3 convertases of complement. *J. Biol. Chem.* 281: 2128–2132.
26. Spitzer, D., L. Mitchell, J. P. Atkinson, and D. E. Hourcade. 2007. Properdin can initiate complement activation by binding specific target surfaces and providing a platform for de novo convertase assembly. *J. Immunol.* 179: 2600–2608.
27. Gommerman, J. L., D. Y. Oh, X. Zhou, T. F. Tedder, M. Maurer, S. J. Galli, and M. C. Carroll. 2000. A role for CD21/CD35 and CD19 in responses to acute septic peritonitis: a potential mechanism for mast cell activation. *J. Immunol.* 165: 6915–6921.
28. Wirthmueller, U., B. Dewald, M. Thelen, M. K. Schäfer, C. Stover, K. Whaley, J. North, P. Eggleton, K. B. Reid, and W. J. Schwaeble. 1997. Properdin, a positive regulator of complement activation, is released from secondary granules of stimulated peripheral blood neutrophils. *J. Immunol.* 158: 4444–4451.

References

Abraham, S. N. and Malaviya, R. (1997). Mast Cells in Infection and Immunity. *Infect. Immun.* **65,** 3501-3508.

Aguilar, A., Merino, S., Merce-Nagueras, M., Regue, M. and Tomas, J.M. (1999). Two genes from the capsule of *Aeromonas hydrophila* (serogroup O:34) confer serum resistance to *Escherichia coli* K12 strains. *Res. Microbio.*, **150**, 395-402.

Alexandrakis, M., Letourneau, R., Kempuraj, D., Kandere-Grzybowska, K., Huang, M., Christodoulou, S., Boucher, W., Seretakis, D. and Theoharides, T. C. (2003). Flavones Inhibit Proliferation and Increase Mediator Content in Human Leukemic Mast Cells (HMC-1). *Eur. J. Haematol.* **71,** 448-454.

Al-Nedawi, K., Szemraj, J. and Cierniewski, C. S. (2005). Mast Cell-Derived Exosomes Activate Endothelial Cells to Secrete Plasminogen Activator Inhibitor Type 1. *Arterioscler. Thromb. Vasc. Biol.* **25,** 1744-1749.

Andrasfalvy, M., Prechl, J., Hardy, T., Erdei, A. and Bajtay, Z. (2002). Mucosal Type Mast Cells Express Complement Receptor Type 2 (CD21). *Immunol. Lett.* **82,** 29-34.

Angel, C. S., Ruzek, M. and Hostetter, M. K. (1994). Degradation of C3 by *Streptococcus Pneumoniae*. *J. Infect. Dis.* **170,** 600-608.

Anisimov, A. P., Dentovskaya, S. V., Titareva, G. M., Bakhteeva, I. V., Shaikhutdinova, R. Z., Balakhonov, S. V., Lindner, B., Kocharova, N. A., Senchenkova, S. N., Holst, O., Pier, G. B. and Knirel, Y. A. (2005). Intraspecies and Temperature-Dependent Variations in Susceptibility of *Yersinia Pestis* to the Bactericidal Action of Serum and to Polymyxin B. *Infect. Immun.* **73,** 7324-7331.

Avery, V. M., Adrian, D. L. and Gordon, D. L. (1993). Detection of Mosaic Protein mRNA in Human Astrocytes. *Immunol. Cell Biol.* **71,** 215-219.

Bathum, L., Hansen, H., Teisner, B., Koch, C., Garred, P., Rasmussen, K. and Wang, P. (2006). Association between Combined Properdin and Mannose-Binding Lectin Deficiency and Infection with Neisseria Meningitidis. *Mol. Immunol.* **43,** 473-479.

Bein, K. and Simons, M. (2000). Thrombospondin Type 1 Repeats Interact with Matrix Metalloproteinase 2. Regulation of Metalloproteinase Activity. *J. Biol. Chem.* **275,** 32167-32173.

Benoist, C. and Mathis, D. (2002). Mast Cells in Autoimmune Disease. *Nature* **420,** 875-878.

Bentley, C., Fries, W. and Brade, V. (1978). Synthesis of Factors D, B and P of the Alternative Pathway of Complement Activation, as well as of C3, by Guinea-Pig Peritoneal Macrophages in Vitro. *Immunology* **35,** 971-980.

Benton, K. A., Everson, M. P. and Briles, D. E. (1995). A Pneumolysin-Negative Mutant of Streptococcus Pneumoniae Causes Chronic Bacteremia rather than Acute Sepsis in Mice. *Infect. Immun.* **63,** 448-455.

Bergeron, Y., Ouellet, N., Deslauriers, A. M., Simard, M., Olivier, M. and Bergeron, M. G. (1998). Cytokine Kinetics and Other Host Factors in Response to Pneumococcal Pulmonary Infection in Mice. *Infect. Immun.* **66,** 912-922.

Bischoff, S. C. (2007). Role of Mast Cells in Allergic and Non-Allergic Immune Responses: Comparison of Human and Murine Data. *Nat. Rev. Immunol.* **7,** 93-104.

Boes, M., Prodeus, A. P., Schmidt, T., Carroll, M. C. and Chen, J. (1998). A Critical Role of Natural Immunoglobulin M in Immediate Defense Against Systemic Bacterial Infection. *J. Exp. Med.* **188,** 2381-2386.

Bongrazio, M., Pries, A. R. and Zakrzewicz, A. (2003). The Endothelium as Physiological Source of Properdin: Role of Wall Shear Stress. *Mol. Immunol.* **39,** 669-675.

Braconier, J. H., Sjoholm, A. G. and Soderstrom, C. (1983). Fulminant Meningococcal Infections in a Family with Inherited Deficiency of Properdin. *Scand. J. Infect. Dis.* **15,** 339-345.

Broudy, V. C. (1997). Stem Cell Factor and Hematopoiesis. *Blood* **90,** 1345-1364.

Brouwer, N., Dolman, K. M., van Zwieten, R., Nieuwenhuys, E., Hart, M., Aarden, L. A., Roos, D. and Kuijpers, T. W. (2006). Mannan-Binding Lectin (MBL)-Mediated Opsonization is Enhanced by the Alternative Pathway Amplification Loop. *Mol. Immunol.* **43,** 2051-2060.

Brown, J. S., Hussell, T., Gilliland, S. M., Holden, D. W., Paton, J. C., Ehrenstein, M. R., Walport, M. J. and Botto, M. (2002). The Classical Pathway is the Dominant Complement Pathway Required for Innate Immunity to *Streptococcus Pneumoniae* Infection in Mice. *Proc. Natl. Acad. Sci. U. S. A.* **99,** 16969-16974.

Burry, R. W. (2000). Specificity Controls for Immunocytochemical Methods. *J. Histochem. Cytochem.* **48,** 163-166.

Butterfield, J. H., Weiler, D., Dewald, G. and Gleich, G. J. (1988). Establishment of an Immature Mast Cell Line from a Patient with Mast Cell Leukemia. *Leuk. Res.* **12,** 345-355.

Caby, M. P., Lankar, D., Vincendeau-Scherrer, C., Raposo, G. and Bonnerot, C. (2005). Exosomal-Like Vesicles are Present in Human Blood Plasma. *Int. Immunol.* **17,** 879-887.

Cairns, J. A. (1998). Mast Cell Tryptase and its Role in Tissue Remodelling. *Clin. Exp. Allergy* **28,** 1460-1463.

Canvin, J. R., Marvin, A. P., Sivakumaran, M., Paton, J. C., Boulnois, G. J., Andrew, P. W. and Mitchell, T. J. (1995). The Role of Pneumolysin and Autolysin in the Pathology of Pneumonia and Septicemia in Mice Infected with a Type 2 Pneumococcus. *J. Infect. Dis.* **172,** 119-123.

Carroll, M. C. (2004). The Complement System in Regulation of Adaptive Immunity. *Nat. Immunol.* **5,** 981-986.

Cesta, M. F. (2006). Normal Structure, Function, and Histology of the Spleen. *Toxicol. Pathol.* **34,** 455-465.

Chi, D. S., Fitzgerald, S. M., Pitts, S., Cantor, K., King, E., Lee, S. A., Huang, S. K. and Krishnaswamy, G. (2004). MAPK-Dependent Regulation of IL-1- and Beta-Adrenoreceptor-Induced Inflammatory Cytokine Production from Mast Cells: Implications for the Stress Response. *BMC Immunol.* **5,** 22-33.

Choy, L. N. and Spiegelman, B. M. (1996). Regulation of Alternative Pathway Activation and C3a Production by Adipose Cells. *Obes. Res.* **4,** 521-532.

Chronos, N. A., Goodall, A. H., Wilson, D. J., Sigwart, U. and Buller, N. P. (1993). Profound Platelet Degranulation is an Important Side Effect of some Types of Contrast Media used in Interventional Cardiology. *Circulation* **88,** 2035-2044.

Coleman, M. P., Murray, J. C., Willard, H. F., Nolan, K. F., Reid, K. B., Blake, D. J., Lindsay, S., Bhattacharya, S. S., Wright, A. and Davies, K. E. (1991). Genetic and Physical Mapping Around the Properdin P Gene. *Genomics* **11,** 991-996.

Crivellato, E., Beltrami, C., Mallardi, F. and Ribatti, D. (2003). Paul Ehrlich's Doctoral Thesis: A Milestone in the Study of Mast Cells. *Br. J. Haematol.* **123,** 19-21.

Cunliffe, N. A., Snowden, N., Dunbar, E. M. and Haeney, M. R. (1995). Recurrent Meningococcal Septicaemia and Properdin Deficiency. *J. Infect.* **31,** 67-68.

de Paula, P. F., Barbosa, J. E., Junior, P. R., Ferriani, V. P., Latorre, M. R., Nudelman, V. and Isaac, L. (2003). Ontogeny of Complement Regulatory Proteins – Concentrations of Factor H, Factor I, C4b-Binding Protein, Properdin and Vitronectin in Healthy Children of Different Ages and in Adults. *Scand. J. Immunol.* **58,** 572-577.

Del Conde, I., Cruz, M. A., Zhang, H., Lopez, J. A. and Afshar-Kharghan, V. (2005). Platelet Activation Leads to Activation and Propagation of the Complement System. *J. Exp. Med.* **201,** 871-879.

Densen, P., Weiler, J. M., Griffiss, J. M. and Hoffmann, L. G. (1987). Familial Properdin Deficiency and Fatal Meningococcemia. Correction of the Bactericidal Defect by Vaccination. *N. Engl. J. Med.* **316,** 922-926.

Derkx, H. H., Kuijper, E. J., Fijen, C. A., Jak, M., Dankert, J. and van Deventer, S. J. (1995). Inherited Complement Deficiency in Children Surviving Fulminant Meningococcal Septic Shock. *Eur. J. Pediatr.* **154,** 735-738.

Derrico, C. A. and Goodrum, K. J. (1996). Interleukin-12 and Tumor Necrosis Factor Alpha Mediate Innate Production of Gamma Interferon by Group B Streptococcus-Treated Splenocytes of Severe Combined Immunodeficiency Mice. *Infect. Immun.* **64,** 1314-1320.

Distler, J. H., Huber, L. C., Gay, S., Distler, O. and Pisetsky, D. S. (2006). Microparticles as Mediators of Cellular Cross-Talk in Inflammatory Disease. *Autoimmunity* **39,** 683-690.

Dommett, R. M., Klein, N. and Turner, M. W. (2006). Mannose-Binding Lectin in Innate Immunity: Past, Present and Future. *Tissue Antigens* **68,** 193-209.

Drexler, H. G. and MacLeod, R. A. (2003). Malignant Hematopoietic Cell Lines: *In Vitro* Models for the Study of Mast Cell Leukemia. *Leuk. Res.* **27,** 671-676.

Duncan, R. C., Wijeyewickrema, L. C. and Pike, R. N. (2008). The Initiating Proteases of the Complement System: Controlling the Cleavage. *Biochimie* **90,** 387-395.

Dvorak, A. M. (2005). Ultrastructural Studies of Human Basophils and Mast Cells. *J. Histochem. Cytochem.* **53,** 1043-1070.

Echtenacher, B., Mannel, D. N. and Hultner, L. (1996). Critical Protective Role of Mast Cells in a Model of Acute Septic Peritonitis. *Nature* **381,** 75-77.

Edelson, B. T., Li, Z., Pappan, L. K. and Zutter, M. M. (2004). Mast Cell-Mediated Inflammatory Responses Require the Alpha 2 Beta 1 Integrin. *Blood* **103,** 2214-2220.

Edelson, B. T., Stricker, T. P., Li, Z., Dickeson, S. K., Shepherd, V. L., Santoro, S. A. and Zutter, M. M. (2006). Novel collectin/C1q Receptor Mediates Mast Cell Activation and Innate Immunity. *Blood* **107,** 143-150.

Ekdahl, K. N., Norberg, D., Bengtsson, A. A., Sturfelt, G., Nilsson, U. R. and Nilsson, B. (2007). Use of Serum Or Buffer-Changed EDTA-Plasma in a Rapid, Inexpensive, and Easy-to-Perform Hemolytic Complement Assay for Differential Diagnosis of Systemic Lupus Erythematosus and Monitoring of Patients with the Disease. *Clin. Vaccine Immunol.* **14,** 549-555.

Erdei, A., Andrasfalvy, M., Peterfy, H., Toth, G. and Pecht, I. (2004). Regulation of Mast Cell Activation by Complement-Derived Peptides. *Immunol. Lett.* **92,** 39-42.

Esmon, C. T. (2004). The Impact of the Inflammatory Response on Coagulation. *Thromb. Res.* **114,** 321-327.

Farries, T. C. and Atkinson, J. P. (1989). Biosynthesis of Properdin. *J. Immunol.* **142,** 842-847.

Favoreel, H. W., Van de Walle, G. R., Nauwynck, H. J. and Pensaert, M. B. (2003). Virus Complement Evasion Strategies. *J. Gen. Virol.* **84,** 1-15.

Fearon, D. T. and Austen, K. F. (1975). Properdin: Binding to C3b and Stabilization of the C3b-Dependent C3 Convertase. *J. Exp. Med.* **142,** 856-863.

Feger, F., Varadaradjalou, S., Gao, Z., Abraham, S. N. and Arock, M. (2002). The Role of Mast Cells in Host Defense and their Subversion by Bacterial Pathogens. *Trends Immunol.* **23,** 151-158.

Ferguson, A. R., Youd, M. E. and Corley, R. B. (2004). Marginal Zone B Cells Transport and Deposit IgM-Containing Immune Complexes onto Follicular Dendritic Cells. *Int. Immunol.* **16,** 1411-1422.

Figueroa, J. E. and Densen, P. (1991). Infectious Diseases Associated with Complement Deficiencies. *Clin. Microbiol. Rev.* **4,** 359-395.

Fijen, C. A., Derkx, B. H., Kuijper, E. J., Mannens, M., Poort, S. R., Peters, M., Daha, M. R. and Dankert, J. (1995). Fulminant Meningococcal Septic Shock in a Boy with Combined Inherited Properdin and Protein C Deficiency. *Clin. Exp. Immunol.* **102,** 290-296.

Fijen, C. A., Kuijper, E. J., Drogari-Apiranthitou, M., Van Leeuwen, Y., Daha, M. R. and Dankert, J. (1998). Protection Against Meningococcal Serogroup ACYW Disease in Complement-Deficient Individuals Vaccinated with the Tetravalent Meningococcal Capsular Polysaccharide Vaccine. *Clin. Exp. Immunol.* **114,** 362-369.

Fijen, C. A., Kuijper, E. J., Hannema, A. J., Sjoholm, A. G. and van Putten, J. P. (1989). Complement Deficiencies in Patients Over Ten Years Old with Meningococcal Disease due to Uncommon Serogroups. *Lancet* **2,** 585-588.

Fijen, C. A., Kuijper, E. J., te Bulte, M. T., Daha, M. R. and Dankert, J. (1999a). Assessment of Complement Deficiency in Patients with Meningococcal Disease in the Netherlands. *Clin. Infect. Dis.* **28,** 98-105.

Fijen, C. A., van den Bogaard, R., Daha, M. R., Dankert, J., Mannens, M. and Kuijper, E. J. (1996). Carrier Detection by Microsatellite Haplotyping in 10 Properdin Type 1-Deficient Families. *Eur. J. Clin. Invest.* **26,** 902-906.

Fijen, C. A., van den Bogaard, R., Schipper, M., Mannens, M., Schlesinger, M., Nordin Fredrikson. G., Dankert, J., Daha, M. R., Sjoholm, A. G., Truedsson, L. and Kuijper, E. J. (1999b). Properdin Deficiency: Molecular Basis and Disease Association. *Mol. Immunol.* **36,** 863-867.

Fremeaux-Bacchi, V., Le Coustumier, A., Blouin, J., Kazatchkine, M. D. and Weiss, L. (1995). Partial Properdin Deficiency Revealed by a Septicemia Caused by *Neisseria Meningitidis*. *Presse Med.* **24,** 1305-1307.

Furitsu, T., Tsujimura, T., Tono, T., Ikeda, H., Kitayama, H., Koshimizu, U., Sugahara, H., Butterfield, J. H., Ashman, L. K. and Kanayama, Y. (1993). Identification of Mutations in the Coding Sequence of the Proto-Oncogene c-Kit in a Human Mast Cell Leukemia Cell Line Causing Ligand-Independent Activation of c-Kit Product. *J. Clin. Invest.* **92,** 1736-1744.

Gaboriaud, C., Teillet, F., Gregory, L. A., Thielens, N. M. and Arlaud, G. J. (2007). Assembly of C1 and the MBL- and Ficolin-MASP Complexes: Structural Insights. *Immunobiology* **212,** 279-288.

Gallagher, R., Collins, S., Trujillo, J., McCredie, K., Ahearn, M., Tsai, S., Metzgar, R., Aulakh, G., Ting, R., Ruscetti, F. and Gallo, R. (1979). Characterization of the Continuous, Differentiating Myeloid Cell Line (HL-60) from a Patient with Acute Promyelocytic Leukemia. *Blood* **54,** 713-733.

Galli, S. J. and Tsai, M. (2008). Mast Cells: Versatile Regulators of Inflammation, Tissue Remodeling, Host Defense and Homeostasis. *J. Dermatol. Sci.* **49,** 7-19.

Gasque, P. (2004). Complement: A Unique Innate Immune Sensor for Danger Signals. *Mol. Immunol.* **41,** 1089-1098.

Gasser, O., Hess, C., Miot, S., Deon, C., Sanchez, J. C. and Schifferli, J. A. (2003). Characterisation and Properties of Ectosomes Released by Human Polymorphonuclear Neutrophils. *Exp. Cell Res.* **285,** 243-257.

Gasser, O. and Schifferli, J. A. (2005). Microparticles Released by Human Neutrophils Adhere to Erythrocytes in the Presence of Complement. *Exp. Cell Res.* **307,** 381-387.

Geelen, S., Bhattacharyya, C. and Tuomanen, E. (1992). Induction of Procoagulant Activity on Human Endothelial Cells by *Streptococcus Pneumoniae*. *Infect. Immun.* **60,** 4179-4183.

Gelfand, E. W., Rao, C. P., Minta, J. O., Ham, T., Purkall, D. B. and Ruddy, S. (1987). Inherited Deficiency of Properdin and C2 in a Patient with Recurrent Bacteremia. *Am. J. Med.* **82,** 671-675.

Genel, F., Atlihan, F., Gulez, N., Sjoholm, A. G., Skattum, L. and Truedsson, L. (2006). Properdin Deficiency in a Boy with Fulminant Meningococcal Septic Shock. *Acta Paediatr.* **95,** 1498-1500.

Gilchrist, M. and Befus, A. D. (2007). Interferon-Gamma Regulates Chemokine Expression and Release in the Human Mast Cell Line HMC-1: Role of Nitric Oxide. *Immunology*. **123**, 209-217.

Gillespie, S. H. and Balakrishnan, I. (2000). Pathogenesis of Pneumococcal Infection. *J. Med. Microbiol.* **49,** 1057-1067.

Gingles, N. A., Alexander, J. E., Kadioglu, A., Andrew, P. W., Kerr, A., Mitchell, T. J., Hopes, E., Denny, P., Brown, S., Jones, H. B., Little, S., Booth, G. C. and McPheat, W. L. (2001). Role of Genetic Resistance in Invasive Pneumococcal Infection: Identification and Study of Susceptibility and Resistance in Inbred Mouse Strains. *Infect. Immun.* **69,** 426-434.

Glaum, M. C., Wang, Y., Raible, D. G. and Schulman, E. S. (2001). Degranulation Influences Heparin-Associated Inhibition of RT-PCR in Human Lung Mast Cells. *Clin. Exp. Allergy* **31,** 1631-1635.

Gommerman, J. L., Oh, D. Y., Zhou, X., Tedder, T. F., Maurer, M., Galli, S. J. and Carroll, M. C. (2000). A Role for CD21/CD35 and CD19 in Responses to Acute Septic Peritonitis: A Potential Mechanism for Mast Cell Activation. *J. Immunol.* **165,** 6915-6921.

Gonzalez de Peredo, A., Klein, D., Macek, B., Hess, D., Peter-Katalinic, J. and Hofsteenge, J. (2002). C-Mannosylation and O-Fucosylation of Thrombospondin Type 1 Repeats. *Mol. Cell. Proteomics* **1,** 11-18.

Goodall, A. H. and Appleby, J. (2004). Flow-Cytometric Analysis of Platelet-Membrane Glycoprotein Expression and Platelet Activation. *Methods Mol. Biol.* **272,** 225-253.

Goundis, D., Holt, S. M., Boyd, Y. and Reid, K. B. (1989). Localization of the Properdin Structural Locus to Xp11.23-Xp21.1. *Genomics* **5,** 56-60.

Goundis, D. and Reid, K. B. (1988). Properdin, the Terminal Complement Components, Thrombospondin and the Circumsporozoite Protein of Malaria Parasites Contain Similar Sequence Motifs. *Nature* **335,** 82-85.

Grutzkau, A., Kruger-Krasagakes, S., Kogel, H., Moller, A., Lippert, U. and Henz, B. M. (1997). Detection of Intracellular Interleukin-8 in Human Mast Cells: Flow Cytometry as a Guide for Immunoelectron Microscopy. *J. Histochem. Cytochem.* **45,** 935-945.

Guckian, J. C. (1975). Effect of Pneumococci on Blood Clotting, Platelets, and Polymorphonuclear Leukocytes. *Infect. Immun.* **12,** 910-918.

Guo, D., Henriksson, R. and Hedman, H. (2002). The iCycler iQ^{TM} Detection System for Evaluating Reference Gene Expression in Normal Human Tissue. *BioRad tech note,* **2804**.

Harris, C. L., Pettigrew, D. M., Lea, S. M. and Morgan, B. P. (2007). Decay-Accelerating Factor must Bind both Components of the Complement Alternative Pathway C3 Convertase to Mediate Efficient Decay. *J. Immunol.* **178,** 352-359.

Hartert, H. (1948). Blutgerinnungsstudien Mit Der Thromboelastographie, Einem Neuen Untersuchungsverfahren. *Klin. Wochenschr.* **26,** 577-583.

Hartmann, S. and Hofsteenge, J. (2000). Properdin, the Positive Regulator of Complement, is Highly C-Mannosylated. *J. Biol. Chem.* **275,** 28569-28574.

Hayat, M. A. (1981). Fixation for Electron Microscopy. Academic Press, London.

Heijnen, H. F., Schiel, A. E., Fijnheer, R., Geuze, H. J. and Sixma, J. J. (1999). Activated Platelets Release Two Types of Membrane Vesicles: Microvesicles by Surface Shedding and Exosomes Derived from Exocytosis of Multivesicular Bodies and Alpha-Granules. *Blood* **94,** 3791-3799.

Higgins, J. M., Wiedemann, H., Timpl, R. and Reid, K. B. (1995). Characterization of Mutant Forms of Recombinant Human Properdin Lacking Single Thrombospondin Type I Repeats. Identification of Modules Important for Function. *J. Immunol.* **155,** 5777-5785.

Holme, E. R., Veitch, J., Johnston, A., Hauptmann, G., Uring-Lambert, B., Seywright, M., Docherty, V., Morley, W. N. and Whaley, K. (1989). Familial Properdin Deficiency Associated with Chronic Discoid Lupus Erythematosus. *Clin. Exp. Immunol.* **76,** 76-81.

Horny, H. P., Sotlar, K. and Valent, P. (2007). Mastocytosis: State of the Art. *Pathobiology* **74,** 121-132.

Hostetter, M. K. (2000). Opsonic and Nonopsonic Interactions of C3 with *Streptococcus Pneumoniae*. In *Streptococcus Pneumoniae*: Molecular Biology and Mechanisms of Disease, pp. 309-313. Mary Ann Liebert, New York.

Hourcade, D. E. (2006). The Role of Properdin in the Assembly of the Alternative Pathway C3 Convertases of Complement. *J. Biol. Chem.* **281,** 2128-2132.

Ikeda, K., Sannoh, T., Kawasaki, N., Kawasaki, T. and Yamashina, I. (1987). Serum Lectin with Known Structure Activates Complement through the Classical Pathway. *J. Biol. Chem.* **262,** 7451-7454.

Ivanovska, N. D., Dimitrova, P. A., Luckett, J. C., El-Rachkidy Lonnen, R., Schwaeble, W. J. and Stover, C. M. (2008). Properdin Deficiency in Murine Models of Nonseptic Shock. *J. Immunol.* **180,** 6962-6969.

Jacobson, A. C., Weis, J. J. and Weis, J. H. (2008). Complement Receptors 1 and 2 Influence the Immune Environment in a B Cell Receptor-Independent Manner. *J. Immunol.* **180,** 5057-5066.

Janoff, E. N. and Rubins, J. B. (2000). Invasive Pneumococcal Disease in the Immunocompromised Host. In *Streptococcus Pneumoniae: Molecular Biology and Mechanisms of Disease*, pp. 321-341. Mary Ann Liebert, New York.

Jarva, H., Jokiranta, T. S., Wurzner, R. and Meri, S. (2003). Complement Resistance Mechanisms of Streptococci. *Mol. Immunol.* **40,** 95-107.

Jedrzejas, M. J. (2001). Pneumococcal Virulence Factors: Structure and Function. *Microbiol. Mol. Biol. Rev.* **65,** 187-207.

Jounblat, R., Clark, H., Eggleton, P., Hawgood, S., Andrew, P. W. and Kadioglu, A. (2005). The Role of Surfactant Protein D in the Colonisation of the Respiratory Tract and Onset of Bacteraemia during Pneumococcal Pneumonia. *Respir. Res.* **6,** 126-137.

Kadioglu, A. and Andrew, P. W. (2004). The Innate Immune Response to Pneumococcal Lung Infection: The Untold Story. *Trends Immunol.* **25,** 143-149.

Kadioglu, A. and Andrew, P. W. (2005). Susceptibility and Resistance to Pneumococcal Disease in Mice. *Brief Funct. Genomic Proteomic* **4,** 241-247.

Kadioglu, A., Gingles, N. A., Grattan, K., Kerr, A., Mitchell, T. J. and Andrew, P. W. (2000). Host Cellular Immune Response to Pneumococcal Lung Infection in Mice. *Infect. Immun.* **68,** 492-501.

Kadioglu, A., Weiser, J. N., Paton, J. C. and Andrew, P. W. (2008). The Role of *Streptococcus Pneumoniae* Virulence Factors in Host Respiratory Colonization and Disease. *Nat. Rev. Microbiol.* **6,** 288-301.

Kandere-Grzybowska, K., Letourneau, R., Kempuraj, D., Donelan, J., Poplawski, S., Boucher, W., Athanassiou, A. and Theoharides, T. C. (2003). IL-1 Induces Vesicular Secretion of IL-6 without Degranulation from Human Mast Cells. *J. Immunol.* **171,** 4830-4836.

Keller, S., Sanderson, M. P., Stoeck, A. and Altevogt, P. (2006). Exosomes: From Biogenesis and Secretion to Biological Function. *Immunol. Lett.* **107,** 102-108.

Kemper, C., Mitchell, L. M., Zhang, L. and Hourcade, D. E. (2008). The Complement Protein Properdin Binds Apoptotic T Cells and Promotes Complement Activation and Phagocytosis. *Proc. Natl. Acad. Sci. U. S. A.* **105,** 9023-9028.

Kerr, A. R., Paterson, G. K., Riboldi-Tunnicliffe, A. and Mitchell, T. J. (2005). Innate Immune Defense Against Pneumococcal Pneumonia Requires Pulmonary Complement Component C3. *Infect. Immun.* **73,** 4245-4252.

Kimura, Y., Miwa, T., Zhou, L. and Song, W. C. (2007). Activator-Specific Requirement of Properdin in the Initiation and Amplification of the Alternative Pathway Complement. *Blood*. **111**, 732-740.

Kindt, T. J., Goldsby, R. A. and Osborne, B. A. (2007). Kuby Immunology – 6th ed. W.H. Freeman and company, New York.

Kirshenbaum, A. S., Akin, C., Wu, Y., Rottem, M., Goff, J. P., Beaven, M. A., Rao, V. K. and Metcalfe, D. D. (2003). Characterization of Novel Stem Cell Factor Responsive Human Mast Cell Lines LAD 1 and 2 Established from a Patient with Mast Cell sarcoma/leukemia; Activation Following Aggregation of FcεRI Or FcγRI. *Leuk. Res.* **27,** 677-682.

Kolble, K., Cant, A. J., Fay, A. C., Whaley, K., Schlesinger, M. and Reid, K. B. (1993). Carrier Detection in Families with Properdin Deficiency by Microsatellite Haplotyping. *J. Clin. Invest.* **91,** 99-102.

Kouoh, F., Gressier, B., Luyckx, M., Brunet, C., Dine, T., Ballester, L., Cazin, M. and Cazin, J. C. (2000). A Simple Method for Isolating Human and Rabbit Polymorphonuclear Neutrophils (PMNs). *Biol. Pharm. Bull.* **23,** 1382-1383.

Kraal, G. (2008). Antigens Take the Shuttle. *Nat. Immunol.* **9,** 11-12.

Kulah, B., Tezeren, D., Aksaray, S., Ozmutlu, A., Coskun, F., Toyran, A. and Guvener, E. (2006). Changes in Serum C3 Complement Protein Levels during Early and Late Experimental Sepsis. *16th European congress of clinical microbiology and infectious disease*, Nice, Abstract.

Lachmann, P. (2006). Complement before Molecular Biology. *Mol. Immunol.* **43,** 496-508.

Landskroner, K. A., Olson, N. C. and Jesmok, G. J. (2005). Thromboelastography Measurements of Whole Blood from Factor VIII-Deficient Mice Supplemented with rFVIII. *Haemophilia* **11,** 346-352.

Lanie, J. A., Ng, W. L., Kazmierczak, K. M., Andrzejewski, T. M., Davidsen, T. M., Wayne, K. J., Tettelin, H., Glass, J. I. and Winkler, M. E. (2007). Genome Sequence of Avery's Virulent Serotype 2 Strain D39 of *Streptococcus Pneumoniae* and Comparison with that of Unencapsulated Laboratory Strain R6. *J. Bacteriol.* **189,** 38-51.

Law, S. K. and Dodds, A. W. (1997). The Internal Thioester and the Covalent Binding Properties of the Complement Proteins C3 and C4. *Protein Sci.* **6,** 263-274.

Lee, J. D., Kato, K., Tobias, P. S., Kirkland, T. N. and Ulevitch, R. J. (1992). Transfection of CD14 into 70Z/3 Cells Dramatically Enhances the Sensitivity to Complexes of Lipopolysaccharide (LPS) and LPS Binding Protein. *J. Exp. Med.* **175,** 1697-1705.

Lepow, I. H. (1980). Presidential Address to American Association of Immunologists in Anaheim, California, April 16, 1980. Louis Pillemer, Properdin, and Scientific Controversy. *J. Immunol.* **125,** 471-475.

Letiembre, M., Echchannaoui, H., Bachmann, P., Ferracin, F., Nieto, C., Espinosa, M. and Landmann, R. (2005). Toll-Like Receptor 2 Deficiency Delays Pneumococcal Phagocytosis and Impairs Oxidative Killing by Granulocytes. *Infect. Immun.* **73,** 8397-8401.

Lin, T. J., Gao, Z., Arock, M. and Abraham, S. N. (1999). Internalization of FimH+ *Escherichia Coli* by the Human Mast Cell Line (HMC-1 5C6) Involves Protein Kinase C. *J. Leukoc. Biol.* **66,** 1031-1038.

Linton, S. M. and Morgan, B. P. (1999). Properdin Deficiency and Meningococcal Disease – Identifying those most at Risk. *Clin. Exp. Immunol.* **118,** 189-191.

Lyubchenko, T., dal Porto, J., Cambier, J. C. and Holers, V. M. (2005). Coligation of the B Cell Receptor with Complement Receptor Type 2 (CR2/CD21) using its Natural Ligand C3dg: Activation without Engagement of an Inhibitory Signaling Pathway. *J. Immunol.* **174,** 3264-3272.

Malaviya, R., Ikeda, T., Ross, E. and Abraham, S. N. (1996). Mast Cell Modulation of Neutrophil Influx and Bacterial Clearance at Sites of Infection through TNF-Alpha. *Nature* **381,** 77-80.

Mallett, S. V. and Cox, D. J. (1992). Thrombelastography. *Br. J. Anaesth.* **69,** 307-313.

Manco, S., Hernon, F., Yesilkaya, H., Paton, J. C., Andrew, P. W. and Kadioglu, A. (2006). Pneumococcal Neuraminidases A and B both have Essential Roles during Infection of the Respiratory Tract and Sepsis. *Infect. Immun.* **74,** 4014-4020.

Markiewski, M. M., Nilsson, B., Nilsson Ekdahl, K., Mollnes, T. E. and Lambris, J. D. (2007). Complement and Coagulation: Strangers Or Partners in Crime? *Trends Immunol.* **28,** 184-192.

Marshall, J. S. and Jawdat, D. M. (2004). Mast Cells in Innate Immunity. *J. Allergy Clin. Immunol.* **114,** 21-27.

Mathew, S. and Overturf, G. D. (2006). Complement and Properdin Deficiencies in Meningococcal Disease. *Pediatr. Infect. Dis. J.* **25,** 255-256.

Maves, K. K., Guenthner, S. T., Densen, P., Moser, D. R. and Weiler, J. M. (1995). Cloning and Characterization of the cDNA Encoding Guinea-Pig Properdin: A Comparison of Properdin from Three Species. *Immunology* **86,** 475-479.

Maves, K. K. and Weiler, J. M. (1992). Detection of Properdin mRNA in Human Peripheral Blood Monocytes and Spleen. *J. Lab. Clin. Med.* **120,** 762-766.

Maves, K. K. and Weiler, J. M. (1993). Properdin: Approaching Four Decades of Research. *Immunol. Res.* **12,** 233-243.

Maves, K. K. and Weiler, J. M. (1994). Human Liver-Derived Hep G2 Cells Produce Functional Properdin. *J. Lab. Clin. Med.* **124,** 837-842.

Mebius, R. E. and Kraal, G. (2005). Structure and Function of the Spleen. *Nat. Rev. Immunol.* **5,** 606-616.

Metcalfe, D. D., Baram, D. and Mekori, Y. A. (1997). Mast Cells. *Physiol. Rev.* **77,** 1033-1079.

Metz, M. and Maurer, M. (2007). Mast Cells – Key Effector Cells in Immune Responses. *Trends Immunol.* **28,** 234-241.

Minta, J. O. (1988). Biosynthesis of Complement Factor P (Properdin) by the Human Pre-Monocyte Cell Line (U-937). *Mol. Immunol.* **25,** 1363-1370.

Morgan, B. P. and Orren, A. (1998). Vaccination Against Meningococcus in Complement-Deficient Individuals. *Clin. Exp. Immunol.* **114,** 327-329.

Mueller-Ortiz, S. L., Drouin, S. M. and Wetsel, R. A. (2004). The Alternative Activation Pathway and Complement Component C3 are Critical for a Protective Immune Response Against *Pseudomonas Aeruginosa* in a Murine Model of Pneumonia. *Infect. Immun.* **72,** 2899-2906.

Nakamura, M., Tomita, A., Nakatani, H., Matsuda, T. and Nadano, D. (2006). Antioxidant and Antibacterial Genes are Upregulated in Early Involution of the Mouse Mammary Gland: Sharp Increase of Ceruloplasmin and Lactoferrin in Accumulating Breast Milk. *DNA Cell Biol.* **25,** 491-500.

Nauta, A. J., Trouw, L. A., Daha, M. R., Tijsma, O., Nieuwland, R., Schwaeble, W. J., Gingras, A. R., Mantovani, A., Hack, E. C. and Roos, A. (2002). Direct Binding of C1q to Apoptotic Cells and Cell Blebs Induces Complement Activation. *Eur. J. Immunol.* **32,** 1726-1736.

Nelson, R. A.,Jr. (1958). An Alternative Mechanism for the Properdin System. *J. Exp. Med.* **108,** 515-535.

Nielsen, H. E. and Koch, C. (1987). Congenital Properdin Deficiency and Meningococcal Infection. *Clin. Immunol. Immunopathol.* **44,** 134-139.

Nielsen, H. E., Koch, C., Magnussen, P. and Lind, I. (1989). Complement Deficiencies in Selected Groups of Patients with Meningococcal Disease. *Scand. J. Infect. Dis.* **21,** 389-396.

Nielsen, H. E., Koch, C., Mansa, B., Magnussen, P. and Bergmann, O. J. (1990). Complement and Immunoglobulin Studies in 15 Cases of Chronic Meningococcemia: Properdin Deficiency and Hypoimmunoglobulinemia. *Scand. J. Infect. Dis.* **22,** 31-36.

Nielsen, V. G. and Crow, J. P. (2004). Peroxynitrite Decreases Rabbit Tissue Factor Activity in Vitro. *Anesth. Analg.* **98,** 668-671.

Nilsson, G., Blom, T., Kusche-Gullberg, M., Kjellen, L., Butterfield, J. H., Sundstrom, C., Nilsson, K. and Hellman, L. (1994). Phenotypic Characterization of the Human Mast-Cell Line HMC-1. *Scand. J. Immunol.* **39,** 489-498.

Nolan, K. F., Kaluz, S., Higgins, J. M., Goundis, D. and Reid, K. B. (1992). Characterization of the Human Properdin Gene. *Biochem. J.* **287,** 291-297.

Nolan, K. F., Schwaeble, W., Kaluz, S., Dierich, M. P. and Reid, K. B. (1991). Molecular Cloning of the cDNA Coding for Properdin, a Positive Regulator of the Alternative Pathway of Human Complement. *Eur. J. Immunol.* **21,** 771-776.

Nordahl, E. A., Rydengard, V., Nyberg, P., Nitsche, D. P., Morgelin, M., Malmsten, M., Bjorck, L. and Schmidtchen, A. (2004). Activation of the Complement System Generates Antibacterial Peptides. *Proc. Natl. Acad. Sci. U. S. A.* **101,** 16879-16884.

Nordin Fredrikson, G., Gullstrand, B., Westberg, J., Sjoholm, A. G., Uhlen, M. and Truedsson, L. (1998). Expression of Properdin in Complete and Incomplete Deficiency: Normal in Vitro Synthesis by Monocytes in Two Cases with Properdin Deficiency Type II due to Distinct Mutations. *J. Clin. Immunol.* **18,** 272-282.

Nordin Fredrikson, G., Westberg, J., Kuijper, E. J., Tijssen, C. C., Sjoholm, A. G., Uhlen, M. and Truedsson, L. (1996). Molecular Characterization of Properdin Deficiency Type III: Dysfunction Produced by a Single Point Mutation in Exon 9 of the Structural Gene Causing a Tyrosine to Aspartic Acid Interchange. *J. Immunol.* **157,** 3666-3671.

Okayama, Y., Ra, C. and Saito, H. (2007). Role of Mast Cells in Airway Remodeling. *Curr. Opin. Immunol.* **19,** 687-693.

Oksjoki, R., Kovanen, P. T., Mayranpaa, M. I., Laine, P., Blom, A. M., Meri, S. and Pentikainen, M. O. (2006). Complement Regulation in Human Atherosclerotic Coronary Lesions Immunohistochemical Evidence that C4b-Binding Protein Negatively Regulates the Classical Complement Pathway, and that C5b-9 is Formed Via the Alternative Complement Pathway. *Atherosclerosis*. **192**, 40-48.

Olsson, N., Piek, E., Sundstrom, M., ten Dijke, P. and Nilsson, G. (2001). Transforming Growth Factor-Beta-Mediated Mast Cell Migration Depends on Mitogen-Activated Protein Kinase Activity. *Cell. Signal.* **13,** 483-490.

Pangburn, M. K. (1989). Analysis of the Natural Polymeric Forms of Human Properdin and their Functions in Complement Activation. *J. Immunol.* **142,** 202-207.

Peerschke, E. I., Yin, W., Grigg, S. E. and Ghebrehiwet, B. (2006). Blood Platelets Activate the Classical Pathway of Human Complement. *J. Thromb. Haemost.* **4,** 2035-2042.

Pensky, J., Hinz, C. F.,Jr, Todd, E. W., Wedgwood, R. J., Boyer, J. T. and Lepow, I. H. (1968). Properties of Highly Purified Human Properdin. *J. Immunol.* **100,** 142-158.

Perdikoulis, M. V., Kishore, U. and Reid, K. B. (2001). Expression and Characterisation of the Thrombospondin Type I Repeats of Human Properdin. *Biochim. Biophys. Acta* **1548,** 265-277.

Pillemer, L., Blum, L., Lepow, I. H., Ross, O. A., Todd, E. W. and Wardlaw, A. C. (1954). The Properdin System and Immunity. I. Demonstration and Isolation of a New Serum Protein, Properdin, and its Role in Immune Phenomena. *Science* **120,** 279-285.

Prieto-Alamo, M. J., Cabrera-Luque, J. M. and Pueyo, C. (2003). Absolute Quantitation of Normal and ROS-Induced Patterns of Gene Expression: An in Vivo Real-Time PCR Study in Mice. *Gene Expr.* **11,** 23-34.

Prodeus, A. P., Zhou, X., Maurer, M., Galli, S. J. and Carroll, M. C. (1997). Impaired Mast Cell-Dependent Natural Immunity in Complement C3-Deficient Mice. *Nature* **390,** 172-175.

Prussin, C. and Metcalfe, D. D. (2006). 5. IgE, Mast Cells, Basophils, and Eosinophils. *J. Allergy Clin. Immunol.* **117,** S450-6.

Quah, B. J. and O'Neill, H. C. (2005). The Immunogenicity of Dendritic Cell-Derived Exosomes. *Blood Cells Mol. Dis.* **35,** 94-110.

Ratajczak, J., Wysoczynski, M., Hayek, F., Janowska-Wieczorek, A. and Ratajczak, M. Z. (2006). Membrane-Derived Microvesicles: Important and Underappreciated Mediators of Cell-to-Cell Communication. *Leukemia* **20,** 1487-1495.

Rautemaa, R. and Meri, S. (1999). Complement-Resistance Mechanisms of Bacteria. *Microbes Infect.* **1,** 785-794.

Reid, K. B. and Gagnon, J. (1981). Amino Acid Sequence Studies of Human Properdin – N-Terminal Sequence Analysis and Alignment of the Fragments Produced by Limited Proteolysis with Trypsin and the Peptides Produced by Cyanogen Bromide Treatment. *Mol. Immunol.* **18,** 949-959.

Reis, E. S., Barbuto, J. A. and Isaac, L. (2006). Human Monocyte-Derived Dendritic Cells are a Source of several Complement Proteins. *Inflamm. Res.* **55,** 179-184.

Ren, B., McCrory, M. A., Pass, C., Bullard, D. C., Ballantyne, C. M., Xu, Y., Briles, D. E. and Szalai, A. J. (2004). The Virulence Function of *Streptococcus Pneumoniae* Surface Protein A Involves Inhibition of Complement Activation and Impairment of Complement Receptor-Mediated Protection. *J. Immunol.* **173,** 7506-7512.

Reynes, M., Aubert, J. P., Cohen, J. H., Audouin, J., Tricottet, V., Diebold, J. and Kazatchkine, M. D. (1985). Human Follicular Dendritic Cells Express CR1, CR2, and CR3 Complement Receptor Antigens. *J. Immunol.* **135,** 2687-2694.

Reynolds, E. S. (1963). The use of Lead Citrate at High pH as an Electron-Opaque Stain in Electron Microscopy. *J. Cell Biol.* **17,** 208-212.

Ricevuti, G. (1997). Host Tissue Damage by Phagocytes. *Ann. N. Y. Acad. Sci.* **832,** 426-448.

Robinet, A., Emonard, H., Banyai, L., Laronze, J. Y., Patthy, L., Hornebeck, W. and Bellon, G. (2008). Collagen-Binding Domains of Gelatinase A and Thrombospondin-Derived Peptides Impede Endocytic Clearance of Active Gelatinase A and Promote HT1080 Fibrosarcoma Cell Invasion. *Life Sci.* **82,** 376-382.

Rosenbauer, F. and Tenen, D. G. (2007). Transcription Factors in Myeloid Development: Balancing Differentiation with Transformation. *Nat. Rev. Immunol.* **7,** 105-117.

Rosenkranz, A. R., Coxon, A., Maurer, M., Gurish, M. F., Austen, K. F., Friend, D. S., Galli, S. J. and Mayadas, T. N. (1998). Impaired Mast Cell Development and Innate Immunity in Mac-1 (CD11b/CD18, CR3)-Deficient Mice. *J. Immunol.* **161,** 6463-6467.

Rottem, M., Miron, D., Shiloah, E., Horovitz, Y. and Schlezinger, M. (1998). Properdin Deficiency: Rare Presentation with Meningococcal Bone and Joint Infections. *Pediatr. Infect. Dis. J.* **17,** 356-358.

Saladino, R. A., Stack, A. M., Fleisher, G. R., Thompson, C. M., Briles, D. E., Kobzik, L. and Siber, G. R. (1997). Development of a Model of Low-Inoculum *Streptococcus Pneumoniae* Intrapulmonary Infection in Infant Rats. *Infect. Immun.* **65,** 4701-4704.

Schifferli, J. A., Steiger, G., Hauptmann, G., Spaeth, P. J. and Sjoholm, A.G. (1985). Formation of Soluble Immune Complexes by Complement in Sera of Patients with Various Hypocomplementemic States. Difference between Inhibition of Immune Precipitation and Solubilisation. *J. Clin. Invest.* **76**, 2127-2133.

Schlesinger, M., Mashal, U., Levy, J. and Fishelson, Z. (1993). Hereditary Properdin Deficiency in Three Families of Tunisian Jews. *Acta Paediatr*. **82,** 744-747.

Schlesinger, M., Nave, Z., Levy, Y., Slater, P. E. and Fishelson, Z. (1990). Prevalence of Hereditary Properdin, C7 and C8 Deficiencies in Patients with Meningococcal Infections. *Clin. Exp. Immunol.* **81,** 423-427.

Schwaeble, W., Dippold, W. G., Schafer, M. K., Pohla, H., Jonas, D., Luttig, B., Weihe, E., Huemer, H. P., Dierich, M. P. and Reid, K. B. (1993). Properdin, a Positive Regulator of Complement Activation, is Expressed in Human T Cell Lines and Peripheral Blood T Cells. *J. Immunol.* **151,** 2521-2528.

Schwaeble, W., Huemer, H. P., Most, J., Dierich, M. P., Strobel, M., Claus, C., Reid, K. B. and Ziegler-Heitbrock, H. W. (1994). Expression of Properdin in Human Monocytes. *Eur. J. Biochem.* **219,** 759-764.

Segura, M. A., Cleroux, P. and Gottschalk, M. (1998). *Streptococcus Suis* and Group B Streptococcus Differ in their Interactions with Murine Macrophages. *FEMS Immunol. Med. Microbiol.* **21,** 189-195.

Senzolo, M., Coppell, J., Cholongitas, E., Riddell, A., Triantos, C., Perry, D. and Burroughs, A. (2007). The Effects of Glycosaminoglycans on Coagulation: A Thromboelastographic Study. *Blood Coagul. Fibrinolysis* **18,** 227-236.

Siebenhaar, F., Syska, W., Weller, K., Magerl, M., Zuberbier, T., Metz, M. and Maurer, M. (2007). Control of *Pseudomonas Aeruginosa* Skin Infections in Mice is Mast Cell-Dependent. *Am. J. Pathol.* **170,** 1910-1916.

Sjoholm, A. G. (1990). Inherited Complement Deficiency States: Implications for Immunity and Immunological Disease. *APMIS* **98,** 861-874.

Sjoholm, A. G., Braconier, J. H. and Soderstrom, C. (1982). Properdin Deficiency in a Family with Fulminant Meningococcal Infections. *Clin. Exp. Immunol.* **50,** 291-297.

Sjoholm, A. G., Jonsson, G., Braconier, J. H., Sturfelt, G. and Truedsson, L. (2006). Complement Deficiency and Disease: An Update. *Mol. Immunol.* **43,** 78-85.

Sjoholm, A. G., Kuijper, E. J., Tijssen, C. C., Jansz, A., Bol, P., Spanjaard, L. and Zanen, H. C. (1988a). Dysfunctional Properdin in a Dutch Family with Meningococcal Disease. *N. Engl. J. Med.* **319,** 33-37.

Sjoholm, A. G., Selander, B., Ostenson, S., Holmstrom, E. and Soderstrom, C. (1991). Normal Human Serum Depleted of C1q, Factor D and Properdin: Its use in Studies of Complement Activation. *APMIS* **99,** 1120-1128.

Sjoholm, A. G., Soderstrom, C. and Nilsson, L. A. (1988b). A Second Variant of Properdin Deficiency: The Detection of Properdin at Low Concentrations in Affected Males. *Complement* **5,** 130-140.

Skokos, D., Le Panse, S., Villa, I., Rousselle, J. C., Peronet, R., David, B., Namane, A. and Mecheri, S. (2001). Mast Cell-Dependent B and T Lymphocyte Activation is Mediated by the Secretion of Immunologically Active Exosomes. *J. Immunol.* **166,** 868-876.

Smith, C. A., Pangburn, M. K., Vogel, C. W. and Muller-Eberhard, H. J. (1984). Molecular Architecture of Human Properdin, a Positive Regulator of the Alternative Pathway of Complement. *J. Biol. Chem.* **259,** 4582-4588.

Smith, K. F., Nolan, K. F., Reid, K. B. and Perkins, S. J. (1991). Neutron and X-Ray Scattering Studies on the Human Complement Protein Properdin Provide an Analysis of the Thrombospondin Repeat. *Biochemistry* **30,** 8000-8008.

Soderstrom, C., Braconier, J. H., Sjoholm, A. G. and Thuresson, B. (1991). Granulocyte Functions and *Neisseria Meningitidis*: Influence of Properdin-Deficient Serum. *APMIS* **99,** 965-971.

Soderstrom, C., Sjoholm, A. G., Svensson, R. and Ostenson, S. (1989). Another Swedish Family with Complete Properdin Deficiency: Association with Fulminant Meningococcal Disease in One Male Family Member. *Scand. J. Infect. Dis.* **21,** 259-265.

Spath, P. J., Sjoholm, A. G., Nordin Fredrikson, G., Misiano, G., Scherz, R., Schaad, U. B., Uhring-Lambert, B., Hauptmann, G., Westberg, J., Uhlen, M., Wadelius, C. and Truedsson, L. (1999). Properdin Deficiency in a Large Swiss Family: Identification of a Stop Codon in the Properdin Gene, and Association of Meningococcal Disease with Lack of the IgG2 Allotype Marker G2m(n). *Clin. Exp. Immunol.* **118,** 278-284.

Spitzer, D., Mitchell, L. M., Atkinson, J. P. and Hourcade, D. E. (2007). Properdin can Initiate Complement Activation by Binding Specific Target Surfaces and Providing a Platform for De Novo Convertase Assembly. *J. Immunol.* **179,** 2600-2608.

Spurr, A. R. (1969). A Low-Viscosity Epoxy Resin Embedding Medium for Electron Microscopy. *J. Ultrastruct. Res.* **26,** 31-43.

Stover, C. M., Luckett, J. C., Echtenacher, B., Dupont, A., Figgitt, S. E., Brown, J., Mannel, D. N. and Schwaeble, W. J. (2008). Properdin Plays a Protective Role in Polymicrobial Septic Peritonitis. *J. Immunol.* **180,** 3313-3318.

Su, A. I., Cooke, M. P., Ching, K. A., Hakak, Y., Walker, J. R., Wiltshire, T., Orth, A. P., Vega, R. G., Sapinoso, L. M., Moqrich, A., Patapoutian, A., Hampton, G.M., Schultz, P.G. and Hogenesh, J.B. (2002). Large-Scale Analysis of the Human and Mouse Transcriptomes. *Proc. Natl. Acad. Sci. U. S. A.* **99,** 4465-4470.

Sun, Z., Reid, K. B. and Perkins, S. J. (2004). The Dimeric and Trimeric Solution Structures of the Multidomain Complement Protein Properdin by X-Ray Scattering, Analytical Ultracentrifugation and Constrained Modelling. *J. Mol. Biol.* **343,** 1327-1343.

Taylor, M. W., Grosse, W. M., Schaley, J. E., Sanda, C., Wu, X., Chien, S. C., Smith, F., Wu, T. G., Stephens, M., Ferris, M. W. et al. (2004). Global Effect of PEG-IFN-α and Ribavirin on Gene Expression in PBMC in Vitro. *J. Interferon Cytokine Res.* **24,** 107-118.

Taylor, P. R., Martinez-Pomares, L., Stacey, M., Lin, H. H., Brown, G. D. and Gordon, S. (2005). Macrophage Receptors and Immune Recognition. *Annu. Rev. Immunol.* **23,** 901-944.

Theoharides, T. C., Kempuraj, D., Tagen, M., Conti, P. and Kalogeromitros, D. (2007). Differential Release of Mast Cell Mediators and the Pathogenesis of Inflammation. *Immunol. Rev.* **217,** 65-78.

Thery, C., Boussac, M., Veron, P., Ricciardi-Castagnoli, P., Raposo, G., Garin, J. and Amigorena, S. (2001). Proteomic Analysis of Dendritic Cell-Derived Exosomes: A Secreted Subcellular Compartment Distinct from Apoptotic Vesicles. *J. Immunol.* **166,** 7309-7318.

Thurman, J. M. and Holers, V. M. (2006). The Central Role of the Alternative Complement Pathway in Human Disease. *J. Immunol.* **176,** 1305-1310.

Tong, Z. Y. and Brigstock, D. R. (2006). Intrinsic Biological Activity of the Thrombospondin Structural Homology Repeat in Connective Tissue Growth Factor. *J. Endocrinol.* **188,** R1-8.

Truedsson, L., Sturfelt, G., Offenbartl, K. and Sjoholm, A. G. (1990). The Spleen is Not a Major Synthetic Site of Alternative Pathway Components. *Complement Inflamm.* **7,** 52-56.

Truedsson, L., Westberg, J., Nordin Fredrikson, G., Sjoholm, A. G., Kuijper, E. J., Fijen, C. A., Spath, P. J. and Uhlen, M. (1997). Human Properdin Deficiency has a Heterogeneous Genetic Background. *Immunopharmacology* **38,** 203-206.

van den Bogaard, R., Fijen, C. A., Schipper, M. G., de Galan, L., Kuijper, E. J. and Mannens, M. M. (2000). Molecular Characterisation of 10 Dutch Properdin Type I Deficient Families: Mutation Analysis and X-Inactivation Studies. *Eur. J. Hum. Genet.* **8,** 513-518.

Vandermeer, J., Sha, Q., Lane, A. P. and Schleimer, R. P. (2004). Innate Immunity of the Sinonasal Cavity: Expression of Messenger RNA for Complement Cascade Components and Toll-Like Receptors. *Arch. Otolaryngol. Head. Neck. Surg.* **130,** 1374-1380.

Veerman, A. J. and van Ewijk, W. (1975). White Pulp Compartments in the Spleen of Rats and Mice. A Light and Electron Microscopic Study of Lymphoid and Non-Lymphoid Cell Types in T- and B-Areas. *Cell Tissue Res.* **156,** 417-441.

Wang, J. and Liang, P. (2003). DigiNorthern, Digital Expression Analysis of Query Genes Based on ESTs. *Bioinformatics* **19,** 653-654.

Welker, P., Grabbe, J., Zuberbier, T., Grutzkau, A. and Henz, B. M. (2001). GM-CSF Downmodulates c-Kit, FcεRIα and GM-CSF Receptor Expression as Well as Histamine and Tryptase Levels in Cultured Human Mast Cells. *Arch. Dermatol. Res.* **293,** 249-258.

Whaley, K. (1980). Biosynthesis of the Complement Components and the Regulatory Proteins of the Alternative Complement Pathway by Human Peripheral Blood Monocytes. *J. Exp. Med.* **151,** 501-516.

WHO. (1998). World Health Organisation Meeting on Maternal and Neonatal Pneumococcal Immunization. *Wkly. Epidemiol. Rec.* **73,** 187-188.

Wirthmueller, U., Dewald, B., Thelen, M., Schafer, M. K., Stover, C., Whaley, K., North, J., Eggleton, P., Reid, K. B. and Schwaeble, W. J. (1997). Properdin, a Positive Regulator of Complement Activation, is Released from Secondary Granules of Stimulated Peripheral Blood Neutrophils. *J. Immunol.* **158,** 4444-4451.

Wubbolts, R., Leckie, R. S., Veenhuizen, P. T., Schwarzmann, G., Mobius, W., Hoernschemeyer, J., Slot, J. W., Geuze, H. J. and Stoorvogel, W. (2003). Proteomic and Biochemical Analyses of Human B Cell-Derived Exosomes. Potential Implications for their Function and Multivesicular Body Formation. *J. Biol. Chem.* **278,** 10963-10972.

Wurzner, R. (2003). Deficiencies of the Complement MAC II Gene Cluster (C6, C7, C9): Is Subtotal C6 Deficiency of Particular Evolutionary Benefit? *Clin. Exp. Immunol.* **133,** 156-159.

Xu, W., Berger, S. P., Trouw, L. A., de Boer, H. C., Schlagwein, N., Mutsaers, C., Daha, M. R. and van Kooten, C. (2008). Properdin Binds to Late Apoptotic and Necrotic Cells Independently of C3b and Regulates Alternative Pathway Complement Activation. *J. Immunol.* **180,** 7613-7621.

Xu, Y., Ma, M., Ippolito, G. C., Schroeder, H. W.,Jr, Carroll, M. C. and Volanakis, J. E. (2001). Complement Activation in Factor D-Deficient Mice. *Proc. Natl. Acad. Sci. U. S. A.* **98,** 14577-14582.

Yang, P. C., Zheng, P. Y. and Wang, C. S. (2005). Lipopolysaccharide Activates Human Mast Cells to Induce Intestinal Epithelial Barrier Dysfunction. *The Internet Journal of Gastroenterology* **4**.

Yirmiya, R., Pollak, Y., Barak, O., Avitsur, R., Ovadia, H., Bette, M., Weihe, E. and Weidenfeld, J. (2001). Effects of antidepressant drugs on the behavoral and physiological responses to lipopolysaccharide (LPS) in rodents. *Neuropsychopharmacology*, **24**, 531-544.

Yuste, J., Botto, M., Paton, J. C., Holden, D. W. and Brown, J. S. (2005). Additive Inhibition of Complement Deposition by Pneumolysin and PspA Facilitates *Streptococcus Pneumoniae* Septicemia. *J. Immunol.* **175,** 1813-1819.

Zelazko, M., Carneiro-Sampaio, M., Cornejo de Luigi, M., Garcia de Olarte, D., Porras Madrigal, O., Berron Perez, R., Cabello, A., Rostan, M. V. and Sorensen, R. U. (1998). Primary Immunodeficiency Diseases in Latin America: First Report from Eight Countries Participating in the LAGID. Latin American Group for Primary Immunodeficiency Diseases. *J. Clin. Immunol.* **18,** 161-166.

Zhang, L. and Insel, P. A. (2004). The Pro-Apoptotic Protein Bim is a Convergence Point for cAMP/protein Kinase A- and Glucocorticoid-Promoted Apoptosis of Lymphoid Cells. *J. Biol. Chem.* **279,** 20858-20865.

Zwirner, J., Felber, E., Schmidt, P., Riethmuller, G. and Feucht, H. E. (1989). Complement Activation in Human Lymphoid Germinal Centres. *Immunology* **66,** 270-277.